2010

THE ROLE OF ABCG2 IN DRUG ACTIVE TRANSPORT IN MILK

Lipeng Wang
University of Kentucky, wanglipeng2000@hotmail.com

ABSTRACT OF DISSERTATION

Lipeng Wang

The Graduate School

University of Kentucky

2010

THE ROLE OF ABCG2 IN DRUG ACTIVE TRANSPORT INTO MILK

ABSTRACT OF DISSERTATION

A dissertation submitted in partial fulfillment of the
requirements for the degree of Doctor of Philosophy in the
College of Pharmacy at the University of Kentucky

By

Lipeng Wang

Lexington, Kentucky

Director: Patrick J. McNamara, Ph.D., Professor of Pharmaceutical Sciences

Lexington, Kentucky

2010

ABSTRACT OF DISSERTATION

THE ROLE OF ABCG2 IN DRUG ACTIVE TRANSPORT INTO MILK

Drug active transport into milk is a major concern for breastfeeding mothers and healthcare providers. Studies from the literature indicated that breast cancer resistance protein (ABCG2) plays an important role in drug transfer into milk. There has been limited study on stereoselective interactions with ABCG2. A mechanistic analysis of flux across cell monolayer model is a critical first step toward extrapolating in vitro results for predicting in vivo disposition (including distribution into milk), drug disposition or drug-drug interactions.

The objectives of this thesis were (1) to establish a “Chemical knockout model” in rat for studying drug accumulation into milk, (2) to investigate the impact of stereoselective interaction between ABCG2/Abcg2 and pantoprazole on drug transport in milk, (3) to understand *in vitro* monolayer flux model using experimental data and a mechanistic mathematical model.

Quantitive PCR, Western blotting and immunohistochemistry results indicated that Abcg2 was up-regulated during lactation and localized on apical side of epithelial cells in mammary gland. *In vitro* and *in vivo* experiments confirmed that Abcg2 is responsible for nitrofurantoin active transport in rat milk and GF120918 was established as a chemical knockout model.

Abcg2 interacts stereoselectively with pantoprazole isomers. A significant different apical flux between two pantoprazole isomers was observed in Abcg2-MDCKII cell line. The milk to serum (M/S) ratio of (-)-pantoprazole was almost 3 times as that of (+)-pantoprazole in lactating rats. Administration GF120918 decreased M/S of (-)-pantoprazole ($p<0.001$) but not (+)-pantoprazole ($p>0.05$).

A stably transfected ABCG2/Abcg2 overexpressing MDCKII cell line was successfully created and used to explore the theoretical relationships in a monolayer flux model. Based on the profiles of pantoprazole isomer transport, a simple three compartment model for drug transfer into breast milk incorporating the permeability-surface area products for passive diffusion (PS_D), paracellular flux (PS_{PC}) and apically efflux ABCG2 ($PS_{A,E}$) transfection was developed. The mathematical model was

developed to more fully understand the interplay of paracellular, passive diffusion, active transport, and flux kinetic parameters (K_m, V_{max}, IC_{50} and K_i). This model provided useful insights into the meaning and limitation of parameters obtained from monolayer flux.

KEYWORDS: ABCG2, transporter, chirality, transwell model, lactation, mathematical modeling.

Lipeng Wang

10-12-10

Date

THE ROLE OF ABCG2 IN DRUG ACTIVE TRANSPORT IN MILK

By

Lipeng Wang

Patrick J. McNamara, Ph.D.
Director of Dissertation

Jim Pauly, Ph. D
Director of Graduate Studies

10-12-10
Date

RULES FOR THE USE OF DISSERTATIONS

Unpublished dissertations submitted for the Doctor's degree and deposited in the University of Kentucky Library are as a rule open for inspection, but are to be used only with due regard to the rights of the authors.

Bibliographical references may be noted, but quotations or summaries of parts may be published only with the permission of the author, and with the usual scholarly acknowledgments.

Extensive copying or publication of the dissertation in whole or in part also requires the consent of the Dean of the Graduate School of the University of Kentucky.

A library that borrows this dissertation for use by its patrons is expected to secure the signature of each user.

Name	Date

DISSERTATION

Lipeng Wang

The Graduate School

University of Kentucky

2010

THE ROLE OF ABCG2 IN DRUG ACTIVE TRANSPORT IN MILK

DISSERTATION

A dissertation submitted in partial fulfillment of the
requirements for the degree of Doctor of Philosophy in the
College of Pharmacy at the University of Kentucky

By

Lipeng Wang

Lexington, Kentucky

Director: Patrick J. McNamara, Ph.D., Professor of Pharmaceutical Sciences

Lexington, Kentucky

2010

DEDICATION

With deepest appreciation, this dissertation is dedicated to my husband and my parents for their love and support over the years.

ACKNOWLEDGEMENTS

This dissertation contains many years of not only my own effort on study and work but also support and encouragement from many generous and inspiring people. Without their support this dissertation would not have been completed. First and foremost, I thank my mentor, Dr. Patrick J. McNamara for providing this wonderful opportunity for me to develop a scientist. He devoted an inordinate amount of time guiding me through the challenges in my graduate student life. He is a thoughtful research scientist who has deep insight to discover the theory under the surface of experiment results. He always could see the problems and difficulties in my study and research where I was experiencing even sometimes I did not really realize them. He was always there to listen and to give guidance, encouragement and help in both my research career and personal life whenever how busy he was. The almost 5 years graduate student life that I have worked with him has been fun, rewarding, interesting and challenging, and along the way I am getting mature as a scientist. I will always appreciate for his education, advice, patience and help. His passion, dedication and diligence towards the work made the best example for me to follow in my future career.

I also acknowledge the contributions of each of my committee members Drs. Mary Vore, Peter Wedlund and Markos Leggas. Their advice, discussions and challenging, thoughtful questions helped me to achieve a nice PhD research. I would like to thank Dr. Arthur Cammers as my outside examiner for his time and attention. I also would like to thank Drs. Paul Bummer and Brad Anderson for their suggestion and help. I am appreciative for several previous students in Dr. McNamara's lab: Phillip Empey, Maggie Abbassi, Phillip Gerk and Jane Alcorn for sharing experiment methods and giving help on my work. Collaboration played a key role in the success of this project. I would like to thank colleagues in Dr. Leggas's lab, Mamta Goswami for her assistance of ABCG2 transfection in MDCKII cell line and Sf9 cell line, Jamie Horn for helping me to solve the HPLC problems, Kuei-ling Kuo for the research experience which we have been through together and Elefthefia for her time spending on LC-MS method development in lab rotation. I would also express my specially appreciation to Catina Rossoll for assisting me with the administrative tasks for completing my doctoral program.

I appreciate the assistance of Dr. Jennifer Strange and Dr. Greg Bauman at the Flow Cytometry Core Facility, John May at ERTL center. Then, I would like to

acknowledge the financial support of the Graduate School and the Department of Pharmaceutical Sciences, American Association of Pharmaceutical Science for the travel support to the meetings to present my work.

Last but not least, I would like to thank my parents, Shumei Zai and Shengtai Wang for raising me up and always encouraging me to pursue the knowledge, my husband, Chengjun Huo for his love, patience and support. They gave me the courage and strength to overcome the difficulties over the years.

TABLE OF CONTENTS

LIST OF TABLES

LIST OF FIGURES

CHAPTER 1: Introduction

A. The benefit of breastfeeding and breastfeeding trends in the United States

Breast milk has been recommended by many advocacy groups as the optimal nutrition for infants, such as the American Academy of Pediatrics (AAP), the American Medical Association (AMA), the American Dietetic Association (ADA) and the World Health Organization (WHO). An ideal feeding pattern for infants would include exclusive breastfeeding for the first 6 months of life and breastfeeding with complementary foods from 6 months until at least 12 months of age; such consideration would provide optimal nutrition and health protection for both infants and mothers (James and Lessen, 2009).

Breast milk is considered to be most advantageous for providing protective nutrients for infants. Some components, including transforming growth factor (TGF)-β, interleukin (IL)-10 (Penttila, 2010), erythropoietin, and lactoferrin (Rodriguez-Palmero et al., 1999) can reduce the inflammatory response in the newborn intestine. These special components from breast milk work individually or in concert to modulate the neonatal immature anti-inflammatory response. Milk appears to decrease the incidence of ear infections, diarrhea, lung infections and urinary tract infections in babies; such that breast-feeding babies are admitted to the hospital less often than the infants fed formula. Moreover, the composition of breast milk appears to change according to the newborn infant's needs for passive protection at the different ages. Some clinical evidence suggests its protective effect against age-related infectious gastroenteritis (Walker, 2010). Some elements in breast milk can actively stimulate development of the newborn's host defense systems to establish a continuous mucosal protection after breastfeeding is terminated (Walker, 2010). There is some evidence that breastfeeding improves cognitive development and has an important impact on children’s IQ, brain size and white matter development (Kramer et al., 2008; Isaacs et al., 2009). Furthermore, those who were breastfed are less likely to acquire adult illnesses such as type 1 and 2 diabetes (Kostraba et al., 1993; Pettitt et al., 1997; Gunderson, 2008), some cancers (Davis, 1998; Bener et al.,

2001), asthma (Gdalevich et al., 2001; Chulada et al., 2003), hypertension, metabolic syndrome (Nobili et al., 2009) and obesity (Gillman et al., 2001; Armstrong and Reilly, 2002; Plagemann and Harder, 2005). For the mother, breastfeeding also improves health outcomes, including a reduced risk of breast and ovarian cancer (Titus-Ernstoff et al., 2009), type 2 diabetes (Villegas et al., 2008), rheumatoid arthritis (Mason et al., 1995) and maternal postpartum depression (Ip et al., 2009).

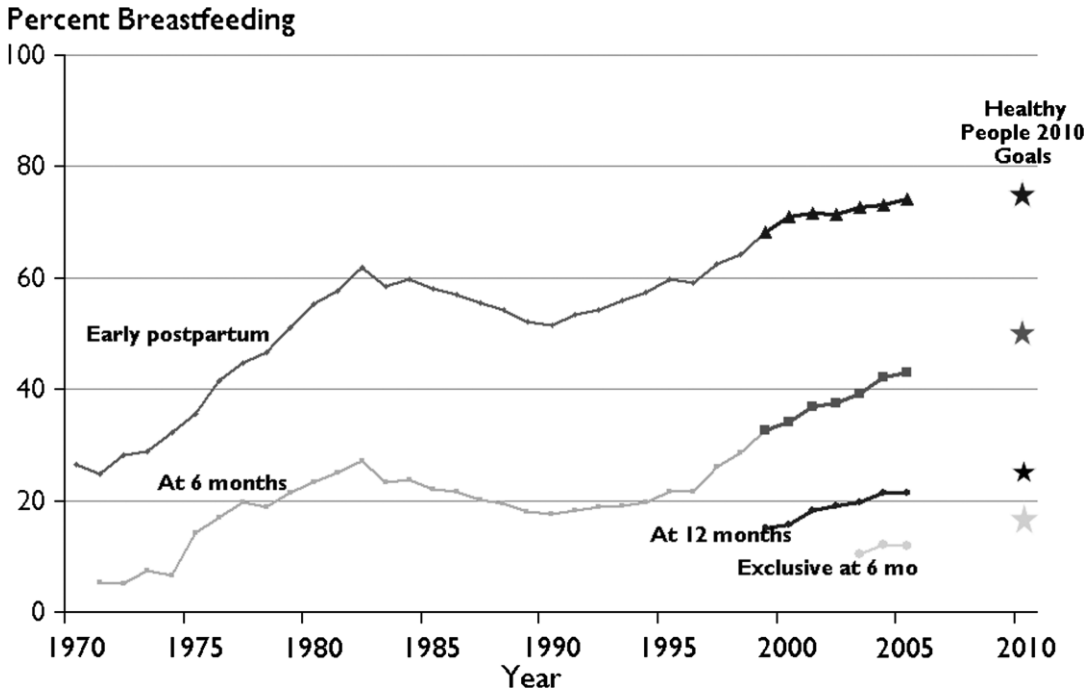

Figure 1-1 National trends in rate of breastfeeding. Data source: pre-1999, Ross Mothers Survey; 1999–present, CDC NIS (The figure was cited from (Grummer-Strawn and Shealy, 2009))

Notes: Ross Laboratory Mothers Survey (RLMS), a survey whose primary goal was to track usage of infant formula by manufacturing brand. CDC: the Centers for Disease Control and Prevention; NIS: the National Immunization Survey.

Breastfeeding benefits not only the health of mother and infant but also provides societal and economic advantages as well as convenience of life issues of parenting (Rohde, 1981). These health benefits decrease acute and chronic illness in short-term and long-term for both mother and child help to reduce health care-related expenses. It has become an important public health strategy for decreasing infant and child morbidity and maternal morbidity, and helping to

control health care costs. During the last 39 years (1970-2009) the rate of breastfeeding had improved in the United States (Figure 1-1)(Grummer-Strawn and Shealy, 2009). Rates of initiation of breastfeeding more than doubled from a lowest rate of 26.5% in 1970 to 61.9% in 1982. This trend was slightly decreased from 1982 until the mid 1990s. In 1990 the rate of initiation of breastfeeding fell to 51.5%; after that time point, the breast feeding rate again rose and reached 74.2% in 2005. Trends in breastfeeding at 6 months have paralleled initiation trends. In order to drive the maximal benefit for mother, infant and society, new Healthy People 2010 set objectives to call for breastfeeding with targets of 75% initiation and 50% continuation at 6 months (Grummer-Strawn and Shealy, 2009).

B.Drug use during breastfeeding

A societal concern of drug transfer into human milk has drawn more attention following the trend of increasing breastfeeding rate. It was reported the more than 90% of women take at least one medication during the first week after delivery (Bennet, 1988). Drug surveys have indicated that about 17% of the mothers who were still breast-feeding at 4 months had taken at least the equivalent of one daily dose of one drug. Moreover, 5% of the mothers who continued to breast-feed were receiving medication for asthma, allergy, hypertension, arthritis, diabetes, and epilepsy or migraine (Bennet, 1988). Drug use for infection, pain relief and other acute and chronic disease symptoms during breast feeding is very common (Hernadez et al., 2009).

Most drugs and their metabolites in maternal blood pass the barrier of the mammary gland and distribute into the milk. They can modify the production, volume and composition of the milk to produce possible short- or long-term harmful effects on the infant. Significant drug-related symptoms in breast-fed infants [such as irritability, vomiting, sedation, respiratory depression and shock] have been reported in clinical cases. One extreme example of clinical case reports is the fatal opioid poisoning in a breastfed neonate whose codeine-prescribed mother was a CYP2D6 (Cytochrome P450 2D6) ultrarapid

metabolizer (UM) (Madadi et al., 2009). CYP2D6 is a member of the cytochrome P450 system and it is one of the most important enzymes involved in the metabolism of xenobiotics in the body. The pathway of codeine and morphine metabolism is shown in Figure 1-2. Although codeine has been recommended by the American Academy of Pediatrics as being compatible with breastfeeding, a polymorphism of breastfeeding mother in CYP2D6 added complexity to this case. Codeine is a prodrug and its analgesic properties are primarily dependent on its biotransformation into morphine by the cytochrome enzyme P450 2D6 (CYP2D6). Its active product, M6G is almost exclusively catalyzed by the enzyme uridyl glucuronosyltransferase 2B7 (UGT2B7). Therefore, the breastfed infant of a mother who is CYP 2D6 UMs combined with the UGT2B7*2/*2 genotype may result in increased in dose exposure level and as a result an increased risk of life-threatening CNS depression for the newborn (Madadi et al., 2009). These observations prompted the Food and Drug Administration to issue a Public Health Advisory on the topic (Use of Codeine By Some Breastfeeding Mothers May Lead To Life-Threatening Side Effects In Nursing Babies)

There also may be long term, more subtle developmental effects of drug exposure at early stages of life which are very difficult to monitor or ascribe cause and effect (Arendt, 1997; Khaksari et al., 2009). Likewise there may be consequences for mother and child if maternal pharmacotherapy is forgone. For example, untreated depression may have a deleterious effect on the emotional development of their children and significant depression, especially if complicated by delusions, may lead to the mother attempting suicide and infanticide (Gentile, 2005). Consequently maternal medication during lactation must consider not only benefit of breastfeeding but also health of mother and infant. Doctors need to help mothers weigh the risks of prenatal exposure to drugs for their babies against the potential risks of untreated illness or to forego the benefits of breastfeeding. These therapeutic considerations include susceptibility to drug toxicity of the very young or premature infant, significant individual variations in drug response, the dose-response relationship with

respect to drug toxicity and the role of pharmacogenetics in both the mother and the infant (Berlin et al., 2009).

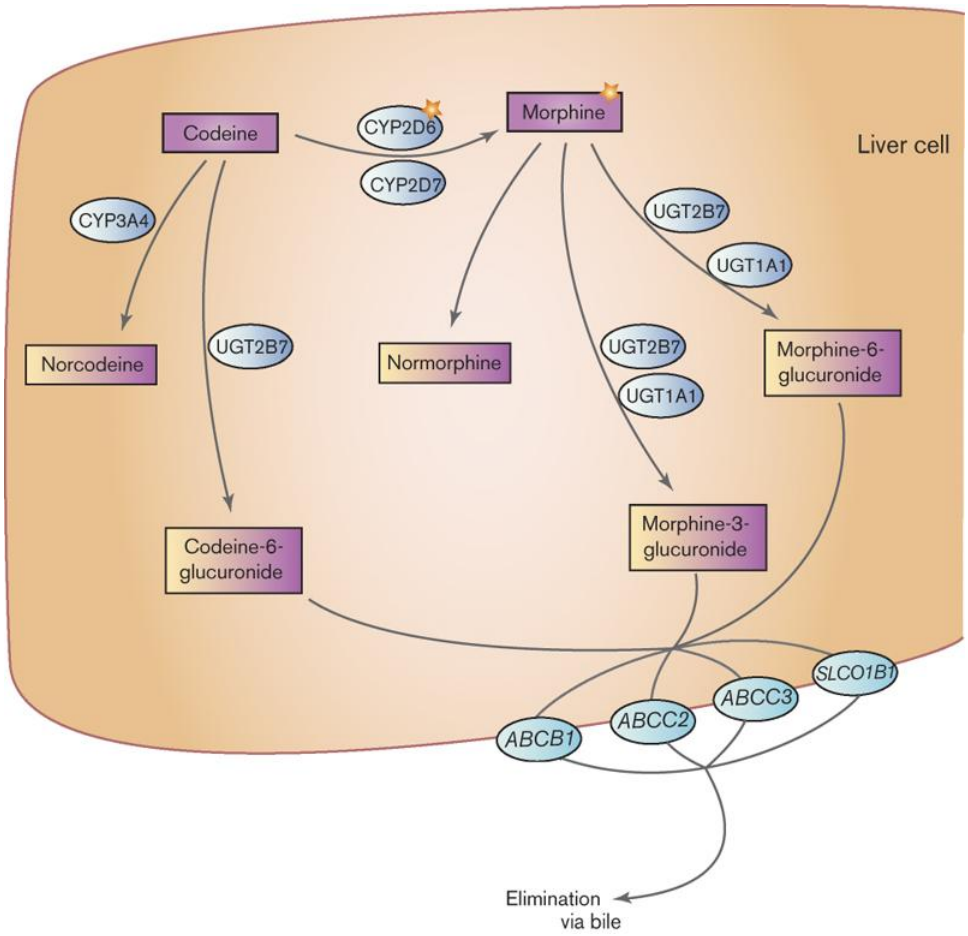

Figure 1-2 The pathway of codeine and morphine metabolism. Figure is cited from (Thorn et al., 2009)

While the above consideration is warranted, there are very few studies conducted in breastfeeding women and their infants to make an appropriate risk assessment for drug use in lactation. A 2003 FDA analysis of the prescribing information of the 1022 drugs in the Physician's Desk Reference illustrates the problem (Uhl et al., 2003). Only 25% of drug labels had information of drug transport in human milk and/ or effects in nursing infants. In addition, 16% of drug labels had information on drug excretion into milk in animals and more than half of them had no information at all. The problem is not limited to older drugs. It was estimated that less than 10% of the new molecular entities approved between 1995 and 2002 gave any information on human milk transfer in their

regulatory filings (Uhl et al., 2003). Therefore, considerable confusion in the scientific community regarding this issue exists (Friguls et al., 2010): should a woman breastfeed her baby while continuing to use prescription drugs and/or drugs of abuse? What is the mechanism of drug transfer into milk? What is the extent of drug exposure and does this present a significant risk to the newborn? The discussion of the mechanism of drug transfer into milk is one of the critical steps to address these questions.

C.Physiological mechanisms of drug transfer into milk

1.Physiology of mammary gland

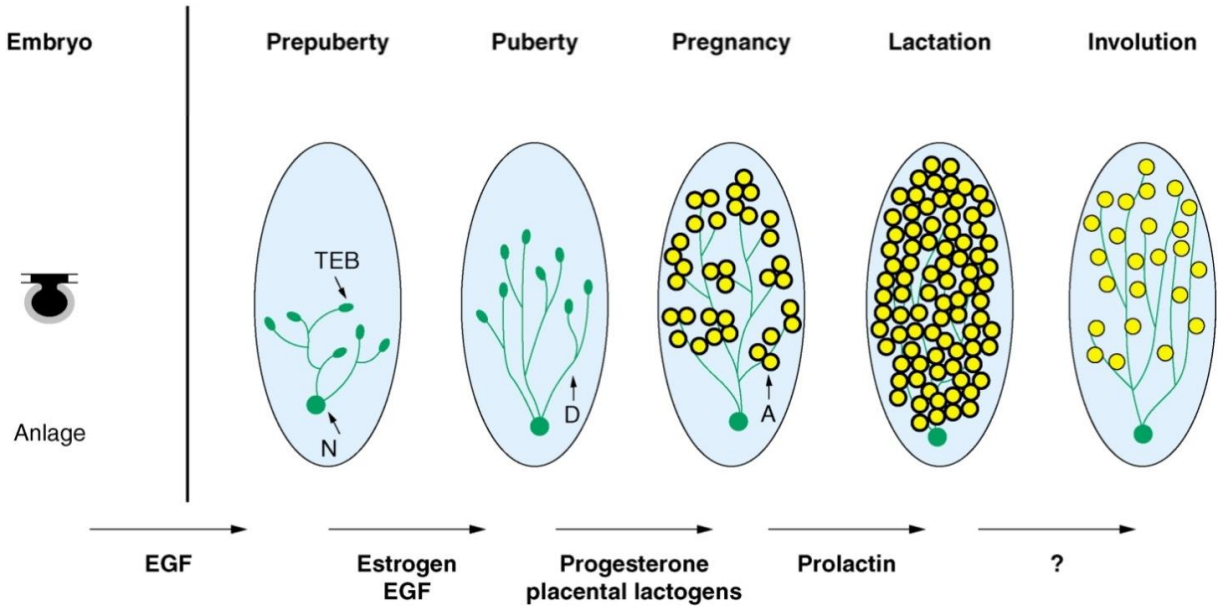

Figure 1-3 The development of structure of mouse mammary gland under the control of hormones in ontogeny. The proportion of epithelial cells in lactating are obviously increased than in non-lactating and involution. The solid green circle represents the nipple (N) from which the ducts originate. The ends of growing ducts form terminal end buds (TEB) during puberty. Mammary ducts (D) are shown as solid lines and the lobuloalveolar structures are presented as yellow circles (A). Epidermal growth factor (EGF) signals through the stroma and controls early ductal outgrowth. Together with estrogen, it also controls ductal elongation and branching during puberty. Progesterone, placental lactogens, prolactin, and the osteoclast differentiation factor signal alveolar proliferation and differentiation during pregnancy and possibly lactation. The figure was modified from Lothar Hennighausen's paper (Hennighausen and Robinson, 2001).

Briefly, the mammary gland is comprised of epithelium and stroma. The functional unit of milk production is alveoli which are formed by two types of epithelial cells. The majority are luminal secretory cells which produce breast milk and secrete it into a central lumen. These cells can form the barrier between the breast milk and the maternal circulation. The development of the mammary gland is different from most of other organs. It estabolishes in embryo and further development, predominant differentiation and proliferation of mammary gland, occurs after birth and under the control of hormones (Figure 1-3). The embryonic, prepubertal, pubertal, pregnancy, lactation and involution stages are connected with sexual development and reproduction. Following initial embryonic and prepubertal stages, the growth and development of mammary gland is dependent on the stimulation of hormones. The steroid hormones control ductal and alveolar development. It has been proposed that progesterone through activating Wnt signaling pathway is essential for the cell proliferation of mammary gland (Brisken et al., 2000). Both estrogen and progesterone induce ductal side branching in mice (Xu et al., 2000). The proliferation and differentiation of secretory mammary gland epithelium are dependent on the interaction between prolactin and prolactin receptor (PrIR) (Ormandy et al., 1997) and the downstream Jak-Stat5 pathway. Jak-Stat5 signaling pathway controls cell proliferation, differentiation and specification in development of mammary gland. During a successful pregnancy, hormonal changes associated with pregnancy induce series changes in the maternal hypothalamus, stimulating maternal body development to prepare for lactation. The size and number of alveoli grows and develops under hormonal stimulation and intercellular gaps close for the preparation of lactation (Neville and Watters, 1983). The inner structure and ratio of cell types in mammary gland undergoes significant change. The proportion of epithelial cells in lactation is obviously increased than in non-lactation (Figure 1-3).

2. Milk components and secretion pathways

Drug is likely to be transported into milk via the same pathways which milk components secreted from serum or secretary cells into lactating mammary

gland. Therefore, to fully understand drug accumulation into milk it is helpful to examine the mechanism of milk formation itself.

Breast milk has evolved in mammals to enrich all necessary nutrients for the growth and development of the newborn. The various milk components include lipids, protein, carbohydrates, water, calcium and phosphorus, iron, zinc, copper, manganese, selenium, iodine, vitamins D, K, A, E, C, thiamine, riboflavin, niacin, pantothenic acid, pyridoxine, biotin, folate, and cyanocobalamine (Nichols and Nichols, 1981).

From the cell biology of lactating alveolar cells in mammary gland, there are a number of potential barriers to the transfer of exogenous substances from blood to milk side: (1) vascular or stromal membranes; (2) basement membrane; (3) basal epithelial membranes, (4) paracellular junctional complexes, (5) Golgi membranes and (6) apical epithelial membranes (McManaman and Neville, 2003). Some proteins in milk are synthesized and secreted by the epithelial cells themselves. The major amounts of lactation-specific proteins present in milk are synthesized in rough endoplasmic reticulum (Larson, 1979) and then secreting into the Golgi apparatus to finish post-translational modifications and ejected into the lumen with other milk components (Larson, 1979). Substances derived from maternal circulation get into milk by overcoming the various barriers between blood and milk. The five pathways for solute to enter milk by transcellular and paracellular routes are summarized in Figure 1-4 (McManaman and Neville, 2003).

Pathway I: Aqueous solutes include the major milk proteins, oligosaccharides, and nutrients such as lactose, citrate, phosphate and calcium. They are secreted through an exocytotic pathway.

Pathway II: Primarily triglycerides and lipid-associated proteins are secreted by a process unique to mammary epithelial cells (Mather and Keenan, 1998).

Pathway III: It is a transcytosis pathway and transports a wide range of macromolecular substances derived from plasma or stromal cells, including endocrine hormones such as prolactin, insulin and estrogen (Koldovsky, 1995;

Ollivier-Bousquet, 1998); serum proteins such as albumin, transferrin and immunoglobulins (Hunziker and Kraehenbuhl, 1998); and stromal derived agents such as secretory immunoglobulin A, cytokines and lipoprotein lipase (Goldman et al., 1996; McManaman and Neville, 2003).

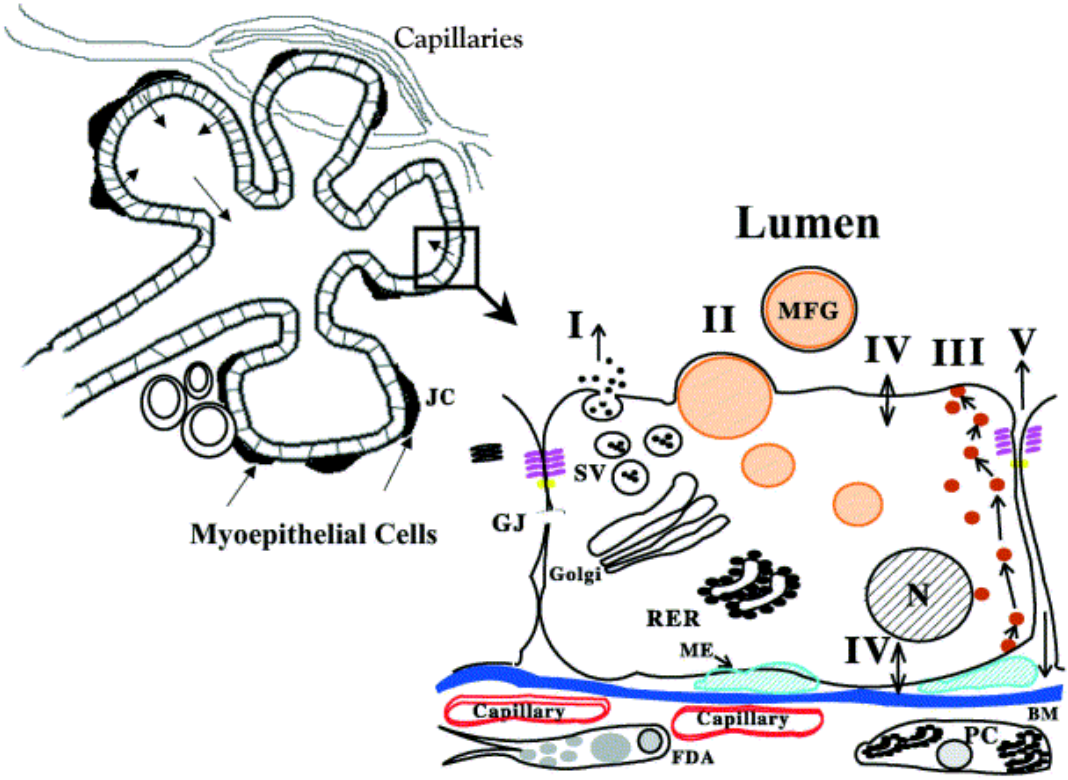

Figure 1-4 Diagram of mammary alveolus and alveolar epithelial cell showing pathways for milk secretion. Abbreviations: SV, secretory vesicle; RER, rough endoplasmic reticulum; BM, basement membrane; N, nucleus; PC, plasma cell; FDA, fat depleted adipocyte; JC, junctional complex containing the tight and adherens junctions; GJ, gap junction; ME, myoepithelial cell. MFG, membrane bound milk fat globule. Figure is cited from (McManaman and Neville, 2003).

Pathway IV: For the transfer of ions and small molecules, such as glucose, amino acids, and water across basolateral and apical plasma membranes.

Pathway I and II are for secretion of endogenously generated substances. Pathway III and IV exist for transport of exogenous substances to milk.

Pathway V: Paracellular transport provides an entry of plasma components, leukocytes, serum and interstitial substances into milk (Nguyen and Neville, 1998). Pathway V is typically open but becomes very restricted during lactation. This pathway is open during pregnancy, involution and in inflammatory states such as mastitis.

D.The pathway of drug transfer into milk

1. Paracellular transport

Paracellular transport (Pathway V) plays minimal role in drug accumulation in milk. One would anticipate that some small, polar molecules are candidates for diffusion through the paracellular pathway since molecular size is the most relevant parameter relating to rate of diffusion through the restricted paracellular route. Pathway V is closed by the tight junctions between epithelial cells during lactation in humans and most other species except rabbit (McManaman and Neville, 2003) (Figure 1-4). Therefore drugs are transferred at a slow rate and in very low amounts by paracellular transport; hence, this pathway is generally considered negligible for most drugs.

2. Transcellular passive diffusion

Theoretically, passive diffusion is expected to be a common pathway for most endogenous or exogenous substances (including drugs, environment toxins and their metabolites) in blood circulation to pass through the barriers of alveolar epithelial cell and distribute into milk. Smaller, more lipophilic molecules partition into lipid bilayers and pass more readily through the epithelial membranes. The equilibrium between serum and milk tends to be rapid and there is no need for the assistance of transporters.

The drug concentration in milk is proportional to the corresponding concentration in maternal serum based on the passive diffusion pathway. The parameter, milk to serum (M/S) ratio, which compares milk with maternal plasma drug concentrations, serves as an index of the extent of drug excretion in milk. Drug distribution resulting in passive diffusion between serum and milk can be

predicted or estimated by a diffusion model (Fleishaker, 2003) and calculated by Eq.1-1.

$$\frac{M}{S_{Dif}} = \frac{(f_s^u)(f_s)(W)}{(f_m^u)(f_m)(S)} \qquad \text{Eq. 1-1}$$

where f^u is the unionized fraction of drug in serum or milk, f is the free fraction of drug in serum or milk, W/S is the ratio of the drug concentration in whole milk to the drug concentration in skim milk, and the subscripts s and m represent serum and milk, respectively.

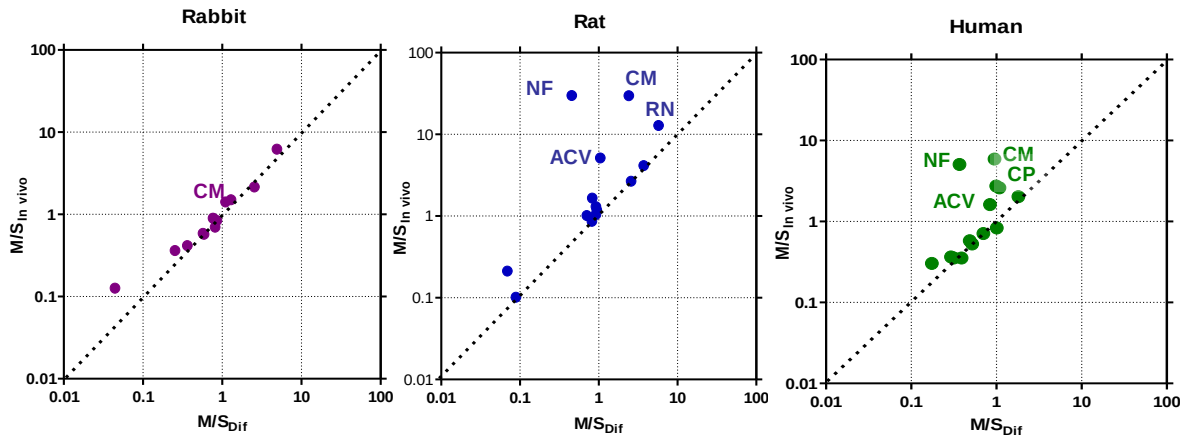

Figure 1-5 M/S predicted vs observed in rabbit, rat and human for a number of drugs. Exceptions include: nitrofurantoin (NF), cimetidine (CM), acyclovir (ACV), ranitidine (RN) and ciprofloxicin (CP).

Figure 1-5 shows that the results of passive diffusion model (M/S_{Dif}) to predict drug M/S ratios from a series of experiments which were conducted in lactating rabbits, rats and humans (Fleishaker and McNamara, 1988a; Fleishaker and McNamara, 1988b; McNamara et al., 1991; McNamara et al., 1992a; McNamara et al., 1992b). It illustrates the relationship observed M/S versus M/S_{Dif} for ten drugs: propranolol, phenobarbital, phenytoin, diazepam, acetaminophen, antipyrine, salicylic acid, caffeine, paraxanthine and cimetidine. The diffusion model predicted well the transport into milk for all drugs in rabbit and many of the drugs in rat and human. For some drugs, such as cimetidine and nitrofurantoin, the observed M/S in rat and human milk clearly exceeded the

diffusion prediction. The prototypical example is nitrofurantoin in rat and clinical studies. Oo et al. showed that an infusion of 0.5 mg/h nitrofurantoin resulted in an $M/S_{\text{in vivo}}$ that was almost 100 times greater than the value from the diffusion prediction (31.1± 4.0 v. 0.3 ± 0.1) in rat. In a clinical study, M/S determined by a ratio of the nitrofurantoin AUC in milk and serum was 22 times as the predicted $M/S_{\text{diff.}}$ (6.21 ± 2.71 vs. 0.28 ± 0.05) (Gerk et al., 2001a). CM and RN transfer into rat milk could be saturated and inhibited (McNamara et al., 1996). Taken together, these results suggest the presence of the active transport processes across the mammary epithelium that are involved in drug accumulation into milk (Oo et al., 2001).

3. Transcellular active transport

In some instances, physical and chemical properties such as size, charge, and hydrophilicity are impediments for drug passage across biological membranes (Klaassen and Aleksunes, 2010). Pathway IV includes some solute-specific mechanisms for the transport of ions and small molecules such as glucose and amino acids. These processes require the presence of specific transporters on the basolateral or apical side of epithelial cells. A number of transporters have been shown to be expressed in lactating mammary epithelial cells and are responsible for various components transport into milk. Some of them are likely to be involved in drug accumulation in milk as well.

E.Transporter expression in lactation

During lactating, the change of alveoli in mammary gland is not only in size and number but also in protein expression on epithelial cells for the preparation of lactation, including glucose, amino acid transporters. In order to exclude the effect of the changes of mammary gland in structure on the investigation of transporter expression during lactation, Alcorn et al first isolated a pure population of epithelial cells from human breast milk and reduction mammoplastic clinical samples to investigate 30 transporter expressions in lactating mammary gland by quantitative reverse transcription-polymerase chain reaction (Alcorn et al., 2002). In order to cover a broader array of transporter

expression in lactating mammary gland, Phil Empey (Thesis) used a similar approach to isolate a pure population of epithelial cells for subsequent gene expression profiling by microarray. From his dissertation work, the results of microarray analysis discovered that ABCG2, SLC15A2, SLC22A12, SLC6A14, and SLCO4C1 were significantly up-regulated during lactation (164-, 70-, 41-, 8-, and 2-fold, respectively). ABCC10, SLC10A1, SLC16A1, SLC22A4, SLC22A5, SLC22A9, SLC28A3, SLC29A1, SLC29A2, and SLCO4A1 had an expression level similar to, or greater than, levels in the kidney or liver (Table 1-1, from Phil Empey's dissertation).

PEPT2 is an oligopeptide transporter generally characterized as an apical uptake transporter (Shen et al., 1999) and if a similar location/function were also true for lactating mammary epithelium, an associated flux would more likely to diminish drug concentration in milk. SLC22A12 (an organic anion/urate transporter) and SLC6A14 (amino acid transporter) are also present at increased RNA expression level, but these transporters appear to play a less likely role in drug transport (Anderson et al., 2008; Ohtsu et al., 2010). However, one investigation showed 1-Methyltryptophan, which is an inducer of immune surveillance against tumor cells by inhibiting indoleamine dioxygenase, is a substrate for SLC6A14 [ATB(0,+)](Karunakaran et al., 2008). Therefore, additional studies should be performed to investigate whether ATB (0, +) has a role in drug transport into milk. The significant up-regulation of SLCO4C1 is a novel finding. SLCO4C1 has not been widely studied, but is considered to be an uptake basolateral transporter (Chu et al., 2007; Cheng and Klaassen, 2009). SLCO4C1 belongs to the organic anion transporting polypeptides (OATP) family of influx transporters expressed in numerous tissues (liver, brain, intestine, kidney) and facilitate the tissue uptake of substrate drugs (Kalliokoski and Niemi, 2009). A number of recent reports have shown that OATP uptake transporters (e.g, OATP1B1) on the basolateral membrane can function in concert with apical efflux transporters (e.g., P-gp, MRP2 and ABCG2) to facilitate the transcellular transport of drugs (Matsushima et al., 2005). The most important and established efflux transporter on apical side of epithelial cells in lactating mammary gland is

ABCG2. Therefore, a reasonable hypothesis is that SLCO4C1 coordinates with ABCG2 to regulate substrate movement into breast milk. However, unpublished data from our group studies (Kuei-ling Kuo) suggests that SLCO4C1 is on the apical instead of the basolateral membrane.

Table 1-1 Comparison of Affymetrix U133 plus 2.0 array transporter probeset expression levels in human LMEC (lactating luminal mammary epithelial cell) vs. MEC (mammary epithelial cell). Genes are grouped based on whether they are increased or decreased during lactation. Probesets for the same gene were grouped into sections of the table sorted by fold change in expression (From Phil Empey's dissertation).

Gene Symbol	Probeset ID	p-Value	LMEC		MEC		Fold Change
			Mean	SD	Mean	SD	
Higher during lactation (p < 0.05, fold change >1)							
ABCG2	209735_at	3.69E-02	17536	5964	107	75	**164.04**
SLCO4C1	222071_s_at	2.39E-03	3362	294	48	31	**69.70**
SLC15A2	205316_at	3.62E-03	3936	421	96	47	**40.80**
	205317_s_at	2.16E-03	868	182	89	62	**9.72**
	240159_at	8.99E-04	243	31	76	10	**3.18**
SLC22A12	237799_at	2.79E-02	184	80	24	19	**7.84**
SLC6A14	219795_at	4.13E-02	3988	1193	1773	500	**2.25**

F. ABCG2

1.General introduction of ABCG2

The ATP binding cassette (ABC) transporter family is a large protein superfamily. ABC transporters are widely distributed in membranes of all organisms from bacteria to mammals, such as in the brush border membrane of intestinal cells, the canalicular and sinusoidal membrane of hepatocytes, the luminal and basolateral membrane in the proximal tubules of the kidney and in the endothelial cell of the brain capillaries (Kos and Ford, 2009; Wang et al., 2009a; Klaassen and Aleksunes, 2010). They are responsible for transport of a wide variety of compounds through cell membranes against concentration gradient using the energy of ATP hydrolysis for the process of substrate translocation (Rocchi et al., 2000). The existence of ABC transporters can have a significant effect on the absorption distribution metabolism elimination (ADME), toxicity and the adverse drug-drug interactions of substrate drugs.

ABCG2 is a member of ABC family subfamily G and it has been confirmed as an important transporter in mammalian defense system. ABCG2 is also named as mitoxantrone resistance-associated protein (MXR) or breast cancer resistance protein (BCRP) because it was first cloned from a multidrug-resistant breast cancer cell line (Doyle et al., 1998); however, subsequent studies indicate that BCRP is not a unique or special characteristic for breast cancer cells and many of these cells were found lacking BCRP expression (van Herwaarden and Schinkel, 2006). A growing body of evidence strongly suggests that ABCG2 is one of the more important efflux transporters having a strong impact on the pharmacokinetic profile, pharmacodynamics, and toxicity of drugs.

The typical structure of the majority of mammalian ABC transporters contains 2 types of structural domains: the hydrophobic membrane spanning domain (MSD) comprising several transmembrane α-helices and the hydrophilic, intracellular nucleotide binding domain (NBD) (Mao and Unadkat, 2005). The mRNA of ABCG2 encodes a 655 amino acid protein (72-kDa) that contains a single N-terminal ATP binding cassette followed by six trans-membrane

segments. Comparison of protein sequences with that of P-gp and MRP1, ABCG2 proteins are half transporters that are composed of a single NBD followed by one MSD. Hence, the structure of ABCG2 appears to be a half transporter and functions as a homodimer (Doyle and Ross, 2003) or heterodimers (Xu et al., 2004). Kage et al demonstrated that the breast cancer resistance protein (BCRP, ABCG2) forms an S-S homodimer (Kage et al., 2002) and Cys-603 is an important residue in the formation of the covalent bridge between BCRP monomers (Kage et al., 2005). Recently the results from mutation of Cys at different position of ABCG2 indicated that Cys-mediated covalent dimerization is not required for ABCG2 to function as a transporter and that Cys-603, Cys-608 may also be involved in BCRP dimmer formation (Figure 1-6) (Shigeta et al., 2010).

ABCG2 polymorphisms that alter expression or function of protein have been observed and it has been reported that variants of ABCG2 greatly impact the oral bioavailability and clearance of ABCG2 substrates (Ishikawa et al., 2005). Some studies have characterized the possible physiological relevance of the ABCG2 polymorphism and functional variants (Mao and Unadkat, 2005). To date, sequencing of the ABCG2 gene from human samples has discovered over 80 different, naturally occurring sequence variations (Ishikawa et al., 2005). In general, the studies of polymorphisms of ABCG2 have been focused on resistance of anticancer drugs. For example, a variant at position 482 which is responsible for the resistance to mitoxantrone, doxorubicin, and daunorubicin, reduces daunorubicin accumulation and retention, and causes an ATP-dependent enhancement of the efflux of rhodamine 123 in the cloned transfected cells. At least three variant forms of ABCG2 have been documented on the basis of their amino acid moieties (i.e.,arginine, glycine and threonine) at position 482 (Mitomo et al., 2003). They have been reported causing change of drug resistance profile and substrate specificity.

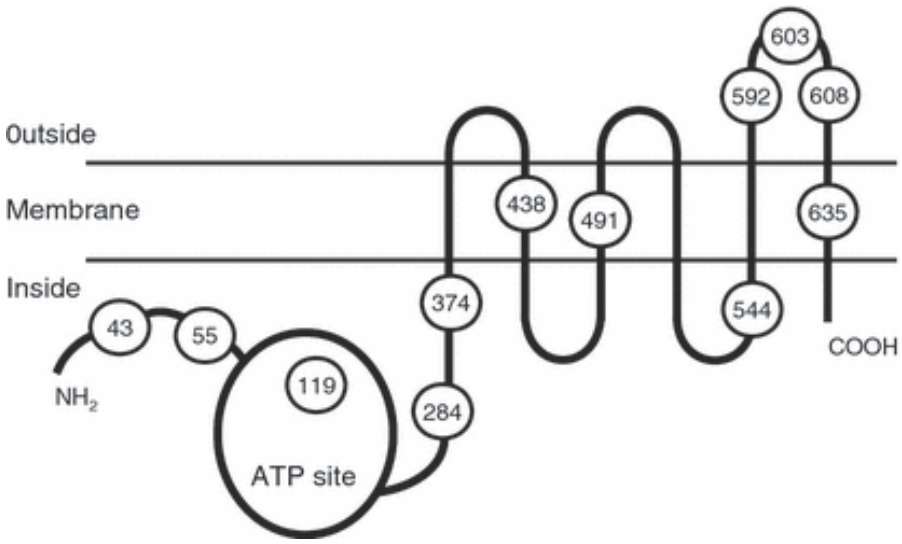

Figure 1-6 Schematic depiction of the breast cancer resistance protein (BCRP) with 12 cysteine residues indicated. Three of these residues, Cys-592, Cys-603, and Cys-608, are localized in the third extracellular domain (Shigeta et al., 2010).

ABCG2 is abundant in the luminal membrane of endothelial cells of blood capillaries in the brain, epithelial cells of placenta, kidney, liver and intestine to limit endogenous or exogenous xenotoxins into body (van Herwaarden and Schinkel, 2006), and importantly in most of cancer cells where ABCG2 plays important roles to resist chemotherapy or acquire resistance during treatment.

2. ABCG2 and drug transfer into milk

As mentioned in previous section, nitrofurantoin and cimetidine are actively transported into human and rat milk, and result in drug accumulation much greater than predicted by the diffusion model. However, the mechanism remained unknown until studies at the Netherlands Cancer Institute (Jonker et al., 2005; Merino et al., 2005b) which indicated that ABCG2 was strongly up-regulated in the mammary gland of mice, cows and humans during lactation and was responsible for the active secretion of clinically and toxicologically important substrates into mouse milk, such as the dietary carcinogen PhIP, the anticancer drug topotecan and the antiulcerative cimetidine (Jonker et al., 2005).

ABCG2 and P-glycoprotein are generally considered to be protective transporters. In general, they play a role in barrier systems (e.g., blood brain

barrier, placenta, gut wall) that protect more vulnerable entities (e.g., brain, fetus, and whole body) from harmful xenobiotics. Hence, the physiologic function of ABCG2 in lactating mammary epithelium is not fully understood, since high concentration of drugs and environment toxins in milk may be harmful to infants. Evolution would tend to favor physiology that is efficient and protects the developing newborn. ABCG2 transporting drug and toxin to milk would run counter to this tenet. The study of riboflavin suggests a possible physiological role for ABCG2 in lactating mammary epithelial cells. As an important vitamin, riboflavin can be converted to the essential coenzymes which participate as electron carriers in many important redox reaction chains in body (Powers, 2003); however, riboflavin cannot be synthesized by mammals. Riboflavin is an ABCG2 substrate and is transferred into milk by ABCG2 (van Herwaarden et al., 2007) which could imply that ABCG2 may be serve as a milk vitamin and nutrient transporter.

G. *In vivo* model to study drug transport

Knockout mouse models are the most popular *in vivo* approaches for the function study of transporter or other proteins (Kooij et al., 2009; Lagas et al., 2009a; O'Byrne et al., 2009). The alteration of drug disposition following the knockout of a specific transporter provides compelling evidence for the significance of the transporter (Agarwal et al., 2010; de Waart et al., 2010; Kodaira et al., 2010). However, mammalian physiology is a complex, interconnected system and no one protein or pathway is truely independent. In some transporter knockout mice models, the mice cannot survive from disease or nutritive deficiency, such as deletion of the taurine transporter gene (taut) which results in all taut-/- mice succumbing to infections (Delic et al., 2010), whereas in other examples, the homeostasis is maintained in a relative normal state even if one important pathway has been impaired. This would imply that the pathway associated with the transporter may not be the only one responsible for function or there are adjustments on compensatory mechanism. The body is under an integrated regulation control to maintain the normal physiologic function.

It has been observed that the expression of other proteins changes after knocking out a specific protein in several transporter knockout studies (Chu et al., 2006; Kooij et al., 2009). For example, Mdr1a deficient mice express 3 times as much Abcg2 compared to wild-type mice (Cisternino et al., 2004); the level of Mrp4 mRNA and protein expression in liver and kidney of Mrp2 (-/-) mice increase approximately 6- and 2-fold, respectively (Chu et al., 2006). Whether or not these increased expressions of other transporters provide a compensatory mechanism in these knockout mice models will depend upon the particular substrates (or biochemical pathway). Nonetheless, there may be unintended and unknown consequences following the knockout of a specific gene.

Inhibition of transport of a compound by a specific inhibitor is often used for transporter studies in *in vitro* experiment, and a chemical knockout could be an alternative way to overcome shortcomings of a knockout mouse model if the function of a transporter *in vivo* can be completely inhibited. A critical criterion in selecting an inhibitor is specificity. Many inhibitors are nonspecific and they interact with several transporters and even drug metabolism enzyme (Matsson et al., 2009). The inhibitor specificities of P-gp, BCRP and MRP2 were shown to be overlapping. Moreover, P-gp and CYP3A4 have significant overlap in substrate specificity (Kim et al., 1999). So the specificity of an inhibitor as a “chemical knockout” should be considered carefully when correlating the organ with multiple different transporter expressions, such as kidney and liver. GF120918 (N-(4-[2-(1, 2, 3, 4-tetrahydro-6,7-dimethoxy-2-isoquinolinyl)ethyl]-phenyl)-9,10-dihydro-5-methoxy-9-oxo-4-acridine carboxamide) is an inhibitor for both P-gp and ABCG2; however, P-gp is not expressed in mammary gland. The rat is the most common animal model for drug development. A functional blockade of rAbcg2 by a specific inhibitor (a “chemical knock out”) resulting in a decrease in active drug transport into milk would be a useful *in vivo* model for verification of *in vitro* experiments.

H. *In vitro* models to study drug transport

Optimal pharmaceutical therapy delivers drug to the target site(s) in the body at concentrations adequate to obtain a positive pharmacological effect. One factor affecting drug reaching the target site, as well as systemic exposure is drug transport into and out of cells (David T. Rossi, 2002). The presence of transporter(s) has been shown to affect the therapeutic consequence of many important drugs. Therefore, in order to decrease the cost in drug development and optimize the pharmacokinetic properties of drug candidates during the early stages, characterizing drug transporter interaction is a widely accepted strategy (White, 2000; Roberts, 2001). Broadly, *in vitro* methods are the most common choice to evaluate key pharmacokinetic properties of drugs in pharmaceutical industry. These *in vitro* systems tend to focus on drug metabolism enzymes and transporter (Yamashita et al., 2002; Schwab et al., 2003; Zhou et al., 2010). In general, the range of these available *in vitro* tools scale from relatively simple biochemical approaches to complex cell culture model.

1. ATPase assay for ABC transporters

ATPase assay is one of a limited number of traditional biochemical available methods for the assessment of drug transporter function (Stanley et al., 2009). The method is based on the realization that transporters utilize the energy from ATP hydrolysis for substrates translocation (Figure 1-7). It measures the utilization of ATP and indirectly provides an estimate of transporter mediated drug transport (Gannon et al., 2009; Robey et al., 2009). For example, ATPase activity measured in the presence of orthovanadate represents non-P-gp ATPase activity and can be subtracted from the activity generated without orthovanadate to yield vanadate-sensitive ATPase activity (Schwab et al., 2003). In this method, isolation of intact membranes is important to estimate vectorial transport but it is controllable and easier than other biological systems (transwell monolayer or Sf9 vesicles). It can be used for high throughput screening since we do not have to develop a specific assay for each drug. However, this method is, at best, a proxy for actual directional transport (Stanley et al., 2009). Also some substrates that are transported do not stimulate ATPase activity and, hence, this approach would result in false negatives.

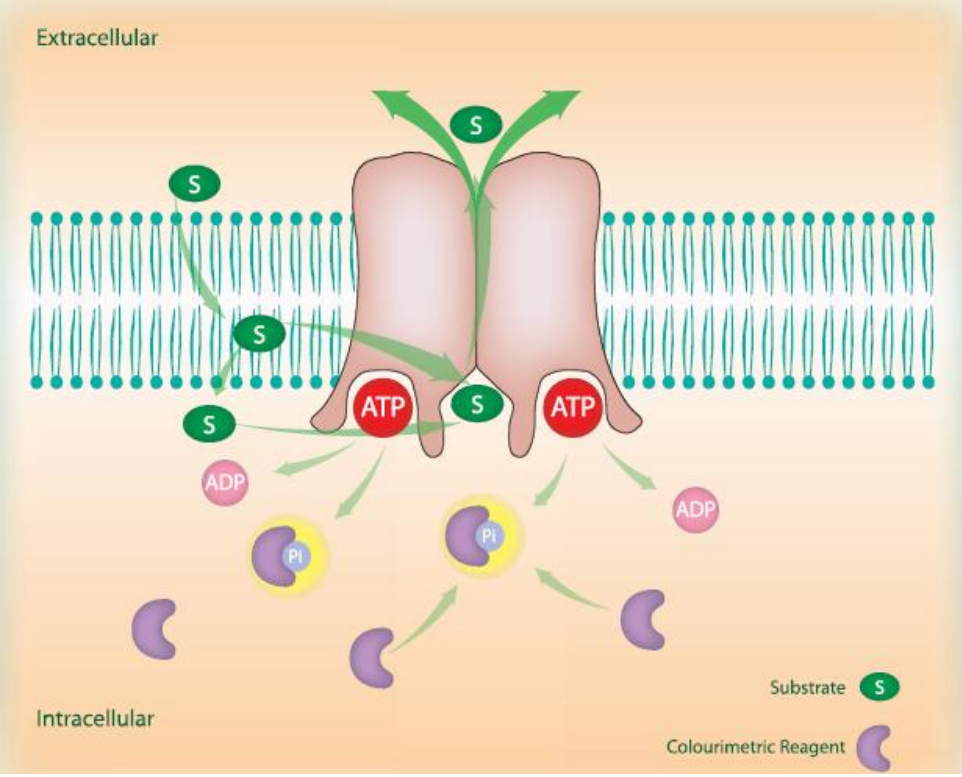

Figure 1-7 The mechanism of ATPase assay for ABC transporters. This figure is cited from the homepage of SOLVO Biotechnology Company (http://www.solvobiotech.com/Solvo%20Solutions/atpase_assays.html)

2. Monolayer flux model for transcellular transport assay

Flux across a monolayer of cells grown on a porous plexiglass filter (i.e., sometimes referred to as Transwell after the name of the filter system) is the most popular method to study transporter. Monolayer flux model provides an efficient, low throughput pathway to screen new molecule entries in drug discovery (Balimane et al., 2004; Xiao et al., 2006), or study drug-drug interaction (Marchetti et al., 2007; Wang et al., 2009b) and drug transport mechanism (Wang et al., 2009b). It mimics *in vivo* environment by culturing specific cell lines on the permeable supports. These cells can polarize and form an integrated monolayer with tight junction on the support membrane. This model produces a separate apical or basolateral domain for the different purpose studies, uptake, efflux or secretion. Selection of an appropriate cell line is a key step to establish an appropriate model system. The cell lines which are often used for monolayer flux studies include the following:

Primary cell lines

Primary cell culture involves the use of cells that are directly isolated from tissues or organs and may most closely mimic *in vivo* environment. Cultures are established either as explants, using mixed cell populations from small fragments of tissues, or using purified populations of defined cell types. For the explant culture, one type cell could adapt *in vitro* environment quickly than other cell types by proliferating rapidly and outgrowing (Burdall et al., 2003). It should be noted that explants culture may be significantly different from the original structure of tissue or organ. This is a particular problem with explants, and so primary cultures may be more desirable and controllable. Primary culture typically involves the preparation of the cells every time and not as a continuous culture; hence, it tends to be labor intensive and may lack the necessary reproducibility to compare results across a series of experiments (Stanley et al., 2009).

Continuous culture cell lines

In order to overcome the disadvantages of primary cell culture and meet the preference for cell culture that is reproducible and easy to work with, several continuous cell lines have been established for drug transporter study. They also can be used as host (parent cell lines) to overexpress a single or double specific transporter(s) for further function study.

CaCo-2 is a human colon tumor-derived cell line that has been widely used for the high-throughput screening of drug permeability and identification of substrates, inhibitors, and inducers of intestinal transporters (Sun et al., 2008). The CaCo-2 screening system has remained a popular *in vitro* model to test compounds for intestinal permeability and efflux liability for more than a decade (Press and Di Grandi, 2008). CaCo-2 was considered by the pharmaceutical industry for the development of cell culture systems that could mimic intestinal mucosa and thereby mimic drug absorption. The CaCo-2 cell line has a well-differentiated brush border on the apical surface and tight junctions, and expresses typical small-intestinal microvillus hydrolases and nutrient

transporters. In addition, since differentiated CaCo-2 cells express various cytochrome P450 isoforms and phase II enzymes such as UDP-glucuronosyltransferases, sulfotransferases and glutathione-S-transferases, this model could also allow the study of presystemic drug metabolism (Meunier et al., 1995). The CaCo-2 is popular because it is of human origin, easy to maintain (Ohashi et al., 2009) and derived from a colon cancer. In addition, as a single cell line, it expresses the appropriate polarized phenotype as *in vivo* but it is free of mucus and underlying submucosal and muscular tissue, which could interfere with drug transport.

LLC-PK1, the porcine kidney cell line, LLC-PK1, has been used as a model for drug-transport studies for around 15 years (Aszalos, 2004). LLC-PK1 cells have a polarized phenotype in culture and express some endogenous P-gp activity (porcine P-gp). The presence of porcine P-gp in LLC-PK1 cells may compromise the results of *in vitro* studies using this cell line (Yamazaki et al., 2001). The main disadvantage of the LLC-PK1 cell line is it is non-human and non-rodent origin. However, this cell line is easy to work with and responds well to transduction with adenoviral vectors (Brimer et al., 2000).

MDCKII (Madin-Darby canine kidney strain II cells), has been used as a model for drug-transport studies for around 20 years (Aszalos, 2004). This cell line has been widely used to establish transporter transfection model, such as P-gp (Shirasaka et al., 2009; Tachibana et al., 2010), MRP2 (Lechner et al., 2010) and ABCG2 (Tournier et al., 2009). MDCKII cells grow fast, form relatively tight junction, produce interpretable data of relevance for clinicians (Keogh and Kunta, 2006a) and with low expression level of MDR1, MRP1 and MRP2. MDCKII has been well characterized as a good host cell line for transfection.

Overexpressing transporter cell lines

The overexpressing transporter system is an effective tool for studying the activity of individual transport processes. It brought into perspective the possibility to investigate transporter interaction with substrate on monolayer. Usually, the difference between efflux ratios on the transfected and parental cell

lines is regarded as transporter mediated active uptake or efflux process (van Herwaarden et al., 2007; Zhou et al., 2008; Lagas et al., 2009b). To date, overexpressing transporter in a host cell line has been a widely accepted technique. P-gp, MRP2, ABCG2 and other transporters have been overexpressed in CaCo-2, LLC-PK1 and MDCKI or II for different study purposes. The expression level and the function of specific transporter can be characterized and provide some pharmacokinetic insights, however, this method may not reflect the *in vivo* condition.

3. Membrane vesicles with transporter protein

Another popular method to study transporter is membrane vesicle of insect or mammalian cells which also introduces the overexpressing transporter system into a host cell line. Target transporter can be expressed on membrane of cells by either stable transfection (heterologously overexpressed) or baculovirus-mediated expression in insect cells. In general, stable overexpression is most often chosen for mammalian cell lines, such as MDCKII, LLC-PK1 and CaCo2 (Burger et al., 2005; de Wolf et al., 2008; Zhao et al., 2009; Zhang et al., 2010). Although it is possible to perform in insect cell lines (Kohler et al., 2000; Kempf et al., 2002); however, single insect cells are not easy to grow and the establishment of a monoclonal cell line is difficult following transfection. Hence, there is a limited number of studies which include other proteins (such as receptor) overexpressed in Sf9 insect cells. In most of situations these cells were used as a population after selection and the percentage of expression cells would be estimated (Kohler et al., 2000; Kempf et al., 2002).

Baculovirus-mediated expression in insect cells is a well-accepted approach to produce recombinant transporter protein. It is frequently used because it is relatively easy to use and the high likelihood of acquiring expected expression level of heterologous protein and the high probability of obtaining a biologically active protein. Insect cell is a popular alternative host to bacteria for expression of recombinant proteins. Several factors contribute to this widespread use, including the development of vectors with features that provide ease-of-use and

high expression levels of recombinant protein, post-translational modifications such as glycosylation and phosphorylation which mimic those modifications in mammalian cells. Hence, Baculovirus-mediated transporter expressing in insect cells could be used for mammalian transporter study of qualitative pharmacokinetic estimates (Pedersen et al., 2008; Lagas et al., 2009b; Vaidya et al., 2009).

Membrane fractions can be isolated from overexpressing transporter in either mammalian cells or insect cells. The membrane fraction including functional transporter would form vesicles. Theoretically, the orientations of these vesicles are half and half (50% is “inside in” and 50% is “inside out”). Thus, efflux transporter study can take advantage of “inside out” membrane vesicle where the ATP binding site is exposed. The technique also changes the efflux study paradigm to one of vesicle accumulation, so that the experiment can be specific, ATP dependent and controllable.

I. *In vitro* models to estimate kinetic parameters of drug transporters

The most common *in vitro* models to estimate kinetic parameters of drug transporter are based on transporter overexpressing systems; either membrane fraction or whole cell system. Both approaches utilize overexpressing transporter into cell lines (mammalian or insect) to conduct a range of studies to determine Michaelis-Menten type kinetic parameters and K_i or IC_{50} values either directly or indirectly.

1.Transporter ATPase (K_m and V_{max})

As mentioned previously, ATPase assay is a cost effective assay to identify interaction between test compounds and transporters since it is not necessary to establish a method for each compound. The membrane fractions are isolated from transporter over-expressing in Sf9 (Feng et al., 2008) or other mammalian cell lines (Robey et al., 2009; Cai et al., 2010). ATPase activities were calculated in terms of nanomoles of phosphate per milligram of total vesicle protein per minute of incubation time. Apparent affinity values (K_m) of ATPase, could be

estimated from the concentration-response data by nonlinear regression (Feng et al., 2008). Affinities of substrates for transporter can be ranked differently according to the range of K_m of transporter ATPase (Feng et al., 2008). In some cases, the value of V_{max}/K_m is used to compare the transport property of different mutants of transporters (Cai et al., 2010). In addition, the parameter estimation of transporter ATP_{ase} avoids the culture of intact monolayer and basolateral transport limitation from Transwell. However, K_m and V_{max} of transporter ATP_{ase} are not equivalent to the K_m and V_{max} of transporter-substrate complex. They provide a useful indication of activity of transporter but not real translocation parameters.

2. Transporter from cellular transport (K_m and V_{max})

Intracellular accumulation of substrates is a popular method for the functional study of transporter to identify either uptake or efflux (Pan et al., 2009; Zheng et al., 2009; Agarwal et al., 2010; Pan et al., 2010). In some studies intracellular transport (also called cellular accumulation) is used to determine the kinetic parameters of efflux transporter, such as K_m and V_{max} of ABCG2 (Pollex et al., 2010). In this method, it was assumed that the permeability of empty cell line (as nonsaturable transport or passive diffusion) was same as in a transporter overexpressing cell line. Time dependent transport and concentration dependent experiments were performed. The data were fit into nonlinear regression analysis to determine K_m and V_{max} of ABCG2.

The driving forces for this transport process can be described in Figure 1-8. In this *in vitro* model there are a passive diffusion, an efflux transport on the membrane but no paracellular transport between cells. Although there is no passive diffusion presentation from basolateral as in Transwell model; they do have passive diffusion exposure on the membrane for efflux transport. The drugs or substrates to be effluxed out of cell must first diffuse into the cell. It should be recognized that the donor concentration of substrate is not the driving force for efflux transport process, but is the cellular concentration. As a result, functional

qualitative characterization may be acceptable; however, the K_m and V_{max} of transporter estimated from accumulation experiment may also be inaccurate.

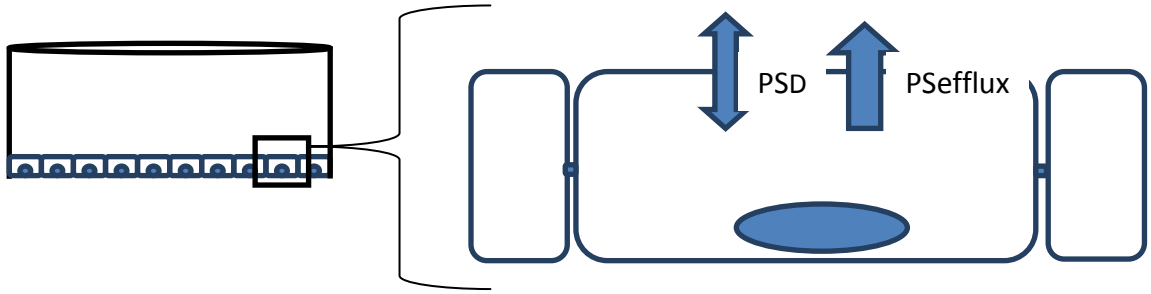

Figure 1-8 The model of drug accumulation in cell on plate.

3. Cell monolayers (K_m and V_{max})

Transwell is a method used to estimate Michaelis-Menten type kinetic parameters (K_m and V_{max}) of a substrate for a transporter (Breedveld et al., 2004; Petri et al., 2004). The substrate obtained from the receiver side of the Transwell is detectable by HPLC or LC-MS. In Figure 1-9, there is an example in which the $K_{1/2}$ (K_m) of pantoprazole was obtained from Transwell data (Breedveld et al., 2004) and estimated to be 100-200 µM. However, several issues with this approach need to be fully understood before the information can be utilized effectively. First consideration is one of correlating flux with concentration. For vectorial drug transport from basolateral to apical side or apical side to basolateral, the driving force for efflux transporters is the drug concentration in the cell, not donor concentration. Second consideration, is the realization that as with any process, the overall flux rate is controlled by the slowest step in a series. Permeability associated with diffusion across the basolateral side (PS_D) may be the limiting step controlling the appearance of drug in the apical compartment, thus masking the apical flux process. Bentz et al reported the steady-state Michaelis-Menten analysis of P-glycoprotein mediated transport through a confluent cell monolayer cannot predict the correct Michaelis constant (K_m) (Bentz et al., 2005). Kalvass and Pollack demonstrated that PS_D on the basolateral membrane limits the apical directional transport of substrate so that ER_A (the apical efflux ratio can be defined as the ratio of the initial rate of flux in the B-to-A direction in overexpressing cell line divided by the initial rate of flux in

the B-to-A direction in parent cell line) of substrate in Transwell should not exceed 2 (Kalvass and Pollack, 2007). Therefore, understanding the mechanism of drug transport in Transwells is a critical step to estimating Michaelis-Menten type kinetic parameters (K_m and V_{max}) of transporter using this approach.

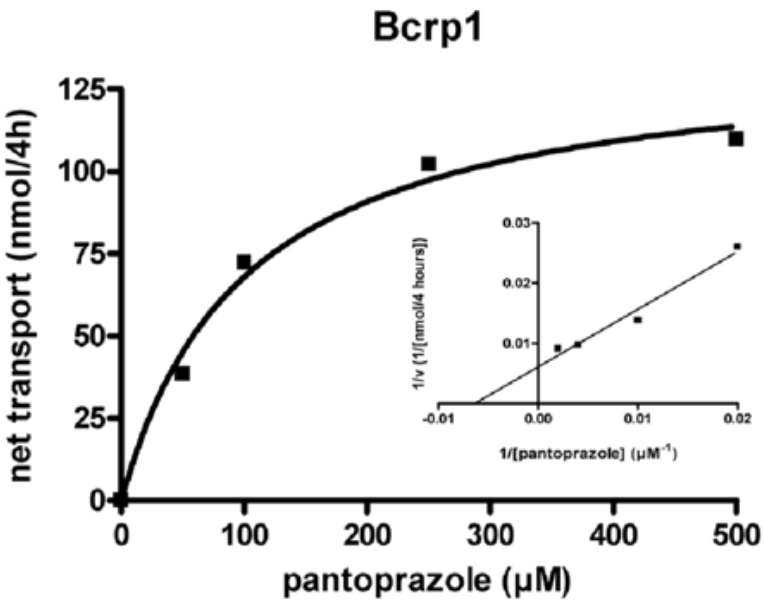

Figure 1-9 Saturation kinetics of pantoprazole transport by Bcrp1 in the MDCKII cell line. The difference in transport of pantoprazole in MDCKII-Bcrp1 and MDCKII-Parental cell lines at t = 4 h is plotted against the pantoprazole concentration (in μM). *Inset*, Lineweaver-Burk transformation of these results. The apparent K1/2 value at t = 4 h is 0.1–0.2 mM (Breedveld et al., 2004)

4.Kinetic parameters (K_m and V_{max}) from Sf9 vesicles

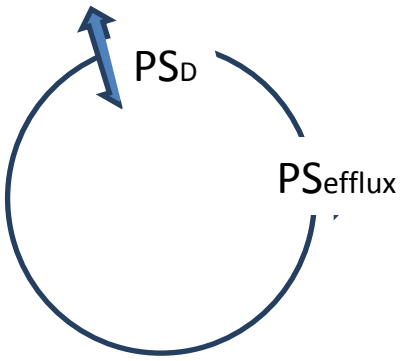

Figure 1-10 The model of efflux transporter in Sf9 membrane vesicle.

As described previously, Baculovirus-mediated expression in insect cells has become well-established for the production of recombinant transporter proteins (Figure 1-10). Overexpressing transporter in Sf9 cells is convenient, fast and controllable. For efflux transporters, inside-out Sf9 membrane vesicles expose ATPase site of transporter and substrate concentration directly so that ATP dependent substrate accumulation can be quantitiated. Because of these advantages, estimation of K_m and V_{max} for efflux transporters from Sf9 vesicles has been widely used (Breedveld et al., 2004). The disadvantage of Sf9 vesicle experiment is assay limitation. The amount of substrate accumulation in vesicle is very low and hence, requires highly sensitivity of assay. The samples from vesicle experiment are difficult to detect by HPLC or even LC-MS methodology. As a result, a radiolabeled substrate is frequently used for the detection of uptake. However, most target substrates are not commercially available as radiolabeled. Some investigators use inhibition experiments to indirectly characterize parameter values such as the inhibition constant (K_I) (Lagas et al., 2009b). Another consideration is the lipophilicity of the compound. For highly lipophilic drugs, the ability to discern the affinity of compound could not be uniquely defined because of the high background accumulation due to diffusion. In those cases as well, competition experiments may be employed as an indirect estimate of affinity, as in the estimation of gimatecan affinity for human ABCG2 (Marchetti et al., 2007).

J. The understanding and mathematical model of efflux in Transwells

Since the initial paper using a monolayer flux model was published in 1980's, Transwells have been extensively employed in many studies for individual purpose. The discussion about the underlying mechanism of drug transport across cell monolayers has greatly deepened our understanding (Lentz et al., 2000; Tam et al., 2003; Kalvass and Pollack, 2007). A large number of Transwell studies have focused on P-gp substrate screening using the CaCo-2 system. The various complex observations associated with Transwell experiments have caused investigators to consider a number of factors involved in kinetic

processes and establish the kinetic models to understand the Transwell model (Roerig et al., 2004; Janneh et al., 2009). Naruhashi et al have examined whereas the unstirred water layer can be the rate-limiting step for transport of drugs with high membrane permeability in Caco-2 cells and affect the apparent permeability of drug transport (Naruhashi et al., 2003). Therefore, investigators should be cautious in evaluating the contributions of a transporter in the case of drugs with high apparent permeability.The passive permeability may also have influence on results of drug transport mediated by P-gp. Some compounds, such as nicardipine, may pass through the cell membrane faster than P-gp can transfer it. Thus, the high passive diffusion can mask drug flux across the apical membrane via P-gp and resulted in that efflux ratio does not affect active transport (Lentz et al., 2000). Also Liu et al indicated that the filter membrane is a permeability barrier for the low mass balance compounds (Liu et al., 2009). It is very important to define the hydrodynamic conditions in these small chambers with use of *in vitro* experimental apparatus (Transwell or Snapwell) for transport experiments (Naruhashi et al., 2003). To date, a relatively comprehensive approach to explain flux in monolayer system has been presented as a kinetic efflux model (Kalvass and Pollack, 2007) and Caco-2 cell monolayer theoretical model (Sun and Pang, 2008).

1. Kalvass and Pollack kinetic model

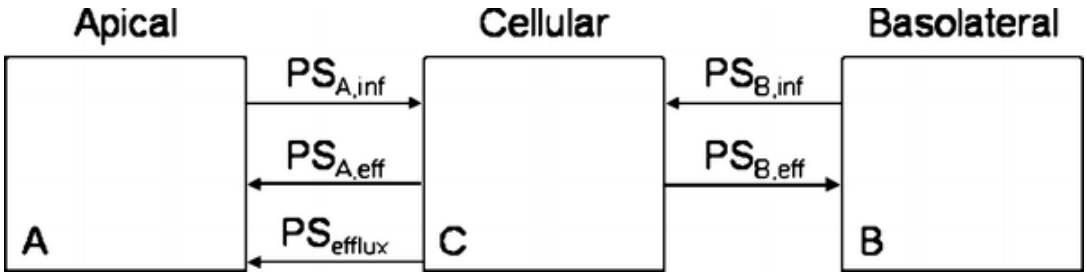

Figure 1-11 Kalvass's three-compartment model consistent with efflux attenuating the initial rate of flux in the A-to-B direction. $PS_{A,inf}$ and $PS_{A,eff}$, represent the passive permeability–surface area product of the apical membrane, whereas, $PS_{B,inf}$ and $PS_{B,eff}$ represent the passive permeability–surface area products of the basolateral membrane. PS_{efflux} represents the permeability–surface area product of efflux activity. It is assumed $PS_{A,inf} = PS_{A,eff} = PS_A$ and $PS_{B,inf} = PS_{B,eff} = PS_B$ (Kalvass and Pollack, 2007).

Kalvass et al (Kalvass and Pollack, 2007) constructed the three compartments kinetic model based on the efflux transporter P-gp in monolayer system (Figure 1-11). Compared with previous P-gp kinetic models (Lentz et al., 2000; Adachi et al., 2001), it is a system with relative complete and derived from first principles. It considers all the interactions in the system, such as passive diffusion on both membranes (apical and basolateral) and efflux on apical side, the role of cellular concentration in determination of K_m, the relationship between various efflux ratios (ER_A: apical efflux ratio ($PS_{0,B\rightarrow A}/PS_{B\rightarrow A}$) or steady-state ($C_{A,0}/C_A$); ER_B: basolateral efflux ratio ($PS_{I,A\rightarrow B}/PS_{A\rightarrow B}$) or steady-state ($C_{B,I}/C_B$); ER_α : asymmetry efflux ratio ($PS_{B\rightarrow A}/PS_{A\rightarrow B}$) or steady-state ($C_A/C_B$) and ER_C: cellular efflux ratio ($PS_{I,A\rightarrow C}/PS_{A\rightarrow C}$) or steady-state ($C_{C,I,}/C_C$))and efflux activity.

Permeability-surface area product was introduced to the mathematic model. It derived the theorectical relationships between PS_{efflux} and experiment parameters, such as Michaelis-Menten constant (K_m), 50% inhibitory concentration (IC_{50}) and the degree of efflux inhibition (Φ_i). This model is helpful in illuminating our interpretation of the apical efflux in the monolayer Transwell model. Overall, it makes the following points:

1). Apical efflux would attenuate the basolateral directional flux and enhances the apical directional flux. However, neither attenuation nor enhancement of flux is proportional to the efflux activity.

2). The flux should not be used to calculate the K_m or IC_{50} directly since the substrate concentration and inhibitor concentration do not relate to flux directly and the flux is not proportional to PS_{efflux}.

3). Measuring the effect of efflux on permeability in the B to A is uninformative because it is minimally sensitive to PS_{efflux} by passive diffusion on basolateral side. Therefore, the maximal ER_A is approaching to 2. ER_A is not a right parameter to estimate the efflux activity.

However, some assumptions upon which this model is based may produce a significant bias of observation significantly: (1) it did not consider the effect of paracellular permeability (PS_{PC}) on the kinetic parameters and assumed the

PS_{PC} can be ignored; (2) it did not consider the effect from unstirred water layer and filter permeability. For P-gp substrates with high lipophilic property, the high passive permeability and unstirred water layer may become limiting step or mask the active flux on the membrane. While insightful, the model of Kalvass and Pollac (Kalvass and Pollack, 2007) has some shortcomings that came to light while analyzing the pantoprazole – ABCG2 flux data and compelled us to explore a more complex mechanistic model.

2.Theoretical Caco-2 model

Caco-2 is widely accepted for assessment of permeability to oral drug absorption. Usually it is used to test whether compounds are substrates of efflux transporter, especially P-gp (Sun and Pang, 2008). As mentioned earlier, Caco-2 also expresses various CYP 450 isoforms and phase II enzymes, so the theoretical model of Caco-2 cell monolayer is a comprehensive system which described both the kinetic parameters from transporter as other monolayer systems (MDCKII or PK-LLC) and also metabolic contribution from cellular enzymes (Sun and Pang, 2008).

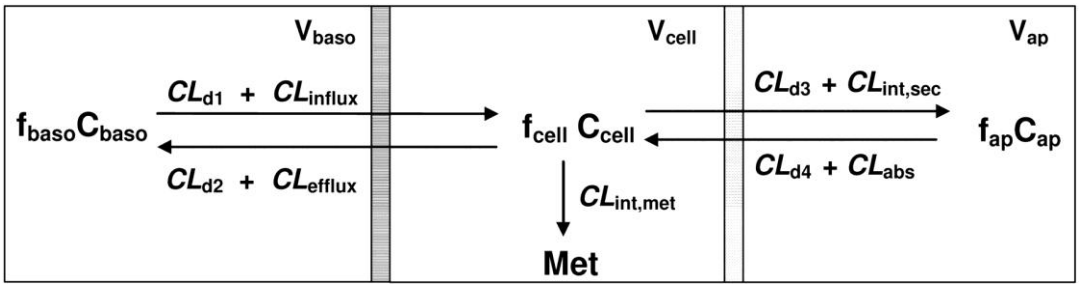

Figure 1-12 Sun's three compartment CaCo-2 model. Schematic presentation of the Caco-2 cell-based system by a catenary model comprising the basolateral (baso), cell, and apical (ap) compartments. *V*, f, and C denote volume, unbound fraction, and the concentration of drugs of each compartment, respectively; M denotes formed metabolite(s). CL_{d1} and CL_{d2},CL_{d4}, and CL_{d3} denote the influx and efflux and passive diffusion clearance on the basolateral and apical membrane, respectively. CL_{influx} and CL_{efflux} represent the transporter-mediated influx and efflux intrinsic clearances on the basolateral membrane; CL_{abs} and $CL_{int,sec}$ denote transporter-mediated intrinsic clearances of absorption and efflux on the apical membrane, respectively; $CL_{int,met}$ is the metabolic intrinsic clearance. Under nonlinear conditions, CL_{influx},CL_{efflux},CL_{abs} and $CL_{int.sec}$, and $CL_{int,met}$ may be replaced by the $V_{max}/(K_m + C_u)$, where C_u is the unbound drug concentration(Sun and Pang, 2008).

In Sun and Pang's three compartment Caco-2 model (Figure 1-12), apparent permeability, P_{app} (is called effective permeability in the paper) and efflux ratio ER_{α} (is called EfR in the paper) were also introduced as in Kalvass's kinetic model. They added two more detailed elements to the model, volume and unbound fraction of each compartment. Also, a parameter, clearance was used to represent the drug "in or out " the cell membranes either by transporters mediated efflux or influx, or cellular enzymes mediated metabolic intrinsic clearance. Compared with other kinetic models, this Caco-2 system considered both sink and nonsink conditions; no assumptions were made for nonsink condition. They established an "improvised equation" which reflects the relationship between flux and passive diffusion and active transport; also V_{max}, K_m and the number of binding site were also introduced to express active transport. The effect of high or low passive diffusion on apparent permeability and efflux ratio was discussed in the paper. However, there was no consideration of paracellular permeability either in this model. In the improvised equation, the donor concentration but not cellular concentration of substrate was used to calculate V_{max} and K_m. The cellular concentration of substrate is significantly different from donor concentration so this calculation can result in deviation from the right value. For the efflux ratio, they conducted same implication equation as Kalvass's model (Eq. 1-2 is equal to Eq.1-).

$$EfR = 1 + \frac{Cl_{int,sec}}{Cl_4}$$

Eq.1-2

$$ER\alpha = 1 + \frac{PS_{AE}}{PS_D}$$

Eq.1-3

In this CaCo-2 model the cellular metabolism was another factor which contributes to the observation of drug efflux or influx on either direction. Briefly, cellular metabolism can affect the apparent permeability of each direction but the effects on both directions (A→B and B→A) are same, so the efflux ratio remains unchanged.

Overall, both Kalvass and Sun's theoretical models were based on the efflux transporters, P-gp, and both provided insights into flux across a monolayer system in Transwell. Both recognized that the Transwell monolayer model is not just a single barrier but two barriers in series; and both utilized a three compartment model to better reflect the interaction between substrate and membrane barriers. The description of apparent permeability, efflux ratio, passive diffusion, active transport, intracellular metabolism and saturation process indicated the complexities of the system. Due to the large number of parameters to be ascribed and that saturation may involve in more than one process (transporter and enzymes), these models are typically limited to theoretical considerations and are difficult to fit actual observations.

K. Chirality and effect on drug disposition

1.Molecular chirality

In 1848, Louis Pasteur separated the first isomers of fasfasic acid into its left-handed (*levo*-tartaric acid) and right-handed (*dextro*-tartaric acid) forms by using a hand lens and a pair of tweezers. This experiment established the theory of chirality in chemical molecules: the compounds contain chiral center and one is related to another as non-superimposable mirror images. Ten years after Pasteur first discovered enantiomers of tartaric acid, he indicated that the mold *Penicillium glaucum* destroyed two enantiomers of ammonium tartrate differently and established that enantioselectivity is exist in biological environment and proteins can recognize the molecular asymmetry (DE, 1993). Since then, stereoselectivity of compounds has been documented to give rise to differences in drug metabolism, pharmacokinetics and toxicity (Prost and Thormann, 2003; Ha and Follath, 2004; Afshar and Thormann, 2006; Sun and Scott, 2009).

By definition, enantiomeric compounds are composed of the same chemical entity and have the same structural formulas, but differ with respect to their three-dimensional structure. Some stereoisomers could have two or more chiral centers which have 4 or more non-superimposable mirror images, such as diastereoisomers. Chirality exists not only in chemical molecules, but also in the

biological world. Many endogenous substances, such as proteins and amino acids have chirality feature. The recognition between two enantiomers of endogenous or exogenous substances and chiral macromolecule, such as an enzyme, receptor or transporter, could result in different outcomes. In some situations stereoselectivity is required for biological function and the higher affinity enantiomer dominates the reaction, or the metabolic or transport pathway.

2. Effect of chirality on drug disposition

It has been estimated that about 50% of therapeutic drugs are currently administered as a racemate, a mixture of equal proportions of two enantiomers (Andersson and Weidolf, 2008). When administered as a racemate, two enantiomers can display a qualitative and quantitative difference in pharmacokinetic processes (absorption, distribution, metabolism and excretion). Molecular chemical properties, such as lipophilicity, total hydrogen bond strength and dipole/polarize-ability are related with passive diffusion. The passive transcellular membrane transport is generally identical between two enantiomers (Sugano et al., 2010). By contrast, the active transport tends be significantly affected by chirality. The interaction of three dimensional structures of active transporter and chiral substrates can cause different transport profiles.

To date, a large number of studies have focused on enantiomer drugs stereoselective interaction involving CYP450 in many drug pharmacokinetic, pharmacodynamic and toxicology areas (Campo et al., 2009; Choong et al., 2010; Schmitz et al., 2010; Tenberken et al., 2010). Steroselective interactions may make some drug utilization problematic (e.g., antiarrhythmics), especially drugs that have a narrow therapeutic index. Drug response is dependent on many processes including administration route, first-pass effect, inhibition of enzymes and polymorphisms, receptor sensitivity, etc. Stereoselectivity contributes to the problem of individual variability to many of these processes (Ha and Follath, 2004) .

In recent years, the studies have shown that steoroselective interactions not only occur with metabolic enzymes (Gunaratna and Kissinger, 1998), but also

with transporters (Bhatia et al., 2008). For example, efflux transporters P-gp and MRPsexhibit enantioselectivity in the absorption and efflux of cetirizinein in CaCo-2 monolayer. The results indicated that enantiomers interaction with P-gp and MRP2 caused potential drug-drug interaction and might significantly changed the cetirizine pharmacokinetics (He et al., 2009). Moreover, several *in vitro* and *in vivo* evidences indicated an enantioselective drug transport at the human blood-brain barrier and implied that significant enantioselective activity of P-gp might be clinically relevant (Choong et al., 2010). As an important efflux transporter, ABCG2 is involved in the disposition of many drugs in body and has a significant impact on drug pharmacokinetic and pharmacodynamic profile. However, to date, there are no reports demonstrating steroselective interaction between substrate drugs and ABCG2.

L. Pantoprazole

Pantoprazole (Protium and Protonix**)** is a proton pump (H^+/K^+-ATPase) inhibitor (PPI) which binds specifically and irreversibly to the proton pump to reduce gastric acid secretion [150]. Pantoprazole is a prodrug which is more stable than other substituted benzimidazole PPI drugs in neutral to moderately acidic environment and is active and tends to accumulates in an acid environment (Sachs, 1997). It is more effective than H_2-antagonists in the treatment of moderate to severe gastro-oesophageal reflux disease (GERD) (Schoenfeld et al., 1999; Scott et al., 2002). The mechanism of action of pantoprazole on proton pump is shown in Figure 1-13. The prodrug form is ampholytic in that three nitrogen atoms can accept or donate protons. Briefly, pantoprazole accumulates under an acidic environment; then is catalysed and converts to active principal, cyclic sulfenamide. This active principle has an ability to react with key cysteines present in the gastric acid pump (Kohl et al., 1992; Huber et al., 1995).

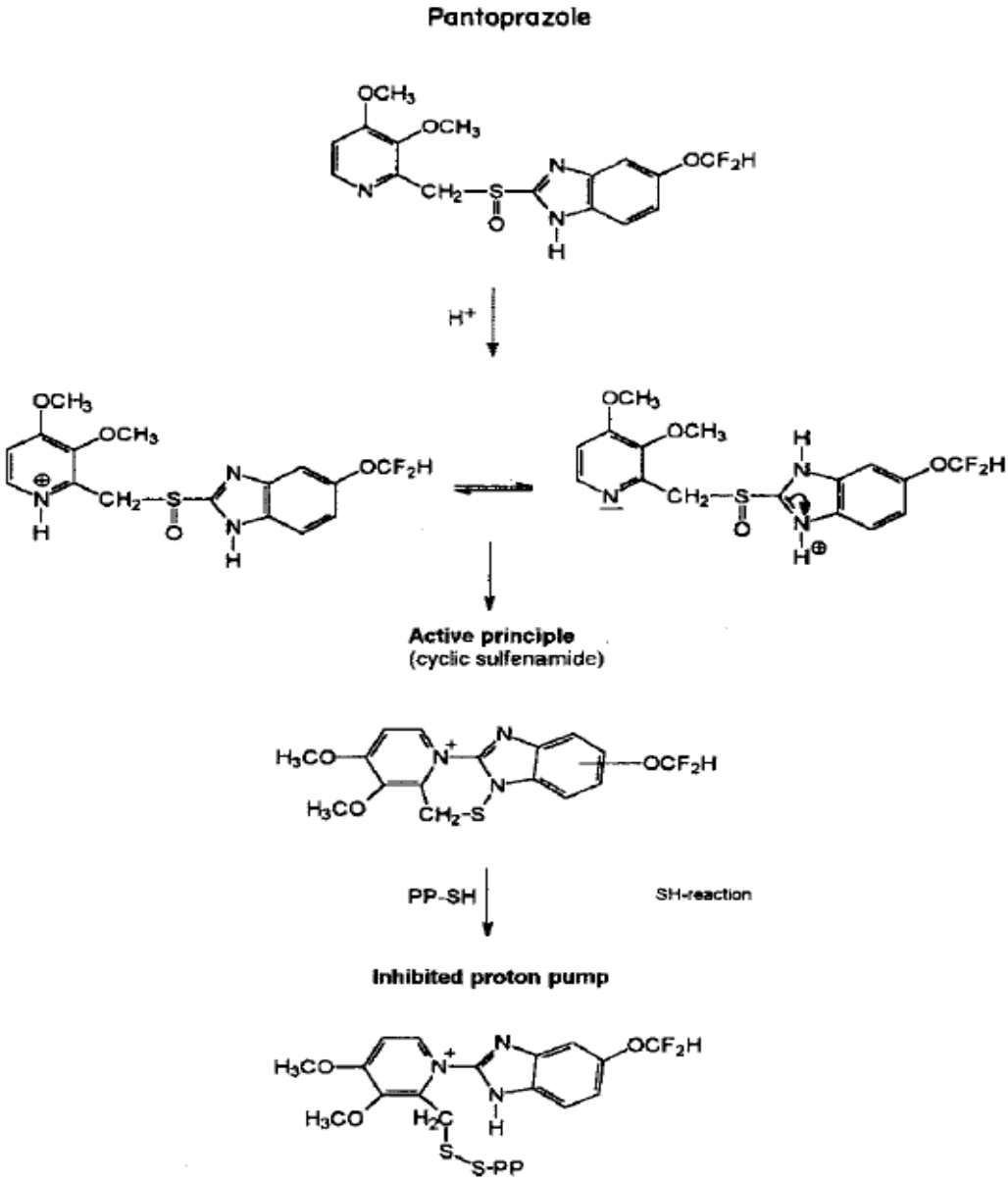

Figure 1-13 Acid activation of pantoprazole and inhibition of the gastric proton pump by binding of the active principle to a cysteine SH group of the enzyme (Huber et al., 1995).

Pantoprazole is completely metabolized to inactive metabolites M1, M2 and M3 by the cytochrome P450 isoforms CYP2C19 (> 80%) and most of rest of them by CYP3A4 (Andersson, 1996; Noubarani et al., 2010) and rest of them by a conjugating enzyme, a cytosolic sulfotransferase (Meyer, 1996). The time course of covalent interaction of pantoprazole with the acid pump is prolonged compared to the time the compound is in plasma (Huber et al., 1995).

Pantoprazole is rapidly eliminated from plasma and almost completely metabolized in the human liver. The initial metabolic step is oxidation via CYP450 system and then it undergoes further metabolism as shown in Figure 1-14. M2, the main metabolite of pantoprazole, is formed by demethylation at the 4-position in the pyridine ring to give a hydroxyl group, then conjugated with sulphate. Both M1 and M3 are sulphate conjugates in an analogous fashion to M2. There are additional oxidation and reduction of the sulphoxide group to sulphone for forming M1 and M3 (Figure 1-15). None of these metabolites are active (Huber et al., 1995).

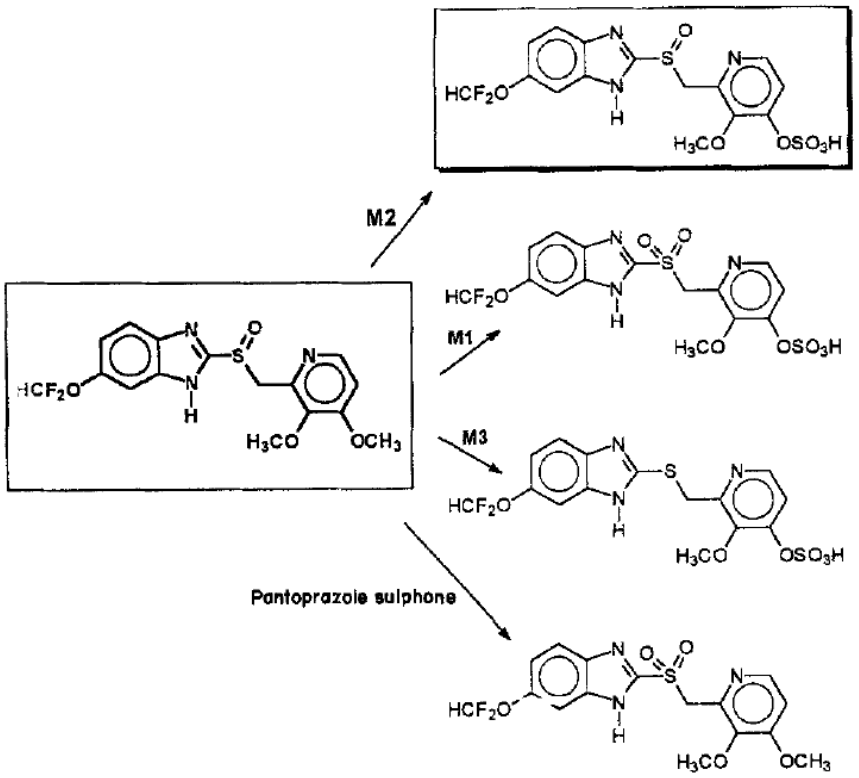

Figure 1-14 Pattern of pantoprazole metabolites in human plasma (M2: main metabolite; pantoprazole sulphone: minor metabolite: relative plasma concentrations: M2>M1>M3> sulphone) (Huber et al., 1995).

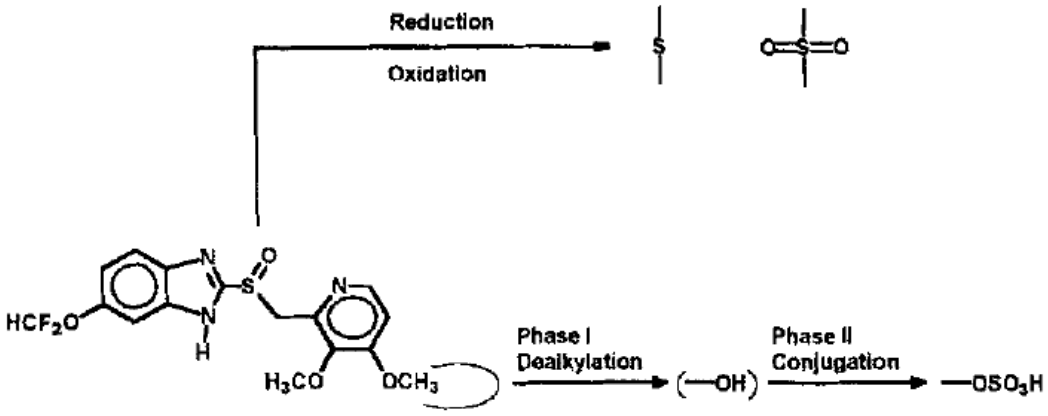

Figure 1-15 Biotransformation of pantoprazole in the human liver (Huber et al., 1995).

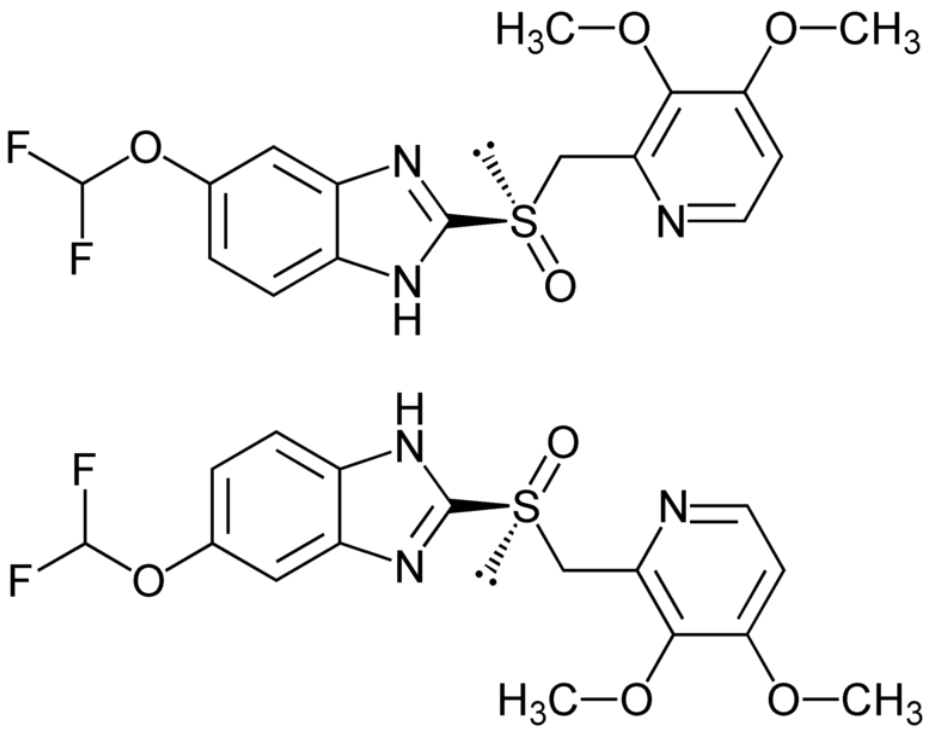

Figure 1-16 The structure of pantoprazole isomers.

Pantoprazole is a typical ABCG2 substrate that has been widely used as a specific inhibitor of ABCG2. PAN is a chiral benzimidazole sulfoxide (Figure 1-16). Currently it is administered as a racemic mixture. In human study, the pharmacokinetics of PAN enantiomers was different in extensive metabolizers

(EMs) and poor metabolizers (PMs). In EMs, the serum concentrations of (-)-PAN were slightly higher than (+)-PAN. In PMs, the concentrations of both PAN isomers were higher than in EMs. The half life of (+)-PAN is 2.67-3.77 times longer than that of (-)-PAN (Tanaka et al., 1997). It demonstrated a stereoselective interaction between pantoprazole enantiomers and metabolic enzymes. In rat pharmacokinetic study, the mean area under the curve value of (-)-PAN was 1.5 times greater than (+)-PAN after oral administration of racemic PAN. It suggested stereoselective pharmacokinetics of pantoprazole isomers are due to the steroselective metabolism that contributed by all the metabolic pathways (Xie et al., 2005). In addition, the chiral inversion was observed after administration of (+)-PAN in rat but not (-)-PAN (Masubuchi et al., 1998).

M. Summary

Breastfeeding is considered to be the best choice of nutrition for most infants, with numerous benefits to infant, mother and society. Drug use during breastfeeding is common. Limited information on drugs disposition in lactation adds uncertainty and concern for both lactating mother and caregiver. Most drugs and their metabolites readily diffuse into milk; however, some drugs are actively transported into milk, leading to accumulation in milk. To fully understand drug accumulation into milk as a critical first step in risk assessment, it is necessary to establish experimental paradigms and mathematical models to be able to put observations into a more integrated form. ABCG2 is an efflux transporter on the apical side of epithelial cell in lactating mammary gland that is responsible for drug active transport into milk. Clinical studies and knockout mice studies have confirmed the role of ABCG2/Abcg2 in nitrofurantoin, cimetidine, Phip(toxin 2-amino-1-methyl-6-phenylimidazo[4,5-b]pyridine) and other xenobiotics accumulation in milk. In this dissertation we propose to investigate the possible role of interaction between substrate and transporter on drug accumulation in milk using both *in vivo* and *in vitro* experimental paradigms focusing on the following aspects:

a) To determine the role of Abcg2 in drug accumulation in rat milk.

b) To establish a “chemical rAbcg2 knockout” for drug active transport into milk.
c) To understand the stereoselective interaction between ABCG2 and substrate by *in vitro* and *in vivo* experiments.
d) To fully understand cell monolayer flux data by using a mechanistic mathematic model.

CHAPTER 2:The plan of study and hypothesis

ABCG2/Abcg2 appears to play a major role in the bioavailability and systemic clearance as well as contribute to the active transport into milk for a number of drugs. The following hypothesis and specific aims are designed to fully understand the interaction of substrates with ABCG2/Abcg2 and its role in drug accumulation into milk.

Overall Hypothesis: ABCG2 substrates accumulate in milk, resulting in high M/S ratios

Hypothesis 1: Drugs which are rAbcg2 substrates will accumulate in rat milk.

To validate the rat as a suitable animal model for assessing the role of Abcg2 in drug transfer into milk, the following three aims will be pursued:

- *Specific Aim 1a*: Quantitate the expression and localization of Abcg2 in lactating mammary gland in rat compared to non-lactating mammary gland or other organs (kidney and liver).
- *Specific Aim 1b:* Characterize the transport of nitrofurantoin in a rAbcg2-MDCKII cell line.
- *Specific Aim 1c:* Validate an *in vivo* model in lactating rat using GF120918, a chemical inhibitor of ABCG2, to block the transfer of nitrofurantoin into milk.

Genetic knockout mice have been used to confirm the role of ABCG2 in drug accumulation in milk. The benefits of using the rat as an animal model for drug development also apply to understanding drug accumulation in milk (e.g., similar drug accumulation in milk between rat and humans, ease of sample collection and the potential compensatory mechanisms associated with genetic knockout mice). To establish a clear role for Abcg2 in drug accumulation in rat milk and to validate the chemical knockout rat Abcg2 model could be valuable tools for drug development.

Hypothesis 2: ABCG2 substrates accumulate in milk with high M/S ratio and interact stereoselectively with ABCG2/Abcg2.

To further challenge the use of the rat as a suitable animal model and to explore the stereoselectivity of ABCG2, the following three aims will be pursued:

- *Specific Aim 2a:* Characterize the M/S ratio of pantoprazole isomers in lactating rats.
- *Specific Aim 2b:* Test the ability of a passive diffusion model to predict the M/S ratios of pantoprazole isomers in rat.
- *Specific Aim 2b:* Utilize the "chemical knockout" Abcg2 rat model to characterize the differential influence of Abcg2 on the distribution of pantoprazole isomers into milk.

ABCG2 is highly expressed in mammary gland of mice, cows and humans during lactation, and is responsible for the active secretion of clinically and toxicologically important substrates. Pantoprazole, a typical ABCG2 substrate has been used as a competitive inhibitor to identify other ABCG2 substrates. However, pantoprazole has a very low M/S at 0.022 in one clinical report (Plante et al., 2004). Pantoprazole is an ABCG2 substrate that exists as a racemic mixture. Although chirality has been described as an important characteristic for a number of enzymes and receptors, there have been few reports of stereoselective interactions with transporters. The objective of this series of experiments is to determine if there is a stereoselective interaction between pantoprazole and ABCG2 and, if present, does the stereoselectivity manifest itself in the M/S ratios of pantoprazole isomers.

Hypothesis 3: Pantoprazole transport properties are consistent across species (rat and human).

To fully assess interspecies differences ABCG2 transport, the following two aims will be pursued:

- *Specific Aim 3a:* Characterize pantoprazole isomers transport in ABCG2/Abcg2-expressing MDCKII cell line.
- *Specific Aim 3b:* Compare transport property parameters of rat Abcg2 and human ABCG2.

To effectively utilize animal model data to predict human exposure, a clear understanding of similarities and differences across species is warranted. We have advocated for the use of the rat as an animal model, hence a comparison of transporter kinetic parameters is required. In addition to kinetic assessments, it is also of interest to compare the extent to which stereoselective differences between enantiomers exist across species.

Hypothesis 4: Drug transport in ABCG2-MDCKII monolayer in Transwells can predict drug accumulation in milk.

To fully develop an overall conceptual framework for pantoprazole interaction with ABCG2, the following two aims will be pursued:

- *Specific Aim 4a*: Develop a mechanistic model and characterize the impact of assumptions of the model with respect to cell monolayer flux data (Transwell).
- *Specific Aim 4b:* Evaluate the parameters from Transwell such as PS_D, PS_{PC}, ER_α, ER_A, K_m, V_{max}, IC_{50} and K_i based on mathematical three compartments model.

In general, there is no broadly accepted in vitro exposure system to mimic in vivo environment. However, several in vitro methods offer the unique possibility to focus the question and derive a more specific inference as to the role of a specific drug characteristic or protein (e.g., transporter) feature. Although the use of cell monolayers of transporter transfected cell lines grown on Transwell is widespread, a clear understanding of parameters from such data remains a challange. The purpose of this section of the thesis is to build a mechanism based model and explore the limits and implications of the model utilizing pantoprazole isomers as model substrates.

CHAPTER 3: GF120918 as a chemical Abcg2 knockout model to study nitrofurantoin transfer into milk

3.1 Summary

Genetic knockout mice studies suggested ABCG2/Abcg2 translocates nitrofurantoin at the mammary – blood barrier resulting in drug accumulation in milk. The purpose of this study was to establish the role of Abcg2 in nitrofurantoin accumulation in rat milk using GF120918 as a "chemical knockout" equivalent. The inhibitory effect of GF120918 was verified in MDCKII cells stably expressing rat Abcg2 with Hoechst 33342 and nitrofurantoin flux in transwells. Nitrofurantoin was infused (0.5 mg/h) in the absence and presence GF120918 (10 mg/kg in DMSO) to Sprague Dawley lactating female rats using a balanced crossover design. Administration of GF120918 increased nitrofurantoin concentration in serum (from 443±51 to 650±120 ng/ml) and decreased concentration in milk (from 18.1±0.9 to 1.9±1.2 μg/ml), resulting in corresponding mean values for M/S of 41.4±19.1 vs. 3.04±2.27 in the absence and presence of GF120918 ($p<0.05$), respectively. There was a decrease in the systemic clearance with GF120918 (2.8±0.5 L/h/kg) compared to vehicle controls (4.1±0.5 L/h/kg; $p<0.05$). Western blot analysis revealed good expression of Abcg2 and no P-gp expression in mammary gland while immunohistochemistry confirmed the apical expression of Abcg2 in lactating mammary gland epithelia. Nitrofurantoin active transport into rat milk can be inhibited by GF120918 resulting in a 10-fold lower M/S. Although GF120918 inhibits both Abcg2 and P-gp, the high expression of Abcg2 and the absence of detectable P-gp expression in lactating mammary gland validates an important role for Abcg2 in nitrofurantoin accumulation in rat milk. GF120918 is particularly useful as a rat "chemical knockout" model to establish ABCG2's role in drug transfer into milk during breastfeeding.

3.2 Introduction

Most xenobiotics are transferred into milk by passive diffusion and the extent of their accumulation in milk (as measured by milk to serum concentration ratio, (M/S)) can be predicted by in vitro measurements of drug binding and ionization in milk and serum as well as lipid partitioning into milk (Fleishaker et al., 1987; Fleishaker and McNamara, 1988a). Such an approach successfully predicted the M/S for a number of drugs (Fleishaker and McNamara, 1988b); however, this approach was unable to estimate the large M/S observed for drugs like nitrofurantoin (Gerk et al., 2001a). In fact, the observed ratios for nitrofurantoin in the human and rat were 20 and 100 times greater (Gerk et al., 2001a; Oo et al., 2001), respectively than could be accounted for by passive diffusion alone, clearly implicating an active transport process.

The transport of nitrofurantoin across a murine mammary epithelial cell culture model has been shown to be saturable and sodium dependent in the basal-to-apical direction (Toddywalla et al., 1997; Gerk et al., 2002). Merino et al described that nitrofurantoin was efficiently transported by murine Bcrp1 and human BCRP by using polarized cell lines (Merino et al., 2005b). Importantly, they also demonstrated that the milk-to-plasma ratio of nitrofurantoin was almost 80 times higher in wild-type compared with Bcrp1 knockout lactating female mice (Merino et al., 2005b). Nitrofurantoin, therefore, was identified as an excellent BCRP/Bcrp1 substrate that is translocated at the blood–mammary barrier resulting in its accumulation in milk.

A growing number of studies have shown compensatory mechanisms in genetic knockout mouse models. The most impressive evidence was from recent literature. In Bcrp (-/-) mice, several transporters, like Abca5, Abcb4, Abcc2, and Abcc4, were significantly up- or down-regulated, the most pronounced differential expression observed with Abcg5 and Abcg8, which showed a 20- to 100-fold up-regulation in Bcrp (-/-) mice (Huls et al., 2008). Therefore, compensatory mechanisms in transport function in genetic knockout mice may complicate the

interpretation of drug metabolism and disposition studies as well as active transport into milk.

In present study, we systematically evaluated the role of Abcg2 (Bcrp) in nitrofurantoin accumulation in rat milk. GF120918 pretreatment was administered to generate a “chemical knockout” equivalent of Abcg2 in lactating rat and nitrofurantoin was employed as the prototypical Abcg2 substrate. The results obtained from these studies provide new insights into the utility of the rat model for ABCG2 substrates in drug active transport into milk and other drug metabolism and disposition studies.

3.3 Materials and Methods

Chemicals

Nitrofurantoin and furazolidone were purchased from Sigma Chemical Co. (St. Louis, MO). N-(4-[2-(1,2,3,4-tetrahydro-6,7-dimethoxy-2-isoquinolinyl)ethyl]-phenyl)-9,10-dihydro-5-methoxy-9-oxo-4-acridine carboxamide (GF120918) was a gift from GlaxoSmithKline (Research Triangle Park, NC). Hoechst-33342 was from Invitrogen (Carlsbad, CA). All organic solvents (HPLC grade) and PEG400 were purchased from Fisher (Pittsburgh, PA) and all other chemicals were obtained from Sigma (St. Louis, MO) unless specified otherwise.

Animals

Five adult female lactating Sprague-Dawley rats (250 to 350 g) with 1 or 3 day old pups were purchased from Harlan Laboratories (Indianapolis, IN). Animals were maintained under a 12 h/12 h light/dark cycle and had access to food and water during the experiments. The rats were acclimatized for at least 1 week before the experiment. All procedures were approved by the University of Kentucky Institutional Animal Care and Use Committee.

Expression and Functional Characterization of Rat Abcg2 in MDCK-II Cells

Total RNA was isolated from a frozen liver of a Sprague Dawley rat using RNAeasy kit (Qiagen, Valencia, CA) and reverse transcribed to cDNA using oligo dT primers and Thermoscript RT PCR kit (Invitrogen, Carlsbad, CA). Rat Abcg2 cDNA was amplified using forward (5'-CCGCTCGAGGCATAGATCCTAAAGATGTCTC-3') and reverse 5'-CTAGTCTAGAGGAGTACTATCAATAGTCCTTTC-3') primers and Phusion DNA polymerase enzyme (NEB, Ipswich, MA). The PCR product was cloned into the pcDNA3.1 vector (Invitrogen) between XhoI and XbaI restriction sites. The Abcg2 sequence in this vector was confirmed (Davis Sequencing, Davis, CA) and it had 100% homology with the published rat Abcg2 sequence (Gene Bank accession number AB105817). MDCKII cells were maintained in MEM with Earle's salts (Mediatech, Manassas, VA) with 5% FBS (GIBCO/Invitrogen) and 1X Penicillin Streptomycin (Invitrogen) at 37ºC in 5% CO_2. Cells were transfected with pcDNA3.1 or pcDNA3.1-rAbcg2 using Fugene 6 transfection reagent (Roche Diagnostics, Indianapolis, IN) according to the manufacturer's instructions. After 48 hours, cells were selected with 800 µg/ml G418 (Invitrogen) for 10 days.

Abcg2 expression was confirmed by Western blot analysis with polyclonal anti-ABCG2 antibody from Kamiya Biomedical Company (Seattle, WA). Rat Abcg2 function was assessed using the Hoechst-33342 (10 µM) accumulation assay (Leggas et al., 2006). Single clones were isolated by fluorescence-activated cells sorting (FACS) (MoFlo^{TM}, DakoCytomation, Fort Collins, CO) on the basis of reduced accumulation of the Hoechst 33342 dye. The clone with the highest functional activity was chosen for in-vitro studies.

Inhibition of rAbcg2 by GF120918

To assess the utility of GF120918 as a chemical inhibitor of rat Abcg2, first, we incubated MDCKII-rAbcg2 cells with Hoechst 33342 in the presence and absence of 1 µM GF120918. Briefly, cells were incubated with dye-containing medium at 37°C for 45 minutes. GF120918 was added at the indicated

concentrations 10 minutes before the dye incubation. All flow cytometry assays used 10 µM Hoechst 33342 (Leggas et al., 2006). Secondly, the effect of GF120918 on nitrofurantoin directional transport was evaluated using MDCKII cells expressing rat Abcg2 or empty vector (pcDNA3.1). Cells were seeded on microporous membrane filters (3.0-µm pore size, 24-mm diameter; Transwell 3414; Corning Glassworks, Corning, NY) at a density of 1.0×10^6 cells per well. Cells were grown for 4 days to achieve TEER (transepithelial electrical resistance) >200 $\Omega\cdot cm^2$ and medium was replaced every other day. Prior to the experiment, the medium at both the apical and basolateral side of the monolayer was replaced with 2 ml of OpitiMEM medium (Invitrogen) without serum, and either 1 µM GF120918 or vehicle-only (0.1% DMSO) with 10 µM nitrofurantoin containing 0.2 µCi/ml [^{3}H]-Mannitol. Cells were incubated at 37^{o}C in 5% CO_2. To ensure the tightness of each monolayer, 50 µl aliquots were collected to assess the paracellular flux of [^{3}H]-Mannitol into the opposite compartment. We required that layers restricted mannitol transport to <1% of the total radioactivity per hour. For nitrofurantoin transport, 140 µl aliquots were taken at 0.5, 1, 2 and 3 hours. Samples were stored at -80 ^{o}C until the time of analysis by HPLC assay.

In-vivo Studies

The jugular and femoral veins of Sprague-Dawley lactating female rats were cannulated under ketamine/xylazine anesthesia on day 10 to 12 post partum. After a day of recovery, each dam (n = 5) was randomized to receive an intravenous infusion of nitrofurantoin in PEG400 (0.5 mg/0.25ml/h) for 5 hours either with pretreatment of the inhibitor (GF120918, 10 mg/kg in DMSO) or with equivalent volume (about 0.15 ml DMSO) of vehicle administered intravenously over 10 min and crossed over on the second day to complete both phases (Gerk et al., 2001b; Edwards et al., 2005). One ml normal saline was given hourly to prevent dehydration during infusion. The dams were separated from the pups prior to the infusion. Blood samples were drawn hourly for the last 4 h of the infusion. The blood samples were protected from light, allowed to clot, centrifuged to harvest serum, and frozen at -80°C until analysis. Milk samples were obtained by manual manipulation under light anesthesia (ketamine) at the

end of the infusion, protected from light, and also frozen at −80°C until analysis. Mammary gland and kidney samples were harvested from a separate group of lactating rats on day 16 to18 post partum, frozen in liquid nitrogen, and stored at -80°C until analysis.

Nitrofurantoin HPLC Analysis

To each aliquot (70 µl) of serum, 15 µl of a 5 µg/ml furazolidone HCl was added as an internal standard and was precipitated with 85 µl of cold methanol, vortexed for 5 min, and then centrifuged at 16,000g for 10 min at 4°C. Fifty microliters of the supernatant plus 50 µl mobile phase was mixed for 10 seconds and injected onto the HPLC. To each aliquot of milk, 25 µl of a 25 µg/ml furazolidone HCl was added as an internal standard to 50 µl milk sample and was precipitated with 200 µl of cold methanol, vortexed for 5 min, and then centrifuged at 16,000g for 10 min at 4°C. Then, 50 µl of the supernatant was mixed with 50 µl mobile phase and injected onto the HPLC. The HPLC system consisted of a Lichrosorb 5 RP18 125 × 4.0-mm column (Phenomenex, Torrance, CA) and eluted with 20% acetonitrile: 80% 25 mM potassium phosphate buffer (pH 3.0) at 1.0 ml/min. UV absorbance was measured at 366 nm. Peak height ratios (nitrofurantoin/furazolidone) were used for comparison with the standard curve. The standard curve range for nitrofurantoin in serum was 62.5 to 4000 ng/ml. The milk samples were diluted if the concentration was greater than the linear range for the standard curve (0.725 to 29 µg/ml). Aliquots of nitrofurantoin in OptiMEM medium were directly injected onto the HPLC. The standard curve range was 7.8 to 2000 ng/ml. All standard curves demonstrated an intra- and inter-day variability of less than 10% and r^2 >0.99.

Western Blot Analysis for P-gp and Abcg2

Crude membrane fractions were prepared from lactating mammary gland and kidney. Briefly, the tissue samples were homogenized in Dounce Buffer (Tris buffer pH 7.6 at 4ºC, 0.5 mM magnesium chloride) with protease inhibitors (Complete Mini EDTA-free tablets, Roche Diagnostics, Indiapolis, IN) and the

tonicity restored to 150 mM with sodium chloride. Following centrifugation at 1200 g for 5 min at 4ºC, the supernatant was removed and EDTA was added to a final concentration of 5 mM. The sample was then centrifuged further at 100,000 g for 1 hour at 4ºC to pellet the crude membrane fractions. Pellets were resuspended in resuspension buffer (0.2 M mannitol, 0.07 M sucrose, 50 µM Tris HCl, 1 µM EDTA). Rat Abcg2- and pcDNA3.1 (empty vector)-MDCKII cell pellets were resuspended in RIPA buffer (50 mM Tris pH 8.0, 150 mM NaCl, 1% NP40, 0.5% deoxycholate, 0.1% SDS, protease inhibitor cocktail), rotated for 30 minutes at 4^{o}C, then centrifuged at 13000 rpm for 20 minutes at 4ºC. Supernatants were collected for immunoblot. Protein concentrations were measured using the BCA Protein Assay kit (Pierce, Rockford, IL). PNGase F (New England Biolabs, Ipswich, MA) was used for deglycosylation of rat Abcg2 following manufacturer instructions. Briefly, 60 µg (lactating mammary gland), 100 µg (kidney) and 7 µg (pcDNA3.1 expressed MDCKII cell and Abcg2 expressed MDCKII cell) of membrane fractions were incubated with 10X denaturing buffer supplied and PNGase F (4 µl) at 37 °C for 2.5 h. Then the samples were mixed with 2X SDS-loading buffer and reducing buffer at 37°C for 30 minutes as the non-PNGase treatment group. Western blotting was performed as described previously (Edwards, 2005). P-gp expression was determined using the C219 (mouse anti-human P-gp; 1:100) monoclonal antibody which was obtained from Signet Laboratories (Dedham, MA) and Abcg2 was determined using the PC-138 (1:1000) antibody which was obtained from Kamiya Biomedical (Seattle, WA). Antibody binding was detected using a horseradish peroxide linked IgG (H+L) (goat anti-rabbit) and IgG (H+L) (rabbit anti-mouse) antibodies (1:20000) obtained from Pierce, Inc. (Rockford, IL). The bands were visualized using a SuperSignal Pico Chemiluminescent substrate detection kit (Pierce, Rockford, IL).

Immunohistochemistry for Abcg2 localization in lactating mammary gland

Six-micrometer sections of paraffin blocks were cut using microtomy. After deparaffinization and rehydration, endogenous peroxidase was blocked with

H_2O_2 in methanol for 20 min. The sections were blocked using an avidin biotin blocking kit (Vector Laboratories, Burlingame, CA), and PC-138 (1:1000) was applied for kidney and lactating mammary gland. For non-specific staining control, rabbit IgG (Invitrogen) was applied to the slide instead of PC-138 (1:1000). The sections were incubated overnight at 4^{o}C with amplifier. Subsequently, the slides were washed in PBS-T and then incubated with biotinylated anti-rabbit antibody (1:600 dilutions) and HRP-conjugated avidin-biotin-complex (Vector Laboratories, Burlingame, CA). The antibody binding sites were visualized by incubation with DAB-H_2O_2 solution to develop a brown color and counterstained with hematoxylin, dehydrated, and coverslipped.

Pharmacokinetic calculations and statistical analysis

Systemic clearance was calculated using the following formula.

$$Cls = \frac{Infusion\ Rate}{C_s}$$

Eq.3-1

Where C_s is the average concentration of nitrofurantoin in serum from 3 to 5 hours.

M/S was calculated by:

$$\frac{M}{S} = \frac{C_m}{C_s}$$

Eq. 3-2

Where C_m is concentration of nitrofurantoin in milk at 5 hours.

All data are expressed as mean ± standard deviation (SD). Analyses were performed to estimate intergroup differences using the One-way ANOVA. A p value of <0.05 was considered statistically significant.

3.4 Results

Functional characterization of rat Abcg2 expressed in MDCKII cells and GF120918 as an inhibitor of rat Abcg2

The full-length rat Abcg2 complementary DNA was expressed in MDCK-II cells. The functional activity of Abcg2 was characterized and high activity clones were selected using FACS based on the ability to limit the accumulation of the prototypical human and mouse ABCG2 substrate, Hoechst 33342. Rat Abcg2 clone was selected and validated as shown (**Figure 3-1 A**). The phenotype of this clone could be reversed with GF120918 (**Figure 3-1 B**). Furthermore, the effect of GF120918 on the transport of nitrofurantoin by rat Abcg2 was investigated in MDCKII-rat Abcg2 and MDCKII-empty cells. These MDCKII-rat Abcg2 cells demonstrated 7.5-fold increase in apically directed transport and a 55% decrease in basolateral transport of nitrofurantoin (**Figure 3-1C**), which was largely reversed by GF120918 treatment (**Figure 3-1D**). These results show the creation of a MDCKII–rat Abcg2 expressing cell line was successful and that GF120918 is an inhibitor of rat Abcg2.

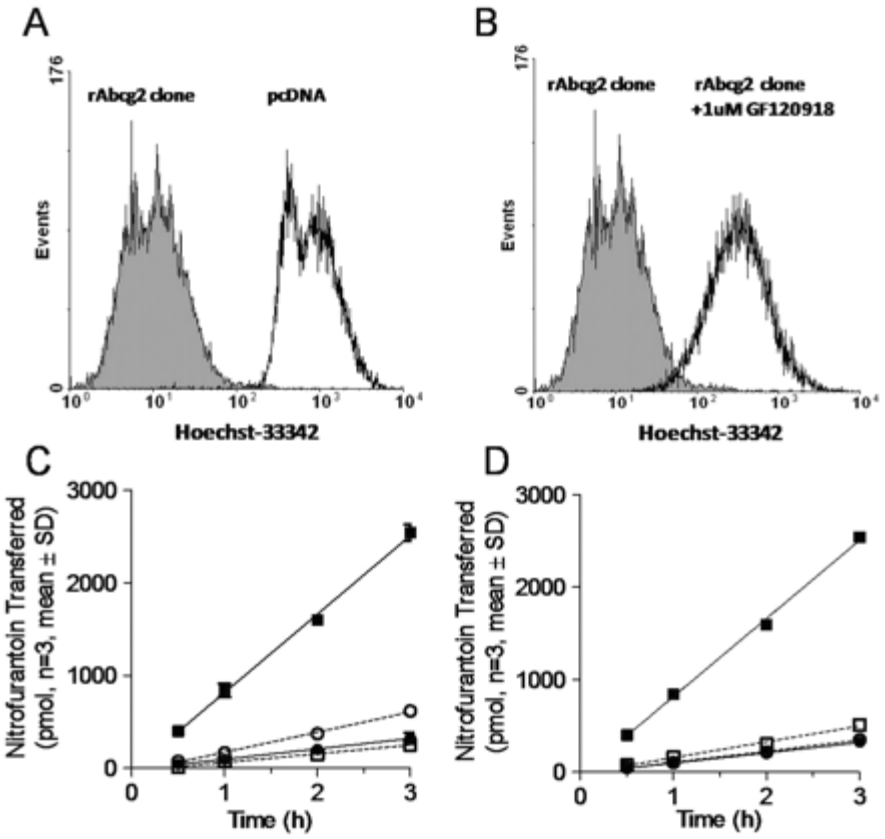

Figure 3-1 Functional characterization of MDCKII-rat Abcg2 expressed cells. The Hoechst 33342 accumulation of MDCKII cells with either empty vector (black unfilled) or rAcbg2 clone cells (shaded) (**Panel A**). Cells were analyzed by flow cytometry following incubation of the ABCG2 substrate Hoescht 33342 in presence (black unfilled) and absence (shaded) of 1 μM of the ABCG2 inhibitor, GF120918 (**Panel B**). The amount of nitrofurantoin appearing in the receiver compartment across MDCKII-empty vector and MDCKII-rAbcg2 monolayers grown on Transwells (**Panels C and D**). Panel C depicts the flux of nitrofurantoin from the basolateral to apical (●■); apical to basolateral (○□) in MDCKII-empty (●○) and MDCKII –Abcg2 (□■); Panel D depicts the transport of nitrofurantoin from the basolateral to apical in MDCKII-empty (●○) and MDCKII –Abcg2 (□■) in MDCKII-rAbcg2 absence (●■) or presence (○□) of 1 □M GF120918.

Expression of rAbcg2 and P-gp in lactating mammary gland and rAbcg2 expressed MDCKII cells

Abcg2 and P-gp expression in rat lactating mammary gland were assayed by Western blot. In contrast to the kidney (positive control), P-gp was not detected in lactating mammary gland (**Figure 3-2A**). Abcg2 expression was detected in lactating mammary gland, kidney and Abcg2 expressing MDCKII cell line (**Figure**

3-2B and 3-2C); however, the native Abcg2 bands were different sizes in the mammary gland (~72kd), rat Abcg2 expressing in MDCKII cell line (~80kd) and the kidney (~80kd). Following deglycosylation (**Figure 3-2B and 3-2C**), all of the native bands were reduced to approximately 60 kDa. Immunohistochemistry showed the localization of Abcg2 in rat lactating mammary gland (**Figure 3-3**). Abcg2 was strongly expressed on the apical side of epithelial cells in lactating mammary gland. As a positive control, Abcg2 staining was mainly observed in the renal proximal tubules in kidney. Abcg2 staining was not found in the nonspecific staining control.

Infusion Studies

Results from the nitrofurantoin infusion study in lactating rats are shown in **Figure 4**. The concentration of nitrofurantoin in serum reached steady-state at 2 hours following the initiation of the infusion and was maintained through 5 hours. Linear regression revealed that the slope (plasma concentration versus time) was not significantly ($p<0.05$) different from zero over this timeframe, however there was a trend for the GF120918 treatment to increase nitrofurantoin concentration with time. The presence of GF120918 resulted in a higher concentration of nitrofurantoin in serum (**Figure 3-4A**). The systemic clearance of nitrofurantoin in lactating rats was 4.12 ± 0.5 L/h/kg and was significantly decreased to 2.78 ± 0.5 L/h/kg ($p<0.05$, **Figure 3-4B**) by coadministration with GF120918. Higher nitrofurantoin serum concentrations and lower milk concentrations (**Figure 3-4A**) in GF120918 treated group resulted in a substantial reduction (93%) in the M/S of nitrofurantoin from 41.5 ± 19.1 to 3.04 ± 2.27 (**Figure 3-4C**).

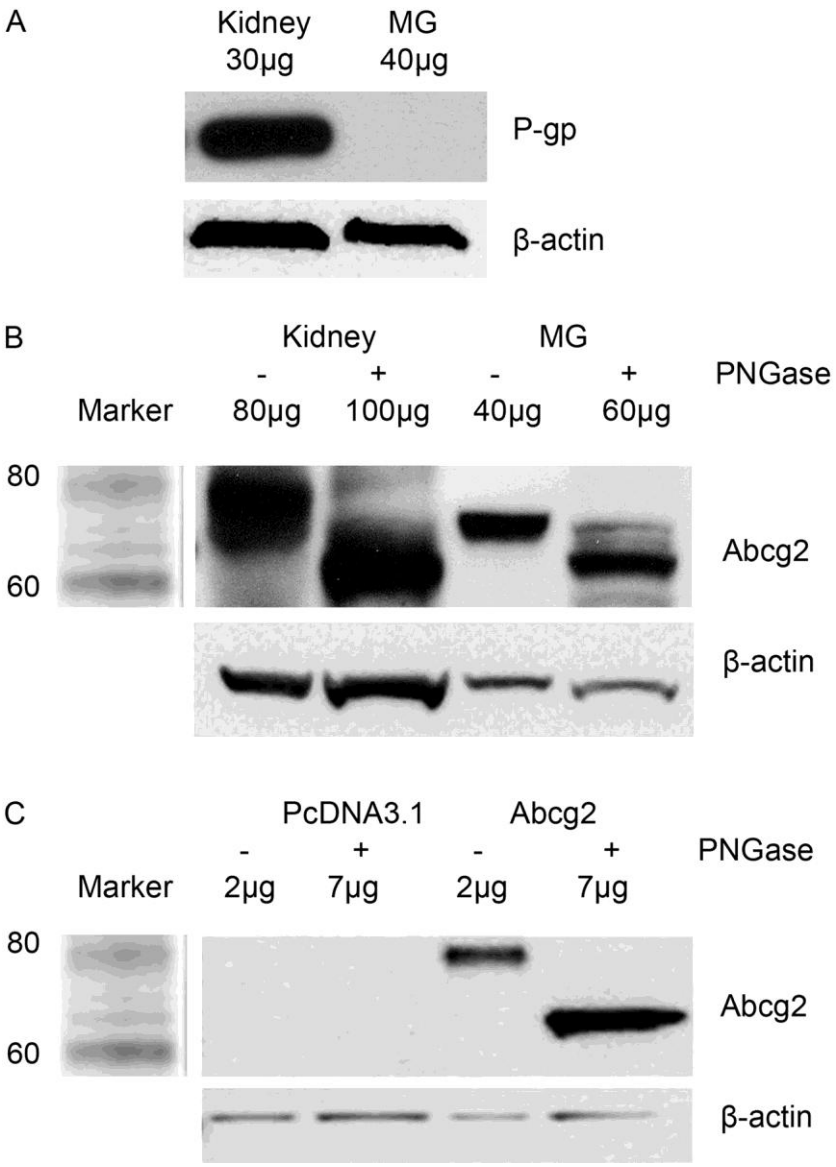

Figure 3-2 Western blot analysis of P-gp and Abcg2 expression. Crude membrane fractions were prepared for all the samples. P-gp expression in rat kidney and lactating mammary gland (**Panel A**). The expression of native and deglycosylated rAbcg2 in lactating mammary gland, kidney (**Panel B**), vector (pcDNA3.1), and rAbcg2 expressed MDCKII cell line (**Panel C**).

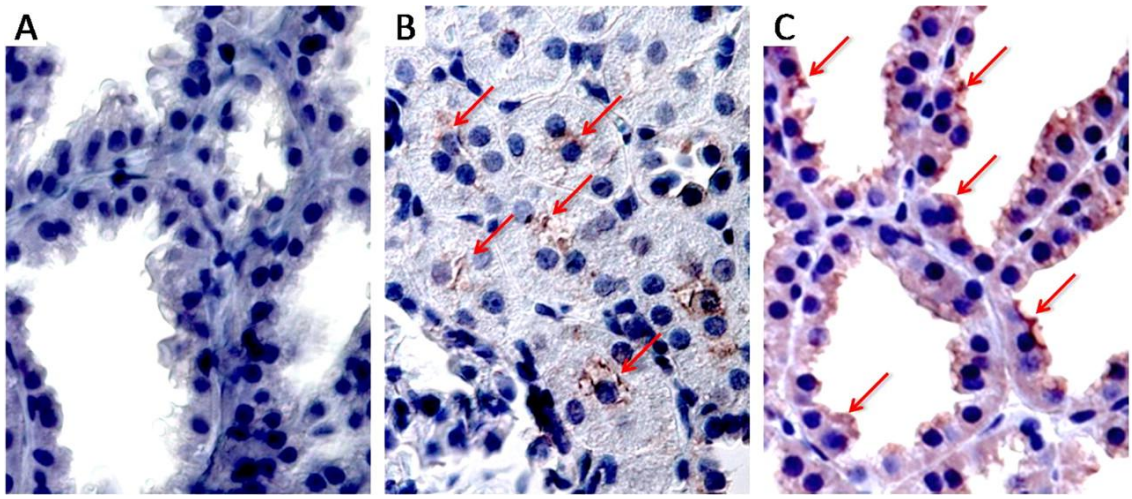

Figure 3-3 Immunohistochemical detection of Abcg2 (magnification, 63x) in rat lactating mammary gland (nonspecific staining control) (**Panel A**), rat kidney (positive control) (**Panel B**) and rat lactating mammary gland (**Panel C**).

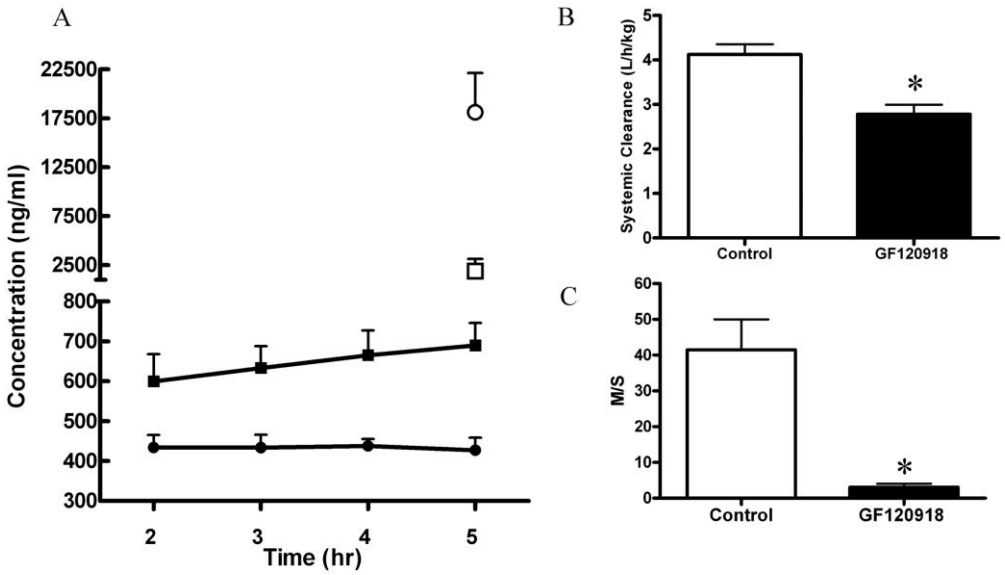

Figure 3-4 Concentration versus time profile (**Panel A**) for serum (●■) and milk (○□) following nitrofurantoin infusion (0.5 mg/hr) in GF120918 (10 mg/kg) treated (□■) or control lactating rats (●○). Nitrofurantoin systemic clearance (**Panel B**) and M/S (**Panel C**). *Asterisks* represent data points that are significantly different from control. * P<0.05. Data is presented as mean ± SD).

3.5 Discussion

In the present study, we have utilized GF120918 as an inhibitor of Abcg2 in order to assess its role in drug transfer into rat milk. GF120918 was originally developed as a second-generation P-gp inhibitor (Tan et al., 2000). It belongs to the family of acridone carboxamide derivatives (Warmann et al., 2002; Boumendjel et al., 2007) and has an IC_{50} value of ~30 to 300 nM on the cellular accumulation of phosphine technetium complexes by human P-gp in Sf9 cells (Luker et al., 1997). GF120918 is also a potent ABCG2 inhibitor with IC_{50} values of ~300 nM on efflux or accumulation in cell lines transfected with human ABCG2 (Ahmed-Belkacem et al., 2005; Pan et al., 2007). Based on our results, GF120918 (1 μM) appeared to effectively inhibit the efflux of Hoechst 33342 and nitrofurantoin from rAbcg2 expressing MDCKII cell line, thus confirming that GF120918 is an effective in vitro inhibitor of rat Abcg2.

Following a 10 mg/kg dose, GF120918 significantly increased the serum concentrations of nitrofurantoin by decreasing its systemic clearance. Previous investigators have noted the systemic clearance of nitrofurantoin to be mediated, in part, by Abcg2-dependent processes (Merino et al., 2005b; Wang and Morris, 2007). Following oral and intravenous administration of nitrofurantoin, the area under the concentration time curve in Bcrp1 knockout mice was 4-fold and 2-fold higher, respectively, than in wild-type mice (Merino et al., 2005b), due to reduced first pass and hepatobiliary excretion of nitrofurantoin. Zhang et al have also shown that Bcrp1 limited the fetal distribution of nitrofurantoin and had a minor effect on the systemic clearance of the drug in the pregnant mouse (Zhang et al., 2007).

In previous work in our lab, the P-gp substrate, nelfinavir, was dosed to lactating rats with GF120918 (Edwards et al., 2005). GF120918 had no effect on M/P (the ratio of drug concentration in milk to in plasma) but did change brain to plasma ratio. Nelfinavir, like other human immunodeficiency virus protease inhibitors are well established substrates of P-gp (Kim et al., 1998; Lee et al., 1998; Washington et al., 1998). These protease inhibitors have been shown to

be inhibitors, but not substrates of Abcg2 (Gupta et al., 2004). This evidence suggests that P-gp does not play a role in drug transfer into rat milk. By contrast, nitrofurantoin has not been shown to be a substrate of other major efflux transporters, such as P-gp, Mrp1 and Mrp2 (Merino et al., 2005b; Wang and Morris, 2007). Hence, the affect GF120918 on the clearance and M/S of nitrofurantoin is not mediated by P-gp, but due largely to Abcg2 inhibition. It should be noted, however, a study of membrane transporters in MDCKII-hMDR1 using GF120918 to inhibit digoxin and loperamide efflux implicated a possible basolateral transporter(s) which could be inhibited by GF120918 (Acharya et al., 2008). The identity or function of basolateral transporter(s) on lactating mammary epithelial cells and their potential impact on M/S has not been established.

Consistent with mammary gland expression in other species (Merino et al., 2005b), our western blotting results show Abcg2 is highly expressed in the lactating rat. P-gp appears to be transcriptionally down-regulated during lactation (Alcorn et al., 2002) and protein expression was not detectable in the lactating rat mammary gland (Figure 2A). All of the native Abcg2 bands were reduced to approximately 60 kDa following deglycosylation. This observation is consistent with the result previous work suggesting that ABCG2 contains N-linked oligosaccharides, probably at both of the putative glycosylation sites (Litman et al., 2002). The native Abcg2 bands in kidney and rAbcg2 - MDCKII cell line had a larger size (approximately 80 kd) than the mammary gland (approximately 70kd), suggesting rat Abcg2 may have tissue or cell specific patterns of glycosylation.

Consistent with the Western blot analysis, immunohistochemistry clearly indicated that Abcg2 is strongly expressed on the apical side of epithelial cells in lactating mammary gland. Apical expression also confirms the role of Abcg2 in actively transporting nitrofurantoin out of the epithelial cells and into rat milk.

The rat is a frequently used animal model in drug development and may be a better animal model under certain experimental paradigms (e.g., multiple

samples, crossover study design). Furthermore, drugs identified as accumulating in rat milk by active transport are consistent with human literature (McNamara et al., 1991; McNamara et al., 1992a). Hence, evidence gathered to date suggest that the rat is a good model for identifying which drugs might undergo active transport into human milk.

As noted in the introduction, genetic knockout models are useful tools to demonstrate transporter function with the assumption that the only difference from wild-type is the abolishment of expression of the intended protein. However, knockout models have been found to undergo additional changes which might further complicate interpretation. For example, brain microvessels from Mdr1a deficient mice express 3 times more Abcg2 RNA than microvessels of wild-type mice (Cisternino et al., 2004). Although the accumulation of Abcg2 substrates, mitoxantrone and prazosin was significantly increased in the presence of GF120918 in both wild-type and P-gp deficient mice there was significant difference between them (Cisternino et al., 2004). Whether or not this increased expression and activity of Abcg2 is a compensatory mechanism for the lack of Mdr1a at the mouse blood-brain barrier remains to be elucidated. There are other compensatory functions which also may be present in genetic knockout animals. In Mrp2 (-/-) mice, Mrp4 mRNA and protein expression in liver and kidney were increased approximately 6- and 2-fold, respectively (Chu et al., 2006). In Mrp2-deficient rats [TR (-)], Mrp3 was significantly up-regulated in the liver (approximately 6-fold) and kidney (approximately 3.5-fold) compared with wild-type controls. Likewise, the expression of the Ugt1 enzyme was increased in the liver and kidney of TR (-) rats by approximately 3.5- and 5.5-fold (Johnson et al., 2006). Therefore, alterations in drug disposition using knockout animals must be interpreted cautiously because of the possibility of compensatory changes in other transport proteins.

The inhibition of Abcg2-associated nitrofurantoin accumulation by GF120918 in the lactating rat (“chemical knockout”) provides support for the use of this alternative to the genetic knockout model for establishing the role of Abcg2 in drug active transport into milk. GF120918 has been tested in phase I clinical

trials and was confirmed to have little toxicity (Planting et al., 2005; Kuppens et al., 2007). Various studies have shown that GF120918 can be tolerated in humans and animals at concentrations sufficient to inhibit ABCG2. Hence, GF120918 is suitable for in vivo animal and perhaps even clinical studies (Mao and Unadkat, 2005).

In summary, Abcg2, but not P-gp is expressed in lactating mammary epithelia and appears to be responsible for nitrofurantoin active transport into rat milk. The rat appears to be a good animal model for identifying those drugs that would accumulate in human milk. GF120918 appears to be an effective in vivo inhibitor ("chemical knockout") tool for confirming the role of Abcg2 in milk transfer. These data are especially valuable for the design of studies of ABCG2 substrates during breastfeeding using the rat as animal model.

CHAPTER 4: Stereoselective drug accumulation in milk: ABCG2 interaction with pantoprazole

4.1 Summary

Drug active transport into milk is a major concern in breastfeeding. Recent evidence has confirmed Abcg2, a xenobiotic transporter, plays a critical role in drug transfer into rat milk which is consistent with human study. Although it is estimated that about half of all therapeutic agents are chiral, there have been few reports of stereoselective interactions with transporters. The purpose of this study is to investigate the interaction of pantoprazole isomers with Abcg2 in drug accumulation in milk by *in vitro* and *in vivo* experiments. For *in vitro* experiments, Abcg2/vector-MDCKII cells were seeded in Transwell. Pantoprazole isomers (30 μM) were loaded on apical/basolateral side and pantoprazole flux was analyzed by HPLC. Jugular and femoral veins of Sprague-Dawley lactating rats were cannulated and each dam (n = 5) received an i.v. infusion of pantoprazole mixture in saline for 8h with/out Abcg2 inhibitor (GF120918) and crossed over on the second day. Samples were analyzed by LC-MS with chiral column. The results indicated pantoprazole isomers were transported in an identical fashion in empty-MDCKII cell lines, whereas a significant difference in flux was observed in Abcg2-MDCKII cell line. In the in vivo experiments, the steady state was achieved after 2 hour infusion and the administration of GF120918 apparently increased both pantoprazole isomer concentrations in serum, but no statistical difference was observed. (+)-PAN (0.57±0.1) had a higher systemic clearance than (-)-PAN (0.44±0.12) ($p<0.01$). Milk to serum ratio of (-)-PAN (1.36±0.20) was almost 3 times as great as that of (+)-PAN (0.54±0.09). Administration of the Abcg2 inhibitor (GF120918) decreased M/S of (-)-PAN to 0.50±0.08 ($p<0.001$) and (+)-PAN to 0.38 ±0.07 ($p>0.05$). Abcg2 interacts stereoselectively with pantoprazole isomers in both *in vitro* and *in vivo* studies. Pantoprazole stereoselectivity for Abcg2 appears to be responsible for a difference in the accumulation of substrate isomers in milk and may have consequences for other aspects of stereoselective drug disposition.

4.2 Introduction

Chirality is a central feature of biology and its existence is essential for many life processes. Specific three dimensional structure-activity relationships in the environment of living systems are required for effect (e.g., enzymes, receptors, transporters, and DNA) (Smith, 2009), which implies that enantiomers of drugs or substrates may elicit a different response or outcome. It is estimated that about half of marketed therapeutic agents are chiral with most available as 50/50 mixtures of their enantiomeric forms (Andersson and Weidolf, 2008). The final decision to market a drug as an enantiomerically pure form or a racemic mixture is made following consideration of all the medical, financial and social risk benefits (Nunez et al., 2009).

Stereoselective metabolism, the transport of chiral drugs as well as genetic polymorphisms of CYP450 and receptors complicate drug dosing and influence pharmacokinetics, pharmacodynamics, and toxicity (Katsuki et al., 2001; Tateishi et al., 2008; Miura and Uno, 2009). It is especially critical for those drugs that have a narrow therapeutic index (e.g., warfarin) (Takahashi, 2008). Additionally, there is a report that two enantiomers of chiral drug can have reverse stereoselective regulation on transporter expression (Shen et al., 2007). As a result of these revelations of the significance of chirality on pharmacodynamic and pharmacokinetic profiles, there has been increasing concern over the use of racemates, and other steroisomeric mixtures, as drugs.

As a widely distributed efflux transporter in such tissues as kidney, liver, blood-brain barrier, placenta, stem cells and mammary gland, ABCG2 (ATP binding cassette transporter isoform G2) exhibits a broad substrate specificity transporting hydrophobic, anionic, and cationic drugs (Mao and Unadkat, 2005). It can significantly influence the absorption, distribution, elimination and toxicity of substrate drugs (Oostendorp et al., 2009).

The role of ABCG2 in xenobiotic distribution into milk has been identified (Jonker et al., 2005; Merino et al., 2006b). A working hypothesis of the present work provides that all ABCG2 substrates accumulate in milk resulting in relatively

high M/S ratios (the ratio of drug concentration in milk to serum); higher than that predicted by simple diffusion. However, a clinical case report with pantoprazole (PAN) would appear to challenge this hypothesis (Plante et al., 2004). PAN has been described as a typical ABCG2 substrate (Breedveld et al., 2004), and yet, the authors found an M/S value of 0.022 for racemic PAN in one volunteer (Plante et al., 2004). It is unclear whether the low M/S ratio for PAN is a result a more limited ability of PAN to act as a substrate for ABCG2, PAN's rapid diffusion across membranes, PAN's extensive serum protein binding, or some other explanation.

PAN undergoes enantioselective hepatic metabolism in both humans and rats (Tanaka et al., 2001; Xie et al., 2005). Poor metabolizers of S-mephenytoin (a CYP2C19 substrate) were less able to metabolize (+) PAN than (–) PAN (Tanaka et al., 2001). There are no reports of PAN isomers interacting with transporters (e.g., ABCG2). Moreover, there do not appear to be any reports on stereoselective drug accumulation in milk.

A chemical knock-out Abcg2 rat model, in which the function of Abcg2 is inhibited by GF120918, has been established (Wang et al., 2008). The major goals of the present work was to take advantage of this unique model to investigate the stereoselective interaction in pantoprazole enantiomers active transport in milk and to further examine the ABCG2 substrate milk accumulation hypothesis by comparing that to predicted M/S from passive diffusion model.

4.3 Materials and methods:

Chemicals Protonix I.V (Pantoprazole sodium, 50:50 stereo mixtures) was obtained from Altana (Konstanz, Germany) and zonisamide sodium was purchased from Sigma-Aldrich (St. Louis, MO). The isomers of PAN were obtained from Altana Pharma AG (Konstanz, Germany). GF120918 was a gift from GlaxoSmithKline (Research Triangle Park, NC). All the organic solvents [high-performance liquid chromatography (HPLC) grade] were purchased from Thermo Fisher Scientific (Waltham, MA).

Animals

Five adult female lactating Sprague-Dawley rats (250–350 g) with 1- or 3-day-old pups were purchased from Harlan Laboratories (Indianapolis, IN). Animals were maintained under a 12/12-h light/dark cycle and had access to food and water during the experiments. The rats were acclimatized for at least 1 week before the experiment. All the procedures were approved by the University of Kentucky Institutional Animal Care and Use Committee.

Flux study

Rat Abcg2 and empty vector (pcDNA3.1) expressed in Madin-Darby Canine Kidney II Cells has been established in our lab (Wang et al., 2008). Cells were seeded on microporous membrane filters (3.0-μm pore size, 24-mm diameter; Transwell 3414; Corning Inc., Corning, NY) at a density of 1.0 x 10^6 cells/well. Cells were grown for 4 days to achieve transepithelial electrical resistance >200 Ω· cm2, and media was replaced every other day. Before the experiment, the media at both the apical and basolateral side of the monolayer was replaced with 2 ml of OptiMEM media (Invitrogen, CA) without serum and either the apical or basolateral side was loaded with 25 μM PAN isomers containing 0.2 μCi/ml [^{3}H]mannitol (Perkin Elmer, Norton, OH). Cells were incubated at 37°C in 5% CO_2. To assess tight junctions of each monolayer, 50 μl aliquots were collected to assess the paracellular flux of [^{3}H] mannitol into the opposite compartment. For PAN isomers transport, 140-μl aliquots were taken at 1, 2, 3 and 4 h. Samples were stored at -80°C until the time of analysis.

In vitro M/S.

M/S ratios for PAN isomers transfer into milk is governed by passive diffusion and can be predicted from an in vitro passive diffusion model (Fleishaker et al., 1987; Fleishaker and McNamara, 1988b):

$$\frac{M}{S}_{predicted} = \frac{(f_s^u)(f_s)(W)}{(f_m^u)(f_m)(S)}$$

Eq.3-1

where f^u is the unionized fraction of drug in serum or milk, f is the free fraction of drug in serum or milk, W/S is the ratio of the drug concentration in whole milk to the drug concentration in skim milk, and the subscripts s and m represent serum and milk, respectively.

The S/W ratios, a measure of the milk fat partitioning of PAN isomers, were determined following LC-MS analysis of the each PAN isomer concentrations in blank rat whole milk and skim milk into which isomer had been added. The unionized fraction in serum and skim milk, a measure of the pH partitioning of drug between serum and milk, was calculated from the pKa of each isomer and from the pHs of serum (pH 7.45) and milk (pH 6.8)(Alcorn and McNamara, 2002). The unbound fraction of PAN isomers in milk and serum were determined by equilibrium dialysis of these fluids against a 0.133 M phosphate buffer (milk pH 6.8 and serum pH 7.45) in plexiglass dialysis cells (single place, 0.5 ml cells). After 8 hours equilibrium at 37^{o}C, samples were taken from both donor and recipient sides. These concentrations were determined by LC-MS.

In vivo studies

The jugular and femoral veins of Sprague-Dawley lactating female rats were cannulated under ketamine/xylazine anesthesia on days 10 to 12 postpartum. After 24 hours of recovery, each dam (n = 5) was randomized to receive an i.v. infusion of PAN in saline (0.4 mg/ml/h) for 8 h either with pretreatment of the inhibitor (GF120918, 10 mg/kg in DMSO) or with equivalent volume (approximately 0.15 ml of DMSO) of vehicle administered i.v. 10 minutes before infusion and all animals were crossed over on the second day to complete both phases (Wang et al., 2008). One milliliter of normal saline was given hourly by i.v. infusion to prevent dehydration during infusion. The dams were separated from the pups 4 hours before the infusion. Blood samples were drawn every 2 hours during the infusion. The blood samples were protected from light in separator tubes (BD Microtainer, Franklin Lakes, NJ), centrifuged to harvest serum, and frozen at -80°C until analysis. Milk samples were obtained by manual manipulation under light anesthesia (ketamine) at the end of the infusion, protected from light, and also frozen at -80°C until analysis.

Sample preparation

To each aliquot (50 µl) of serum, 10 µl 0.2 M NaOH and 20 µl of 10 µg/ml zonisamide sodium (internal standard) were added and the proteins were precipitated with 1ml Ethyl acetate, vortexed for 1 min, and then centrifuged at 2,400 rpm for 15 min at room temperature. The clear layer was collected into another clean glass tube (~0.8 ml) and dried under nitrogen in a 40^{o}C water bath. Samples were then reconstituted in 50 ul mobile phase (15% Acetonitrille and 85% water but without formic acid). To each aliquot of milk, the same amount of NaOH and zonisamide sodium were added to 25 µl of milk sample, protein was precipitated with 1 ml of cold methanol, vortexed for 30 seconds, and then centrifuged at 14,000g for 10 min at 4°C. The clear layer was collected to a clean glass tube (~0.9ml) and dried under nitrogen in a 40°C water bath. Samples were reconstituted in 200 µl water and mixed very well. Then 1 ml ethyl acetate was added, the samples were vortexed and centrifuged (same as serum samples extraction). The collected clear layers were dried under nitrogen in a 40^{o}C water bath and reconstituted in 50 µl mobile phase. This method was adapted from Bharathi (Bharathi et al., 2009). PAN isomers in phosphate buffer samples from *in vitro* predicted M/S ratio experiment were reconstituted in 1 ml water and 2 ml ethyl acetate, vortexed and centrifuged at 2400rpm for 15 minutes. The 1.8 ml organic layer was collected and dried under nitrogen at 40^{o}C water bath and reconstituted in 50 µl mobile phase.

Pantoprazole HPLC analysis

Concentrations of total PAN were assayed by HPLC on a Luna RP18 125 x 4.0-mm column (Phenomenex, Torrance, CA) and eluted with 40% acetonitrile/60% 10 mM potassium phosphate buffer, pH 7.2, at 0.5 ml/min. UV absorb at 290 nm. Aliquots of PAN in Opti-MEM medium were directly injected onto the HPLC. The standard curve range was 7.8 to 2000 ng/ml. All the standard curves showed an intraday and interday variability of <10% and r^2 > 0.999.

Pantoprazole isomer analyses by LC-MS

A Varian 1200L Triple Quadrupole mass spectrometer (Walnut Creek, CA) equipped with an electrospray ionization (ESI) source and a Varian MS Workstation (6.42) data system was employed. The interface was adjusted to the following conditions: positive ion mode; spray needle voltage, 5000V; shield voltage, 600V; capillary voltage, 40V; drying gas (Nitrogen) temperature, 300^{o}C. MS/MS spectra were obtained for selected precursor ions through incidental collision with neutral gas molecules (Argon) at 2.0mTorr in the collision cell of the mass spectrometer. The collision energy was set at 8.50V. The parameters of the selected reaction monitoring transitions for the [M+H]+ to selected product ions were optimized with the following typical values for the analytes and internal standard: PAN m/z 384 to 200 and the internal standard zonisamide m/z 213 to 132. The LC conditions were as follows. The column was a Lux 5 µl Amylose-2 150 x 4.60-mm Chiral column (Phenomenex, Torrance, CA). The initial mobile phase consisting of acetonitrile: water: formic acid (15%:85%:0.02%) was delivered by dual Varian ProStar 210 pumps (Walnut Creek, CA), at a flow rate of 0.3 ml/min. A gradient program was utilized; the acetonitrile phase was increased to 90% over 12 minutes and held constant for an additional 6 minutes. The acetonitrile phase was returned to 15% over 1 minute and held constant for an additional 11 minutes for a total run time of 30 minutes. Twenty microliters of the sample was injected onto the LC-MS. Serum and milk concentrations of PAN were quantified according to standard curves.

Pharmacokinetic Calculations and Statistical Analysis. Systemic clearance was calculated using the following formula:

$$Cl_S = \frac{Infusion\ Rate}{C_S}$$

Eq.3-2

where C_S is the average concentration of PAN in serum from 2 to 8 h. M/S was calculated by:

$$\frac{M}{S} = \frac{C_M}{C_S}$$

Eq.3-3

where C_M is concentration of PAN in milk at 8 h.

All the data are expressed as mean ± S.D. Analyses were performed to estimate intergroup differences using two-way ANOVA analysis of variance with Bonferroni Post test for multiple comparisons. A p value of <0.05 was considered statistically significant.

4.4 Results

Pantoprazole isomers transport in rat-Abcg2 expressed in MDCKII cell line.

The expression level and function of rat Abcg2-MDCKII were confirmed by Western blot, flow-cytometry and nitrofurantoin transport in previous studies (Wang et al., 2008). At 25 μM, the flux for both isomers and in both directions approached steady-state after 3 hour in empty vector and Abcg2-MDCKII cells. Initial rates were calculated during first hour. The flux for both PAN isomers in both directions was identical in empty MDCKII cells (**Figure 4-1A**). The asymmetry efflux ratios (ER_α) of (+)- and (-)- PAN in parent cell line at the one hour time point were 0.90 and 0.95, respectively. In Abcg2-MDCKII cell line, the initial flux rate for basolateral to apical flux was considerably greater than the flux in the opposite direction. The mass transport of (+)-PAN from basolateral to apical side across monolayer appeared greater than (-)-PAN (**Figure 1B**), whereas the flux from apical to basolateral was greater for the (-)-PAN relative to the (+)-PAN. The ER_α of (+)- and (-)-PAN at the one hour time point were 5.15 and 1.51, respectively in Abcg2-MDCKII cell line. These stereoselective differences in initial rates were maintained as the profiles approached steady state of (+)-and (-)-PAN were 3.82 and 1.77, respectively.

A.

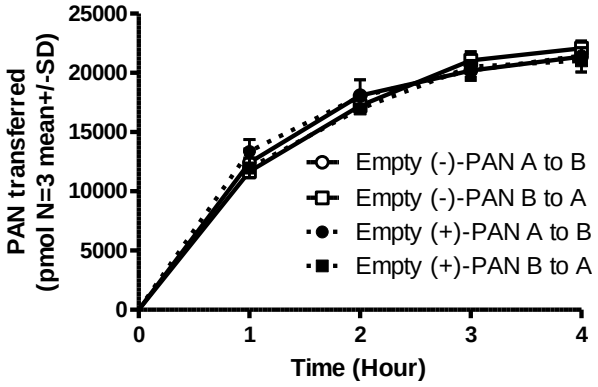

B.

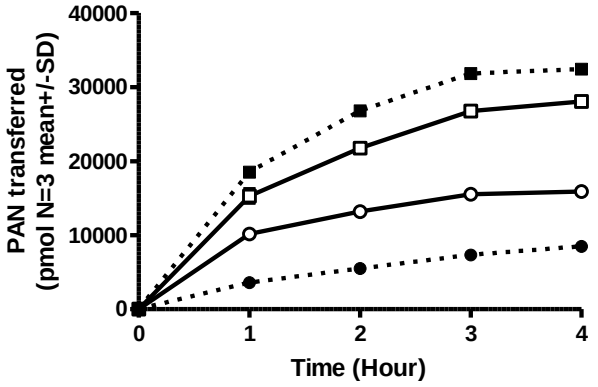

Figure 4-1 The amount (mean±SD, n=3) of PAN isomers appearing in the receiver compartment of MDCKII-empty vector and MDCKII-rAbcg2 monolayers grown on Transwells at donor concentration of 25 uM. PAN isomers: minus (open symbol) and plus (closed symbol) from the basolateral to apical (squares) and apical to basolateral (circles) in MDCKII-empty (**panel A**) and MDCKII-rAbcg2 (**panel B**)

Predicted M/S ratios of pantoprazole isomers

Table 4-1 contains individual parameter estimates that contribute to the diffusion model prediction of M/S ($M/S_{predicted}$) of the PAN isomers. The fraction of unionized approximated 1 for both PAN isomers since their pK_a is lower than the pH of both rat milk (6.8) and serum (7.45). The free fractions of PAN isomers were determined by equilibrium dialysis using serum concentrations in rat infusion study. The serum free faction of (+)-and (-)-PAN were 2.33% and 2.38%, respectively. PAN isomers have lower binding in skim milk (74% and

73%, respectively). The fat partitioning of each isomer was reflected in the S/W ratio which was 0.75 and 0.77 for the (+)- and (-)-PAN, respectively. M/S ratio predicted by the diffusion model was 0.12 for (+)-PAN and 0.11 for (-)-PAN.

Table 4-1 M/S Ratio $_{Observed}$ M/S Ratio $_{Predicted}$ for PAN isomers in lactating Sprague-Dawley rats.* P<0.01. Data is presented as mean.

M/S Ratio and property or rat no.	(+)-PAN	(-)-PAN
Diffusion Model Parameters		
pK_a	3.9	3.9
f^u,serum	~1	~1
f^u,milk	~1	~1
f serum (%)	2.33	2.38
f milk (%)	25.96	27.08
S/W ratio	0.75	0.77
Predicted M/S ($M/S_{Predicted}$)	0.12	0.11
200% $M/S_{Predicted}$	0.24	0.23
50% $M/S_{Predicted}$	0.06	0.06
$(M/S_{Observed})/(M/S_{Predicted})$	4.43*	11.95
Observed M/S ($M/S_{Observed}$)		
1	0.45	1.22
2	0.43	1.34
3	0.62	1.68
4	0.64	1.40
5	0.54	1.17
Mean	0.54*	1.36
SD	0.10	0.20
Lower 95% Cl of mean	0.42	1.11
Upper 95% Cl of mean	0.65	1.61

In vivo study-pantoprazole isomers accumulate in rat milk.

The lactating rats were infused with racemic PAN and each isomer concentration in serum and milk were measured by LC-MS. Chromatographs of PAN isomers and zonisamide are shown in **Figure 4-2**. The standard curve was linear from 80 to 5,000 ng/ml in serum, 10 to 5000 ng/ml in milk and 25-1000 ng/ml in phosphate buffer. All the standard curves showed an intraday and interday variability of <10% and r^2 > 0.99 (**Appendix D-2**) .

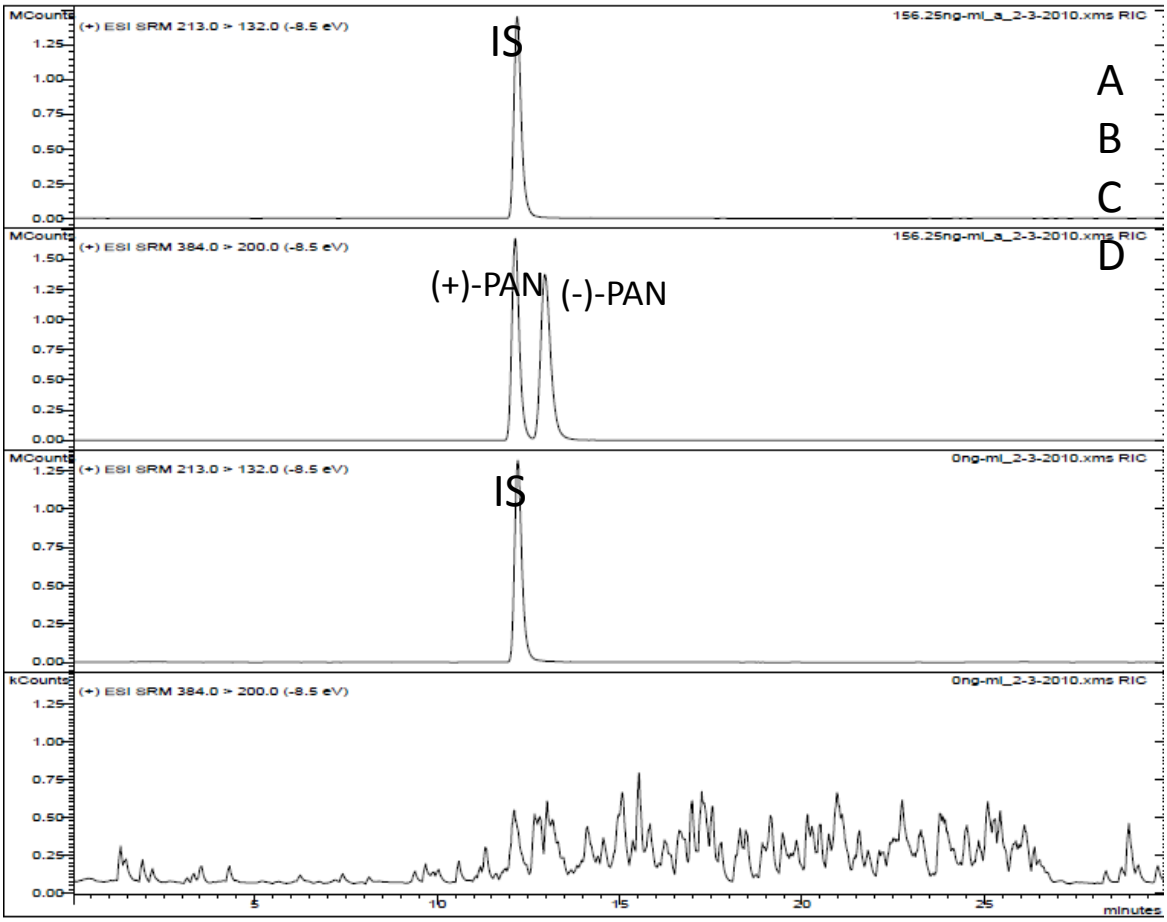

Figure 4-2 Enantiomeric separation of PAN (156 ng/ml) and internal standard zonisamide (4 µg/ml). Panels A and C represent a chromatogram of internal standard alone in one PAN standard serum (156 ng/ml) and blank serum respectively. Panels B and D represent a chromatogram of PAN isomers in one PAN standard serum (156 ng/ml) and blank serum (lower attenuation), respectively.

The mean PAN isomer concentration time profiles in serum are shown in **Figure 4-3**. In the dosing vehicle treatment, both PAN isomers appeared to achieve steady-state serum concentrations by 2 hour time point in the

intravenous infusion protocol with (-)-PAN (1,625 ng/ml) slightly higher than (+)-PAN (1,204 ng/ml). The treatment of GF120918 appeared to increase the serum concentration of both PAN isomers, in particular for (-)-PAN which increased 37%. In the control group, (+)-PAN (0.57±0.1) had greater systemic clearance (**Figure 4-4**) than did (-)-PAN (0.44±0.12). The two-way ANOVA analysis of variance indicated a significant isomer and treatment effect, but no interaction.

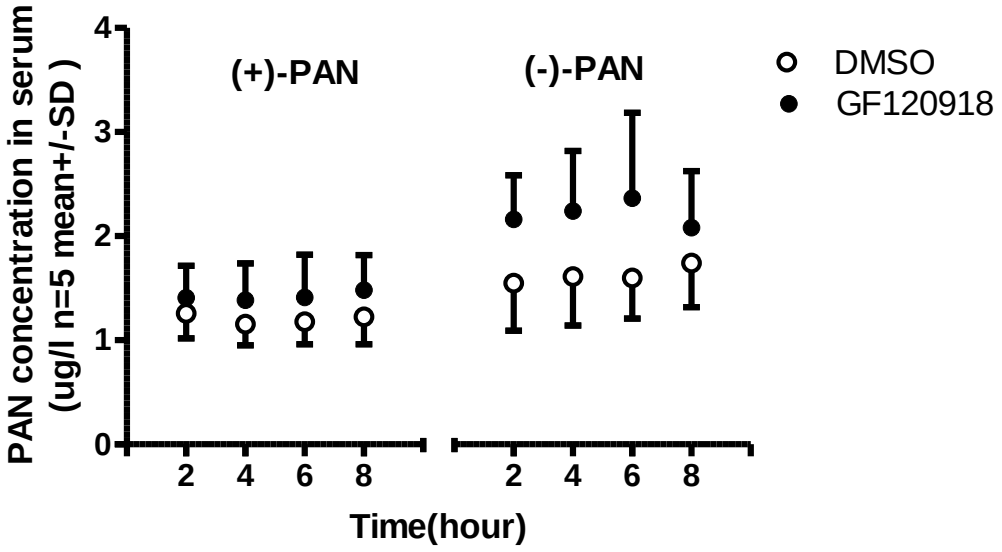

Figure 4-3 PAN isomer concentrations (Mean±S.D., n=5) in serum in lactating Sprague-Dawley rats at 2, 4, 6 and 8 hour infusion (0.4 mg/ml/h) following administration of dosing vehicle alone (DMSO) or GF120918 (10 mg/kg)

PAN isomers were distributed differently into milk in the rat. At 8 hours, the milk concentration of (-)-PAN (2,260 ng/ml) was considerably higher than (+)-PAN (644 ng/ml). The milk concentrations were lower for both isomers and the difference between the isomers diminished [(-)-PAN (1,098 ng/ml) and (+)-PAN (525 ng/ml)] following GF120918 administration. The M/S ratios for PAN isomers are shown in **Figure 4-5**. In control (DMSO) group, M/S ratio of (-)-PAN was nearly 3 times that of (+)-PAN. Administration of GF120918 decreased M/S ratios of (+)-PAN from 0.54±0.09 to 0.38 ±0.07 and (-)-PAN from 1.36±0.20 to 0.50±0.08. The two-way ANOVA analysis of variance indicated a significant

isomer and treatment effect, as well as a significant interaction between isomer and treatment. The mean observed M/S was 4.43 fold for (+)-PAN and 11.95 fold for (-)-PAN greater than the M/S Predicted (**Table 4-1**) and the 95% confidence intervals around the M/S did not overlap the 50 to 200% range of the M/S predicted.

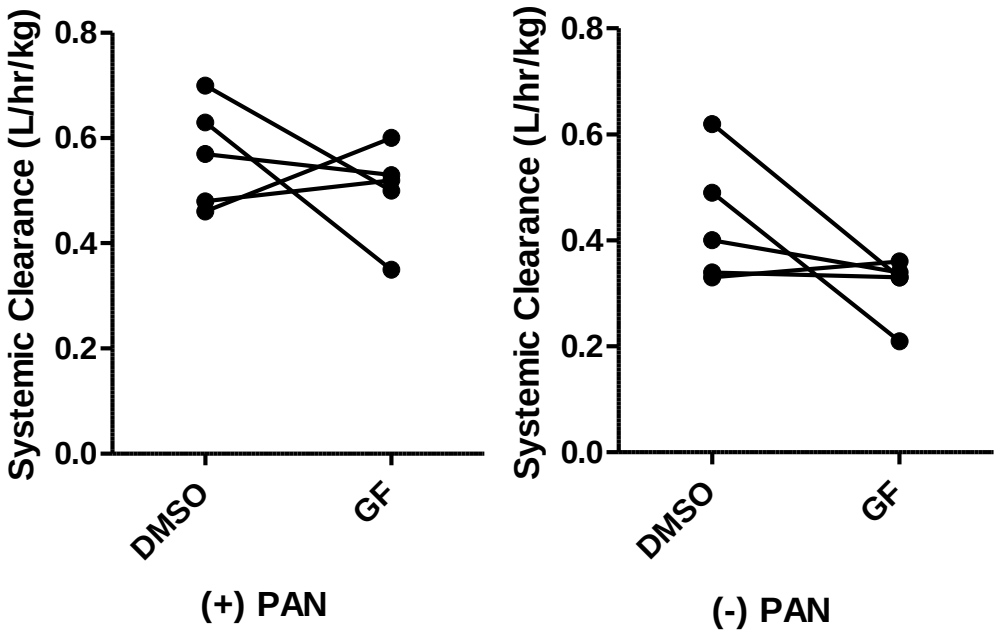

Figure 4-4 The systemic clearance of PAN isomers following administration of dosing vehicle alone (DMSO) or GF120918 (10 mg/kg). Data are presented as paired values from individual rats.

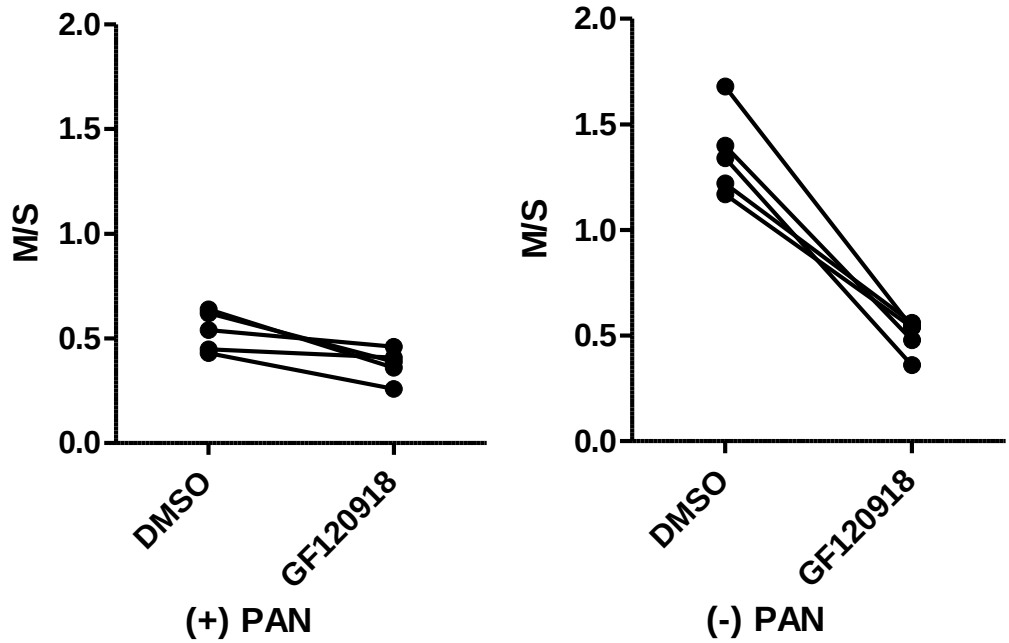

Figure 4-5 The M/S ratios of PAN isomers following administration of dosing vehicle alone (DMSO) or GF120918 (10mg/kg). Data are presented as paired values from individual rats.

4.5 Discussion

ABCG2 is a widely distributed efflux transporter and plays an important role protecting body against endogenous or exogenous xenobiotics. The role of transporter on absorption, distribution, metabolism and excretion (ADME) of drugs has been documented in ABCG2 substrate flux studies (Kruijtzer et al., 2002). There is a growing concern regarding the role of ABCG2 in drug-drug interactions as well (Giacomini et al., 2010; Huang and Woodcock, 2010).

ABCG2 is also found on the apical surface of lactating mammary epithelial cells (Jonker et al., 2005). The physiological function of ABCG2 in lactation is uncertain; however, riboflavin has been shown to be a substrate and ABCG2 may be functioning as a nutrient transporter (van Herwaarden et al., 2007). A number of investigators have demonstrated the importance of this transporter in

the accumulation of drugs in milk (Jonker et al., 2005; Perez et al., 2009). Nitrofurantoin and cimetidine, both ABCG2 substrates, accumulates in human and rat milk (Oo et al., 1995; McNamara et al., 1996; Gerk et al., 2001a; Oo et al., 2001). Others have clearly demonstrated the role of mAbcg2 in drug transfer into milk using knockout mice (Jonker et al., 2005; Merino et al., 2005b). Other ABCG2 substrates which appear to accumulate in milk include: topotecan, acyclovir, dietary carcinogens, ranitidine and ciprofloxicin (Jonker et al., 2005; Merino et al., 2005b; Merino et al., 2006a; van Herwaarden et al., 2007; Vlaming et al., 2009)

A testable supposition would hold that all ABCG2 substrates accumulate in milk, resulting in relatively high M/S ratios, greater than that predicted by simple diffusion. A clinical case report with PAN would appear to challenge the premise (Plante et al., 2004). PAN is highly protein bound (>98%) in human serum (Andersson and Weidolf, 2008) and rat serum (Xie et al., 2005). Data in the current work confirms that the protein binding of both PAN isomers in rat serum is extensive. PAN has a modest octanol to water partitioning (Badwan, 2002) and hence, the fat partitioning is higher (reflected in a lower S/W value) than many drugs. The unionized fractions were assumed to be identical for the two isomers. As a result, M/S ratios predicted by diffusion for both isomers were low and virtually identical. The observed M/S were 4.4 fold [(+)-PAN] and 12.5 fold [(-)-PAN] higher than predicted by diffusion and the 95% confidence intervals around the observed M/S did not overlap the 50 to 200% range of the predicted M/S (Table 4-1) clearly suggesting a potential role of a transporter for PAN accumulation in milk. We have previously utilized this approach as a predictor for a significant role of a transporter in drug accumulation in milk (Alcorn and McNamara, 2002; Edwards et al., 2003). The observed M/S ratios of (+)-PAN and (-)-PAN in the rat were 20-60 times higher than the M/S from the lone human report (Plante et al., 2004). The explanation for the species difference remains unclear.

Stereochemistry is an important aspect of biology and plays a role in many aspects of drug disposition (Bhatia et al., 2008) and yet there are few studies

examining stereoselective transport of drugs. PAN is marketed as a racemic mixture whose stereoselective disposition has been characterized (Masubuchi et al., 1998; Tanaka et al., 2001); however, the interaction of its isomers with transporters (e.g., ABCG2) has not been described. It is unclear whether differences in stereoselective disposition could play any role in the distribution of PAN into milk. The present work characterized PAN isomer flux using rat Abcg2 *in vitro* models as well as PAN isomer distribution into rat milk.

Previously our laboratory had established a stably expressed rat Abcg2 in MDCKII cell line, a cell line commonly used in transport studies (Bartholome et al., 2007; Marchetti et al., 2007; Weinglass et al., 2008). MDCKII cells are believed to express fewer endogenous xenobiotic transporters compared to Caco-2 cells, although some research groups have demonstrated that several xenobiotic transporters are present in MDCKII cells, such as p-gp and MRP2 (Su et al., 2004). Hence, a number of substrates, including nitrofurantoin exhibit directional transport in parent cell line (Kim et al., 1998; van Herwaarden et al., 2007; Wang et al., 2008). Interestingly the PAN isomers transported from apical to basolateral or from basolateral to apical overlaped completely in MDCKII empty cell line; the ER_{α} values were close to unity for both PAN isomers. This would suggest that PAN was not a substrate for any of the endogenous transporters in MDCKII; hence, PAN may serve as a model ABCG2 substrate for a certain mechanistic flux studies.

As a typical ABCG2 substrate, PAN has been used as a competitive ABCG2 inhibitor to identify other ABCG2 substrates or to study drug-drug interaction(Breedveld et al., 2004; Yokooji et al., 2007; Adkison et al., 2009) Our *in vitro* experiment demonstrated a rat Abcg2 mediated apically directed transport of PAN and indicated pantoprazole is a substrate of rAbcg2, which is consistent with the reports that pantoprazole is a substrate for human and mouse ABCG2/Abcg2 (Breedveld et al., 2004; Breedveld et al., 2005; Suzuki et al., 2009). Furthermore, in rat expressing MDCKII cell line, Abcg2 demonstrated stereoselective interaction with pantoprazole. The flux of the (+)-PAN appears to be greater than the (-)-PAN isomer (Figure 4-1B). However, a more detailed

analysis of the in vitro transport data (Chapter 5) suggests that the (-) isomer is, in fact, the better ABCG2 substrate; possessing a greater affinity and overall apical efflux permeability (PS_{AE}) for rAbcg2. The greater flux of (+)-PAN arises due to the interplay between the two membranes (basolateral and apical) in determining the overall flux. At lower concentrations, PAN (both isomers) flux across the apical membrane (due to rAbcg2) is so rapid that the overall rate limiting step is diffusion across the basolateral membrane. At 25 µM concentration, the higher affinity (-)-PAN isomer saturates rAbcg2 at the apical membrane, slowing overall flux across the monolayer. Hence, (+)-PAN appeared to be a better rAbcg2 substrate than (-)-PAN (Figure 4-1) when in reality the opposite is true. A more insightful, mechanistic model is required to fully interpret flux data (theoretical part, Chapter 6) and such an analysis reveals (-)-PAN to be a better rAbcg2 substrate (Chapter 5: in vitro model).

In the chemical Abcg2 knockout rat model, co-administration of GF120918 decreased the systemic clearance of nitrofurantoin (Wang et al., 2008). In the present study of PAN isomers, (-)-PAN had a slightly lower systemic clearance compared to (+)-PAN but there was no statistical difference. This observation is consistent with the report that (-)-PAN had relative longer serum elimination half-life and mean residence time in rat study (Masubuchi et al., 1998). The administration of GF120918 had no significant effect on PAN isomer systemic clearance, which would indicate that Abcg2 does not play a major role in the elimination for the systemic clearance of PAN. In a human study, roughly 80% of an oral or intravenous dose is excreted as metabolites in urine; the remainder is found in feces and appears to originate from biliary secretion (Huber et al., 1996a). The parent drug is predominantly metabolized by CYP2C19 and to a lesser extent by CYP3A (Radhofer-Welte, 1999). The pharmacokinetics of PAN is unaltered in patients with renal failure, but the rate of metabolism was significantly decreased with severe liver cirrhosis patients (Huber et al., 1996b), which indicates systemic clearance of PAN is largely determined by hepatic metabolism of PAN.

The metabolism of PAN isomers in mammary epithelial cell appears to be minimal (no evidence of metabolism in milk samples). The *in vivo* M/S of (+)-PAN was almost 1/3 that of (-)-PAN in DMSO group and the *in vivo* M/S of both isomers converged to a similar value (0.4-0.5) following the administration of GF120918, suggesting Abcg2 contributes to PAN distribution in rat milk with Abcg2 serving as a major contributor for (-)-PAN accumulation.

Based on the results of *in vitro* and *in vivo* studies, we confirmed that Abcg2 recognizes three dimensional structure of PAN. This difference may play a role in the tissue distribution profile for PAN. However, it is likely that such differences would result in minimal differences in the overall pharmacodynamic profiles of PAN. PAN is an acid gradient dependent accumulation prodrug and both isomers are converted to the same active principle, planar sulphenamide. Cyclic sulphenamide has an ability to react with key cysteines present in the gastric acid pump (Huber et al., 1995). The chirality is lost in the conversion from prodrug to active form; hence, for PAN, stereoselective differences in disposition may have limited pharmacologic or clinical effects.

In conclusion, the present work has demonstrated a clear difference in the transport of the isomers of PAN by rAbcg2 with (-)-PAN a better substrate than (+)-PAN. Moreover, PAN stereoselectivity for Abcg2 appears responsible for a difference accumulation of substrate isomers in milk and may have consequences for other aspects of stereoselective drug disposition. The current work also supports the hypothesis that ABCG2 substrates will accumulate in milk, but does not explain the previous clinical observation of a low M/S ratio. Additional studies will be needed to clarify this apparent species difference.

CHAPTER 5: Data based efflux transport transwell model: pantoprazole interaction with rAbcg2/ABCG2

5.1 Summary

CaCo-2 and efflux transporter over-expressing cell lines seeded in Transwell have been broadly used for new molecule entity screening (NME), drug disposition and drug-drug interaction studies which involved efflux transporters, such as P-gp, ABCG2 and MRP2. The interactions between compound and monolayer in Transwell as a NME screening tool have driven more attention than before. In recent years, investigators have employed mathematical models to explain the various experimental observations. Kalvass's efflux theoretical model and Sun's CaCo-2 model expanded our understanding of Transwell flux data and have identified the limitation of some parameters. However, these models also have their limitations as well.

In this section, we characterize the interactions between pantoprazole isomers and rat Abcg2/ human ABCG2 in Transwell system. Both pantoprazole isomers are Abcg2/ABCG2 substrates. There were stereoselective transport of pantoprazole isomers in monolayer of both Abcg2 and ABCG2 expressed in MDCKII cell lines with (-)-PAN having a greater affinity. There was a modest difference observed in kinetic transport parameters between rat Abcg2 and human ABCG2. (-)-pantoprazole is a better substrate than (+)-PAN for both species. The observation of PAN isomers transport in Abcg2 expressing in MDCKII cell line is consistant with the in vivo result from rat study in Chapter 4.

Having identical chemical properties (diffusion controlled), the pantoprazole isomers provide an ideal platform to compare the kinetic parameters derived from Transwell experiments. It is important to use cellular concentration instead of donor concentration to estimate kinetic parameters of transporters, e.g., $PS_{A,E}$, K_m and V_{max}. The theoretical mechanistic model provided a comprehensive understanding of pantoprazole isomers transport in Abcg2/ABCG2, verified the

theory behind the experimental paradigm and helped reinforce our understanding of the monolayer flux experiments.

5.2 Introduction

Efflux transporters such as P-gp, MRP2 and ABCG2 are localized in numerous tissues throughout the body and play important roles in drug absorption, distribution, metabolism and excretion (Giacomini et al., 2010). These transporters can be major determinants of the pharmacokinetic, efficacy and safety profiles of drugs. In order to identify transporter substrates from new discovery libraries or investigate the impact of drug-drug interaction on drug metabolism and pharmacokinetic of marketed drugs or those in development, an *in vitro* method is required that is convenient, specific, high-speed and cost effective.

Flux across a Caco-2 or P-gp-overexpressing polarized epithelial cell lines have become one of the most popular *in vitro* methods to characterize substrate – transporter interactions. Experimental monolayer models produce an environment that mimics the *in vivo* state, permitting cultured cells to polarize and grow on porous membranes that provide an independent access to apical and basolateral plasma membrane domains. Vectorial transport across cell monolayers has been well established and used routinely in pharmaceutical industries world-wide (Balimane et al., 2004; Balimane and Chong, 2005). However, a mechanistic explanation and quantitative description of transport or inhibition data from transwells remains limited (Kalvass and Pollack, 2007). The US Food and Drug Administration and the International Transporter Consortium are trying to develop guidance to assist drug development scientists in conducting informative *in vitro* and follow-up clinical studies, for example, to establish decision trees for the study of P-glycoprotein or BCRP substrate interactions and inhibitor interactions (Zhang et al., 2008; Huang and Woodcock, 2010).

Our laboratory has studied the transfer of drugs into milk in rats, rabbits and humans. While diffusion plays a major role in drug appearance in milk, so does ABCG2. ABCG2 is found on the apical surface of lactating mammary epithelial cells (Jonker et al., 2005) and ABCG2 facilitates the accumulation of drugs in milk including: nitrofurantoin, cimetidine, topotecan, acyclovir, dietary carcinogens, ranitidine and ciprofloxicin (Oo et al., 1995; McNamara et al., 1996; Gerk et al., 2001a; Oo et al., 2001; Jonker et al., 2005; Merino et al., 2005a; Merino et al., 2006b; van Herwaarden et al., 2007; Vlaming et al., 2009). It is unclear if all ABCG2 substrates will accumulate in milk. A clinical report involving pantoprazole (PAN) reported a very low M/S (0.022) which would question the predictability of this generalization (Plante et al., 2004). In a companion chapter, the disposition of PAN in rat milk was explored and revealed a clear stereoselective difference associated with rAbcg2. PAN is marketed as a racemic mixture (**Figure 5-1**) and differences in the overall disposition of the two isomers have been reported both in man (Tanaka et al., 2001) and in rats (Xie et al., 2005). It is unknown if the interaction of PAN with ABCG2 is stereoselective or if it could explain the human M/S report.

In this paper, the transport of PAN isomers in monolayers consisting of rat (rAbcg2) and human ABCG2 expressed in MDCKII cell line was examined. The first objective was to establish whether any difference in the interaction between PAN isomers and rAbcg2/ABCG2 was present. Secondly, a model was proposed to quantify these stereoselective differences in kinetic parameters in order that they might be related to *in vivo* disposition studies. A third objective was to examine the interspecies difference since the rat is frequently used as an animal model.

5.3 Material and methods

Chemicals and materials

PAN mixture (50:50) was purchased from Wyeth (Philadelphia, PA) and the isomers of PAN were obtained from Altana Pharma AG (Konstanz, Germany). Cell culture mediums were obtained from Invitrogen (Carlsbad, CA). All the

organic solvents [high-performance liquid chromatography (HPLC) grade] were purchased from Thermo Fisher Scientific (Waltham, MA), and all of the other chemicals were obtained from Sigma-Aldrich (St. Louis, MO) unless specified.

Over-expressing rAbcg2/ABCG2 in MDCK-II cell lines were used in the transport studies. The establishment of rat Abcg2 or empty vector (pcDNA3.1) alone in MDCKII was described previously (Wang et al., 2008). Human ABCG2 or empty vector (pcDNA3.1) alone in MDCKII was previously established in our laboratory (Phil Empy Thesis). The pcDNA3 plasmid construct alone (empty vector) and the pcDNA3 plasmid containing wild-type ABCG2 were prepared for transfection. MDCKII cell transfection was performed at 50% confluence with the lipid-based FuGENE 6® transfection reagent at a 3:1 ratio per manufacturer's protocol. Success of transfection was initially evaluated at 48 h by Western blot analysis of cell lysates for ABCG2 following procedures described in the Western blot on page 37. Transfected cells were then selected through the addition of 800 µg/mL genecitin to the parent cell line media (MEM containing glutamax, 5% FBS, 100 U/mL penicillin, and 100 µg/mL streptomycin) (From Phil Empey's dissertation).

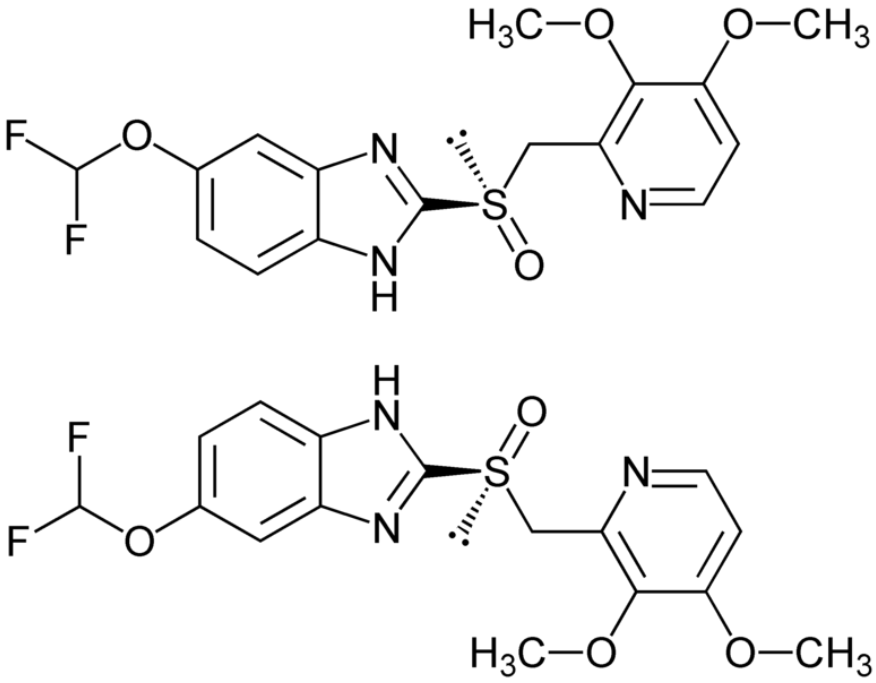

Figure 5-1 The structure of pantoprazole isomers.

PAN isomers transport in rat Abcg2 or human ABCG2 in Madin-Darby Canine Kidney II cells.

Briefly, rat /human ABCG2 or empty vector in MDCKII cells were seeded on microporous membrane filters (3.0-µm pore size, 24-mm diameter; Transwell 3414; Corning Inc., Corning, NY) at a density of 1.0 x 10^6 cells/well. Cells were grown for 4 days to achieve transepithelial electrical resistance >200 $\Omega \cdot cm^2$, and medium was replaced every other day. Before the experiment, the medium at both the apical and basolateral side of the monolayer was replaced with 2 ml of OptiMEM medium (Invitrogen) without serum and either apical or basolateral side was loaded with 3, 10, 30, 50 and 200 µM PAN isomers containing 0.2 µCi/ml [^{3}H]mannitol (Perkin Elmer, Hebron, KY). Cells were incubated at 37°C in 5% CO_2. 50-µl aliquots were collected to assess the paracellular flux of [^{3}H] mannitol into the opposite compartment; layers restricted mannitol transport to <1% of the total radioactivity per hour. For PAN isomers transport, 140-µl aliquots were taken at 0.5 and 1 h. Samples were stored at -80°C until the time of analysis by HPLC assay.

PAN HPLC

Concentrations of PAN were assayed by HPLC on a Luna RP18 125 x 4.0-mm column (Phenomenex, Torrance, CA) and eluted with 40% acetonitrile/60% 10 mM potassium phosphate buffer, pH 7.2, at 0.5 ml/min. UV absorb at 290 nm. Aliquots of PAN in Opti-MEM medium were directly injected onto the HPLC. The standard curve range was from 7.8 to 2000 ng/ml. All the standard curves showed an intraday and interday variability of <10% and r^2 > 0.999.

Permeability

The observed permeability (P_{Obs}, (µL/hr)/cm^2) of PAN isomers or paracellular marker was determined by calculating its initial transfer rate ($\frac{\Delta X}{t}$, pmol/hr) across the cell layer and dividing by the surface area (A, cm^2) of the Transwell and the

initial concentration (C_0, pmol/mL) in the donor chamber. PAN isomers transport data in rat Abcg2 or human ABCG2 were expressed as mean ± S.D.

$$PS_{app} = \frac{\Delta X/t}{A \cdot C_0} \qquad \text{Eq. 5-1}$$

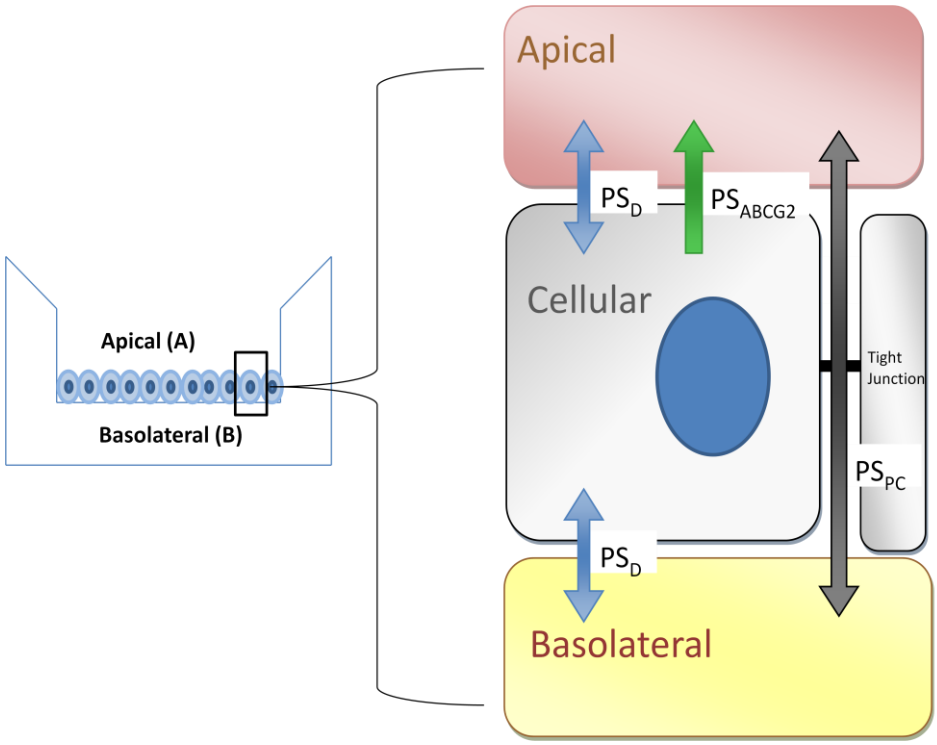

Figure 5-2 Three compartment model of flux across monolayer on Transwell system. PS_D: passive diffusion; PS_{PC}: permeability of paracellular transport; PS_{ABCG2}: active efflux mediated by ABCG2 on apical side.

A three compartment kinetic model of transcellular flux across a monolayer system (e.g., ABCG2 – MDCKII) is shown in **Figure 5-2** and has been recently developed to facilitate the interpretation of flux data (Theoretical part). Briefly, the driving force for drug efflux from basolateral to apical side includes passive diffusion (PS_D) across both basolateral and apical membranes, paracellular transport (PS_{PC}) between cells and active transport efflux on apical side (PS_{AE})

associated with the transporter. The model assumes the substrate does not interact with endogenous transporters, passive diffusion permeability (PS_D) is the same across both membranes, there is no cellular metabolism, and rapid intracellular diffusion. Substrate flux rates in three compartments can be described by the following set of differential equations (Eq.5-2, Eq.5-3 and Eq.5-4).

$$\frac{dX_B}{dt} = C_C(PS_D) - C_B(PS_D) + (C_A - C_B)PS_{PC} \quad \text{Eq. 5-2}$$

$$\frac{dX_A}{dt} = C_C(PS_D + PS_{AE}) - C_A(PS_D) + (C_B - C_A)PS_{PC} \quad \text{Eq. 5-3}$$

$$\frac{dX_C}{dt} = C_A(PS_D) + C_B(PS_D) - C_C(2PS_D + PS_{AE}) \quad \text{Eq.5-4}$$

where X_B, X_A and X_C are the mass of drug in the basolateral, apical and cellular compartment; C_C, C_B and C_A are the concentration of drug in the cellular, basolateral and apical compartment, respectively; PS_{AE} , PS_D and PS_{PC} are the permeability-surface area products for active apical efflux, passive diffusion and paracellular pathways, respectively.

Equation 5-2 and 5-3 can be further refined (Chapter 6) to describe the initial permeability from B to A ($PS_{Obs,B\to A}$) or A to B ($PS_{Obs,A\to B}$)

$$PS_{Obs,B\to A} = \frac{\frac{dX_{A,B\to A}}{dt}}{C_B^0} = \left[\frac{(PS_D)(PS_D + PS_{AE})}{(2PS_D + PS_{AE})} + PS_{PC}\right] \quad \text{Eq.5-5}$$

$$PS_{Obs,A\to B} = \frac{\frac{dX_{B,A\to B}}{dt}}{C_A^0} = \frac{(PS_D)(PS_D)}{(2PS_D + PS_{AE})} + PS_{PC} \quad \text{Eq. 5-6}$$

Paracellular permeability of mannitol was used as a surrogate for PAN PS_{PC}.

PS_D was estimated from the PAN flux in parent MDCKII (PS_{AE}=0) by rearranging Equation 5-5 (or 5-6) as

$$PS_D = 2\left[PS_{\substack{Obs,B\to A \\ \textbf{or}\ Obs,A\to B}} - PS_{PC}\right] \qquad \text{Eq. 5-7}$$

Permeability associated with ABCG2 apical efflux (PS_{AE}) was estimated from B to A or A to B PAN flux in rAbcg2/ABCG2 - MDCKII rearranging Equation 8 or 9, respectively.

$$PS_{AE,B\to A} = \frac{{PS_D}^2 - 2PS_D PS_{Obs,B\to A,}}{\left(PS_{Obs,B\to A} - PS_D\right)} \qquad \text{Eq. 5-8}$$

$$PS_{AE,A\to B} = \frac{{PS_D}^2 - 2PS_D PS_{Obs,A\to B}}{\left(PS_{Obs,A\to B}\right)} \qquad \text{Eq.5-9}$$

Initial transfer flux of from B to A (assuming C_A=0) or A to B can be rewritten (Chapter 6) and used to solve for C_C as Eq. 5-10

$$C_C = \frac{C_B^0(PS_D)}{(2PS_D + PS_{AE})} \qquad \text{Eq. 5-10}$$

ER_α is defined as the ratio of the initial rate of B to A flux divided by the initial rate of A to B.

$$ER_\alpha = \frac{\frac{dX_{Obs,B\to A}}{dt}}{\frac{dX_{Obs,A\to B}}{dt}} \qquad \text{Eq. 5-11}$$

Kinetic Parameter (K_M and T_{Max}) Estimation

The saturation kinetics of PAN isomers apical efflux transport by rAbcg2 or ABCG2 (PS_{AE}) as a function of estimated cellular concentrations (Equation 5-10) can be modeled by Eq. 5-12 where T_{max} is the maximum transport rate and K_m the Michaelis constant, inversely reflecting binding affinity of substrate for

transporter. Non-linear regression using GraphPad Prism (5.02) was employed to determine K_m and T_{max} in Equation 5-12 from PS_{AE}

$$PS_{AE} = \frac{T_{Max}}{(K_M + C_C)}$$

Eq. 5-12

5.4 Results

Pantoprazole isomers transported in rAbcg2 or ABCG2. The expression level and function of transport study of stably expressing rat Abcg2/ human ABCG2 cDNA or vector alone in MDCKII cell lines has been tested in a previous study (Wang et al., 2008) and unpublished data (Phil Empey's Thesis). The mass transport of PAN isomers was studied in empty-MDCKII and rAbcg2-MDCKII cells as shown in **Figure 5-3**. There was no difference observed for flux in either direction (A to B or B to A) or isomer-related flux in PAN isomer transport in empty-MDCKII monolayers at any of the five concentrations examined. In contrast, the transport of PAN isomers exhibited directional flux in rAbcg2-MDCKII cell line. There were marked transport differences between the PAN isomers at 30 and 50 μM for both directions. At lower (3 and 10 μM) concentrations, the difference between the isomers became negligible. At the highest donor concentration (200 μM) both isomers collapsed to flux identical to the empty-

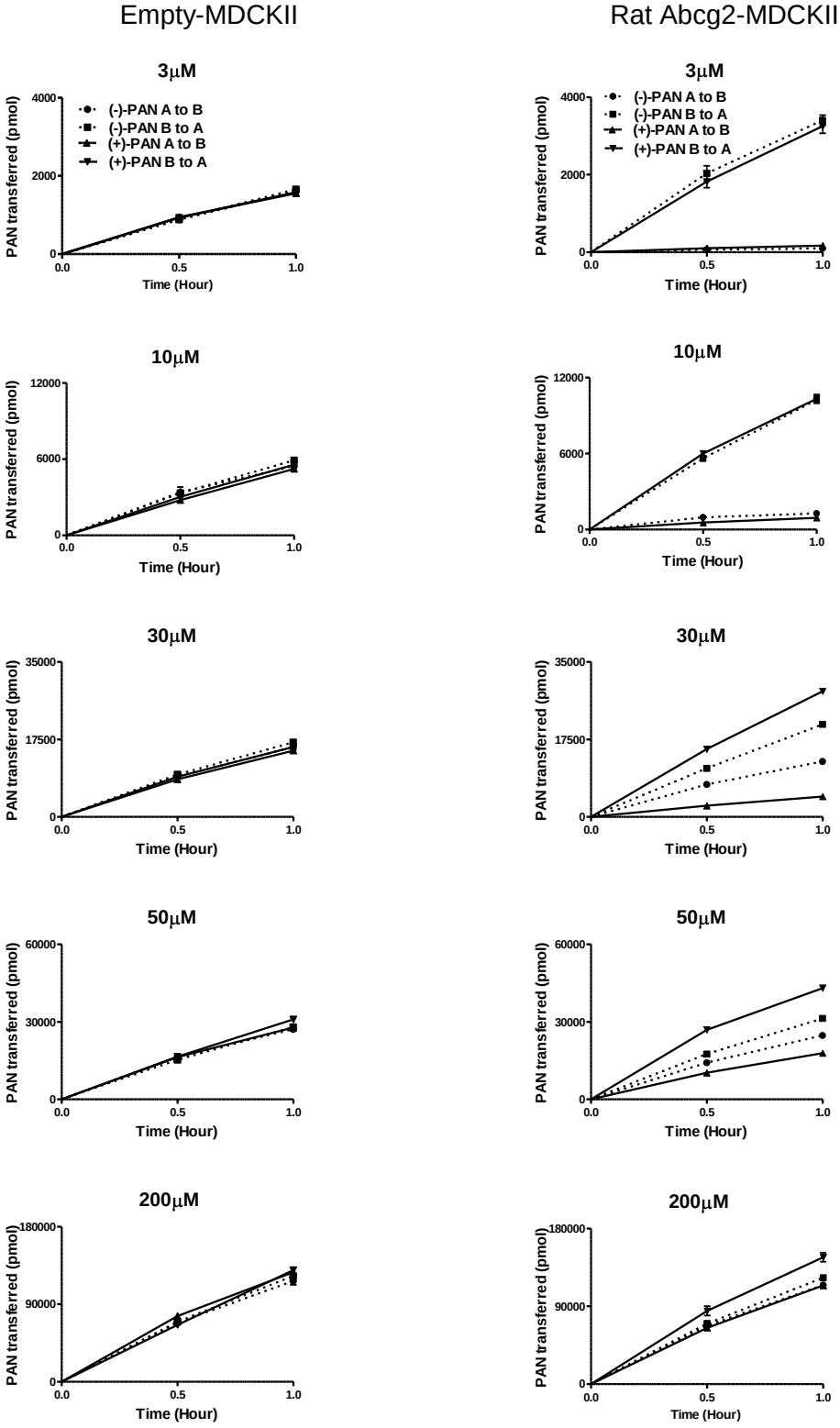

Figure 5-3 Mean (± SD, n=3) PAN isomer transport in pcDNA3.1-MDCKII (left panels) or rAbcg2-MDCKII cells (right panels) at 3, 10, 30, 50 and 200μM.

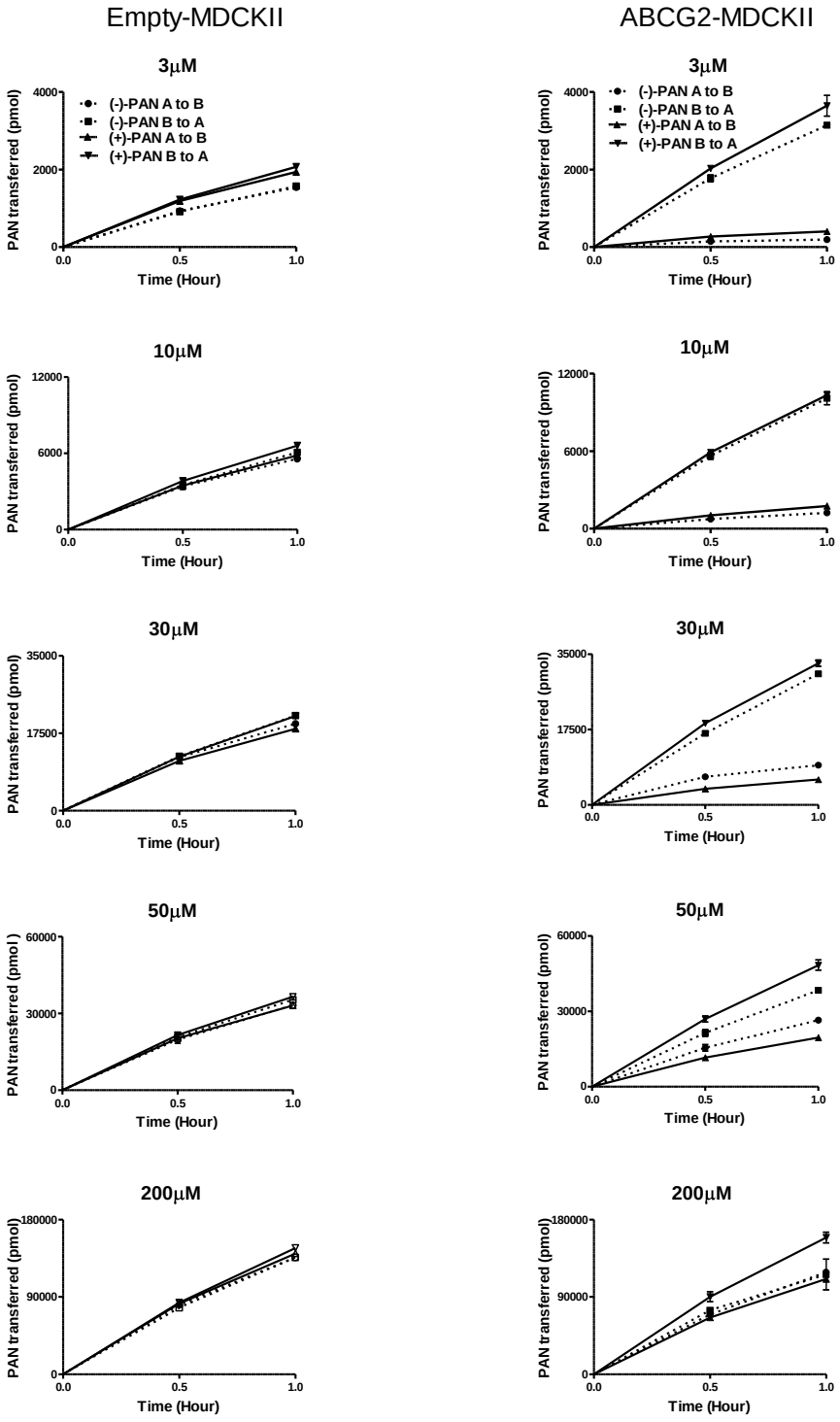

Figure 5-4 Mean (± SD, n=3) PAN isomer transport in pcDNA3.1-MDCKII (left panels) or human ABCG2-MDCKII cells (right panels) 3, 10, 30, 50 and 200μM.

MDCKII. Parallel results were observed in empty-MDCKII and human ABCG2-MDCKII cell line transport study (**Figure 5-4**). The directional transport of the two isomers confirmed that PAN is a substrate for both human and rat ABCG2.

Permeability parameters (PS_{obs}, PS_D and PS_{PC}) and asymmetry efflux ratios (ER_α). Apparent permeability for PS_{obs}, PS_D, PS_{pc} and asymmetry efflux ratios (**Table 5-1 and 5-2**) were obtained for both rat and human ABCG2. Using PS_{obs} of PAN transport in empty-MDCKII, PS_D was estimated from Equation 5-7 at different concentrations and both directions were very close (**Table 5-1 and 5-2**). Assuming the transport permeability of mannitol is similar to PAN isomer transport across paracellular pathway, PS_{pc} values were small and consistent across studies. PS_{pc} values were lower for ABCG2-MDCKII compared to empty-MDCKII. PS_{obs} of PAN isomers in empty-MDCKII cell lines were very similar for both directions at different concentrations resulting in ER_α values approximating unity for all of the experiments. By contrast, the PS_{obs} of both PAN isomers in the transfected cell lines were very different with respect to direction, favoring strong basolateral to apical directional flux at lower PAN concentration. The apparent flux were similar, but with subtle differences. At the lowest PAN concentration, the ER_α(s) of (-)-PAN was nearly double that of (+)-PAN. Flux was decreased from basolateral to apical side in Abcg2/ABCG2-MDCKII and increased from apical side to basolateral as donor concentration increased (**Table 5-1 and 5-2**). As a result, the ER_α(s) of PAN isomers in both rat and human ABCG2 transfected cell lines decreased with increasing donor concentration (**Table 5-1 and 5-2**). The direct driving force of transport is cellular concentration of substrate not donor concentration.

Table 5-1 The asymmetry efflux ratios (ER_{α}) and permeability parameters (PS_{obs}, PS_D and PS_{PC}) of PAN isomers transport in empty vs rat Abcg2-MDCKII as a function of PAN donor concentration (PS units: (μL/hr)/cm^2).

	Isomer	Parameter	Direction	3uM	10uM	30uM	50uM	200uM	Mean	SD
Empty-MDCKII	Minus	PS_{obs}	A->B	118	123	116	121	130	**121**	5
			B->A	120	130	123	126	135	**127**	6
		ER_{α}		1.02	1.06	1.07	1.04	1.04	**1.05**	0.02
	Plus	PS_{obs}	A->B	116	114	110	123	142	**121**	13
			B->A	117	121	116	135	140	**126**	11
		ER_{α}		1.01	1.07	1.06	1.09	0.98	**1.04**	0.05
	PS_D (Both Isomers)			231	242	226	251	271	**244**	18
	PS_{PC} (Mannitol)			2.30	1.14	3.54	0.72	1.39	**1.82**	1.12
rAbcg2-MDCKII	Minus	PS_{obs}	A->B	7.4	30.1	92.5	109	127	n.a.	
			B->A	253	224	151	137	136	n.a.	
		ER_{α}		34.0	7.44	1.63	1.26	1.07	n.a.	
	Plus	PS_{obs}	A->B	12.8	20.9	33.5	79.1	126	n.a.	
			B->A	238	229	206	194	162	n.a.	
		ER_{α}		18.7	11.0	6.16	2.46	1.29	n.a.	
	PS_{PC} (Mannitol)			0.51	0.88	3.44	0.72	1.59	**1.43**	1.20

Table 5-2 The asymmetry efflux ratios (ER_{α}) and permeability parameters (PS_{obs}, PS_D and PS_{PC}) of PAN isomers transport in empty vs human ABCG2-MDCKII as a function of PAN donor concentration (PS units: (μL/hr)/cm^2).

	Isomer	Parameter	Direction	3uM	10uM	30uM	50uM	200uM	Mean	SD
Empty	Minus	PS_{obs}	A->B	126	143	140	137	152	**140**	9
			B->A	128	155	150	146	151	**146**	11
		ER_{α}		1.01	1.08	1.08	1.06	0.99	**1.04**	0.04
	Plus	PS_{obs}	A->B	140	140	137	136	159	**142**	10
			B->A	149	157	156	149	166	**155**	7
		ER_{α}		1.06	1.13	1.14	1.09	1.04	**1.09**	0.04
	PS_D (Both Isomers)			267	291	289	277	309	**287**	16
	PS_{PC} (Mannitol)			2.30	3.29	1.22	3.44	2.29	**2.51**	0.90
Huamn ABCG2	Minus	PS_{obs}	A->B	16.9	31.6	67.6	109	132	n.a.	
			B->A	254	255	211	156	132	n.a.	
		ER_{α}		15.0	8.06	3.12	1.44	1.00	n.a.	
	Plus	PS_{obs}	A->B	30.0	42.2	43.6	79.6	126	n.a.	
			B->A	258	246	240	195	179	n.a.	
		ER_{α}		8.61	5.81	5.50	2.45	1.42	n.a.	
	PS_{PC} (Mannitol)			1.00	1.03	0.76	0.78	0.71	**0.86**	0.15

Cellular concentration profile Simulated cellular concentrations of PAN isomers corresponding to donor concentrations are presented in **Figure 5-5** as estimated from Equation 5-10 for both rAbcg2 and ABCG2-MDCKII based on initial estimates of permeability parameters (PS_{obs}, PS_D and PS_{PC}) of PAN isomers and apparent PS_{AE} values. At low donor concentration (3 μM), cellular concentration is estimated to be 3.2% of donor concentration for (-)-PAN and 5.6% for (+)-PAN for rAbcg2 and 5.5% for (-)-PAN and 11% for (+)-PAN for ABCG2. At high donor concentration (above 50 μM), cellular concentration is predicted to approach ½ of donor concentration (**Figure 5-5**).

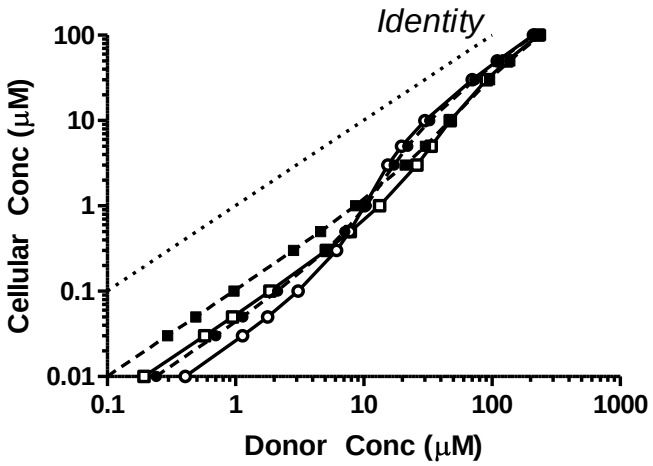

Figure 5-5 Predicted cellular concentration of PAN (Equation 5-10) relative to donor concentration based on PS_D and PS_{PC} described in Table 5-1 and 5-2 as well as fitted parameters T_{MAX} and K_M (Table 5-3) were used. Squares indicate (+)-PAN, circles represent (-)- PAN, open symbols indicate rAbcg2-MDCKII and closed symbols represent ABCG2-MDCKII. The line of identity is also illustrated.

Kinetic parameters K_m and T_{max} for rat Abcg2 and human ABCG2. The profile of apparent PS_{AE} (both directions) as a function of estimated cellular PAN concentration is presented in **Figure 5-6**. Kinetic parameters for the two isomers interaction with Abcg2 and ABCG2 are shown in Table 3. The (-) isomer of PAN has an 8-fold lower K_M compared to the (+)-PAN for both rAbcg2 (0.25 vs 1.85 μM) and ABCG2 (0.6 vs 5.32 μM), indicating a higher affinity of rAbcg2/ABCG2 for the (-) isomer. The (+) isomer of PAN has a 3-fold higher

T_{MAX} compared to the (-)-PAN for both rAbcg2 (7.86 vs 2.49 nmol/hr*cm^2) and ABCG2 (10.2 vs 3.29 nmol/hr*cm^2). rAbcg2 had a lower K_M (a higher affinity) for the PAN isomers compared to human ABCG2, but comparable T_{Max} values. The overall permeability (transport clearance at low PAN concentrations, PS_{AE}) associated with rAbcg2 and ABCG2 was twice that for the (-) isomer compared to the (+) isomer of PAN.

Modeling overall Permeability (PS_{Obs}). Utlizing the PS_D values from the empty –MDCKII (**Table 5-1 and 5-2**) as well as PS_{pc} from the transfected cell lines (**Table 5-1 and 5-2**) and the ABCG2 related kinetic parameters (**Table 5-3**) the overall PS was modeled as a function of donor concentration (**Figure 5-7**). Donor concentrations were back calculated from the intercellular concentrations. The comprehensive relationships (Equations 5-5 and 5-6) were effective in modeling PAN flux in both directions of (-)- PAN (r^2= 0.979) and (+)-PAN (r^2= 0.988) in ABCG2-MDCKII and (-)-PAN (r^2= 0.985) and (+)-PAN (r^2= 0.986) in rAbcg2-MDCKII.

Table 5-3 The permeability parameters (PS_D, PS_{PC} and PS_{AE}) and fitted mean (± SE) kinetic parameters (K_m and T_{max}) in both human ABCG2 and rat Abcg2.

Parameters	Unit	Isomer	Rat Abcg2	Human ABCG2
			Mean	Mean
K_m	µM	(+) PAN	1.85 ± 0.66	5.32 ± 1.62
		(-) PAN	0.25 ± 0.06	0.6 ± 0.12
T_{max}	nmol/hr*cm^2	(+) PAN	7.86 ± 2.20	10.2 ± 2.43
		(-) PAN	2.49 ± 0.41	3.29 ± 0.48
PS_{AE} $[T_{max} / K_m]$	µL/hr*cm^2	(+) PAN	*4,250*	*1,920*
		(-) PAN	*9,960*	*5,480*

A.

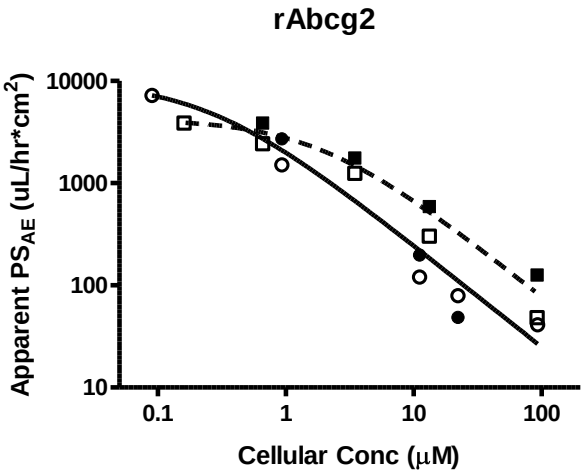

B.

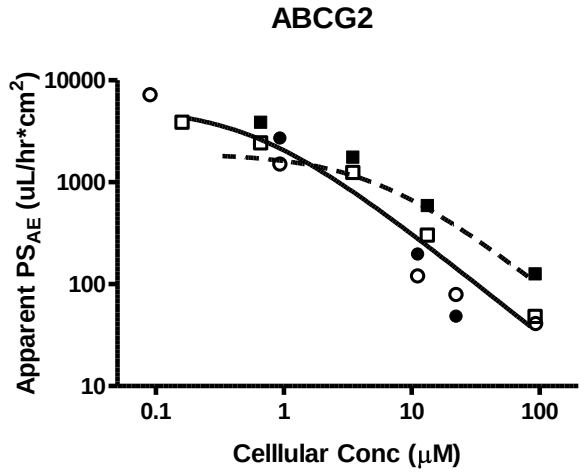

Figure 5-6 Apparent apical efflux permeability (PS_{AE}, Equation 5-12) as a function of simulated PAN cellular concentration (Equation 5-10). Panel A: rat Abcg2; panel B: human ABCG2-MDCKII cell monolayer; Squares indicate (+)-PAN, circles represent (-)-PAN, open symbols indicate basolateral to apical PS_{AE} and closed symbols represent apical to basolateral PS_{AE}. The initial estimates of parameters T_{MAX} and K_M (**Table 5-3**) were used to generate cellular concentration (Equation 5-10) and these concentrations were used in the final estimation process. Both axes were log transformed for easier visualization; fitting was performed using untransformed pooled data from both directional PS_{AE}. The solid and dashed lines are the fitted results for the (-)- and (+)-PAN isomers, respectively.

A.

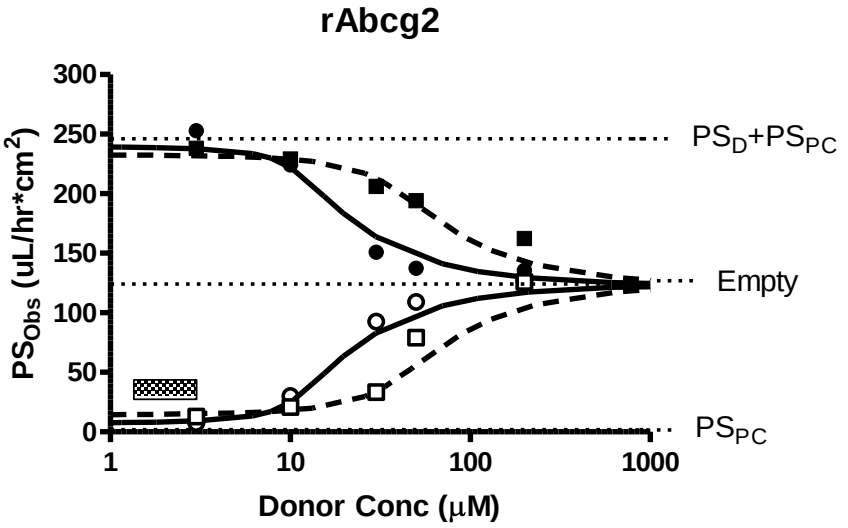

B.

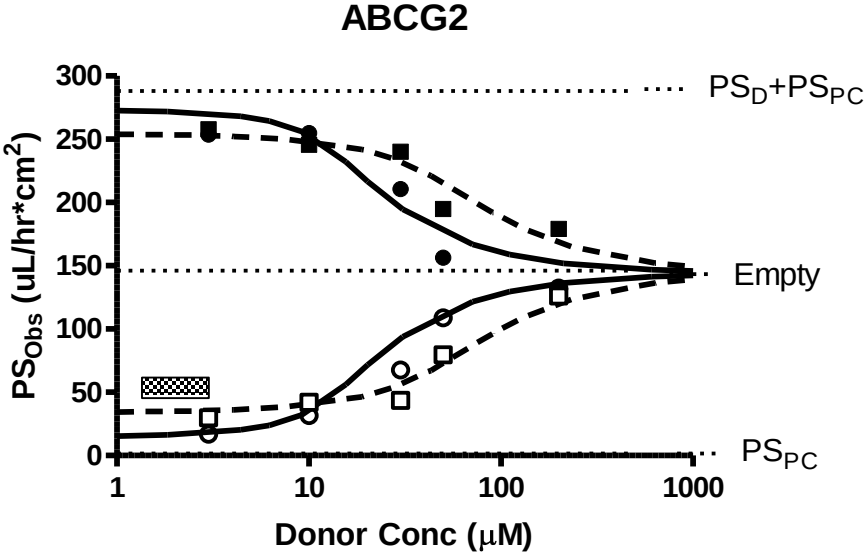

Figure 5-7 Overall permeability (PS_{obs}) as a function of PAN donor concentration. **Panel A**: rat Abcg2; **panel B**: human ABCG2-MDCKII cell monolayer; Squares indicate (+)-PAN, circles represent (-)-PAN, open symbols indicate basolateral to apical and closed symbols represent apical to basolateral flux. The simulation line represents Equation 5-5 and 5-6 for basolateral to apical and apical to basolateral flux, respectively. Fitted parameters T_{MAX} and K_M (Table 5-3) were used to generate cellular concentration (Equation 5-10) and simulation of overall PS_{obs} together with PS_D and PS_{PC} as described in Table 5-1 and 5-2. Model limits for basolateral to apical (PS_D + PS_{PC}), apical to basolateral (PS_{PC}) and empty cell line flux are presented as reference. The small square box presents the range of PAN concentration in serum in rat or pharmacological concentration in human, respectively.

5.5 Discussion

Transporters can play a role in the absorption, distribution, metabolism and excretion as well as a pharmacological effect of a variety of drugs. A recent white paper raised several key issues for drug discovery and development, including which transporters are clinically important in drug absorption and disposition, and which in vitro approaches are predictive for studying drug interactions involving these transporters (Giacomini et al., 2010). Flux across a Caco-2 or P-gp overexpressing polarized epithelial cell lines was one of the prominent in vitro methods proposed in the paper. Recently, our laboratory has described some of the limitations and interpretations of flux across a monolayer using a theoretical model (Chapter 6). The impetus for the model arose, in part, from the PAN isomer flux data presented herein. PAN isomers have almost identical physiochemical properties. PAN isomers transported in ABCG2 overexpressing MDCKII provided a simplified experiment model to compare important kinetic parameters from Transwell.

The apparent permeabilities (PS_{app}) of PAN isomers transport in empty MDCKII cell line (parent cell line) at five different concentrations were virtually identical (**Table 5-1 and 5-2**). There was no directional transport difference observed at any concentration; indicating no interaction of PAN isomers with endogenous transporters in the parent MDCKII cell line. This observation is consistent with other reports from literature (Breedveld et al., 2004) and suggests that PAN is a model substrate for this commonly used polarized epithelial cell line. PAN has been commonly used as an ABCG2 inhibitor in drug-drug interaction or ABCG2 substrate identification studies (Breedveld et al., 2004; Adkison et al., 2009; Oostendorp et al., 2009). In the present study, PAN was transported by human ABCG2 and rat Abcg2; it is particularly evident at 30 and 50 μM (**Figure 5-3 and 5-4**). The results confirm that both PAN isomers are rAbcg2/ABCG2 substrates.

The stereoselective interaction of PAN with rAbcg2/ABCG2 was evident at 30 and 50 μM but was not evident at lower (3 μM and 10 μM) or higher

concentrations (200 μM). The model provides for a clearer interpretation of the isomer flux. The rate limiting steps for PAN flux are associated with diffusion (PS_D and PS_{PC}) and not rAbcg2/ABCG2 associated PS_{AE} under these concentrations. Only at the intermediate donor concentrations when rAbcg2/ABCG2 become saturated is a change in flux observed. Flux studies, including those examining stereoisomer differences, are carried out at low substrate concentrations in high expressing clones to optimize the opportunity for observing a response. It should be noted that under such conditions, it is unlikely that stereoselective interactions would be reported since diffusion pathways dominate overall flux.

Taken together the flux data from empty and rAbcg2/ABCG2-MDCKII cell lines were consistent with the three compartment kinetic model shown in **Figure 5-2,** in which the passive apparent permeability on either apical or basolateral side (PS_D), paracellular apparent permeability through tight junction between cells (PS_{PC}) and the active apparent permeability of ABCG2 on apical side (PS_{AE}) as shown. Isolating the various parameters (PS_D, PS_{PC}, V_{Max} and K_M) allowed the overall PS_{Obs} to be successfully modeled (**Figure 5-7**). PAN flux in the B to A direction at low PAN concentration was very rapid across the apical membrane and overall flux was limited by the rate of diffusional flux across the basolateral membrane plus diffusion via the paracellular pathway. PAN flux in the A to B direction was limited paracellular diffusion since the counter flux associated with PS_{AE} was so efficient that virtually none of the drug which entered the cell from the apical surface fluxed transcellularly to the basolateral compartment.

Relating kinetic parameters (V_{Max} and K_M) to donor concentrations was problematic. Initial attempts to fit flux to permutations of the Micahelis Menton equation as a function of donor concentration resulted in fits which did not mimic the observed data. Fitting flux to donor concentrations would suggest an apparent cooperative interaction with the transporter (Hill coefficient)(Pan et al., 2007). Clearly the driving force for an apical efflux transporter such as rAbcg2/ABCG2 is intracellular not donor concentration. The apparent cooperativity simply reflects the fact that there is relatively more cellular drug

concentration as donor concentration increases due to saturation of the efflux transporter (**Figure 5-5**). Intracellular concentrations were not measured in the current study, but were predicted by the model (**Figure 5-5**) using the apparent PS_{AE} as well as estimates of PS_D and PS_{PC}. These intracellular concentrations were then used to estimate V_{Max} and K_M. The estimated K_M values ranged from 0.25 to 5.3 μM), whereas the donor concentrations around the inflection point (**Figure 5-7**) were in the 20 to 100 μM range. The (-)-PAN had a K_M value that was 10% of the (+) isomer indicating (-)-PAN had an almost 10 fold higher affinity for ABCG2 as well as rAbcg2. The capacity (V_{Max}) was 60% lower for (-)-PAN for ABCG2 and rAbcg2. For normal therapeutic dosing, serum unbound concentrations are likely to be below 0.1 μM, hence cellular concentrations are also expected to be well below the K_M. The effective permeability (PS_{AE} listed in **Table 5-3**) would be more than two fold greater for (-)-PAN compared to the (+) isomer. In the companion Chapter 4, the M/S for (-)-PAN in rats was 1.36 and decreased markedly in response to GF120918 (an inhibitor of rAbcg2/ABCG2) when compared to 0.54 for (+)-PAN (Chapter 4). Hence, the stereoselective effect of PAN and rAbcg2 in vitro did manifest itself in a measureable in vivo difference in disposition.

There may be differences in the human M/S for the two PAN isomers. The current in vitro or rat data does not provide sufficient insight to explain the observed clinical report of a low M/S for pantoprazole (Plante et al., 2004). Differences in the overall disposition of the two isomers have been reported; however most of this difference appears to be related to differences in metabolism. The stereoselective metabolism of (+)-PAN was impaired to a greater extent than (-)-PAN in the poor metabolizers of S-mephenytoin 4'-hydroxylase (CYP2C19) (Tanaka et al., 2001) The stereoselective metabolism via sulfoxide oxidation, 4'-O-demethylation, and 6-hydroxylation results in enantioselective pharmacokinetics; the area under the curve value of (-)-PAN was 1.5 times greater than that of (+)-PAN (Xie et al., 2005). Moreover, it should be realized that both isomers are converted to a common metabolite before achieving pharmacological activity, hence, the ultimate clinical effect of

stereoselective differences in disposition may be limited. As our in vivo rat milk studies demonstrate, stereoselective differences in disposition attributed to ABCG2 can result in tissue concentrations being higher despite comparable systemic concentrations.

In conclusion, there was stereoselective transport of PAN isomers in monolayers of both rat (rAbcg2) and human ABCG2 expressed in MDCKII cell line with the (-) isomer possessing a greater affinity. A mechanism based model was used to quantify differences in kinetic parameters between the two isomers. These kinetic parameters provided insights as to the extent of differences that might arise for in vivo studies. The current work also provided insights into the species difference in ABCG2 transport.

CHAPTER 6:Theoretical framework for transcellular flux across a monolayer system

6.1 Summary

In-vitro cell models are utilized to assess the role of transporter proteins on the vectorial transfer of drug across a polarized epithelial cell monolayer. A mechanistic model is presented to challenge and verify the underlying concepts and boundaries of this approach. Previous investigators have demonstrated the limitations of the apical efflux ratio (ER_A), and proposed the use of the asymmetrical efflux ratio (ER_α) as a more robust parameter. However, the assumption of a nonexistent paracellular transport pathway confounds parameter estimation and gives rise to an underestimation of the contribution of apical efflux ($PS_{A,E}$). Use of donor (and not cellular) concentration gives rise to an apparent positive cooperativty in kinetic parameters. Neither observed permeability (PS_{obs}) nor ER_α plotted as a function of substrate (or inhibitor) concentration provide an accurate estimation of K_M or K_I. Greater appreciation of the consequence of using high expressing clones and the transition of rate limiting steps (from basolateral alone to apical and basolateral processes) provides insight into the interpretation of flux kinetic data (T_{Max} or K_M) as well as inhibition profiles (K_I). The concepts presented in this paper provide a framework for interpreting transcellular flux across a cell monolayer and have implications for the assessment of drug-drug interactions involving transporters.

6.2 Introduction

Approximately 50 efflux and 360 uptake transporter proteins have been identified in mammalian species. These proteins are localized both in intracellular membranes as well as on the cell membrane. They appear to play key roles in homeostasis through their selectivity for ions and larger endogenous molecules, but they also interact with exogenous substances and drugs. Their orientation on either apical or basolateral faces of epithelium or endothelium can greatly control and facilitate substrate passage across biological membranes. This interaction

has led to the realization that transporter proteins can play an important role in the pharmacokinetics and pharmacodynamics of drugs. Initially, much of the interest in transporter–drug interactions was sparked by the role of ATP-binding cassette (ABC) efflux transporters, such as p-glycoprotein (P-gp), multidrug resistance associated proteins (MRPs) and breast cancer resistance protein (BCRP) in resistance to chemotherapy. More recently, the role of select efflux and uptake transporters, which polarize on opposite sides of the same cell and have common substrates, has also been recognized for their capacity to selectively control drug transfer across a variety of epithelial and endothelial blood-tissue barriers.

In the context of drug development, *in-vitro* expression models are being used extensively to characterize transporter-drug interactions. From a regulatory perspective, these analyses are warranted by concerns that interindividual variation in transporter function and drug interactions may influence pharmacokinetics and ultimately pharmacodynamics (Zhang et al., 2008; Zhang et al., 2009). As a result, transporter effects have been included in the drug labeling requirements (Zhang et al., 2008; Zhang et al., 2009). Currently, efforts are ongoing in the industry and at the FDA to develop and evaluate models for predicting the relevance of interactions between drugs and efflux or uptake transporters. These efforts are focused on classifying individual drugs as transporter substrates, inhibitors, and inducers and on providing quantitative measures that will prompt further in-vivo studies for rigorous evaluation of clinical relevance.

Widely accepted systems for such studies include cells that polarize (e.g., MDCKII) and overexpress a cloned transporter. Ideally, this model system has tight junctions and no endogenous transporters that would interact with the drug of interest. While qualitatively useful for identification of substrates, using these expression systems for quantitative assessments should be carefully considered (Kalvass and Pollack, 2007) before making conclusions based on mathematical modeling of the transport data.

Although Michaelis-Menten type relationships analysis is often used to assess drug-transporter interactions, there are multiple assumptions, which if not carefully considered could potentially yield misleading results. Some of the assumptions include minimum contribution by physical barriers such as the unstirred water layer, minimum contribution by passive diffusion, and minimum paracellular transport. Here we examine how these assumptions can potentially influence the quantitative assessments of transport parameters obtained using these monolayer systems and offer insights and guidelines for analyzing vectorial transport data.

Comprehensive Model for Transport Pathways across a Transwell System

Flux across a cell monolayer grown on a support filter (e.g., Transwells) can be represented by a series of sequential and parallel barriers (**Figure 6-1, Panel A**). The barriers include permeability across the unstirred water layer at surfaces (PS_{UWL}), permeability across the filter (PS_F) and ultimately permeability across the monolayer itself (PS_M).

An equation can be written to describe overall permeability ($PS_{Overall}$) that includes consideration of the properties of filter itself as well as flux across the parent cell model monolayer (assuming no active uptake or efflux processes present at basolateral or apical membranes) such that

$$\frac{1}{PS_{Overall}} = \frac{1}{PS_{UWL,B}} + \frac{1}{PS_F} + \frac{1}{PS_M} + \frac{1}{PS_{UWL,A}} \qquad 6\text{-}1$$

Experimentally it is difficult to discern permeability through the unstirred water layer and the filter and these terms are generally combined to yield

$$\frac{1}{PS_{Overall}} = \frac{1}{PS_{F\ \&\ UWL}} + \frac{1}{PS_M} \qquad 6\text{-}2$$

The contribution of diffusion through the porous filter to overall permeability is rather negligible. However, diffusion across the unstirred water layer may present a significant barrier for more lipophilic drugs, whereas the cell monolayer itself is the rate limiting step in the overall permeability for more hydrophilic drugs.

The monolayer presents two distinct parallel pathways through which drug can pass, transcellular (PS_{TC}) and paracellular (PS_{PC}) as shown in **Figure 6-1, Panel B**.

$$PS_M = PS_{TC} + PS_{PC} \quad \text{6-3}$$

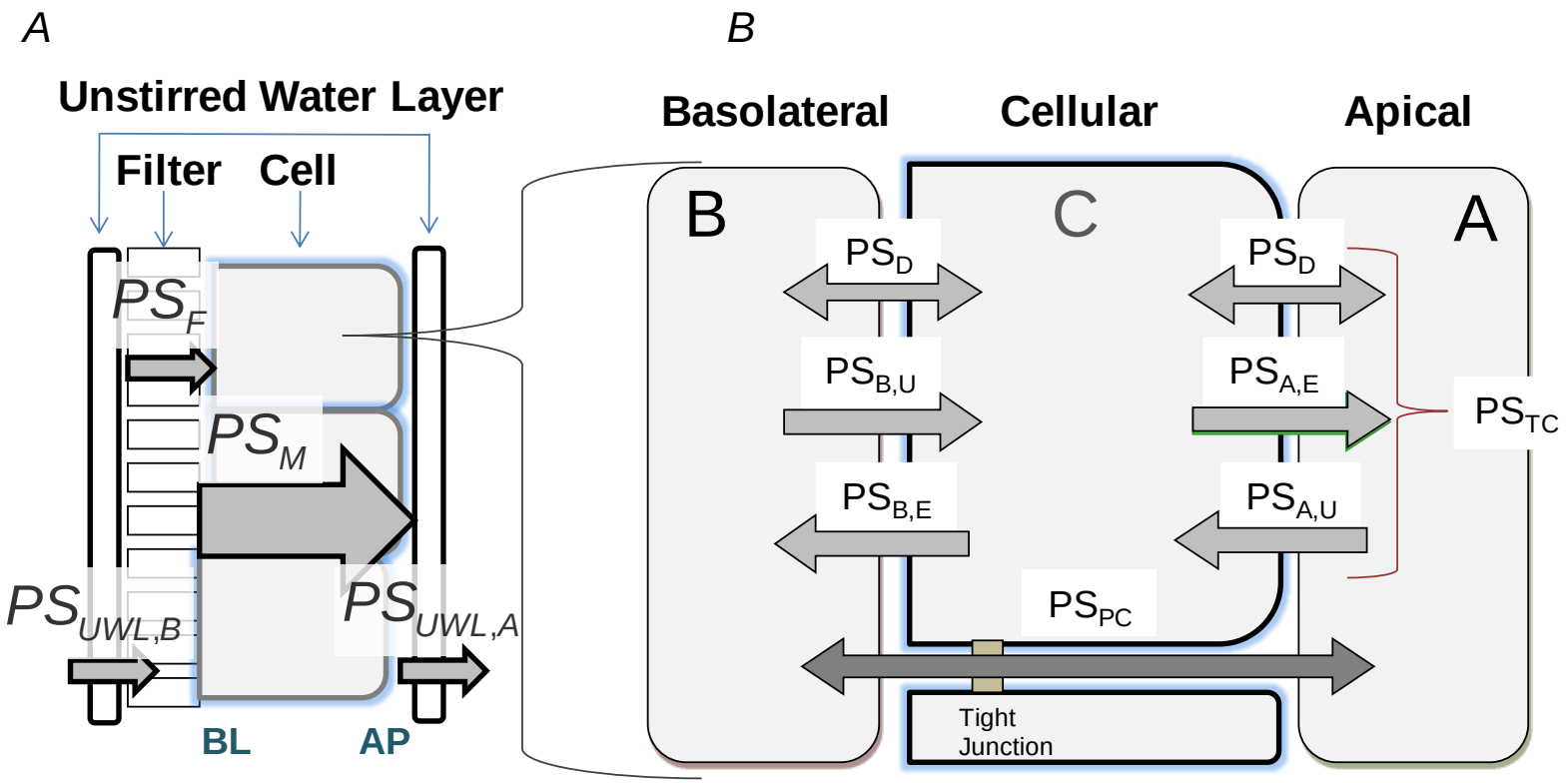

Figure 6-1 Panel A: Model of flux across monolayer on Transwell system, depicting permeability-surface area clearance across unstirred water layers (P_{UWL}), the filter (PS_F) and the cell monolayer itself (PS_M). The subscripts A and B denote the apical (AP) or basolateral (BL) compartments. **Panel B**: Model of flux across a model cell monolayer with all possible active transport processes. The model depicts the processes governing the transfer of drug from the basolateral to apical compartments across the MDCKII (cellular) compartment. Transfer processes include diffusion (PS_D), active uptake on the basolateral and apical membranes ($PS_{B,U}$ and $PS_{A,U}$, respectively), active efflux on the basolateral and apical membranes ($PS_{B,E}$ and $PS_{A,E}$, respectively) as well as paracellular diffusion (PS_{PC}). Transcellular transport processes are denoted as PS_{TC}.

The latter depends largely on the molecular size and the integrity of tight junctions. The former is comprised of two distinct barriers, the basolateral and apical membranes, with each containing multiple pathways that restrict or facilitate passage. At a minimum, diffusion occurs across both membranes (PS_D) and drug must cross these barriers in series.

$$PS_M = \frac{PS_D}{2} + PS_{PC} \qquad 6\text{-}4$$

Careful consideration must be given to passage across the unstirred water layer since it may present the rate limiting barrier for some drugs. While the above analysis is restricted to diffusion (i.e., parent cell line), there are implications for expression systems as well. The observations of Balakrishnan et al (Balakrishnan et al., 2007) suggest that a similar phenomena may occur for less lipophilic drugs for which flux across empty or parent cell monolayers is controlled by diffusion. Their flux in overexpression systems, however, may be so rapid that the unstirred water layer becomes rate limiting. Hence, variation in transporter expression or substrate affinity can readily influence which barrier is rate limiting (Balakrishnan et al., 2007).

For the remainder of the paper, the contribution of the unstirred water layer will be assumed to be negligible.

Integrated Monolayer Model

While the resistance approach is simple and direct, there are limitations in its application and a broader model is warranted to explore the contributions of the two membranes to overall flux. Assuming no endogenous transporters, passive diffusion permeability (PS_D) is the same across both membranes, no cellular metabolism, and rapid intracellular diffusion, a kinetic model (**Figure 6-1, Panel B**) can be described by the following set of differential equations.

Substrate flux into and out of the basolateral compartment, B, can be described by the following equation

$$\frac{dX_B}{dt} = C_C\left(PS_D + PS_{B,E}\right) - C_B\left(PS_D + PS_{B,U}\right) + (C_A - C_B)PS_{PC} \quad \text{6-5}$$

where X_B is the mass of drug in the basolateral compartment; C_C, C_B and C_A are the concentration of drug in the cellular, basolateral and apical compartment, respectively; $PS_{B,E}$, $PS_{B,U}$ and PS_{PC} are the permeability-surface area products for basolateral efflux, basolateral uptake and paracellular pathways, respectively.

Substrate flux into and out of the cellular compartment, C, can be described by the following equation

$$\frac{dX_C}{dt} = C_A\left(PS_D + PS_{A,U}\right) + C_B\left(PS_D + PS_{B,U}\right) - C_C\left(2PS_D + PS_{A,E} + PS_{B,E}\right) \quad \text{6-6}$$

where X_C is the mass of drug in the cellular compartment; $PS_{A,U}$ and $PS_{A,E}$ are the permeability-surface area products for apical uptake and apical efflux pathways, respectively.

Substrate flux into and out of the apical compartment, A, can be described by the following equation

$$\frac{dX_A}{dt} = C_C\left(PS_D + PS_{A,E}\right) - C_A\left(PS_D + PS_{A,U}\right) + (C_B - C_A)PS_{PC} \quad \text{6-7}$$

where X_A is the mass of drug in the cellular compartment.

Flux Across an Untransfected Cell Line

Assuming the absence of both active uptake into and efflux out of the cell, initial permeability for the basolateral to apical direction in the parent untransfected cell line ($PS_{B\rightarrow A,Parent}$) can be written as

$$PS_{B\rightarrow A,Parent} = \left[\frac{PS_D}{2} + PS_{PC}\right] \quad \text{6-8}$$

An identical equation can be written for flux in the apical to basolateral direction. Fluxes via parallel pathways, like diffusion through the cell $\left(\frac{PS_D}{2}\right)$ and between cells (PS_{PC}), are summed, while flux via pathways in series (i.e., diffusion across basolateral and apical membranes) is the reciprocal of the sum of the reciprocals $\left(\frac{1}{PS_D}+\frac{1}{PS_D}\right)$.

Initial Rate of B-to-A flux across a Monolayer

For most experiments, an initial directional flux rate is often used. The initial flux or appearance in the apical compartment for drug transferred from B→A (assuming C_A=0), Equation 6-7 can be written as

$$\frac{dX_{A,B\rightarrow A}}{dt} = C_C\left(PS_D + PS_{A,E}\right) + C_B^0 PS_{PC} \qquad 6\text{-}9$$

If rapid equilibrium between the basolateral and cellular compartment is assumed$\left(\frac{dX_C}{dt}=0\right)$, then Equation 6 can be rewritten as

$$Cc = \frac{C_B^0\left(PS_D + PS_{B,U}\right)}{\left(2PS_D + PS_{A,E} + PS_{B,E}\right)} \qquad 6\text{-}10$$

Substituting Equation 10 into Equation 9 yields

$$\frac{dX_{A,B\rightarrow A}}{dt} = C_B^0\left[\frac{\left(PS_D + PS_{B,U}\right)\left(PS_D + PS_{A,E}\right)}{\left(2PS_D + PS_{A,E} + PS_{B,E}\right)} + PS_{PC}\right] \qquad 6\text{-}11$$

Hence, the initial permeability for the basolateral to apical direction ($PS_{B\rightarrow A}$) can be described by the following equation

$$PS_{B\rightarrow A} = \frac{\frac{dX_{A,B\rightarrow A}}{dt}}{C_B^0} = \left[\frac{\left(PS_D + PS_{B,U}\right)\left(PS_D + PS_{A,E}\right)}{\left(2PS_D + PS_{A,E} + PS_{B,E}\right)} + PS_{PC}\right] \qquad 6\text{-}12$$

Initial Rate of A-to-B flux across a Monolayer

Likewise the directional flux rate in the apical to basolateral direction (assuming C_B=0) can be written as

$$\frac{dX_{B,A\to B}}{dt} = C_C\left(PS_D + PS_{B,E}\right) + C_A^0 PS_{PC} \qquad 6\text{-}13$$

Assuming rapid equilibrium between the apical and cellular compartments $\left(\frac{dX_C}{dt} = 0\right)$, Equation 6-6 can be rewritten as

$$C_C = \frac{C_A^0\left(PS_D + PS_{A,U}\right)}{\left(2PS_D + PS_{A,E} + PS_{B,E}\right)} \qquad 6\text{-}14$$

Substituting Equation 6-14 into Equation 6-13 yields the initial permeability for the apical to basolateral direction ($PS_{B\to A}$)

$$PS_{A\to B} = \frac{\frac{dX_{B,A\to B}}{dt}}{C_A^0} = \left[\frac{\left(PS_D + PS_{A,U}\right)\left(PS_D + PS_{B,E}\right)}{\left(2PS_D + PS_{A,E} + PS_{B,E}\right)} + PS_{PC}\right] \qquad 6\text{-}15$$

Flux Across a Transfected Cell Line

In order to understand the limitations of models describing flux across a monolayer, a broadly encompassing model that includes all of the flux processes can be utilized (**Figure 6-1, Panel B**). Such an approach may be required to explore the relative contributions of the two membranes to overall transcellular flux as well as the contribution of paracellular flux. However, this paper will focus attention on the most frequent analysis and on what is the current focus of the Drug-Drug Interaction Draft Guidance at the FDA; a monolayer in which an apical efflux transporter (i.e., P-gp, ABCG2, MRPs) has been expressed. **Table 6-1** contains various scenarios to describe flux across such a model system.

In a single transfected system like ABCG2 (or MRPs), the other pathways are assumed to be negligible $\left(PS_{B,U}, PS_{A,U}\ and\ PS_{B,E} = 0\right)$ and Equation 6-12 can be rewritten as

$$PS_{B\rightarrow A,ABCG2} = PS_D \left[\frac{\left(1 + \left\{\frac{PS_{AE}}{PS_D}\right\}\right)}{\left(2 + \left\{\frac{PS_{AE}}{PS_D}\right\}\right)}\right] + PS_{PC} \qquad 6\text{-}16$$

Table 6-1 Scenario 2 describes the PS_{Obsl} for the ABCG2 transfected cell line in which passage across both membranes and between cells are contributing to the overall flux.

$PS_{A,E}$ is determined by the properties of the substrate and the transporter, and can be written as in Equation 6-17

$$PS_{A,E} = \frac{T_{Max}}{(K_M + C_C)} \qquad 6\text{-}17$$

where T_{Max} is the maximum transfer rate associated with the active transport process, K_M is the Michaelis-Menten constant (inversely related to affinity) for the transporter substrate complex and C_C is the intracellular drug concentration available to interact with the transporter.

As defined, $PS_{A,E}$ can vary according to inherent substrate characteristics (K_M and T_{Max}) or due to transporter expression level (scaling of T_{Max}). During the development of transfected cell lines, clones with high transporter expression levels are selected in order to develop a positive response model for identifying substrates and predict the role of the transporter in the drug's disposition (i.e., significant change in B→A rate). Thus, this process is inherently biased for selecting clones that can achieve a much greater $PS_{A,E}$ (e.g., 10-fold) than PS_D. Hence, $\frac{dX_{A,B\rightarrow A}}{dt}$ increases with increasing $PS_{A,E}$ until it achieves a maximal flux

that is the upper boundary ($PS_D + PS_{PC}$), as defined by Equation 6-18, which evaluates Equation 6-16 at high $PS_{A,E}$ values relative to PS_D.

Table 6-1 Models depicting initial flux rates for parent and cloned cell model with diffusion across membranes (PS_D), diffusion via paracellular pathway (PS_{PC}) and active transport via an apical efflux transporter (PS_{AE}) as well as the determinants of overall permeability (PS) for parent cell line as well as low and high expressing clones.

Scenario	B→A Flux		A→B Flux	
	Model	**Determinants of overall PS**	**Model**	**Determinants of overall PS**
1. Empty or Parent Cell Line	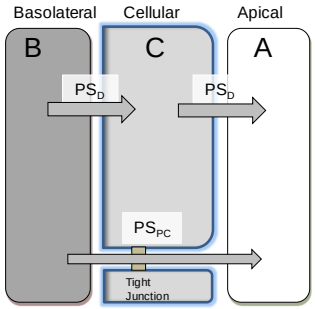	$\frac{PS_D}{2} + PS_{PC}$	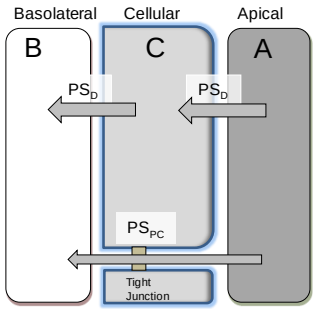	$\frac{PS_D}{2} + PS_{PC}$
2. Apical Efflux Transporter *Low Expression*	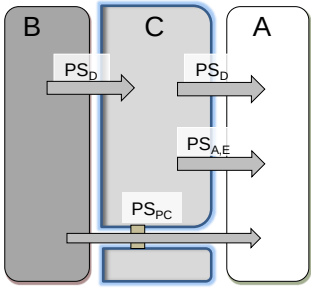	$PS_D \left[\frac{\left(1 + \left\{\frac{PS_{AE}}{PS_D}\right\}\right)}{\left(2 + \left\{\frac{PS_{AE}}{PS_D}\right\}\right)}\right] + PS_{PC}$	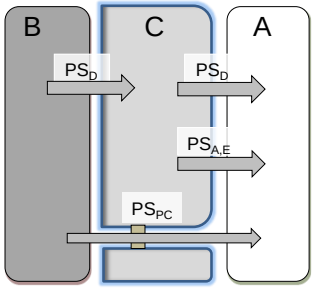	$PS_D \left[\frac{1}{\left(2 + \left\{\frac{PS_{AE}}{PS_D}\right\}\right)}\right] + PS_{PC}$
3. Apical Efflux Transporter *High Expression* (PS_{AE}>>PS_D)	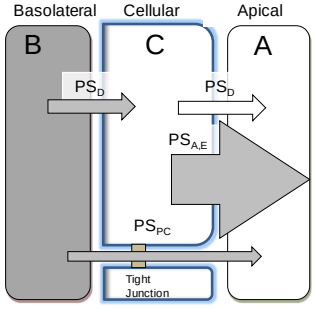	$PS_D + PS_{PC}$ **Upper Boundary** Apical membrane ceases to be a barrier; passage across basolateral membrane is rate limiting for transcellular flux.	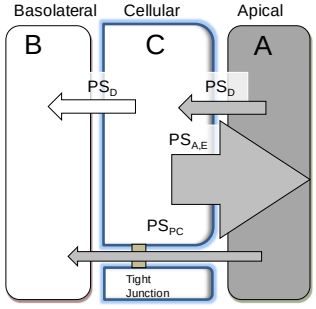	PS_{PC} **Lower Boundary** All drug entering the cell is pumped back into apical compartment; only drug appearing in B is associated with paracellular pathway.

$$\lim_{PS_{A,E} \gg PS_D} PS_{B \to A, \boldsymbol{ABCG2}} = [PS_D + PS_{PC}] \qquad 6\text{-}18$$

In this limiting case, it becomes increasingly difficult to distinguish the role of $PS_{A,E}$ in the overall transport. Flux across the apical membrane becomes so rapid such that overall vectorial flux across the monolayer is controlled by diffusion through the basolateral membrane (PS_D) as well as by the paracellular pathway (**Table 6-1, Scenario 3**). Clearly the B→A flux rate has a fixed dynamic range (2 fold) which is bounded and scaled by PS_D.

In a similar fashion, A→B flux for single transfected system like ABCG2 (Equation 6-15) can be rewritten as

$$PS_{A \to B, ABCG2} = PS_D \left[\frac{1}{\left(2 + \left\{ \frac{PS_{AE}}{PS_D} \right\}\right)} \right] + PS_{PC} \qquad 6\text{-}19$$

Likewise as $PS_{A,E}$ increases, flux in the A→B direction reaches a lower limiting value.

$$\lim_{PS_{A,E} \gg PS_D} PS_{A \to B, ABCG2} = PS_{PC} \qquad 6\text{-}20$$

All drug mass that enters the cell by diffusion across the apical surface is pumped back into the apical compartment and does not cross the basolateral membrane (**Table 6-1**, **Scenario 3**). Hence, only drug diffusing via the paracellular pathway reaches the basolateral compartment.

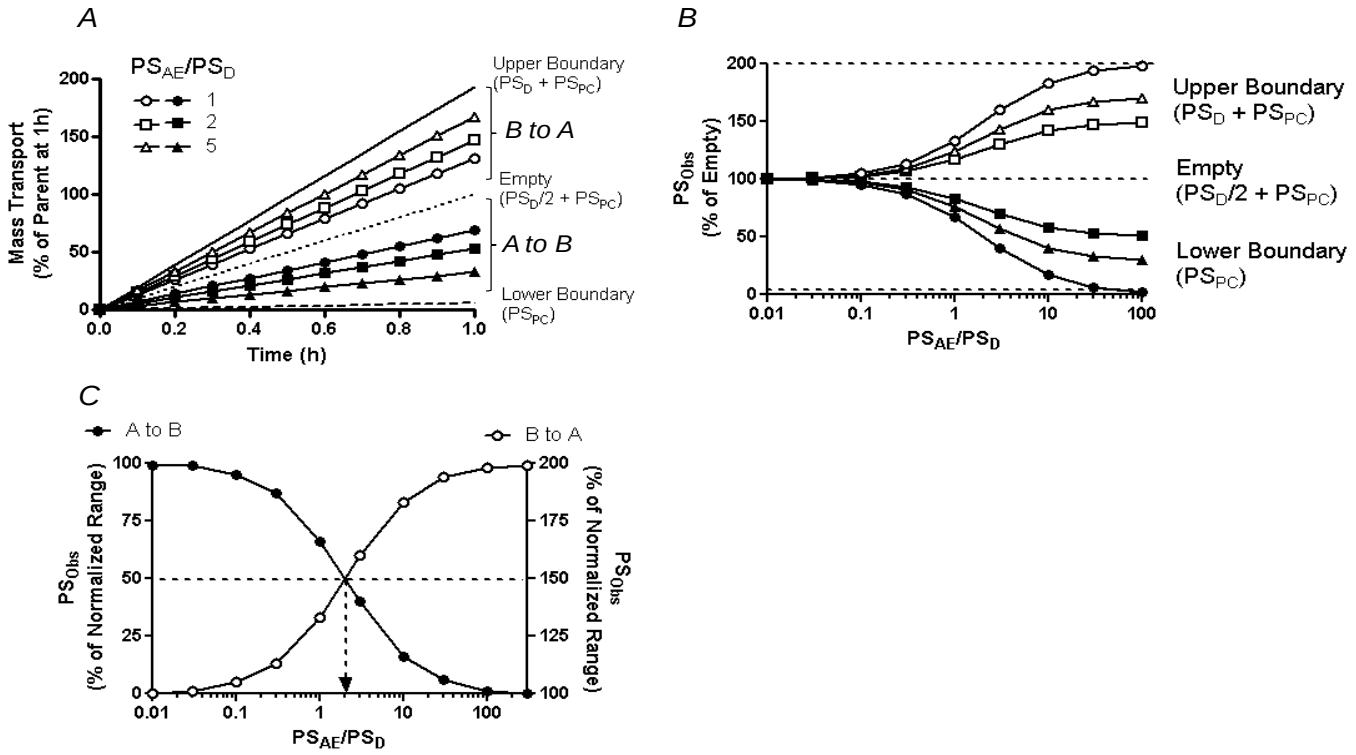

Figure 6-2 Panel A: Effect of increasing permeability-surface area clearance attributed to apical efflux ($PS_{A,E}$) on observed flux (PS_{obs}). B to A flux increases as $PS_{A,E}$ increases to a maximum of diffusion across the basolateral membrane (PS_D) and paracellular pathway (PS_{PC}). A to B flux (dX/dt) decreases as $PS_{A,E}$ increases to a minimum of diffusion across the paracellular pathway (PS_{PC}). As the apparent permeability and permeability-surface area product are proportional to flux, substituting any of these parameters on the y-axis would yield the same relationship. **Panel B**: The influence of $PS_{A,E}$ relative to PS_D on permeability flux (PS_{obs}) for situations where PS_D is two (squares), five (diamonds) or greater than 10 times (circles) the paracellular flux (PS_{PC}). **Panel C**: Data from Panel B is normalized by adjusting for the dynamic range; all of the data from B to A (open circle) or A to B (closed circle) collapse to the identical line.

Numerous published reports utilize the initial B→A vectorial transfer of drug to determine the influence of an apical efflux transporter. While a logical approach, its limitations as a quantitative tool are rarely appreciated (Kalvass and Pollack, 2007). From a practical perspective it is useful to consider those conditions under which an apically expressed transporter contributes to the overall flux of a series of drugs (or a given drug in a series of clones that vary in expression levels of the transporter). **Figure 6-2 Panel A** shows the influence of $PS_{A,E}$ (relative to PS_D) on the mass transfer of drug across a monolayer. As $PS_{A,E}$ increases, the directional flux reaches an upper (B→A) and lower (A→B) boundary that is controlled by the diffusion properties of the basolateral membrane and paracellular passage. Such data could experimentally arise due to clonal selection, i.e., comparing transcellular flux of one drug in different clones ($PS_{A,E}$ varies due to increasing transporter expression) or in comparing various drugs in a single clone (varied $PS_{A,E}$ or PS_D). For either situation, overall flux (PS_{Obs}) is bounded between the flux observed in the parent cell line (Equation 6-8) and the flux observed in the clone when $PS_{A,E} >> PS_D$ (Equation 6-18). At lower $PS_{A,E}$ to PS_D ratios ($PS_{A,E} / PS_D < 0.2$), contributions of active efflux is less apparent. The appearance of drug in the apical compartment is governed by diffusion across both basolateral and apical membrane with contribution from paracellular diffusion. At much higher $PS_{A,E}$ to PS_D ratios (($PS_{A,E} / PS_D > 20.$), flux approaches the boundary (i.e., diffusion across the basolateral membrane and paracellular pathway become rate limiting). **Figure 2 Panel B** further illustrates this phenomena by plotting the measured flux as a function of $PS_{A,E}$ normalized to PS_D. Kalvass and Pollack (Kalvass and Pollack, 2007) presented a similar figure (Figure 6-2 in their reference) however, their model assumed paracellular to be nonexistent ($PS_{PC}=0$). For drugs which have poor diffusion permeability ($PS_D<10*PS_{PC}$) it is clear that paracellular flux cannot be ignored. If the observed permeability surface area product (PS_{obs}) is normalized for the dynamic range (influenced by PS_{PC}) then all of the curves in **Figure 6-2 Panel B** collapse into a one B→A and one A→B flux graph can be seen as in **Figure 6-2 Panel C**. The inflection point in PS_{Obs} (50% in A to B and 150% for B to A)

occurs when PS_{AE} / PS_D = 2. When this ratio is much less than 2, both basolateral and apical membranes contribute to controlling the appearance of drug in the receiver side. When the ratio is much greater than 2, passage across the apical membrane ceases to be a barrier for B→A flux and drug appearance in the donor side is controlled by diffusion across the basolateral membrane and diffusion via paracellular route. For A→B flux ($PS_{A,E}$ / PS_D >> 2) the drug appearance in the receiver side is limited to drug arriving via paracellular passage. Hence, the region near the inflection point is the most sensitive to changes in PS_{AE} and has important implications when considering clonal selection, saturation and inhibition of the transporter (changes in apparent PS_{AE}) and these concepts will be utilized later on in the paper. Normalization (**Figure 6-2 Panel C**) provides a more universal application (a single graphical representation); however, it may also be somewhat misleading. Data transformation as advocated by a number of groups (Kalvass and Pollack, 2007; Giacomini et al., 2010; Lumen et al., 2010), including efflux ratios (ER_A, ER_α) or the ratios of ratios ($ER_{\alpha(+inhibitor}$ / $ER_{\alpha(-inhibitor)}$), can distort the experimental error and may result in a loss of critical insight between the experimental observation and its determinants, e.g., role of PS_{PC} in parameter estimation (see below). While PS has its limitations (Kalvass and Pollack, 2007), PS, like systemic clearance, can be more readily related to underlying principles (i.e., rate limiting steps).

ER_A

Frequently the rate of flux in B→A direction in the transfected cell line is compared to the parent cell line to quantitate the contribution of an apically expressed transporter. This ratio is termed ER_A and is estimated by

$$ER_A = \frac{PS_{B\rightarrow A,AABCG2}}{PS_{B\rightarrow A,Parent}} \qquad 6\text{-}21$$

Substituting Equation 6-16 and 6-19 and assuming $PS_{A,E} \gg PS_D$, Equation 21 yields

$$ER_A = \frac{2(PS_D + PS_{PC})}{(PS_D + 2PS_{PC})} \quad \text{6-22}$$

Equation 6-22 would imply that this ratio is independent of the very parameter of interest, namely $PS_{A,E}$.

Moreover, as PS_{PC} approaches 0 (or is low relative to PS_D), ER_A approaches a limit

$$\lim_{\substack{PS_{A,E} \gg PS_D \\ PS_{PC} \to 0}} ER_A = 2 \quad \text{6-23}$$

This limitation was pointed out in the work by Kalvass and Pollack (Kalvass and Pollack, 2007). **Table 6-2** illustrates this point with ER_A for both murine (Abcg2) and human (ABCG2) derived from the literature. ER_A approaches the limitation of 2 for most drugs, especially for the Abcg2 clones and supports the earlier assumption that for many of these substrates $PS_{A,E} \gg PS_D$ largely due to the high transporter expression level for these clones. Hence, ER_A is not a discriminating parameter since it has limited dynamic range and the numerical value is independent of ABCG2 flux ($PS_{A,E}$). Rather ER_A reflects the fact that flux across the system has changed from one controlled by diffusion across two barriers arranged in series ($PS_D/2$) to diffusion across one barrier (PS_D), the basolateral membrane.

ER_α

In contrast to ER_A, a more robust parameter is the ratio of the rate of flux in one direction (B→A) over the opposite flux (A→B) in the transfected cell line (Kalvass and Pollack, 2007). This ratio is termed the asymmetrical ER (ER_α) and is estimated by

$$ER_\alpha = \frac{PS_{B \to A,Abcg2}}{PS_{A \to B,Abcg2}} \quad \text{6-24}$$

Equation 6-24 can be rewritten using Equations 16 and 18 and experimentally setting $C_A^0 = C_B^0$

$$ER_{\alpha} = \frac{PS_D\left[\frac{\left(1+\left\{\frac{PS_{AE}}{PS_D}\right\}\right)}{\left(2+\left\{\frac{PS_{AE}}{PS_D}\right\}\right)}\right] + PS_{PC}}{PS_D\left[\frac{1}{\left(2+\left\{\frac{PS_{AE}}{PS_D}\right\}\right)}\right] + PS_{PC}} \quad \text{6-25}$$

Moreover, as PS_{PC} approaches 0 (or is low relative to PS_D), ER_{α} approaches a limit

$$\lim_{PS_{PC}\to 0} ER_{\alpha} = 1 + \left\{\frac{PS_{AE}}{PS_D}\right\} \quad \text{6-26}$$

It would appear that ER_{α} can be more readily related to $PS_{A,E}$ (Equation 27) and this relationship has been explored in the work of Kalvass and Pollack (Kalvass and Pollack, 2007).

$$PS_{AE} = PS_D(ER_{\alpha} - 1) \quad \text{6-27}$$

The magnitude of ER_{α} estimates obtained in mouse and human ABCG2 expressing cells is much greater; hence, it appears to be more discriminating compared to ER_A (**Table 6-2**). The ER_{α} for the empty or parent cell is close to unity (+/-20%) for most substrates suggesting that endogenous transporters in MDCKII cells are playing a minor role in the flux of these molecules. Exceptions to this assumption would include cimetidine, estradiol, nitrofurantoin, riboflavin and topotecan; indicating a likely interaction with endogenous MDCKII transporters.

Table 6-2 Comparison of the ER_A and ER_α of several Abcg2/ABCG2 substrates in murine and human Abcg2/ABCG2-transfected MDCKII cell lines in the literature. Apical efflux ratios (ER_A), asymmetry efflux ratios (ER_α), and the ratio of the asymmetry ratios in Abcg2/ABCG2-transfected vs. empty vector-transfected cells (ER_α Ratio) in mouse (mAbcg2) or human (ABCG2) transfected MDCKII cells were calculated using flux data compiled from the literature. Drugs where the mean of ER_α Empty was not within 20% of unity were identified (shaded rows).

Substrate	Empty	mAbcg2		ABCG2		Reference
	ER_α	ER_A	ER_α	ER_A	ER_α	
Aflatoxin	1.12	1.58	9.32	1.15	1.91	(van Herwaarden et al., 2006)
Albendazole	1.14	1.70	18.3	1.36	2.11	(Merino et al., 2005a)
Cimetidine	1.26	3.01	7.14	2.44	3.11	(Pavek et al., 2005)
Ciprofloxacin	0.88	2.52	4.37	1.18	2.13	(Merino et al., 2006a)
Estradiol	0.68	-	-	0.83	0.66	(Pavek et al., 2005)
Imatinib	1.03	2.39	35.3	-	-	(Breedveld et al., 2005)
IQ	1.09	1.84	16.7	1.30	2.47	(van Herwaarden et al., 2006)
Nitrofurantoin	0.64	2.63	8.70	2.66	3.21	(Merino et al., 2005b)
Norfloxacin	0.91	2.92	3.26	1.29	1.32	(Merino et al., 2006a)
Ofloxacin	0.90	2.22	6.17	1.29	1.56	(Merino et al., 2006a)
Oxfendazole	1.14	2.35	5.70	0.87	1.17	(Merino et al., 2005a)
Pantoprazole	1.00	1.34	5.05	-	-	(Breedveld et al., 2004)
PhIP	1.20	1.27	16.43	1.89	12.7	(van Herwaarden et al., 2003; Pavek et al., 2005)
Riboflavin	0.13	2.33	1.65	-	-	(van Herwaarden et al., 2007)
Topotecan	2.23	3.13	14.85	1.46	5.79	(Breedveld et al., 2004; Pavek et al., 2005)
Trp-P-1	1.09	2.89	4.25	1.64	1.39	(van Herwaarden et al., 2006)

While valuable, there are limitations to the use of ER_α. In order to use ER_α as depicted in Equation 6-26, PS_{PC} was assumed to be negligible. In our lab (as in

others), PS_{PC} in MDCKII cells is relatively low, but not zero (1-2% of the amount initially in the donor per hour). PS_{PC} contributes significantly to passage of drugs with lower lipophilicity, the very drugs for which transporters would appear to be most critical. As indicated by the ratio of Equations 6-18 and 6-20, at the limit (i.e., assuming that $PS_{A,E}>>PS_D$ when clones are overexpressing the transporter), ER_α, much like ER_A, reflects the ratio of fluxes that are independent of the transporter protein (Equation 6-28).

$$\lim_{PS_{A,E}\gg PS_D} ER_\alpha = \frac{\lim\limits_{PS_{A,E}\gg PS_D} PS_{B\rightarrow A,ABCG2}}{\lim\limits_{PS_{A,E}\gg PS_D} PS_{A\rightarrow B,ABCG2}} = \frac{[PS_D + PS_{PC}]}{PS_{PC}} \qquad 6\text{-}28$$

Hence, evaluating the vectorial transport of high affinity substrates in overexpressing clones may generate ER_α values that do not correlate with PS_{AE}.

The influence of PS_{PC} on ER_α is demonstrated in **Figure 6-3 Panel A**. When PS_{PC} is zero there is a linear relationship between the ER_α and $PS_{A,E}$ regardless of the PS_D value. However, in the presence of a typical PS_{PC} there is a deviation from linearity such that ER_α is no longer proportional to $PS_{A,E}$. The deviation becomes more problematic as PS_D decreases since the paracellular pathway contributes more to the overall flux in either direction. At high ratios of PS_{AE} / PS_D, ER_α reaches the experimental boundary defined by Equation 6-28. The impact of PS_{PC} on the estimation of PS_{AE} (Equation 6-27) is illustrated in **Figure 6-3, Panel B**. As PS_{PC} approaches zero then $PS_{A,E}$ is accurately estimated. However, in the presence of a typical PS_{PC}, estimates of $PS_{A,E}$ diverge from their true values, and substrates with the lower PS_D are most affected.

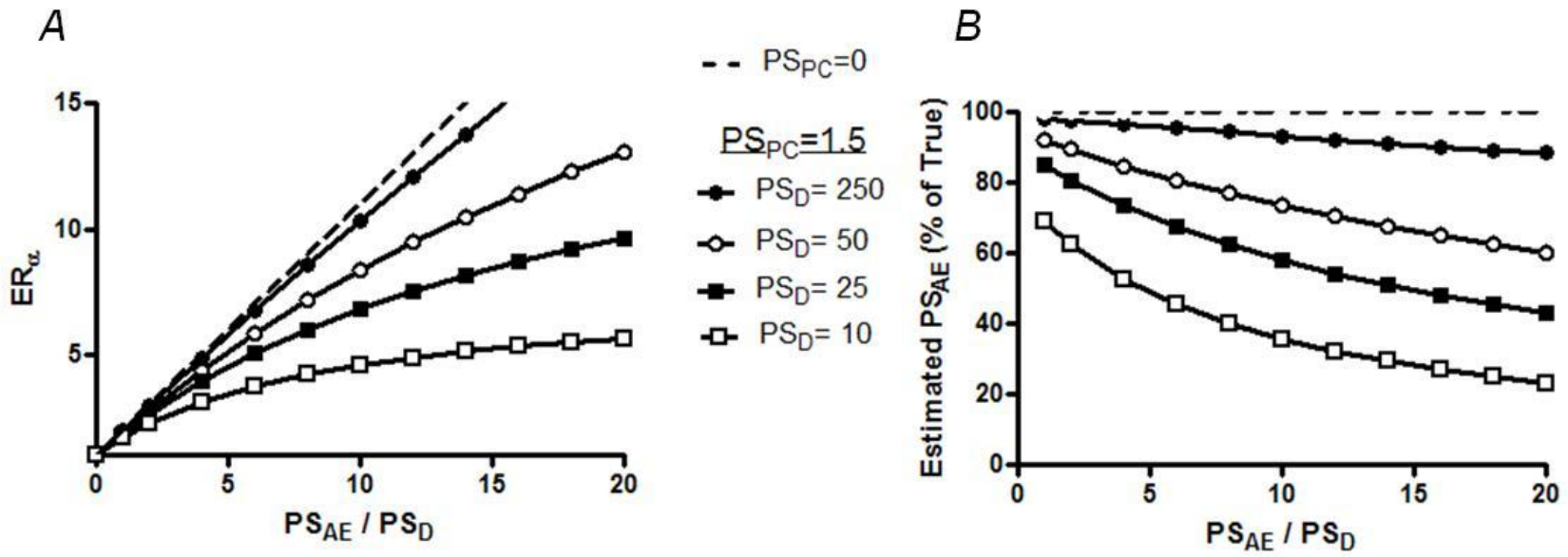

Figure 6-3 Panel A Asymmetrical flux ratio (ER_{α}) as a function of increasing $PS_{A,E}$ relative to PS_D (10, 25, 50 and 250 uL/hr*cm^2) when PS_{PC} is 1.5 uL/hr*cm^2. Dashed line represents the case for all values of PS_D when PS_{PC} is 0. **Panel B** Estimated apical efflux permeability **(**$PS_{A,E}$; Equation 27) relative to the true value of $PS_{A,E}$ as a function of increasing $PS_{A,E}$ relative to PS_D (10, 25, 50 and 250 uL/hr*cm^2) when PS_{PC} is 1.5 uL/hr*cm^2. Dashed line represents the case for all values of PS_D when PS_{PC} is 0.

Saturable $PS_{A,E}$

A number of investigators have characterized the influence of increasing donor concentration on the basolateral to apical flux of drug across a cell monolayer when characterizing an apical efflux transporter (Breedveld et al., 2004; Kitamura et al., 2008). The interpretation of such analysis has several limitations.

If $PS_{A,E}$ is assumed to be a saturable process (Equation 6-17), then Equation 16 can be rewritten to describe the flux of drug from basolateral to the apical side

$$PS_{B\rightarrow A,Abcg2} = PS_D \left[\frac{\left(1+\left\{\frac{T_{Max}}{PS_D(K_M+C_C)}\right\}\right)}{\left(2+\left\{\frac{T_{Max}}{PS_D(K_M+C_C)}\right\}\right)}\right] + PS_{PC} \qquad 6\text{-}29$$

As similar fashion, flux from apical to the basolateral side, Equation 6-19, can be written as

$$PS_{A\rightarrow B,Abcg2} = PS_D \left[\frac{1}{\left(2+\left\{\frac{T_{Max}}{PS_D(K_M+C_C)}\right\}\right)}\right] + PS_{PC} \qquad 6\text{-}30$$

In order to assess an accurate K_M the concentrations to be characterized are cellular and not donor concentration (basolateral or apical compartment). These concentrations are not equivalent; nor is the relationship between them fixed for a saturable efflux system. Earlier in considering the initial flux rates, it was assumed that the cellular concentration comes to rapid equilibrium and can be defined by the model parameters as in Equation 6-10 for (B→A flux) and Equation 6-14 (A→B flux); hence, it is possible to simulate C_C for the initial rate calculation. For a single transfected apical efflux transporter model examining B→A flux (as well as A→B flux), the relationship for C_C approximates the following.

$$C_C = C_B \frac{1}{\left(2+\frac{PS_{A,E}}{PS_D}\right)} \qquad 6\text{-}31$$

A more complex relationship arises when considering saturation of the efflux transporter as in Equation 6-32

$$C_C = C_B \frac{1}{\left(2 + \left\{\frac{T_{Max}}{PS_D(K_M + C_C)}\right\}\right)} \qquad 6\text{-}32$$

that can be rearranged to yield an expression which equates donor concentration (C_B) to a given cellular concentration

$$C_B = C_C \left(2 + \left\{\frac{T_{Max}}{PS_D(K_M + C_C)}\right\}\right) \qquad 6\text{-}33$$

Hence, simulations using cellular concentrations can be performed and donor concentrations derived from Equation 6-33. A much greater challenge is to assess cellular concentrations in an experimental setting; nonetheless simulations provide useful insights that guide experimental design and interpretation of the results.

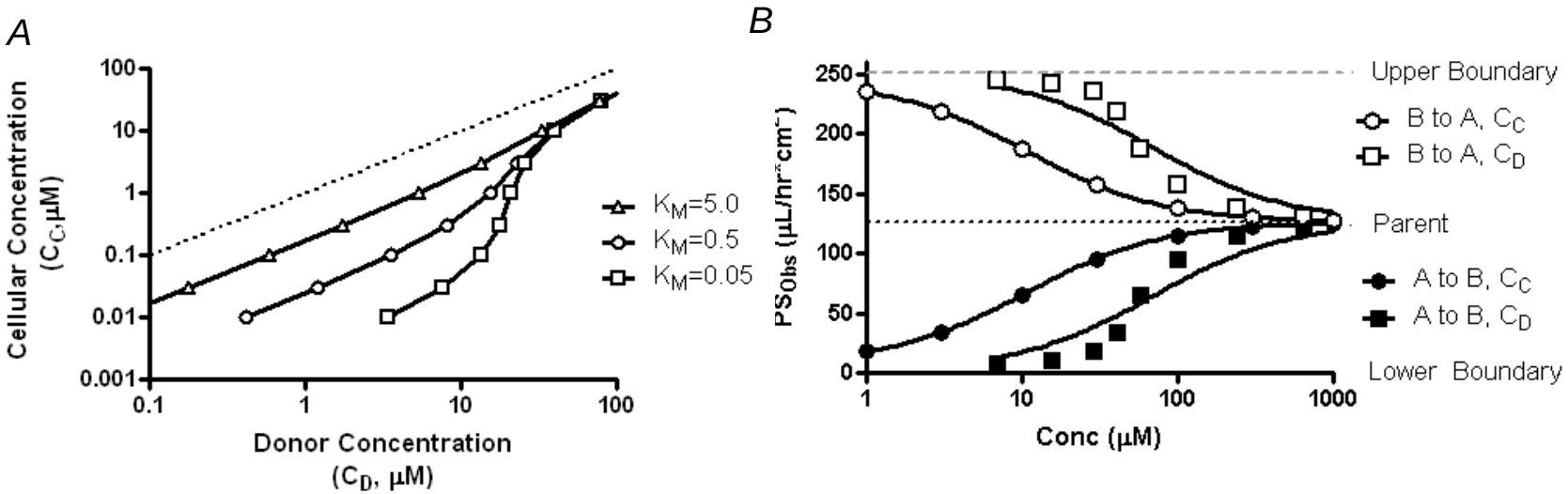

Figure 6-4: Panel A Internal cellular concentration (C_C) as a function of external donor concentration (C_D) for a drug modeled in which PS_D is fixed at 250 uL/hr*cm^2, T_{Max} is fixed at 5,000 pmol/hr/cm^{2}and K_M varies from 0.05 μM to 5 μM (hence, PS_{AE} varies from 100,000 to 1,000 uL/hr*cm^2, respectively). Dotted line represents line of unity. **Panel B** Concentration relationship between apparent PS_{obs} and cellular (C_C, open symbols) or donor (closed symbols) concentration for a drug with PS_D of 250 uL/hr*cm^2, PS_{PC} of 1.5 uL/hr*cm^2,T_{Max} of 5,000 pmol/hr/cm^2 and K_M of 0.5 μM. The simulation was performed using C_C and equations 29 and 30. Subsequently corresponding donor concentrations were solved for using the influence of saturating the apical efflux transporter (Equation 33).

Figure 6-4 Panel A illustrates the predicted relationship between cellular (C_C) and basolateral donor concentration (C_D) for a model system containing an apical efflux transporter. At low donor concentrations, the intercellular concentration is considerably lower for larger $PS_{A,E}$ (i.e., when K_M is smaller) since drug is pumped out of the cell more effectively. At higher donor concentrations, the transporter becomes saturated and the cellular concentration approaches a limit of half the donor concentration (i.e., same concentration achieved in parent cell line). While intuitively obvious, the full impact of this observation is realized when examining the **Panel B** in **Figure 6-4** which illustrates the relationship between observed flux and cellular or donor concentration. The nonlinear function relating cellular and donor concentration causes the relationship between flux and donor concentration (squares Panel B **Figure 6-4**) to be steeper than a simple saturation model. Without an appreciation for the need to model cellular concentration, a saturable model with a positive Hill coefficient (estimated near 2.5) would need to be invoked in order to describe the relationship between flux and donor concentration. If the cellular concentrations could be used, a simple saturation model is sufficient to characterize the model (circles **Figure 6-4 Panel B**).

Another limitation of this type of data is the interpretation of the inflection point on the plot of apparent PS and concentration (donor or cellular). As described earlier (**Figure 6-2**, **Panel B**) the 50% (A→B flux) and the 150% (B→A flux) value of the PS_{Obs} occurs when the value of $PS_{A,E}$ approaches twice that of PS_D. Typically this inflection point ($C_{C,inf\ pt}$) has been interpreted as being representative of K_M; however, this is inaccurate for flux across a monolayer. The concentration corresponding to this inflection point, $C_{C,inf\ pt}$ can be defined as

$$\frac{PS_{AE}}{PS_D} = \frac{\left[{T_{Max}}\Big/{\left(K_M + C_{C,\mathrm{inf\,pt}}\right)}\right]}{PS_D} = 2 \qquad 6\text{-}34$$

which can be rearranged to yield

$$\frac{C_{C,\text{inf pt}}}{K_M} = \frac{{}^{T_{Max}}/_{K_M}}{2PS_D} - 1 \qquad \text{6-35}$$

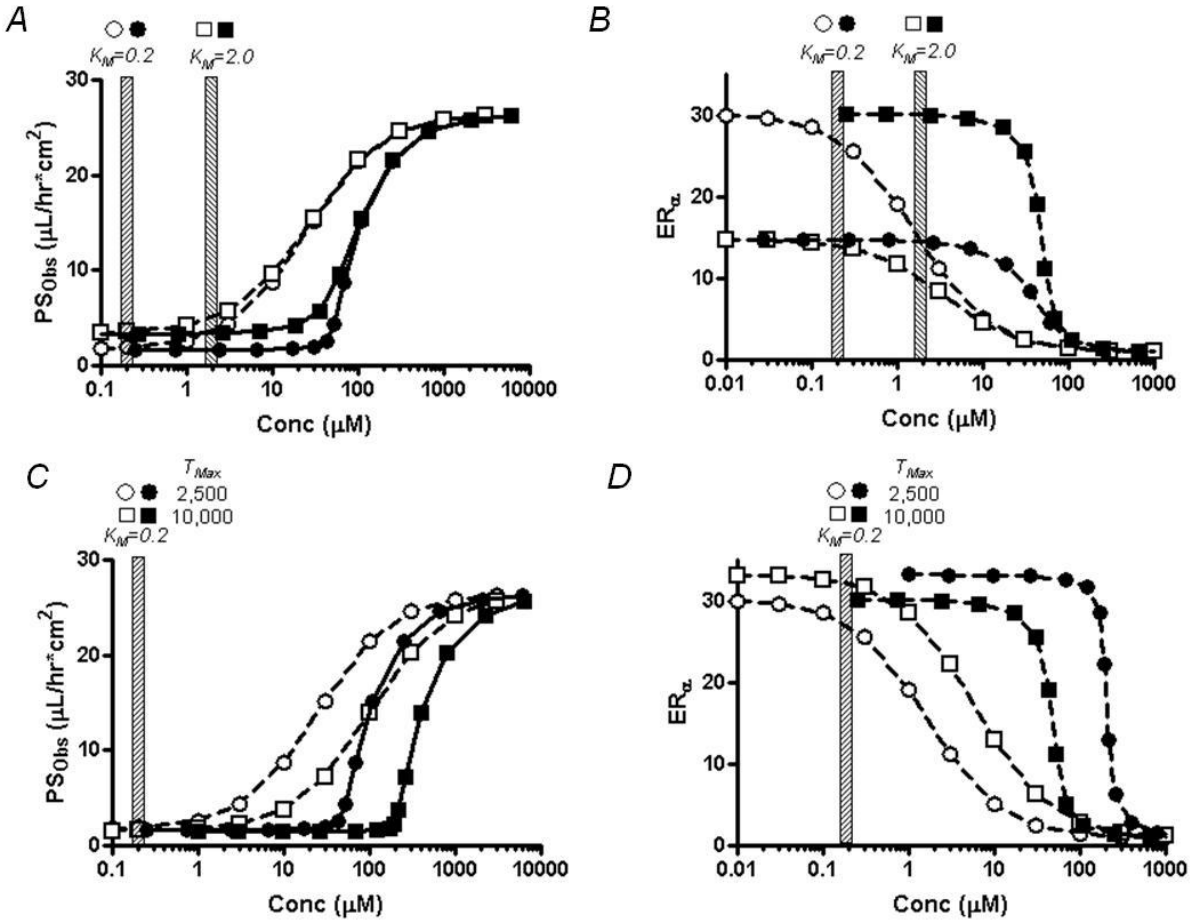

Figure 6-5 Apparent permeability-surface area clearance (PS_{obs}) A→B directional flux (**Panel A** and **C**) and ER_α (**Panel B** and **D**) as a function of substrate concentration (cellular: open symbols; donor: closed symbols). PS_{PC} is 1.5 uL/hr*cm^2 and PS_D is 50 uL/hr*cm^2 . **Panel A** and **B** Substrates vary in K_M with both substrates having a T_{Max} of 2.500 pmol/hr/cm^2. Substrate 1 (circles) has a K_M of 0.2 µM and Substrate 2 (squares) has a K_M of 2.0 µM. **Panel C** and **D** Substrates vary in T_{Max} with both substrates having a K_M of 0.2 µM. Substrate 1 (circles) possessing T_{Max} of 2.500 pmol/hr/cm^2, and Substrate 3 (squares) has a T_{Max} of 10,000 pmol/hr/cm^2.

As evident from Equation 6-17, PS_{AE} (at low C_C) is the ratio of T_{Max} to K_M.

$$\frac{C_{C,\text{inf pt}}}{K_M} = \frac{PS_{A,E}}{2PS_D} - 1 \qquad \text{6-36}$$

Hence, the greater the ratio of apical active efflux to diffusion permeability ($PS_{A,E}/PS_D>>2$) the greater $C_{C,infpt}$ will deviate from K_M. The mechanistic understanding of this deviation can be illustrated for the apical efflux transporter scenario depicted in **Table 6-1**. For high affinity transporter substrates tested in high expression cell monolayers, flux across the apical membrane at 1/2 $PS_{A,E}$ (when $C_C = K_M$) results in apical flux which is many fold greater than PS_D. However, flux across the apical surface will not be rate limiting under those conditions. $PS_{A,E}$ will only begin to approach $2PS_D$ when the C_C is much greater than K_M as defined by Equation 6-36. **Figure 6-5 Panel A** illustrates the change in A→B flux as a function of cellular and donor substrate concentration. [To simplify presentation, only A→B flux is depicted; however, B→A flux is a mirror image of A→B flux relative to the location of the inflection point]. The inflection point of PS_{Obs} (A→B or B→A) as a function of C_C does not correspond to K_M (**Figure 6-5 Panel A**). The cellular $C_{C, infpt}$ values were virtually identical at close to 25 μM for the two substrates despite the tenfold difference in K_M (0.2 and 2.0 μM, respectively). As predicted by Equation 6-36, the inflection point for PS_{Obs} occurs at a cellular concentration which is much larger than the K_M (125-fold for Substrate 1 and 12.5-fold for Substrate 2). Moreover, the corresponding donor concentrations (plotted in most flux experiments) were close to 100 μM for both substrates and the steepness of the relationship is again evident. Kalvass and Pollack (Kalvass and Pollack, 2007) advocate using ER_α rather than PS_{Obs} to estimate kinetic parameters. As can be seen in **Figure 6-5 Panel B** the inflection point is closer to K_M when plotting ER_α as a function of concentration; however, it is not equivalent to K_M even if the cellular concentrations were known (open symbols). The overall flux rate (or ratio of fluxes, ER_α) is dominated by the slow step, i.e., diffusion across the basolateral membrane. For the two examples depicted in **Figure 6-5** (**Panel A** and **B**) flux across the apical membrane at $C_C=K_M$ is 10 to 100 greater than flux across the basolateral membrane. This influence of $PS_{A,E}/2PS_D$ on inflection point for apparent PS can

also be seen in **Figure 6-5 Panel C,** in which K_M is common, but T_{Max} differs for the substrates. The cellular $C_{C,infpt}$ values were different at 25 and 95 μM for the two substrates despite having identical K_M values (0.2 μM). Equation 36 predicts an inflection point which would be 125-fold greater than K_M for Substrate 1 and 500-fold for Substrate 4 under the specified conditions. Again, the inflection point is closer to K_M when plotting ER_α as a function of concentration (**Figure 6-5 Panel D**) but far from identical. Again, the saturation of the apical efflux transporter becomes evident only when its flux rate slows considerably and approaches the diffusion permeability of the drug. Interpretation of monolayer flux data must be done with considerable appreciation for the limitations of the system and an understanding of those factors controlling flux.

Parameter Estimation for Saturable $PS_{A,E}$

Given the complexity of the donor to cellular concentration relationship (**Figure 6-4, Panel A**) and the fact that PS_{Obs} is a hybrid parameter, estimation of kinetic parameters from Transwell flux data is problematic, but not intractable. **Table 6-3** outlines an approach that can provide estimates of T_{Max} and K_M using Transwell flux data. Several key assumptions underpin the analysis such as (1) paracellular flux of the drug can be modeled using the flux of a marker substrate (e.g., mannitol or sucrose), (2) no endogenous transport processes, (3) no cellular metabolism and (4) cellular concentration can be modeled as described.

Our laboratory has investigated the interaction of pantoprazole isomers with ABCG2 in a transfected MDCKII cell model using this approach (Wang and McNamara, 2010). Pantoprazole isomers exhibited many of the properties illustrated in the current analysis; i.e., boundaries illustrated in **Figure 6-4 Panel B** at low and high pantoprazole donor concentrations, inflection point related to T_{Max} not K_M, kinetic analysis with donor concentrations suggesting positive cooperativity. Using the approach outlined in Table 6-3, reasonable parameter estimates were obtained (Wang and McNamara, 2010).

Table 6-3 Iterative approach for the estimation of T_{Max} and K_M using transcellular flux data.

Parameter	Substrate/Cell	Eq	Rearranged to	Comments
Paracellular Permeability (PS_{PC})	Mannitol (or sucrose) / Parent cell line	6-8	$PS_{PC} = \frac{\frac{dX_{A,B\rightarrow A}}{dt}}{C_B^0} \left[or \ \frac{\frac{dX_{BA\rightarrow B}}{dt}}{C_A^0} \right]$	1. Solve for PS_{PC} using mannitol data. 2. Assume that paracellular flux is similar for drug and marker (mannitol or sucrose).
Diffusion Permeability (PS_D)	Drug / Parent cell line	6-8	$PS_D = 2\left\{ \frac{\frac{dX_{A,B\rightarrow A}}{dt}}{C_B^0} \left[or \ \frac{\frac{dX_{BA\rightarrow B}}{dt}}{C_A^0} \right] - PS_{PC} \right\}$	3. Confirm drug is not a substrate for endogenous transporter, ERα is unity for parent cell line. 4. Solve for PS_D using drug data and PS_{PC} from mannitol data.
Transcellular Permeability $\left(PS_{TC,B\rightarrow A}\right)$	Drug / Transfected cell line		$PS_{TC,B\rightarrow A} = \left\{ \frac{\frac{dX_{A,B\rightarrow A}}{dt}}{C_B^0} \left[or \ \frac{\frac{dX_{BA\rightarrow B}}{dt}}{C_A^0} \right] - PS_{PC} \right\}$	5. Solve for transcellular permeability $PS_{TC,B\rightarrow A}$. 6. Similar case for A to B flux $\left(PS_{TC,A\rightarrow B}\right)$
Apparent Apical Efflux Permeability $\left(PS_{AE,B\rightarrow A}^{apparent}\right)$	Drug / Transfected cell line	6-16	$PS_{AE,B\rightarrow A}^{apparent} = \frac{{PS_D}^2 - \left(2PS_D PS_{TC,B\rightarrow A,}\right)}{\left(PS_{TC,B\rightarrow A} - PS_D\right)}$	7. Approximate apparent apical efflux $\left(PS_{AE,B\rightarrow A}^{apparent}\right)$ for B to A direction using $PS_{TC,B\rightarrow A}$, PS_D and PS_{PC}). 8. Approximation is more accurate near the inflection point; error is significant near the boundaries (contribution of PS_{AE} is masked).
Apparent Apical Efflux Permeability $\left(PS_{AE,A\rightarrow B}^{apparent}\right)$	Drug / Transfected cell line	6-19	$PS_{AE,A\rightarrow B}^{apparent} = \frac{{PS_D}^2 - \left(2PS_D\left(PS_{TC,A\rightarrow B}\right)\right)}{\left(PS_{TC,A\rightarrow B}\right)}$	9. Approximate apparent apical efflux $\left(PS_{AE,A\rightarrow B}^{apparent}\right)$ for A to B direction using $PS_{TC,A\rightarrow B}$, PS_D and PS_{PC})
Initial Cellular Concentration (C_C)	Drug / Transfected cell line	6-31	$C_C = C_D \frac{1}{\left(2 + \frac{PS_{AE}^{apparent}}{PS_D}\right)}$	10. Approximate initial cellular concentration (C_C) using C_D, PS_D and $PS_{AE}^{apparent}$.
Kinetic Parameters (T_{Max}, Km)	Drug / Transfected cell line	6-17	$PS_{AE}^{apparent} = \frac{T_{Max}}{Km + C_C}$	11. Nonlinear regression analysis of $PS_{AE,\ apparent}$ as a function of C_C to fit the parameters (T_{Max} and K_M). 12. Steps 4-9 may be repeated to refine estimates of C_C and $PS_{AE,\ apparent}$

Inhibition of $PS_{A,E}$

As mentioned earlier, there is considerable interest in assessing drug-drug interactions involving transporters. Inhibition of transcellular flux has been advocated as a viable approach for screening, however, there is considerable concern regarding the ability to compare results obtained using different model substrates or different cell lines or clones (Giacomini et al., 2010). At low cellular concentrations of substrate ($C_C << K_M$), the influence of a competitive or non-competitive inhibitor on permeability-surface area product associated with the active transport component can be written as:

$$PS_{A,E\ (apparent)} = \frac{T_{Max}}{K_M\left(1+\frac{I_C}{K_I}\right)} = \frac{PS_{A,E}}{\left(1+\frac{I_C}{K_I}\right)} \qquad 6\text{-}37$$

where I_C is the cellular concentration of the inhibitor and K_I is the Michaelis-Menten constant (inversely related to affinity) for the transporter inhibitor complex.

As discussed by Kalvass and Pollack (Kalvass and Pollack, 2007) the use of B→A flux data or ER_A alone can be misleading, resulting in inaccurate estimates of inhibition constants (K_I). **Figure 6-6 Panel A** illustrates the influence of increasing inhibitor concentration on the apparent permeability-surface area A→B flux for a substrate. If the inhibitor is also a substrate for the transporter then the nonlinear nature of the relationship between cellular and donor concentration of the inhibitor needs to be considered (Equation 6-33, **Figure 6-4 Panel A**). As cellular inhibitor concentration increases, the efflux pump becomes inhibited and the substrate flux returns to that of the parent cell line. The difference between the two inhibitors (K_I values of 0.1 and 0.5 μM) is evident in **Figure 6-6 Panel A**; however, it should be noted that the inflection point for these cellular concentration inhibition curves (0.9 and 4.5 μM, respectively) do not correspond to the K_I values.

Again as described earlier (**Figure 6-2**, **Panel B**) the 50% (A→B flux) and the 150% (B→A flux) value of the PS_{Obs} occurs when apparent PS_{AE} approaches a

value which is twice that of PS_D. A drug could be defined as an effective inhibitor if it causes the flux of a known substrate to decrease to half of its maximum for B→A (150%) transport or minimum for A→B (50%). The cellular inhibitor concentration corresponding to this inflection point,$C_{C,inf\ pt}$ can be defined as

$$\frac{PS_{A,E\ (apparent)}}{\mathrm{PS_D}} = \frac{\mathrm{PS_{A,E}}}{\mathrm{PS_D}\left(1 + \frac{\mathrm{I_{C,inf\,pt}}}{\mathrm{K_I}}\right)} = 2 \qquad \text{6-38}$$

Rearranging this equation to yield a relationship which defines the concentration of inhibitor required to cause a 50% decrease in the apparent flux in a transmembrane system relative to the actual K_I and the substrate's active apical efflux ($PS_{A,E}$) and passive diffusion (PS_D) characteristics.

$$\frac{\mathrm{I_{C,inf\,pt}}}{K_I} = \left(\frac{PS_{A,E}}{2PS_D} - 1\right) \qquad \text{6-39}$$

Equation 6-38 would imply that the concentration of inhibitor needed to cause a substantial change in flux is dependent on the characteristics of the substrate ($PS_{A,E}$ and PS_D) in addition to properties of the inhibitor (K_I). Use of ER_α does <u>not</u> provide an accurate estimation of K_I (**Figure 6-6 Panel B)** for either donor or cellular concentration. Again, the influence of an inhibited $PS_{A,E}$ is not evident until it's numerical value approaches twice that of PS_D.

Figure 6-6 Panel C expands on this issue in that a better efflux substrate (higher PS_{AE}) is more difficult to inhibit causing a shift to the right of the inhibition profile ($I_{C,infpt}$ increases from 0.9 to 9.9 μM for the tenfold higher $PS_{A,E}$). In a similar fashion (Equation 6-39), inhibition of a substrate with a higher diffusion permeability (PS_D) occurs at lower inhibitor concentration ($I_{C,infpt}$ decreases as substrate PS_D increases). Again ER_α plotted as a function of inhibitor concentration (donor or cellular) reveals inflection points which are influenced by $PS_{A,E}$ of the substrate (**Figure 6-6 Panel D)**.

The influence of the BCRP inhibitors FTC and GF120918 on the B→A flux for nitrofurantoin, cimetidine and PhIP in BCRP-MDCKII cells were examined in our

laboratory (Philip Empey Thesis, **Figure 6-7**). At a concentration of 10 μM, FTC was shown to be effective at inhibiting flux of all three substrates; however, GF120918 (1 μM) was effective in inhibiting nitrofurantoin and cimetidine, but did not inhibit PhIP B→A flux. One interpretation of such data might be that there are multiple binding sites for BCRP. Giri et al (Giri et al., 2008) suggested that similar inhibition profiles supported evidence for the involvement of multiple binding regions for BCRP. In the context of the current model analysis (Equation 6-38), another interpretation could also be put forth. For the same inhibitor (same K_I), a much higher concentration will be required to see a change in overall flux rate when substrates have a higher $PS_{A,E}$ to PS_D ratio. The concentration needed to cause the apparent PS_{Obs} to decrease by 50% (between the transfected with no drug and the parent cell flux), is greater than K_I. The greater the PS_D at the basolateral surface the less transport at the apical surface has to change in order for overall PS_{Obs} to be altered. Subsequent experiments in our lab (Philip Empey Thesis, data not shown) revealed that higher concentrations of GF120918 (10 μM) decreased the B→A flux of PhiP. Hence, this inconsistency in altering flux of different substrates with a common inhibitor may not be a result of multiple binding sites, but rather a consequence of data interpretation in light of the complexity of the model system.

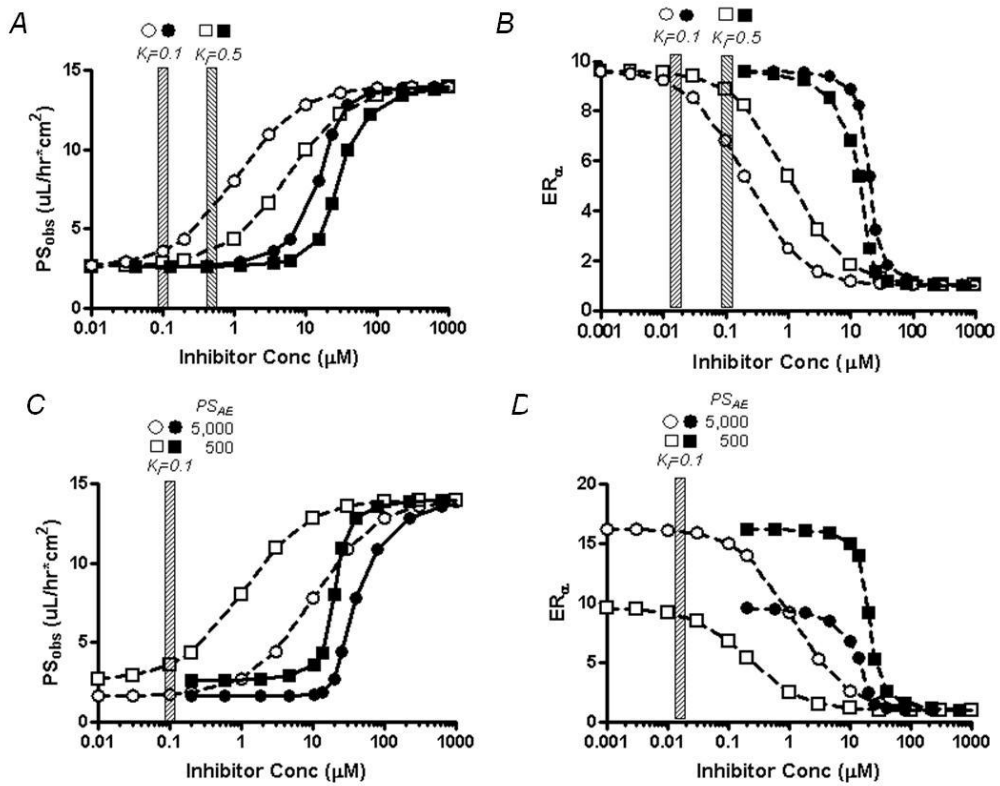

Figure 6-6 Apparent permeability-surface area clearance (PS_{obs}) A→B directional flux (**Panel A** and **C**) and ER_α (**Panel B** and **D**) for a substrate ($PS_{A,E}$ = 500 uL/hr*cm^2 and PS_D of 25 uL/hr*cm^2 at low substrate concentration) as a function of inhibitor concentration (cellular: open symbols; donor: closed symbols) with a PS_{PC} of 1.5 uL/hr*cm^2. **Panel A** and **B** Inhibitors vary in K_I with both inhibitors have a PS_D, and T_{Max} of 25 uL/hr*cm^2 and 500 pmol/hr/cm^2 respectively. Inhibitor 1 (circles) and Inhibitor 2 (squares) have K_I values of 0.1 and 0.5 μM, respectively. **Panel C** and **D** Same inhibitor but substrates vary in $PS_{A,E}$; both substrates having PS_D of 25 uL/hr*cm^2. Substrate 1 (squares) has a $PS_{A,E}$ of 500 uL/hr*cm^2 and Substrate 2 (circles) has a $PS_{A,E}$ of 5,000 uL/hr*cm^2. Inhibitor has PS_D, T_{Max} and K_I values of 25 uL/hr*cm^2, 500 pmol/hr/cm^2 and 0.1 μM, respectively.

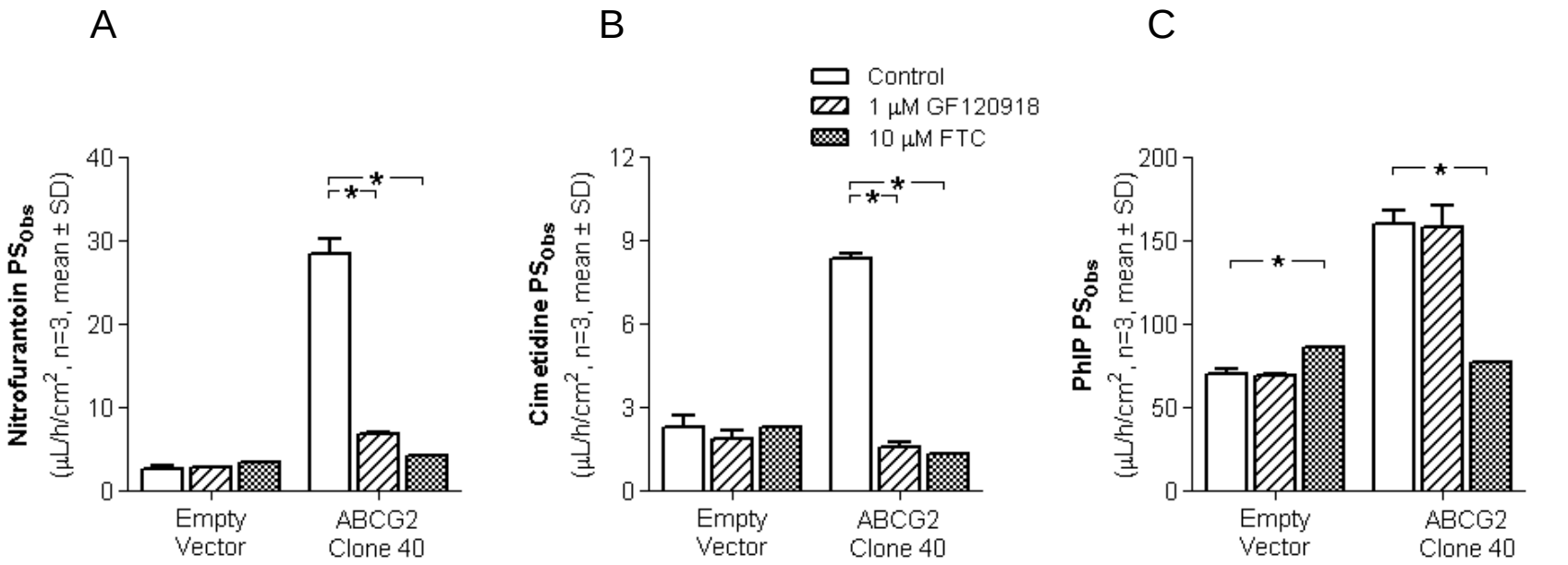

Figure 6-7 Apparent permeability-surface area clearance (PS_{obs}) B→A directional flux for (**Panel A**) Nitrofurantoin at 10 μM, (**Panel B**) Cimetidine at 5 μM and (**Panel C**) PhiP at 2 μM in MDCKII cells transfected with human ABCG2 in the absence or presence of 1 μM GF120918 or 10 μM FTC.

Discussion

Interactions between transporters and drug substrates are of great interest in drug development and in-vitro cell models are constructed to study the importance of a given transporter protein on the vectorial transfer of drug from one side of a polarized epithelial cell barrier to the other. An example includes the use of MDCKII cells into which a transporter gene has been cloned and the protein is usually expressed at high levels. While the experimental paradigm is widely utilized, the limitations and interpretations of the results of such studies are not broadly understood (Bentz et al., 2005; Balakrishnan et al., 2007; Kalvass and Pollack, 2007; Korjamo et al., 2007; Lumen et al., 2010). An appreciation of the underlying conceptual framework and assumptions that provide insights into the mechanisms of drug uptake and efflux when using such in-vitro models is needed in order to make broader inferences regarding drug absorption, disposition and for predicting the potential for drug-drug interactions. The goal of the present analysis was to provide the framework for systematically examining data from such models. An appreciation of controlling (rate limiting steps) or boundary conditions provides insights as to the interpretation of resulting observations.

The work of Kalvass and Pollack (Kalvass and Pollack, 2007) represented an important conceptual step forward illustrating some of the complexities with modeling and interpreting vectorial transport data. They clearly demonstrated the limitations of ER_A, recognizing that transporter overexpression on one surface (e.g., apical) results in diffusion across the opposite surface (i.e., basolateral) being the rate limiting transport process across the monolayer. Hence when studying the role of an apical transporter in B→A flux, in comparison to the untransfected parent cell line, the ER_A metric is an unreliable index for the magnitude of the transporter's contribution to the overall flux because this rate limiting situation yields asymptotic values for a range of affinities. **Table 6-2** provides further experimental evidence supporting the concern that ER_A is not a discriminating parameter. ER_α or the asymmetrical flux, on the other hand, was

thought to be more robust and would more readily correlate with the extent of transporter drug interaction. Again, the current analysis (**Table 6-2**) supports that ER_{α} is a more robust parameter. However, the discriminating power of this parameter relies on the assumption that the paracellular transport pathway contributes negligibly to the overall flux across the membrane, which can be invalid for many experimental paradigms (e.g., MDCKII cell models) and can confound parameter estimation and the values of ER_{α}. The degree to which paracellular flux influences ER_{α} or $PS_{A,E}$ appears to be greatest for those substrates with lower passive diffusion, i.e., substrates for which a transporter would seem most critical for membrane flux.

The current analysis suggests that kinetic parameters (e.g., K_M) derived from vectorial flux data must be interpreted with caution. Kitamura et al (Kitamura et al., 2008) examined the role of multiple transporters in the hepatobiliary transport of rosuvastatin. The K_M values for rosuvastatin uptake into HEK293 cells for OATP1B1 (0.80 μM) was considerably different from those attributed to OATP1B1 obtained using a double transfected (OATP1B1/MRP2) MDCKII model (29.9 μM), and the authors concluded that the transcellular transport of rosuvastatin might not be determined solely by the uptake clearance. Breedveld et al (Breedveld et al., 2004) estimated a $K_{1/2}$ for the B→A flux of pantoprazole in an MDCKII-mBcrp model system of 0.1-1.2mM. Experimental work in our laboratory (Wang and McNamara, 2010) would suggest a much higher affinity (lower K_M) for mBcrp and pantoprazole than might be inferred from the $K_{1/2}$ value.

The active site for an efflux transporter is likely to be intracellular, although the active site for p-GP may be imbedded in the inner membrane itself. Hence, the driving force for efflux transporters is the concentration in a compartment other than the donor. The present examination illustrated that the nonlinear relationship between cellular and donor concentration gives rise to an apparent positive cooperatively relationship when examining flux as a function of donor substrate (or inhibitor) concentration. Several groups have reported positive cooperatively in transcellular flux for p-GP (Keogh and Kunta, 2006b) and BCRP

(Pan et al., 2007). Clearly an alternative explanation is the differential between the internal and external concentration gradients. It is likely this phenomenon of positive cooperatively is also observed for cellular uptake studies.

Giri, et al (Giri et al., 2008) has examined the inhibition of substrate (prozosin, zidovudine, abacavir and imatinib) flux in BCRP overexpressing MDCKII cells by a number of inhibitors. At a fixed concentration, Ko143 inhibited the flux of all of the substrates whereas GF120918, nelfinavir and Pluronic P85 exhibited differential inhibition depending on the substrate. The authors suggested that these observations supported evidence for the involvement of multiple binding regions for BCRP (Giri et al., 2008). Another interpretation of the data might be related to the relative magnitude of active transport and passive diffusion flux for the substrates relative to the K_I for the inhibitors. Again, parameters arising from flux experiments needs to be interpreted with caution.

The concepts presented in this paper provide a framework for interpreting data arising from flux across a cell monolayer. Without the appropriate context, quantitative and qualitative (mechanistic) errors arise that ultimately can misinform our understanding of transporter function and their influence on pharmacokinetics and pharmacodynamics (Zhang et al., 2008; Zhang et al., 2009).

CHAPTER 7: Summary and conclusion

Drug accumulation in milk is a rising concern for the strategy of breastfeeding. Understanding the mechanism of active drug transport into milk is a key step to provide guidance for drug use in lactation. ABCG2 is highly expressed in mammary gland during lactation in mouse, cow and human studies and is responsible for the active transport of some xenobiotics into milk.

In this dissertation, we confirmed that Abcg2, but not P-gp, is highly expressed in rat lactating mammary gland by western blot and immunohistochemistry. Abcg2 was upregulated during lactation compared with non-lactation as shown by Real-time PCR. A rAbcg2-MDCKII cell line has been characterized as functional one by Flow Cytometry and the transport of nitrofurantoin. Utilizing GF120918 as an effective inhibitor of rAbcg2, a "chemical knockout" rat model has been established for milk active transport study. The M/S for nitrofurantoin was decreased dramatically in this viable alternative to the genetic knockout mouse model.

Half of all drugs are marketed as chiral substances. While there are some studies of stereoselective interaction with P-gp transport or chiral metabolism, there is no report demonstrating stereoselective interaction between drugs and ABCG2. From our investigation, pantoprazole is a prototypical substrate of human ABCG2 as well as of rat Abcg2. There is stereoselective interaction between Abcg2/ABCG2 and pantoprazole as demonstrated in both *in vitro* and *in vivo* experiments. ABCG2 recognizes pantoprazole enantiomers differently which resulted in significant differences in M/S ratios for the two isomers in the rat study. M/S ratios of pantoprazole isomers in rat mediated by passive diffusion were determined and predicted by a passive diffusion model. Since chirality does not alter basic physical and chemical properties, no difference was observed between predicted M/S ratios of pantoprazole isomers. The ratios of $(M/S_{Observed})/ (M/S_{Predicted})$ of plus and minus pantoprazole were 4.43 and 11.95, respectively, which supported a role for a transporter in the high M/S ratios of pantoprazole isomers. GF120918 decreased M/S ratios of both isomers but had

a more significant effect on the minus isomer of pantoprazole. Both pantoprazole isomers form an identical active metabolite that does not have a chiral center, so the stereoselective interaction between pantoprazole and ABCG2 is unlikely to result in any significant clinical consequences. However, this stereoselective recognition may have consequences for other chiral drugs. The M/S ratio of either isomer of pantoprazole in rat was much higher (25 time or 68 times) than one human case report (M/S=0.02). The reason for this species difference has not been resolved.

Five concentrations of pantoprazole isomers were transport by either rat Abcg2 or human ABCG2. Having identical chemical properties (diffusion controlled) as well as no interaction with endogenous transporters of the MDCKII cell line, the pantoprazole isomers provided an ideal platform to compare the kinetic parameters derived from Transwell experiments, e.g., PS_D, PS_{AE}, PS_{PC}, K_m and V_{max}. The results demonstrated a consistent trend for pantoprazole transport across these two species. K_m and V_{max} of pantoprazole enantiomers in rat Abcg2 or human ABCG2 were estimated from fitting data with very modest differences between species.

Cell monolayer flux across Transwell or Snapwell is a broadly used method for studying drug transporter or for screening new molecule entity in drug development. Three compartment models instead of a single barrier model have been established by different groups in order to explain the complex observations. Transport of pantoprazole isomers in Abcg2/ABCG2 overexpressing MDCKII cell line provided solid evidence for a mathematic model of the monolayer system. Paracellular transport of a hydrophilic compound may not be assumed negligible compared with transcellular transport. Cellular concentration and not donor concentration is the direct driving force of transcellular transport for an apical efflux transporter like ABCG2. The model confirmed the importance of assessing the data from the context of rate limiting barriers in series or in parallel. For good substrates in highly expressing cell clones passive diffusion on the basolateral side is the limiting step in efflux transporter on the apical side in a monolayer system, so that the ER_A does not

reflect PS_{AE}. ER_{α} is a more robust parameter than ER_A but the expression level of efflux transporter and cellular concentration can still affect the value of ER_{α}. Due consideration should be taken when setting up criteria in drug screening based on the value of ER_{α}. The estimation of K_m, K_i or IC_{50} from monolayer system is not directly related to a property or function of a transporter, but is related to the transition from one rate limiting step (flux across the basolateral membrane) to multiple barriers (flux across both basolateral and apical membranes).

In conclusion, transporters are broadly expressed in barriers (i.e., blood brain barrier, intestine epithelial barrier, renal epithelial barrier, mammary gland epithelial barrier and so on), playing an important biological role for the regulation of endogenous and exogenous substrate concentrations across cells, tissues and systems. A mechanistic three compartment monolayer model with appropriate expression of transporters is critical to our understanding of these *in vivo* biological barriers. Specific transporter expressing cell lines grown in monolayer systems can provide invaluable insights into their function provided that an appropriate expression level of transporter can be correlated with function and flux assessment can be put into the context of limitations of the model system.

APPENDICES

Appendix A: List of Abbreviations

A	Membrane surface area
ABC	ATP-binding cassette transporter superfamily
ACV	Acyclovir
ADME	Absorption, Distribution, Metabolism and Excretion
AUC	Area under the concentration-time curve
BCRP	Breast cancer resistance protein
C_A	Concentration in the apical (milk) compartment
C_B	Concentration in the basolateral (serum) compartment)
C_C	Concentration in the cellular (LMEC) compartment
$C_{milk,\ unbound}$	Unbound concentration in the milk
$C_{serum,\ unbound}$	Unbound concentration in the serum
CDC	The Centers of Disease Control and Prevention
CM	Cimetidine
CP	Ciprofloxicin
DMSO	Dimethyl sulfoxide
ERα	Asymmetry efflux ratio; ratio of the initial rate of B→A flux divided by the initial rate of A→B flux
FACS	Fluorescence-activated cell sorting
f_m	Fraction protein bound in the milk
f_s	Fraction protein bound in the serum
GF120918	N-(4-[2-(1,2,3,4-tetrahydro-6,7-dimethoxy-2-isoquinolinyl)ethyl]-phenyl)-9,10-dihydro-5-methoxy-9-oxo-4-acridine carboxamide

NF	Nitrofurantoin
PAN	Pantoprazole
Papp, (μL/hr)/cm^2	The apparent permeability
PDR	The Physician's Desk Reference
PS_{AE}	Permeability-surface area products of apical efflux
PS_D	Permeability-surface area products of passive diffusion
PS_{PC}	Permeability-surface area products of paracellular flux between cells
MRP	Multiple resistance protein
M/S	Drug concentration in milk to drug concentration in serum
MXR	Mitoxantrone resistance-associated protein
MTX	Methotrexate
NIS	The National Immunization Survey
RER	Rough endoplasmic reticulum
RLMS	Ross Laboratory Mother Survey
RN	Ranitidine
SA	Salicylic acid
TEB	Terminal end buds
X_A	The mass of drug in the apical compartment
X_B,	The mass of drug in the basolateral compartment
X_C	The mass of drug in the cellular compartment

Appendix B: Glossary

ATP	ATP is a molecule which consists of the nitrogenous base adenine linked to the sugar ribose and which has a chain of three phosphate groups attached to the ribose in a linear fashion. ATP is present in all living cells and serves as an energy source for many metabolic processes; energy is released when ATP is hydrolyzed into ADP. It is the single most important molecule in all living things since it serves as the currency for energy in biological systems.
ATPase	Enzyme that catalyzes a process involving the hydrolysis of ATP. A large number of different proteins, including ABC transporters, have ATPase activity.
Baculovirus vectors	They are used for expression of foreign genes in insects.
Caco-2	The Caco-2 cell line is an immortalized line of heterogenous human epithelial colorectal adenocarcinoma cells. Monolayers of Caco-2 cells are widely used to predict the absorption of compounds. This tool is also suitable to study active transport processes.
cDNA	Single-stranded complementary DNA synthesized from an RNA template by the action of RNA-dependent DNA polymerase. cDNA (i.e., complementary DNA) is used in a variety of molecular cloning experiments as well as serving as a specific hybridization probe.
Cloning, Molecular	The insertion of recombinant DNA molecules from prokaryotic and/or eukaryotic sources into a replicating vehicle, such as a plasmid or virus vector, and the introduction of the resultant hybrid molecules into recipient cells without altering the viability of those cells.
DMPK	Drug metabolism and pharmacokinetics
Drug interactions	The action of a drug (termed perpetrator) that may affect the activity, metabolism, or toxicity of another drug (termed victim).
Drug	Any substance which when absorbed into a living organism may modify one or more of its functions. The term is generally accepted for a substance taken for a therapeutic purpose, but is also commonly used for abused substances. Synonymous with medicine, pharmaceutical.

Efflux transporter	Proteins, located in the cell membrane, which transport molecules out of the cell.
Endogenous	Produced inside an organism or cell.
Endothelial cell of the brain capillaries	Monomolecular cell layer separating the blood and brain tissue. Play a major role in blocking xenobiotic and some endogenous substances from entering the brain.
Epithelial cells	Cells that line the inner and outer surfaces of the body.
Flow-cytometry	An instrument that allows one to gather information from single cells by light scattering or fluorescence properties. These provide information on the size and internal complexity (forward scatter and side scatter, respectively) as well as "markers", identified by staining with fluorescent probes such as conjugated antibodies in the case of immunophenotyping, or nucleic acid dyes in the case of reticulocyte enumeration and DNA content analysis.
In vitro	A biological or biochemical process carried out in a test-tube, culture plate or similar vessel.
In vivo	A biological or biochemical process occurring in a living organism.
PCR	Polymerase chain reaction (PCR) is a rapid, inexpensive and simple method for producing relatively large numbers of copies of DNA molecules from minute quantities of source DNA material--even when the source DNA is of relatively poor quality. It has rapidly become one of the most widely used techniques in molecular biology and molecular pathology.
Sf9	An insect ovarian cell, Spodoptera frugiperda (Sf9), has been widely used to express recombinant proteins, as a host cell in the baculovirus expression system.
Vesicle	A relatively small and enclosed compartment, separated from the cytosol by at least one lipid bilayer. Vesicles store, transport, or digest cellular products and wastes.
Xenobiotic	Chemical substances those are foreign to the biological system. They include naturally occurring compounds, drugs, environmental agents, carcinogens, insecticides, etc.

Appendix C: Chemical Structures

1. GF120918

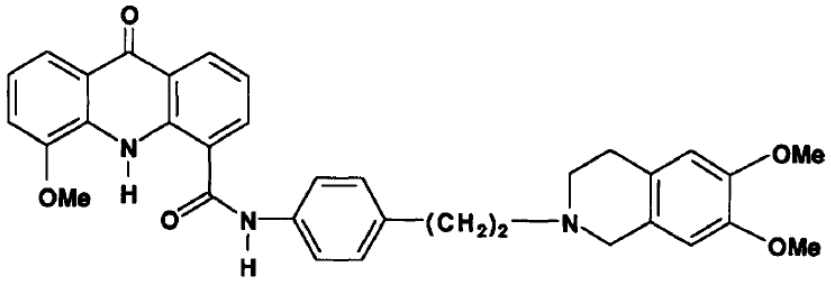

2. Cimetidine

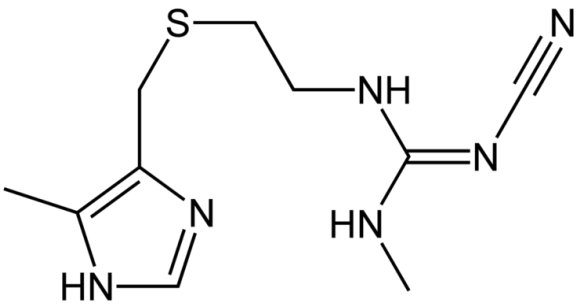

3.Pantoprazole

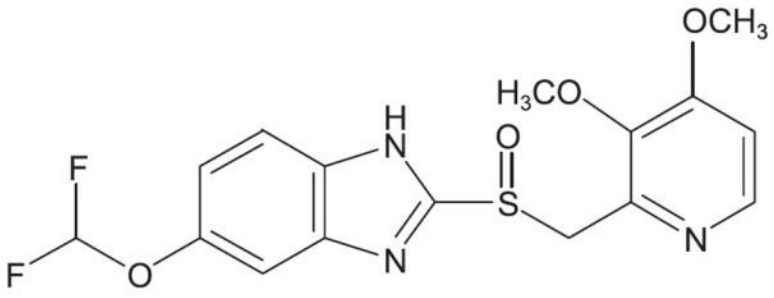

4. Methotrexate

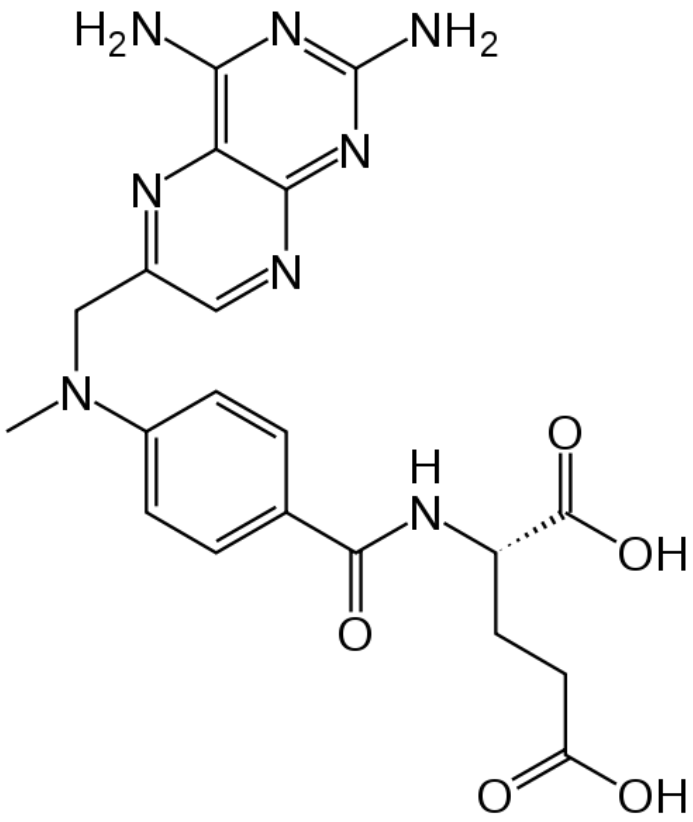

5.Nirofurantoin

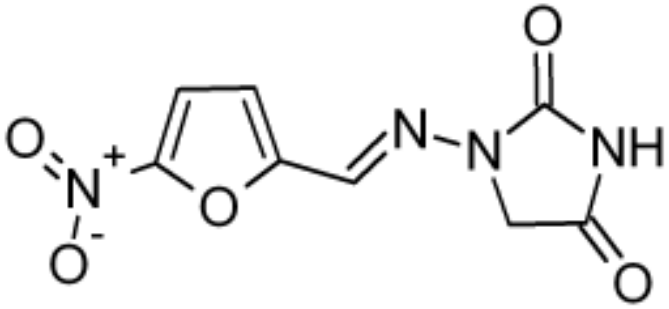

6. Riboflavin

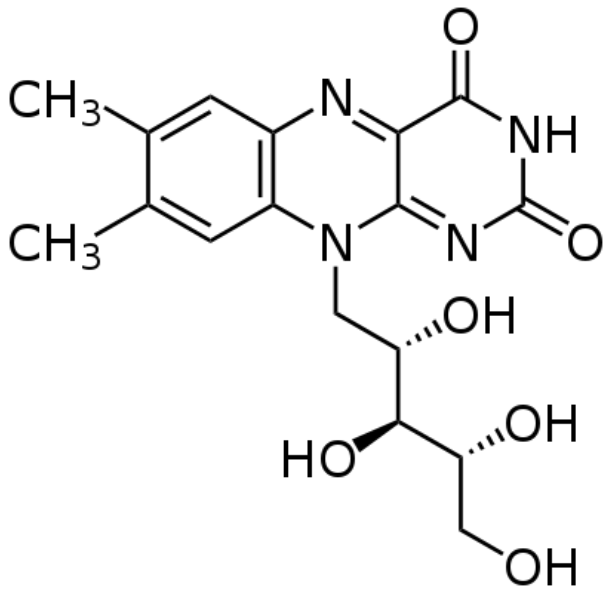

Appendix D: Standard curves for HPLC assay

1. The standard curve of NF in rat serum

   Range: 62.5-8000ng/ml; Y=0.0017x; r^2=0.9999

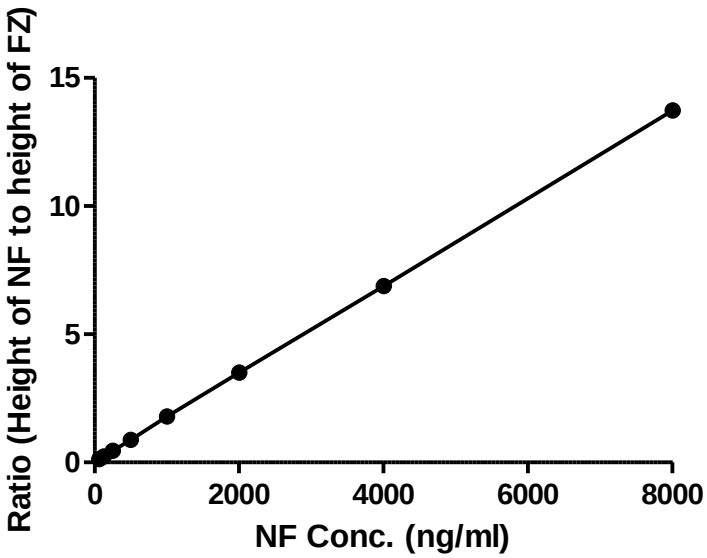

2. The standard curve of NF in rat milk:

   Range: 0.725-29 μg/ml; Y=0.6272x; r^2=0.9993

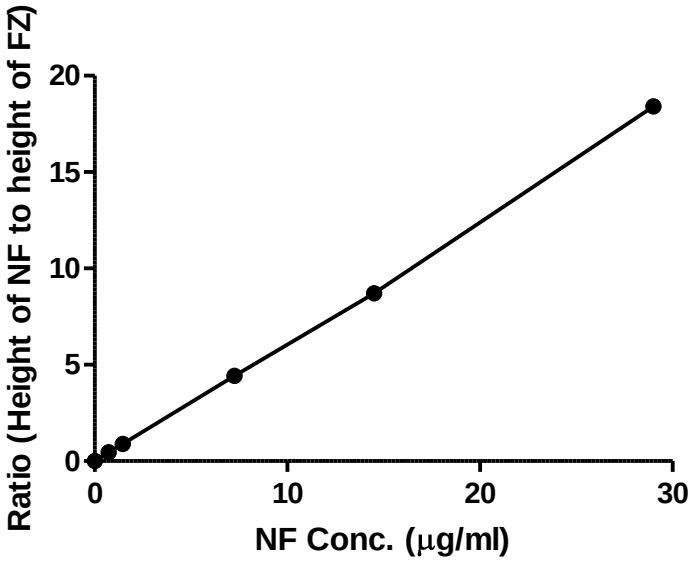

3. The standard curve of NF in cell culture media

   Range: 3.9-8000 ng/ml; Y=16.921x; r^2=0.9999

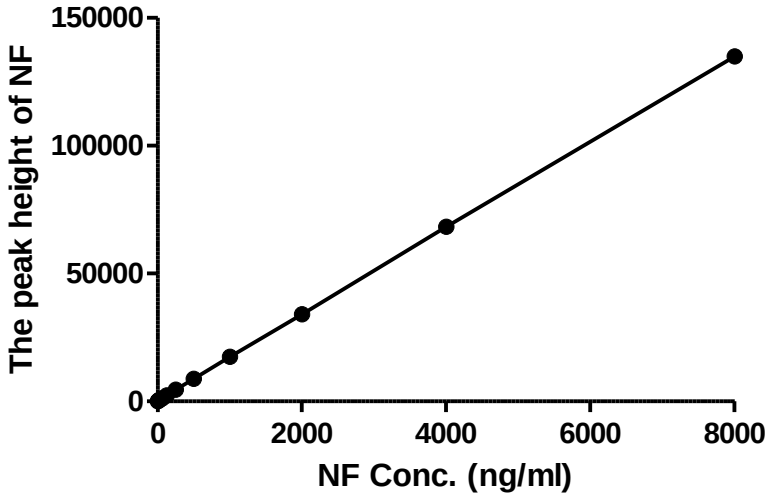

4. The standard curve of pantoprazole in cell culture media (this is one Std curve for 10μM PAN experiment)

   Range: 15.6-8000 ng/ml; Y=130.3093x; r^2=0.9998

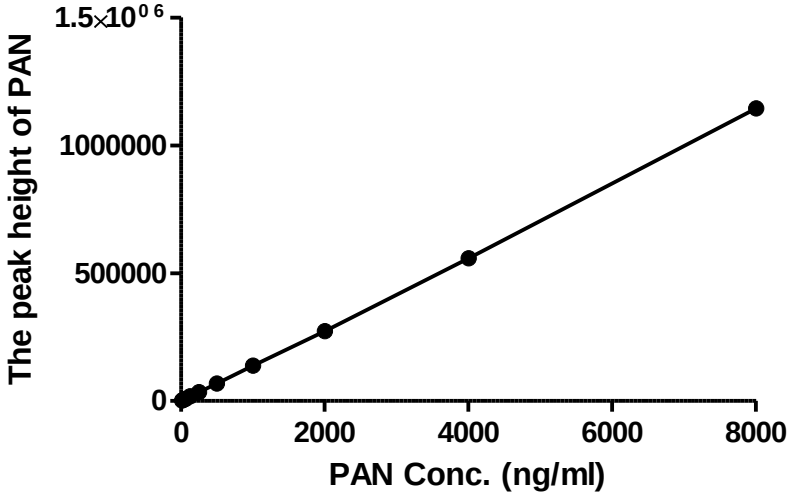

Appendix E-1: Chromatogram of PAN and internal standard of LC-MS

1. Chromatogram of PAN in phosphate buffer: A: 1250 ng/ml PAN mixture; B: 1500ng/ml (-) PAN; C: 1500ng/ml (+) PAN; D: blank.

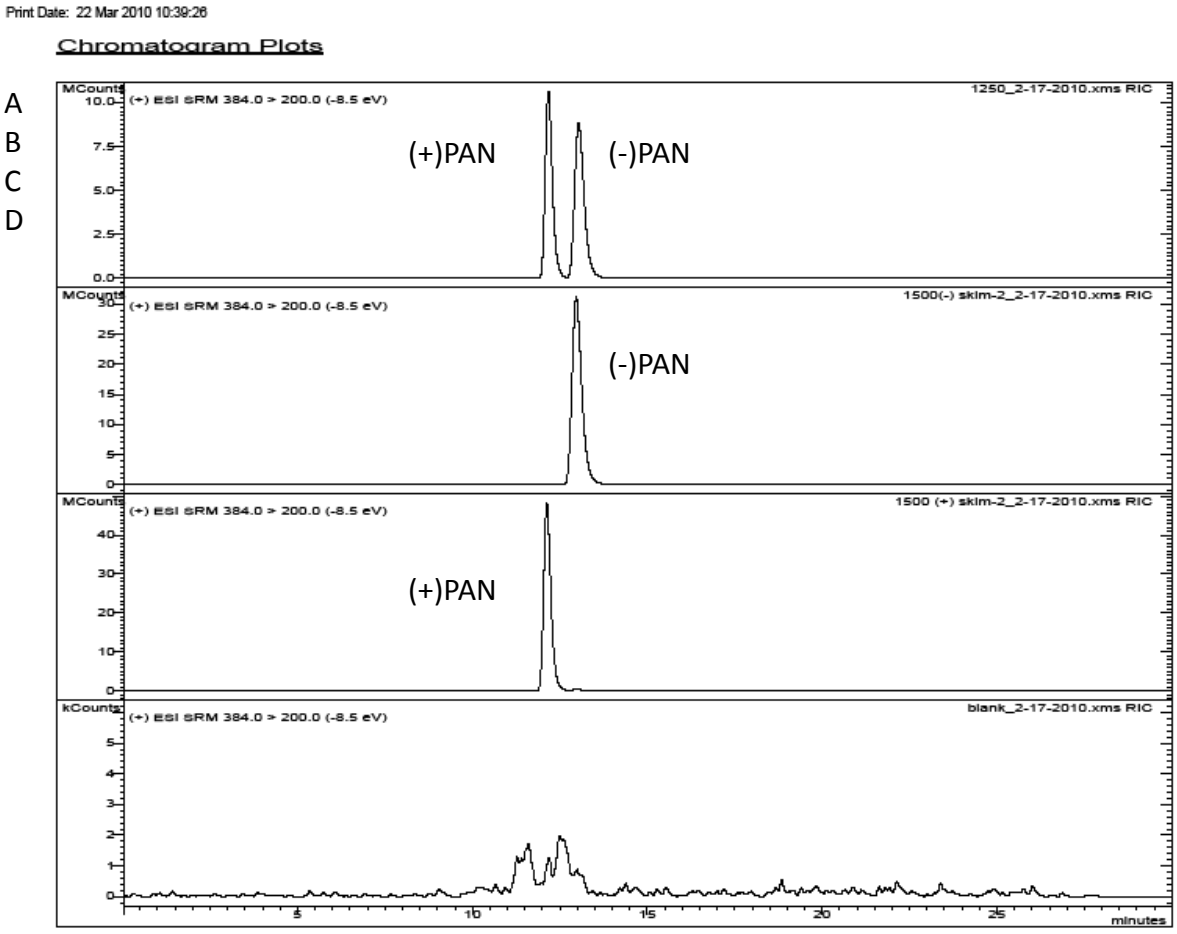

2. Chromatogram of PAN and internal standard in milk sample: A and B: 1250ng/ml PAN and IS in milk sample; C and D: blank milk sample.

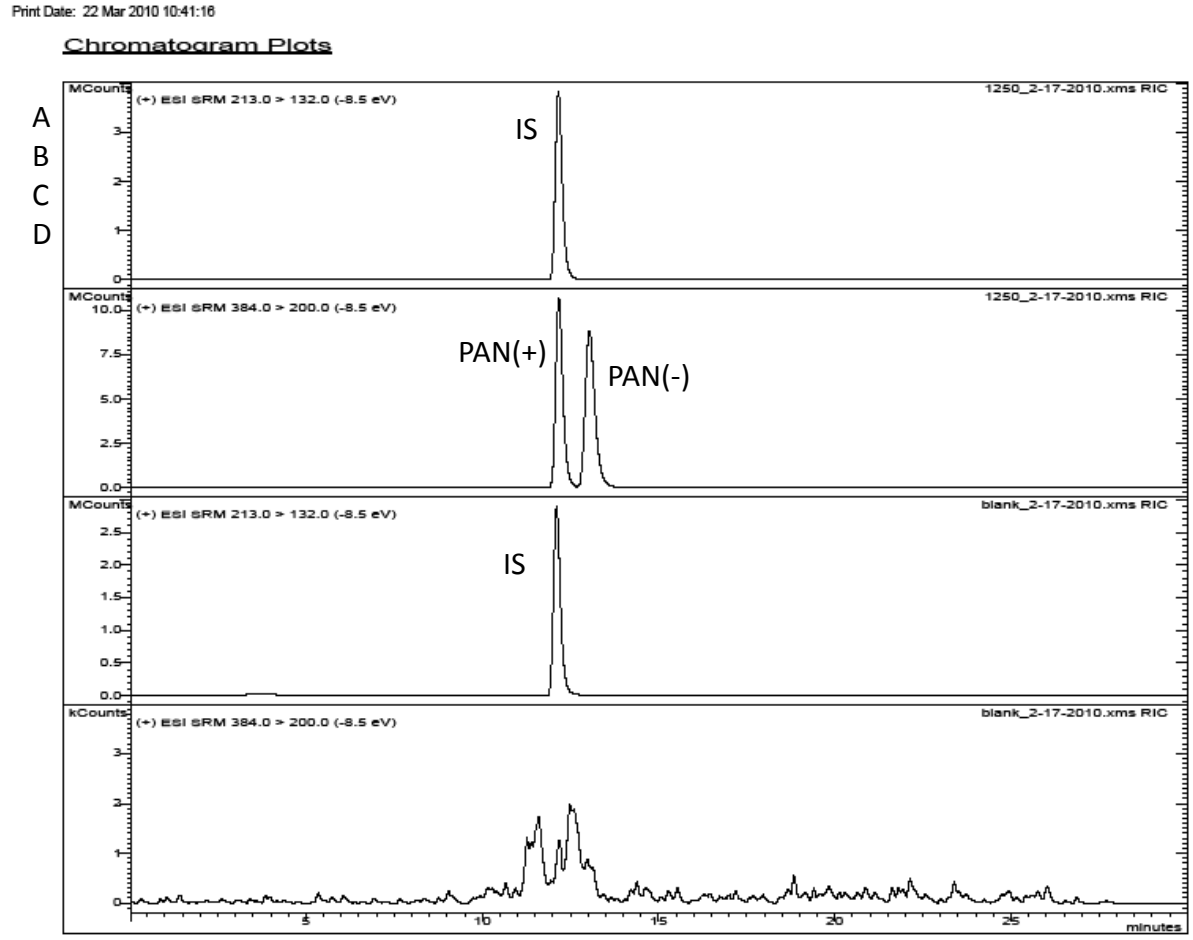

3. Chromatogram of PAN and internal standard in serum sample: A: IS; B: PAN isomers.

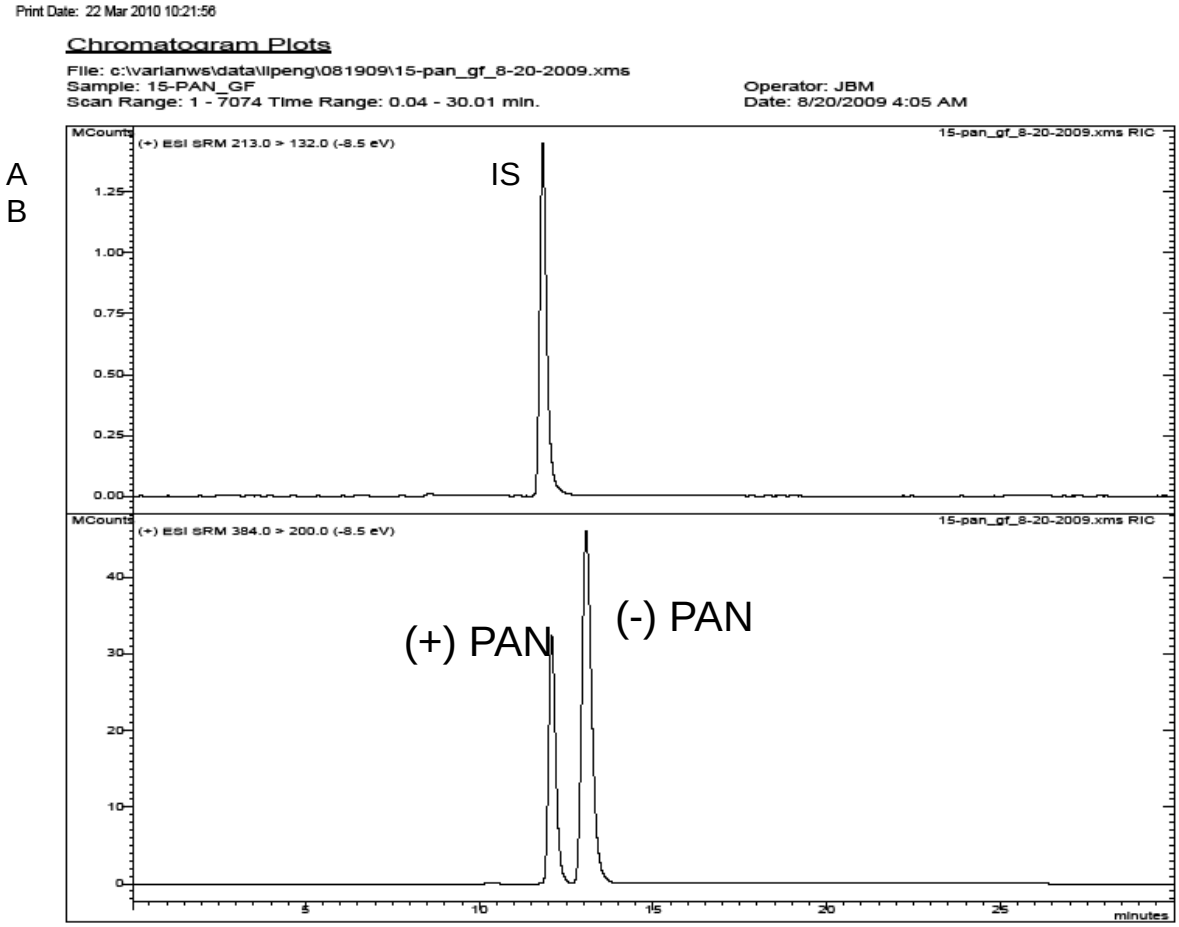

Appendix E-2: Standard curves for LC-MS assay

E-2-1: The standard curve of PAN isomers in phosphate buffer.

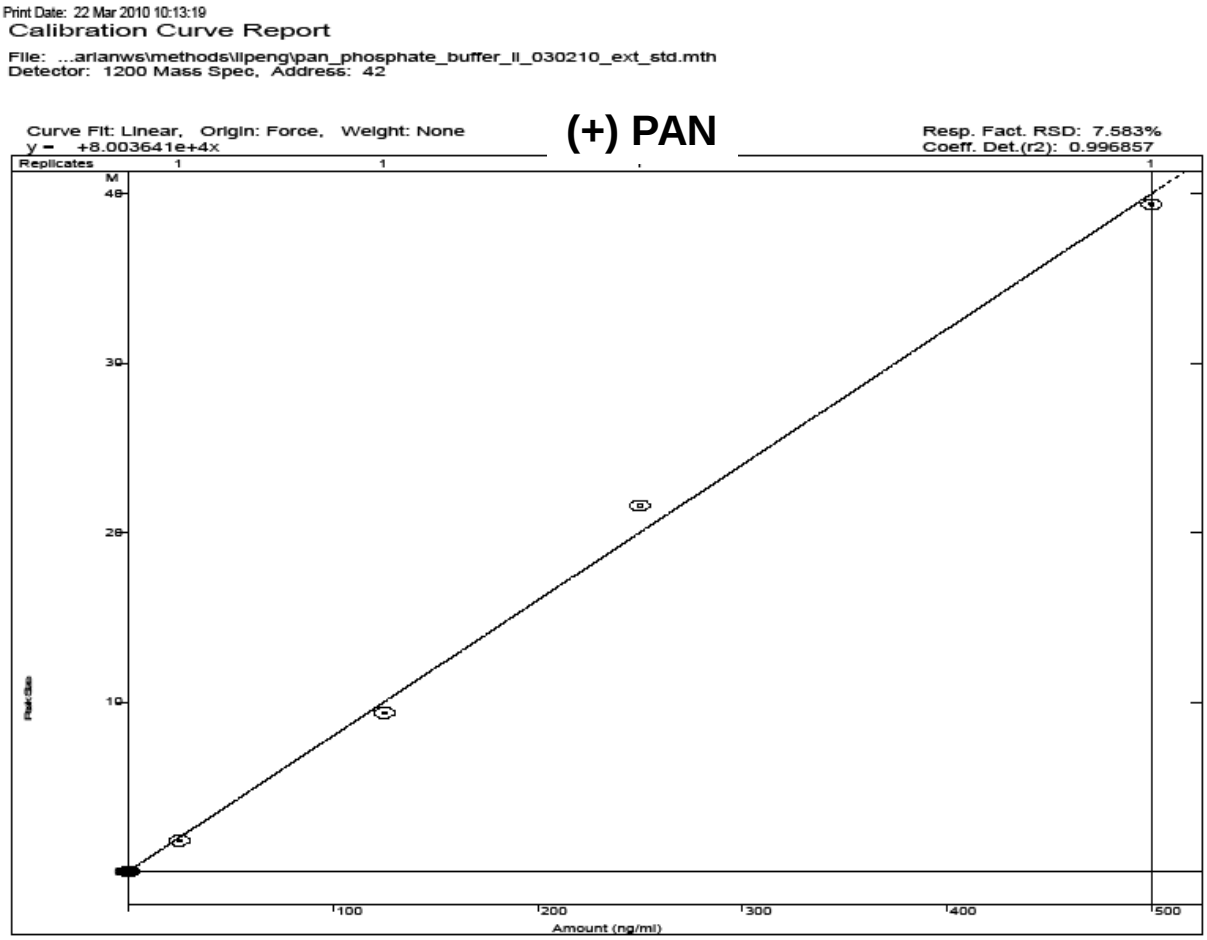

Print Date: 22 Mar 2010 10:13:45

Calibration Curve Report

File: ...arianws\methods\lipeng\pan_phosphate_buffer_ll_030210_ext_std.mth
Detector: 1200 Mass Spec, Address: 42

(-) PAN

Curve Fit: Linear, Origin: Force, Weight: None
y = +8.486797e+4x

Resp. Fact. RSD: 9.537%
Coeff. Det.(r2): 0.996156

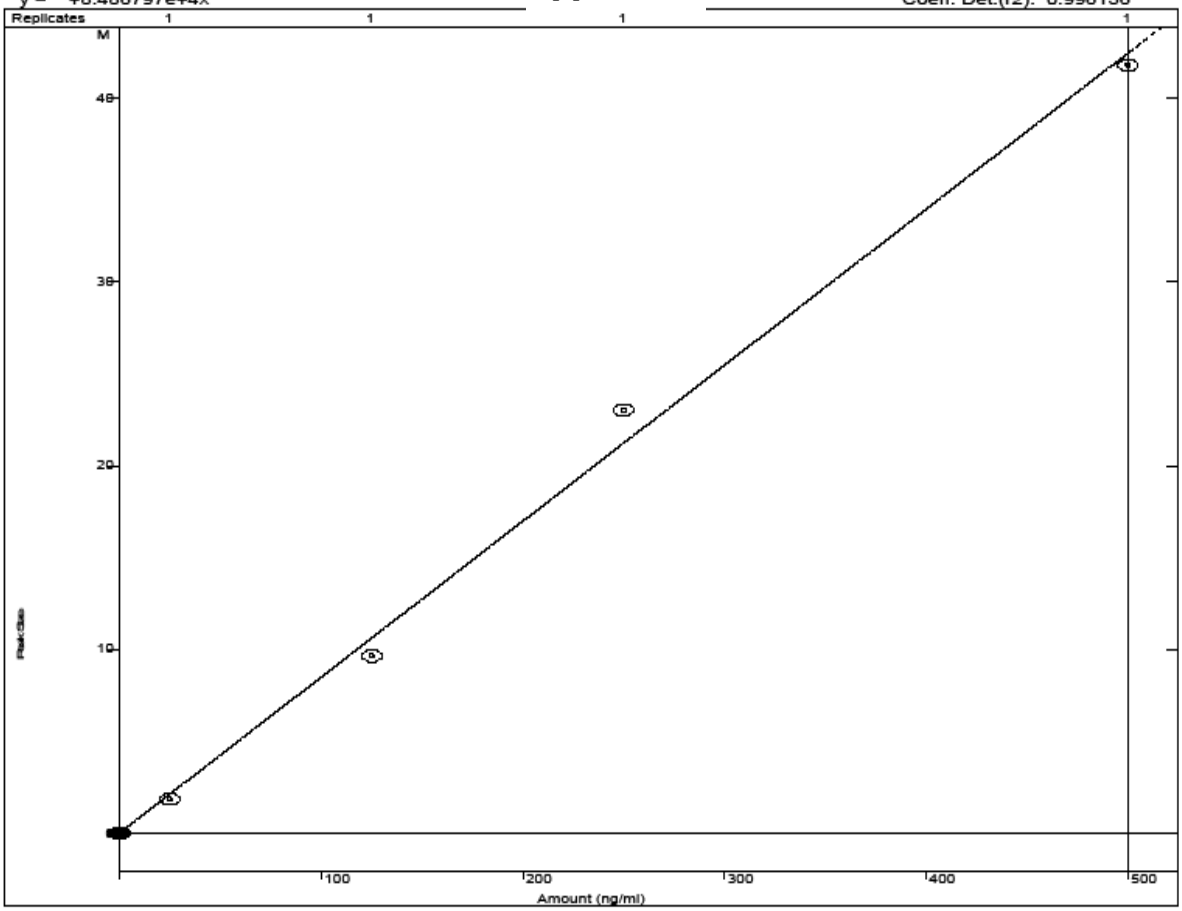

E-2-2: The standard curve of PAN isomers in milk.

Print Date: 22 Mar 2010 10:07:54

Calibration Curve Report

File: c:\varianws\methods\lipeng\pan_milk_II_081809.mth
Detector: 1200 Mass Spec, Address: 42

(+) PAN

Curve Fit: Linear, Origin: Force, Weight: None
y = +18.328550x

Resp. Fact. RSD: 3.508%
Coeff. Det.(r2): 0.999981

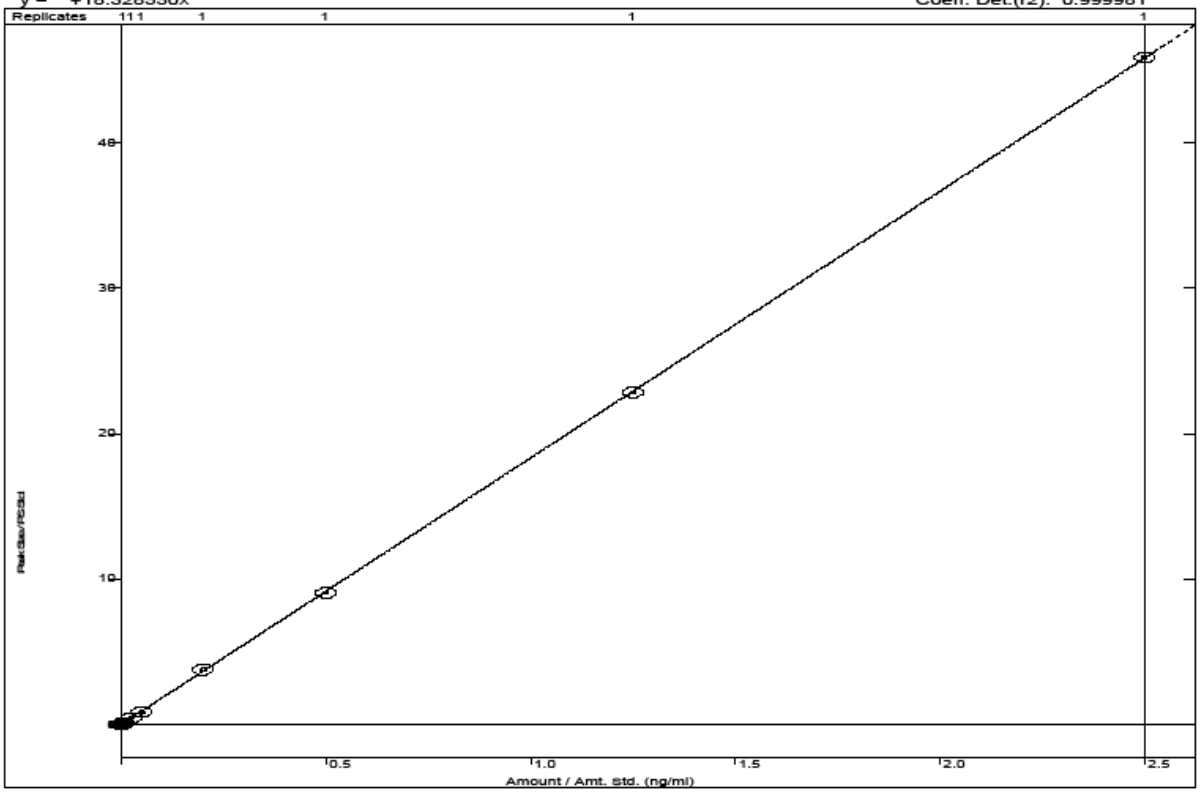

Print Date: 22 Mar 2010 10:08:21

Calibration Curve Report

File: c:\varianws\methods\lipeng\pan_milk_ll_081809.mth
Detector: 1200 Mass Spec, Address: 42

(-) PAN

Curve Fit: Linear, Origin: Force, Weight: None
y = +20.534014x

Resp. Fact. RSD: 4.003%
Coeff. Det.(r2): 0.999781

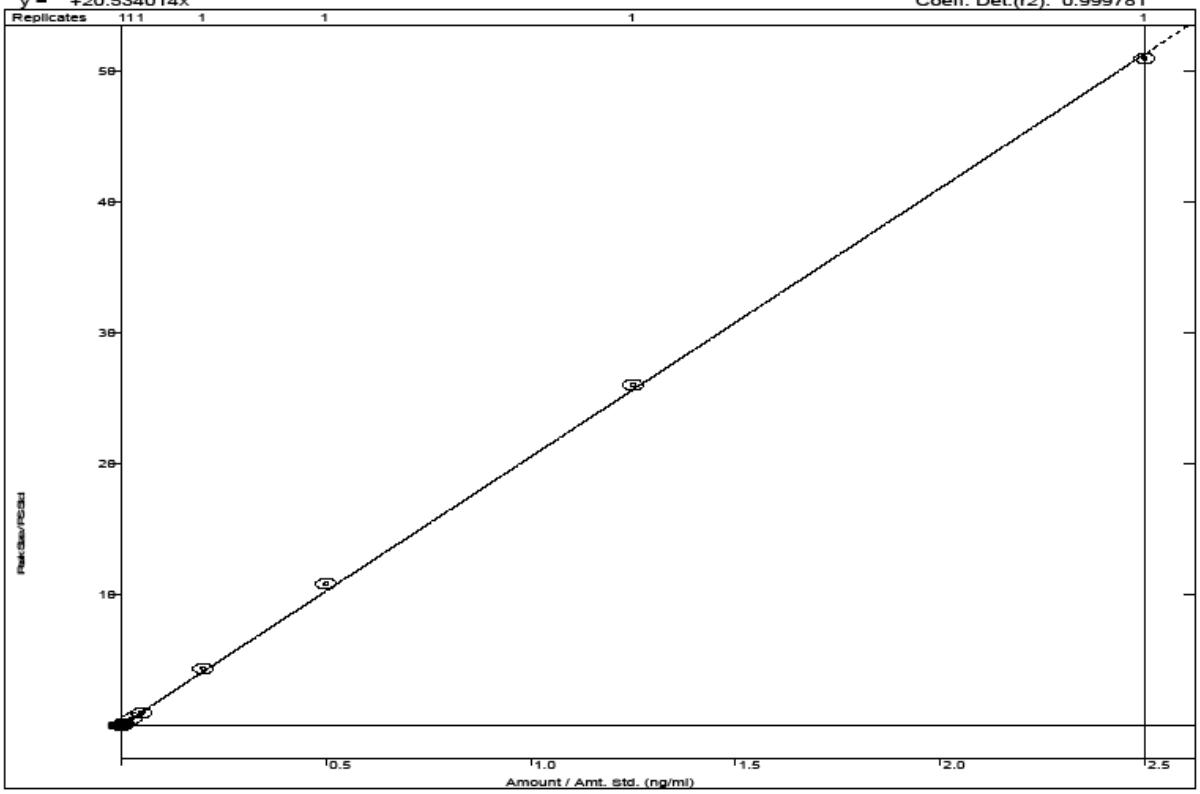

E-2-3: The standard curve of PAN isomers in serum.

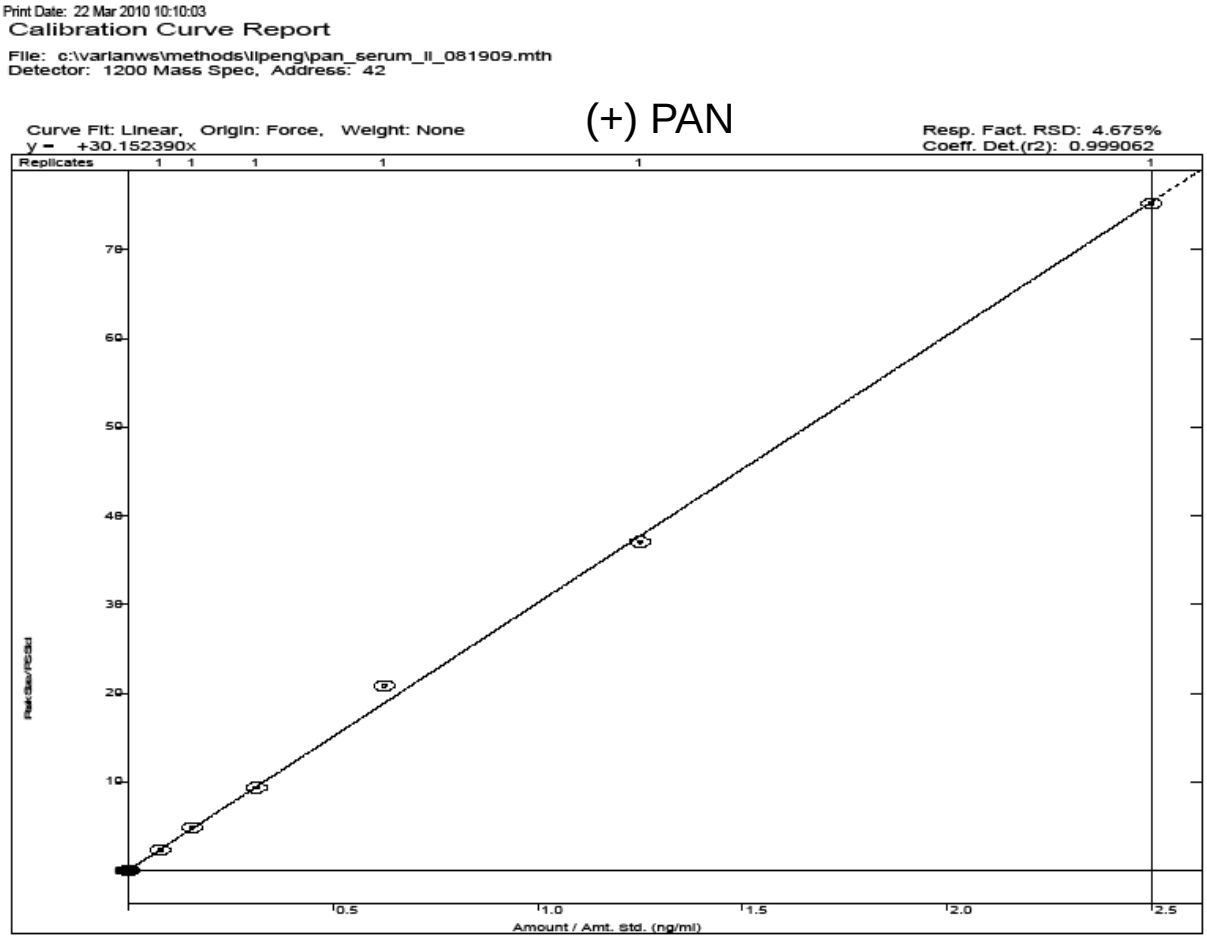

Print Date: 22 Mar 2010 10:10:26

Calibration Curve Report

File: c:\varianws\methods\lipeng\pan_serum_ll_081909.mth
Detector: 1200 Mass Spec, Address: 42

(-) PAN

Curve Fit: Linear, Origin: Force, Weight: None
y = +34.762329x

Resp. Fact. RSD: 4.956%
Coeff. Det.(r2): 0.999446

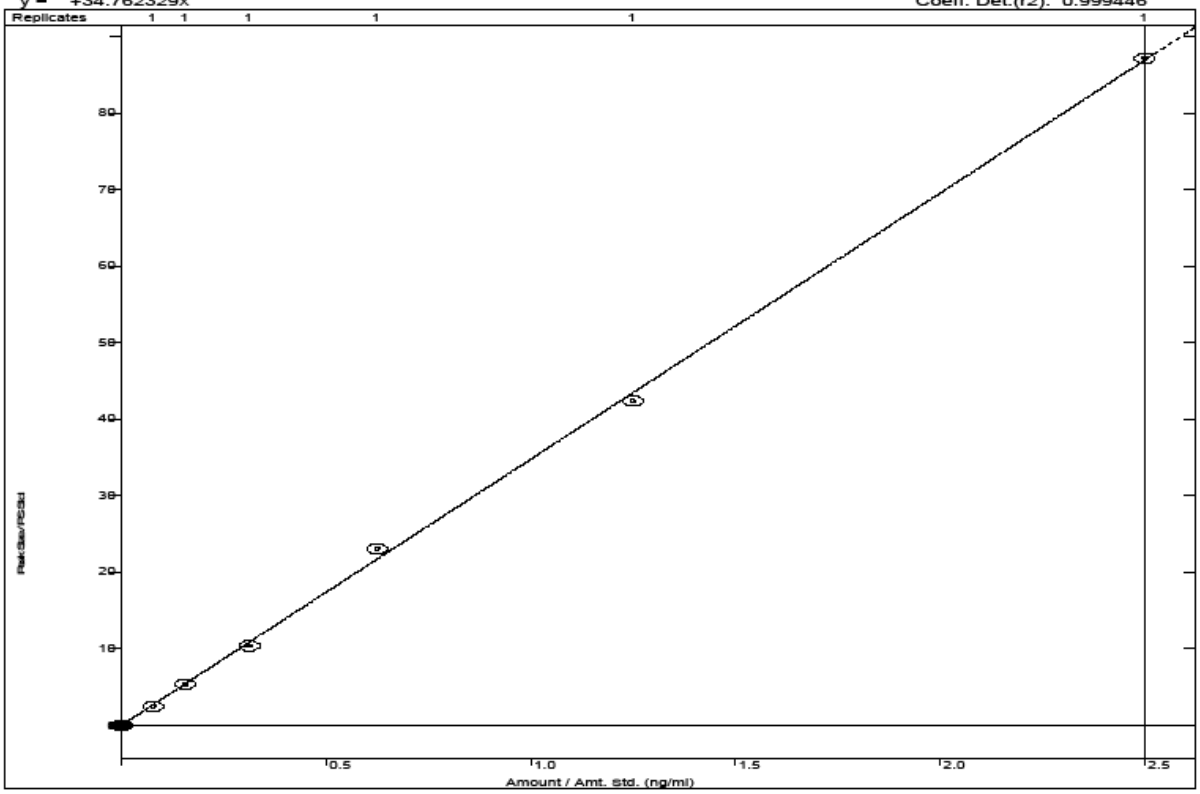

Appendix F: The expression of Abcg2 RNA Ontogeny

Material and Methods

Tissue collection:

Eight adult female Sprague-Dawley rats (four lactating and four non-lactating) were purchased from Harlan Laboratories (Indianapolis, IN). The mammary glands were harvested in lactating rats on day 16 to 18 post partum and all tissues from non-lactating and lactating rats were fresh frozen in liquid nitrogen and then stored at -80 °C until the time of analysis by real time PCR.

RNA isolation and quantitative PCR

Isolation of total RNA from mammary gland was performed using the RNeasy® Micro Kit per manufacturer protocol with sample disruption using Qiashredder® and on-column DNAse treatment. The total RNA concentration was determined by the measurement of optical density at 260 nm with a small volume UV-Vis Spectrophotometer (ND-1000, NanoDrop, Wilmington, DE). Total RNA integrity was verified by an OD260/OD280 absorption ratio greater than 1.9. Reverse-transcription of 1µg RNA to cDNA was performed with the SuperScriptTM First-Strand Synthesis System for RT-PCR kit following manufacturer's protocol using oligo(dT) to prime the reaction preferentially for mRNA. The total cDNA samples of liver and intestine ontogeny were from Maggie Abbassi (Maggie Abbassi Thesis).

Quantification of the expression level of rat Abcg2 was performed using the quantitative polymerase chain reaction (qPCR) on the iCycler Multicolor Real-Time PCR Detection System (Bio-Rad, Hercules, CA). The primer sequences were obtained from published literature and double checked with reference sequences deposited in NCBI's Entrez Gene with the software assistance of Primer3 (*Whitehead Institute for Biomedical Research, Cambridge, MA*) and Oligo Tool Kit (Operon, Huntsville, AL). The primers utilized were confirmed to generate unique products using NCBI's BLAST. Reference accession numbers, primer sequences, and product sizes are provided in table 6-1

Table 0-1 The primer sequences of rat Abcg2 for Qualitative PCR

Gene	Reference Sequence	Forward Primer (5'→3') / Reverse Primer (5'→3')	Prod. Size (bp)	Mg Conc (mM)	Anneal Temp (ºC)	Ref.
Rat Abcg2	AB105817	TAT GAG GTT CTT GCC AAG TGT TAT	181	3.5	60	(Bergman et al., 2005)
		CTA ACA TGA AGT ACA ATA AAC AAG				

qPCR reaction master mixes (50 µL) were made using the SYBR® Green PCR Core Reagents kit and contained 200 nM of each primer, 1.25 mM dNTPs, 1x SYBR Green buffer, 0.025 U/µL Taq polymerase, optimized concentrations of magnesium chloride for each primer pair, 20 nM fluorescein, and 0.10 µg of sample cDNA. The protocol for thermal cycling was:

Cycle 1: (1X)

Step 1: 95.0ºC for 05:00

Cycle 2: (50X)

Step 1: 95.0ºC for 00:45

Step 2: 60.0ºC for 01:00

Step 3: 72.0ºC for 01:00

Data collection and real-time analysis enabled.

Cycle 3: (1X)

Step 1: 95.0ºC for 02:00

Cycle 4: (100X)

Step 1: 95.0ºC for 00:30

Decrease setpoint temperature after cycle 2 by 0.5ºC

Melt curve data collection and analysis enabled.

Cycle 5: (1X)

Step 1: 4.0ºC HOLD

The mammary gland from a lactating rat 16 days post-partum was used as the comparator for relative quantification (to generate the standard curves). The standard curve of each qPCR has correlation coefficients > 0.99 and PCR efficiencies of 95-100%.

Finally, to confirm the generation of a single product of appropriate size, all amplification products were separated by 3% agarose gel electrophoresis in 1 x TBE running buffer for 50 min at 150 mV, visualized by staining with ethidium bromide, and imaged on an Image Station 2000 MM (Eastman Kodak, New Haven, CT).

Results

Expression of Abcg2 in non-lactating vs lactating mammary gland

qPCR was performed to determine if the transcripts for Abcg2 in mammary gland was increased during lactation. Rat Abcg2 amplification curve, standard curve, single products on the melt curve analysis and agarose gel electrophoresis are shown in **Fig. A-1**. After amplification Abcg2 could be detected and the product was confirmed by agarose gel electrophoresis. The RNA expression in mammary gland was increased almost 8 times than non-lactating rats. However one non-lactating rat had relative high Abcg2 level which is close to lactating mammary gland.

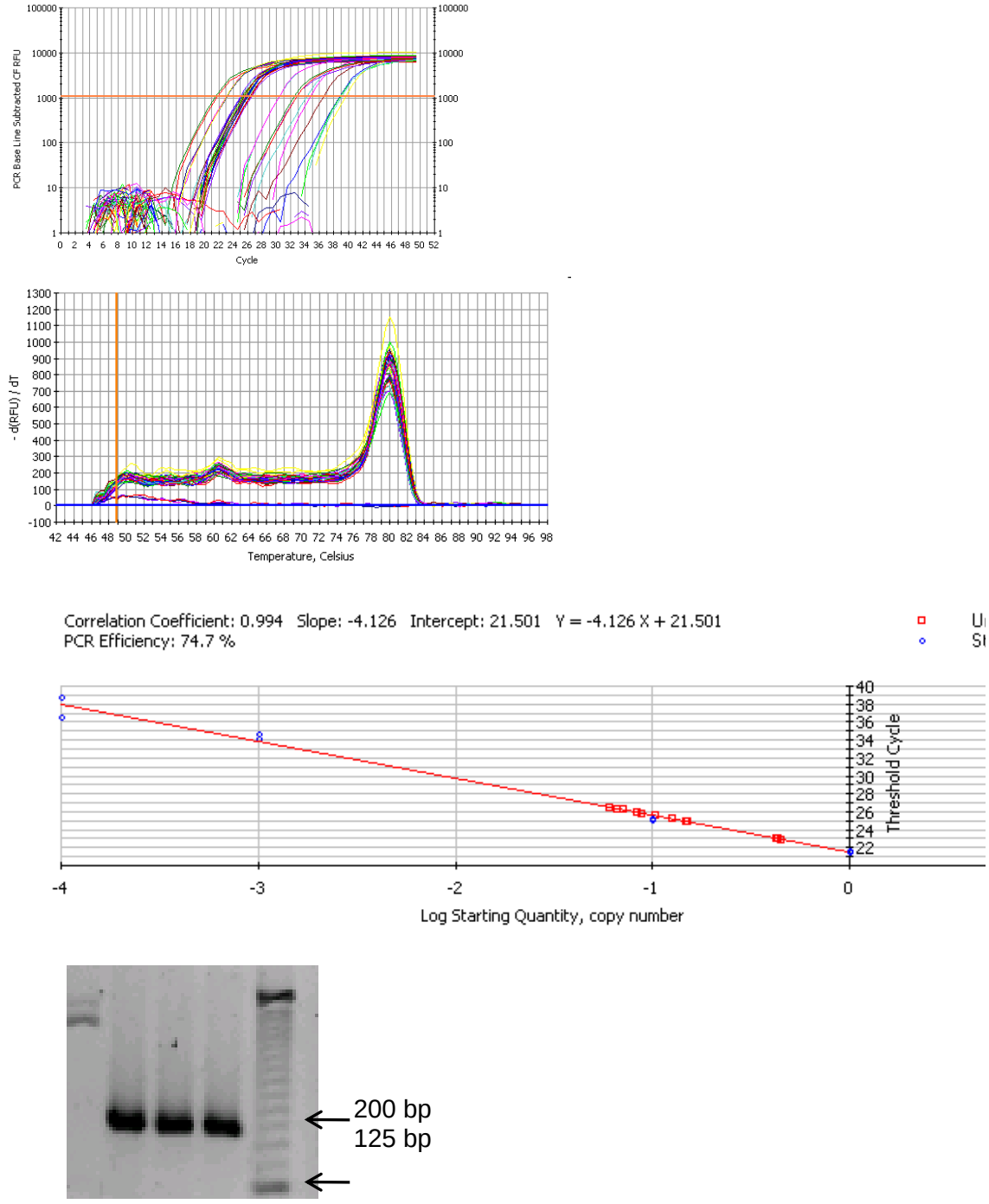

Figure 0-1 Rat Abcg2 amplification curve, melt curve analysis, standard curve, and agarose gel electrophoresis generated from standards over a 4-log10 dilution series for Abcg2 expression in lactating and non-lactating mammary gland.

Table 0-2 mRNA of Abcg2 expression level in lactating and non-lactating mammary gland**.**

Animal #	1	2	3	4	Ave.
Lac	0.141	0.433	0.0657	0.0909	0.183
Non-lac	0.00192	5.39E-05	0.0863	0.00708	0.024
Ratio(Lac/non-lac)					**7.662**

Expression of Abcg2 in intestine and liver ontogeny

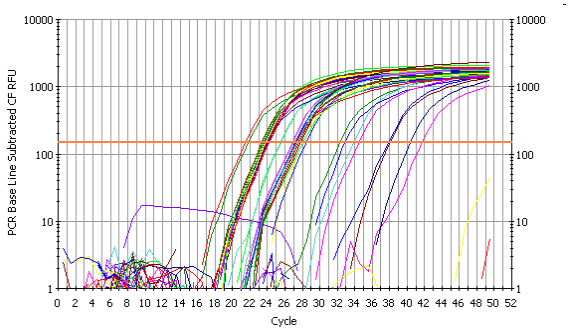

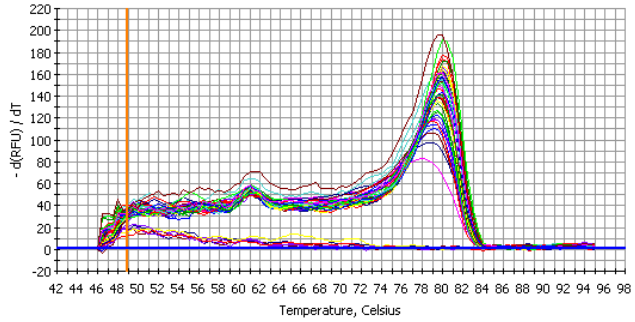

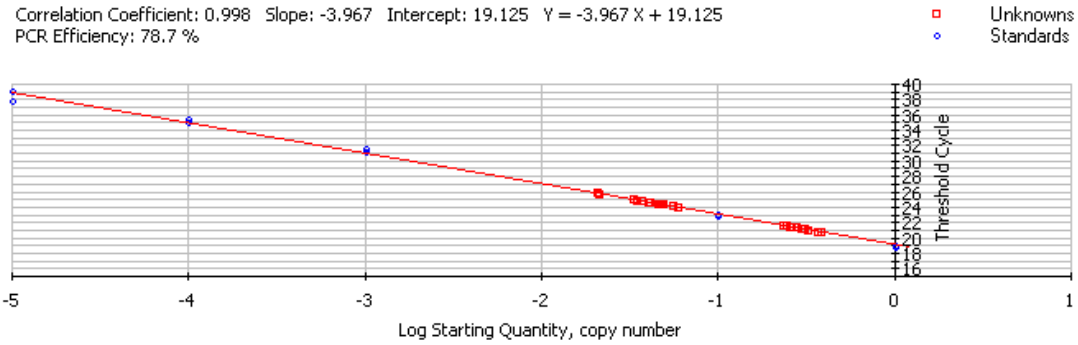

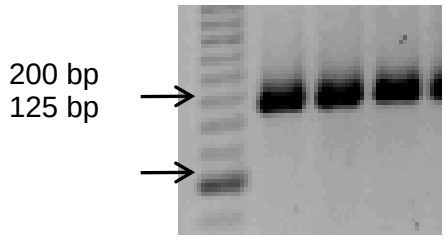

Figure 0-2 Rat Abcg2 amplification curve, melt curve analysis, standard curve, and agarose gel electrophoresis generated from standards over a 4-log10 dilution series for Abcg2 expression in intestine at different age.

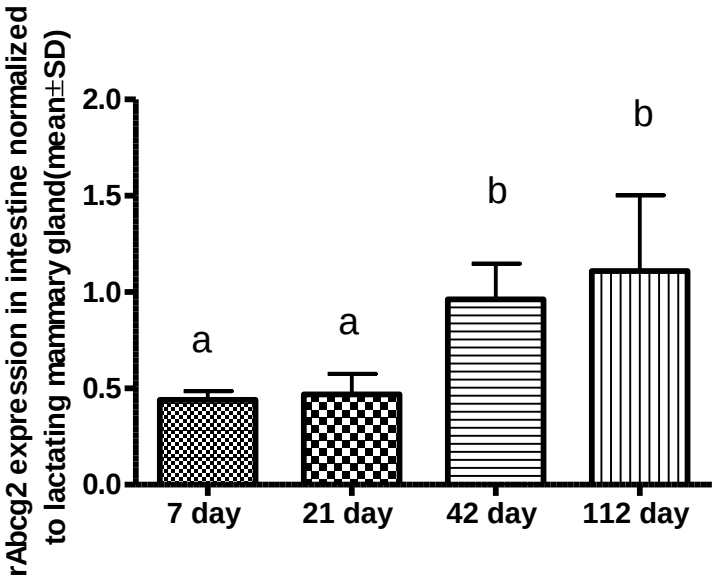

Figure 0-3 The expression level of rAbcg2 in intestine at different ages. Data were obtained from four rats in each group and the values that do not share the same letter are significantly ($P < 0.05$) different from each other.

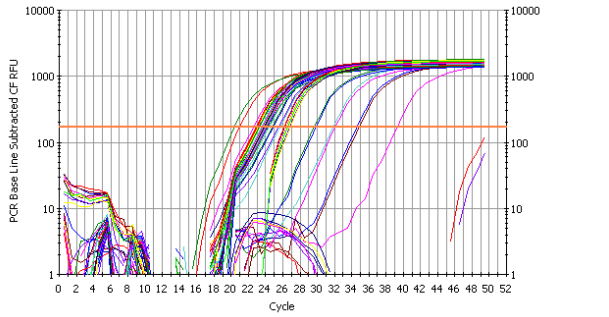

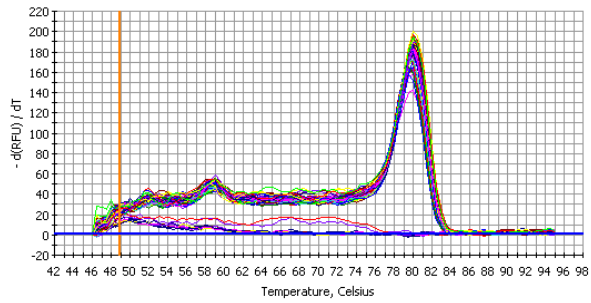

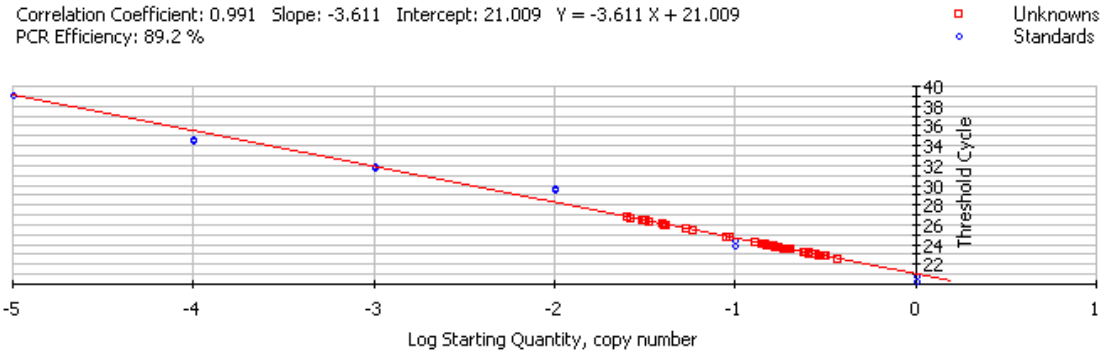

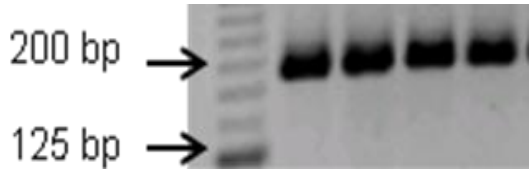

Figure 0-4 Rat Abcg2 amplification curve, melt curve analysis, standard curve, and agarose gel electrophoresis generated from standards over a 4-log10 dilution series for Abcg2 expression in liver at different age.

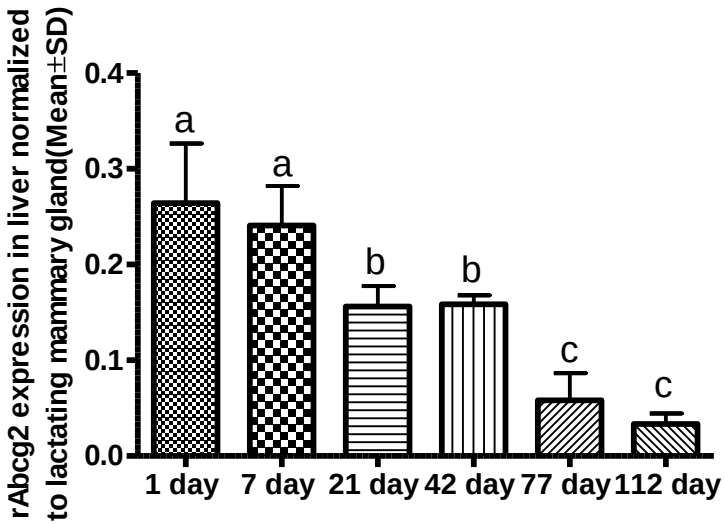

Figure 0-5 The expression level of rAbcg2 in liver at different ages. Data was obtained from four rats in each group and the values that do not share the same letter are significantly ($P < 0.05$) different from each other.

Appendix G: Inhibition of pantoprazole isomers on cimetidine transport across MDCKII empty and MDCKII-Abcg2 monolayer.

Material and Methods

Cells were seeded on microporous membrane filters (3.0-μm pore size, 24-mm diameter; Transwell 3414; Corning Inc., Corning, NY) at a density of 1.0 × 106 cells/well. Cells were grown for 4 days to achieve transepithelial electrical resistance >200 Ω · cm2, and medium was replaced every other day. Before the experiment, the medium at both the apical and basolateral side of the monolayer was replaced with 2 ml of OptiMEM medium (Invitrogen) without serum and either 100μM each pantoprazole isomer or OptiMEM only with 5 μM cimeditine traced with 0.1μM ^{3}H cimetidine containing 0.2 μCi/ml [^{14}C]sucrose. Cells were incubated at 37°C in 5% CO_2. We required that layers restricted sucrose transport to <1% of the total radioactivity per hour. 150-μl aliquots were taken and accounted at 0.5, 1 and 2h for cimetidine and sucrose transport.

Results

A

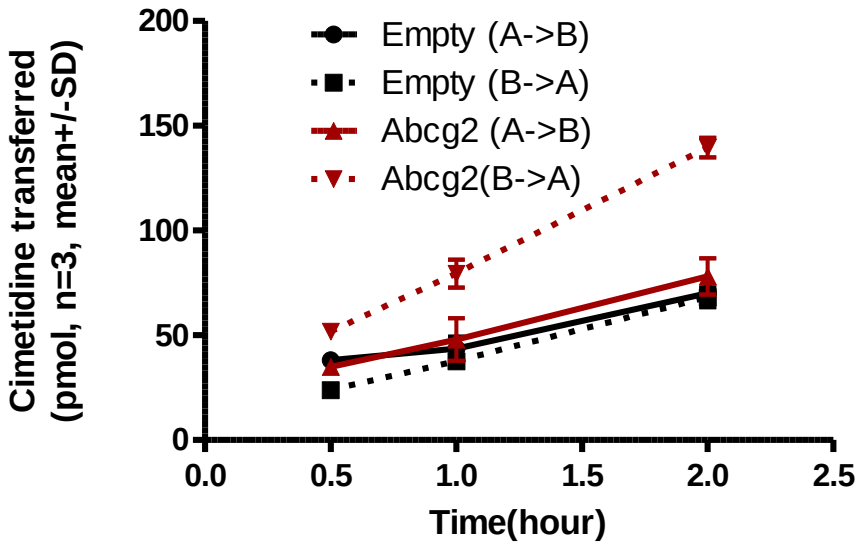

B

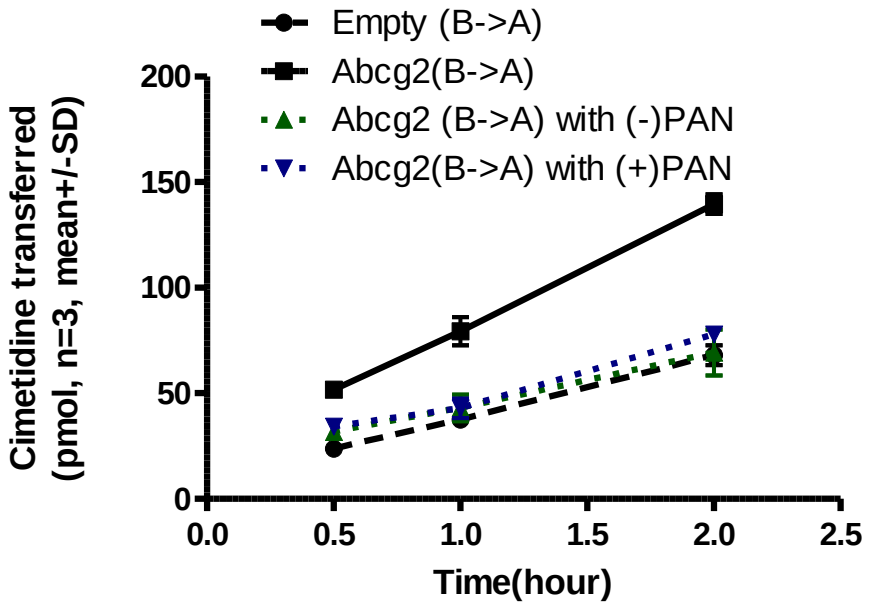

Figure 0-6 Inhibition of pantoprazole isomers on cimetidine transport across MDCKII empty and MDCKII-Abcg2 monolayer. A: Cimetidine transports in empty and rAbcg2-MDCKII cell lines; B: Cimetidine transports in rAbcg2-MDCKII cell line in absence or presence of PAN isomers.

Appendix H: Rat Abcg2 expressed in Sf9 system: the structure of vector, screening procedure, expression level and function study.

Establishment of rAbcg2 in Sf9 system

The total RNA was isolated from rat liver. Specific RNA of Abcg2 was amplified to cDNA which was purified and identified in DNA gel. Both the cDNA of Abcg2 and pENTR vector were digested by enzyme *Not I* and *Asc I.* Abcg2 was inserted into pENTR vector. The structure of pENTR vector and combined pENTR-Abcg2 are shown in **Figure A-7**. Combined pENTR-Abcg2 was amplified in Ecoli. DNA was extracted and purified. After digested at attRI and attRII positions, it was inserted into pIB/V5- His-DEST vector (**Figure A-8**). The pIB/V5-His-DEST vector-rat Abcg2 was transfected into Sf9 cells.

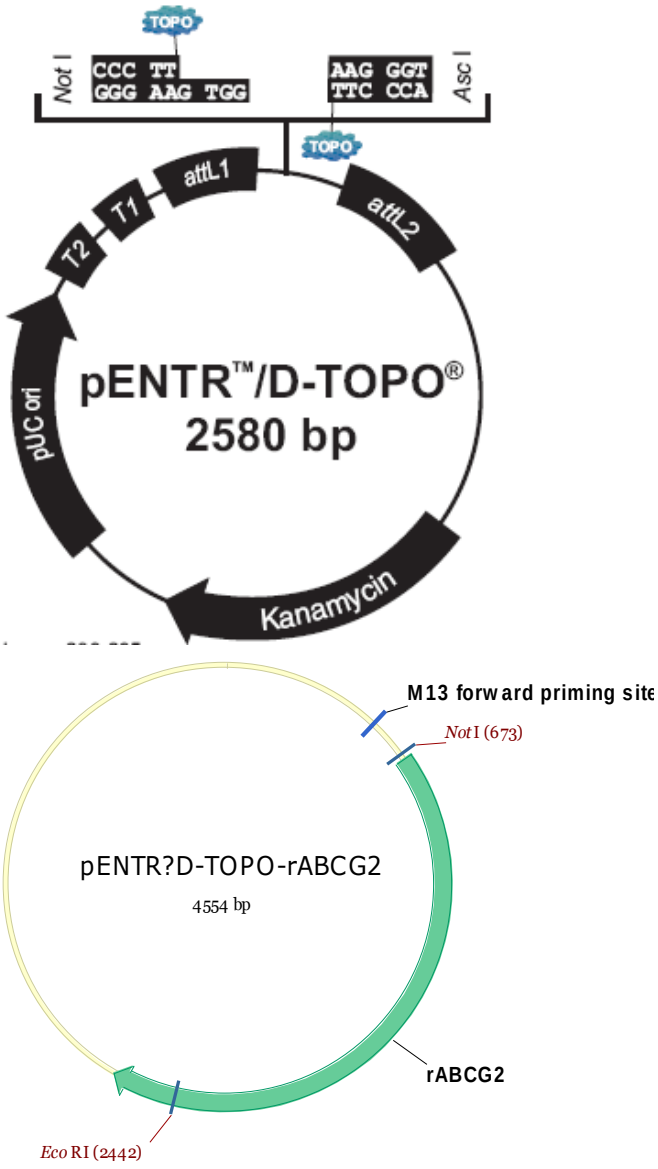

Figure 0-7 The structure of pENTR vector (Left) and combined pENTR-Abcg2 (Right).

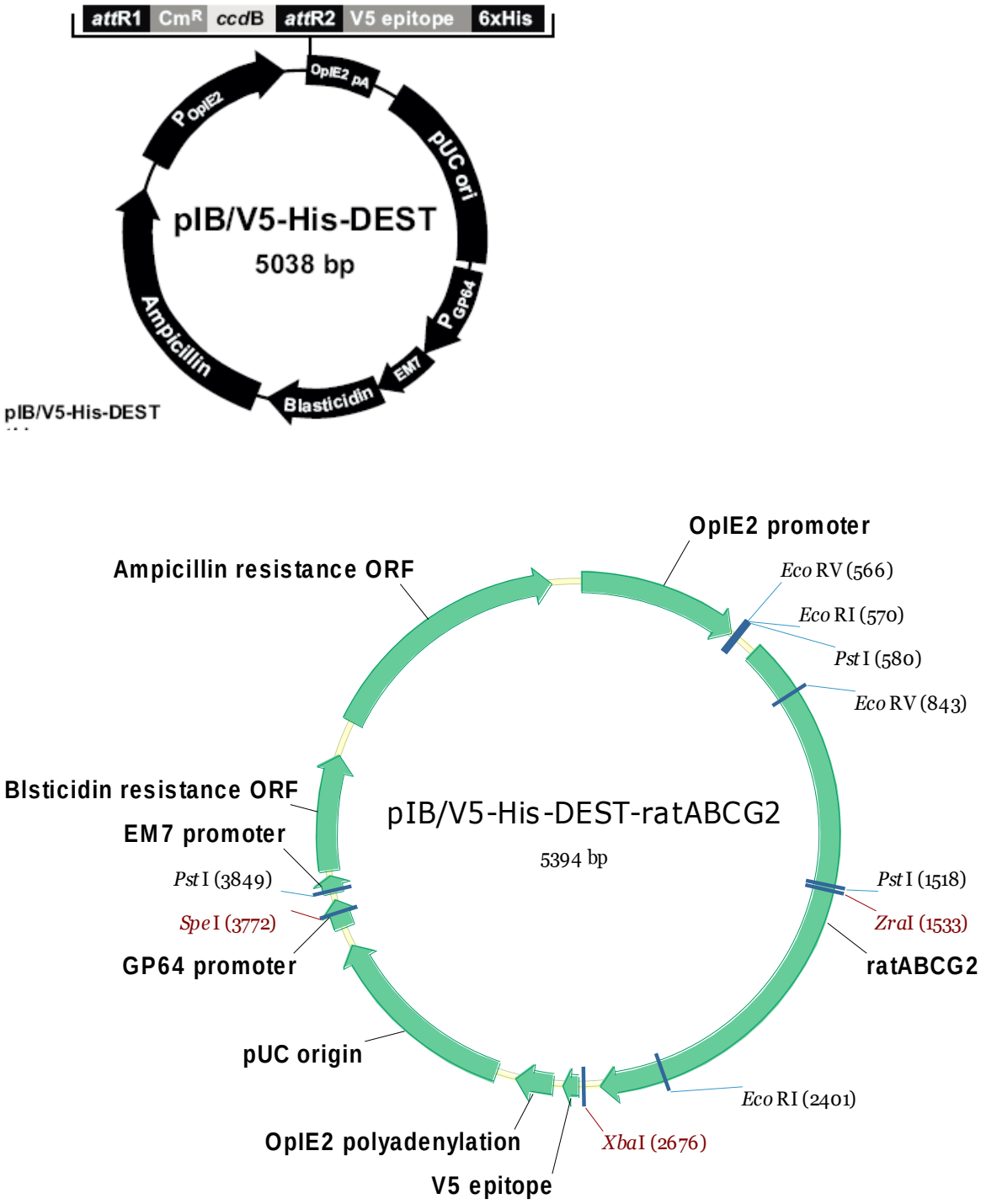

Figure 0-8 The structure of pIB/V5- His-DEST vector (upper) and pIB/V5- His-DEST-rat Abcg2 (lower).

Establishment of rAbcg2 in Sf9 system

Population screening of rAbcg2-Sf9

The rAbcg2-Sf9 population with higher Abcg2 expression level was sorted by Flow-Cytometry. The population was selected according to the comparison of fluoresce intension from Hoechst 33342 in vector and Abcg2-Sf9 combined with the result absence or presence of GF120918 in rAbcg2-Sf9. In order to get better rAbcg2-Sf9 population, they were grew and sorted after first sorting (**Figure A-9**). We tried to grow single clone rAbcg2-Sf9 by growing one cell but it was failed. So at last we chose to grow them as a population.

First sorting

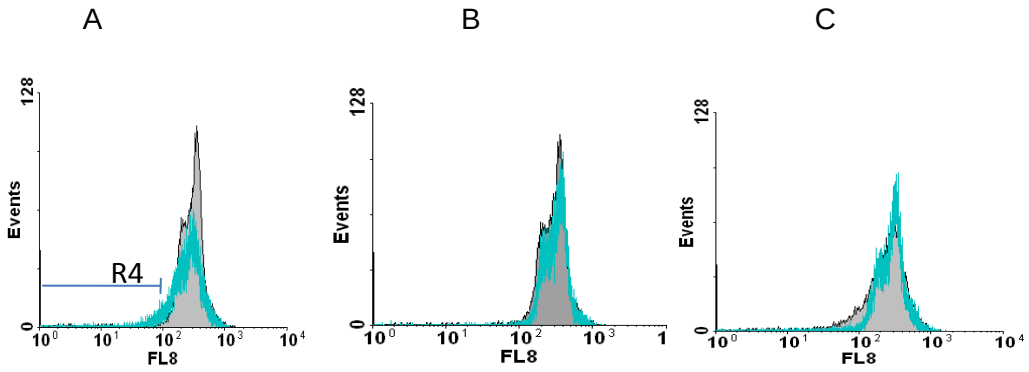

Second sorting

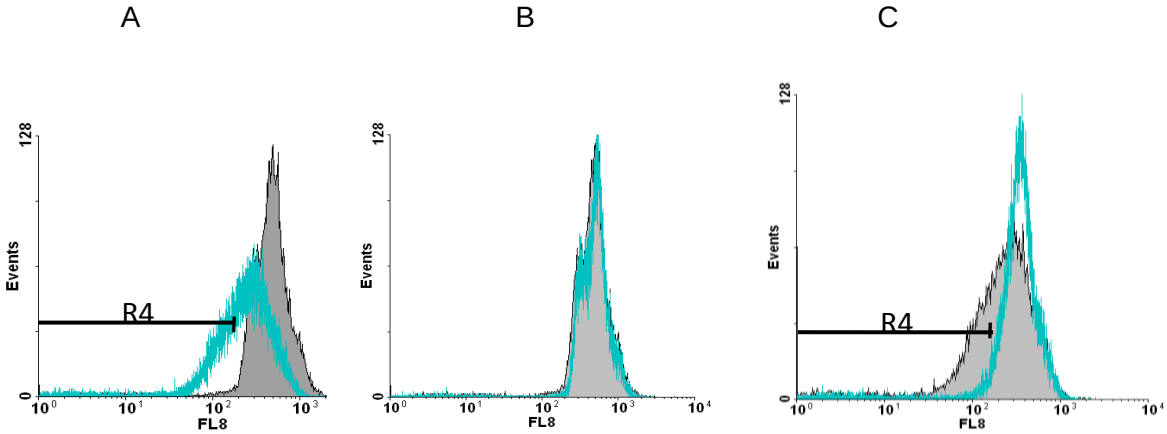

Figure 0-9 The rAbcg2-Sf9 population with higher Abcg2 expression level was sorted by Flow-Cytometry. Upper: first sorting. Lower: second sorting. A: Grey: vector; blue: rAbcg2. B: Grey: vector; blue: Vector+ GF120918. C: Grey: rAbcg2; blue: rAbcg2+ GF120918. R4: sorted rAbcg2 population.

Expression level of rAbcg2 in Abcg2-Sf9

Crude membrane fractions were prepared from vector only or rAbcg2-Sf9 cells, rat lactating mammary gland and kidney. The western blot was performed to test the expression level of Abcg2. The result was shown in **Figure A-10**.

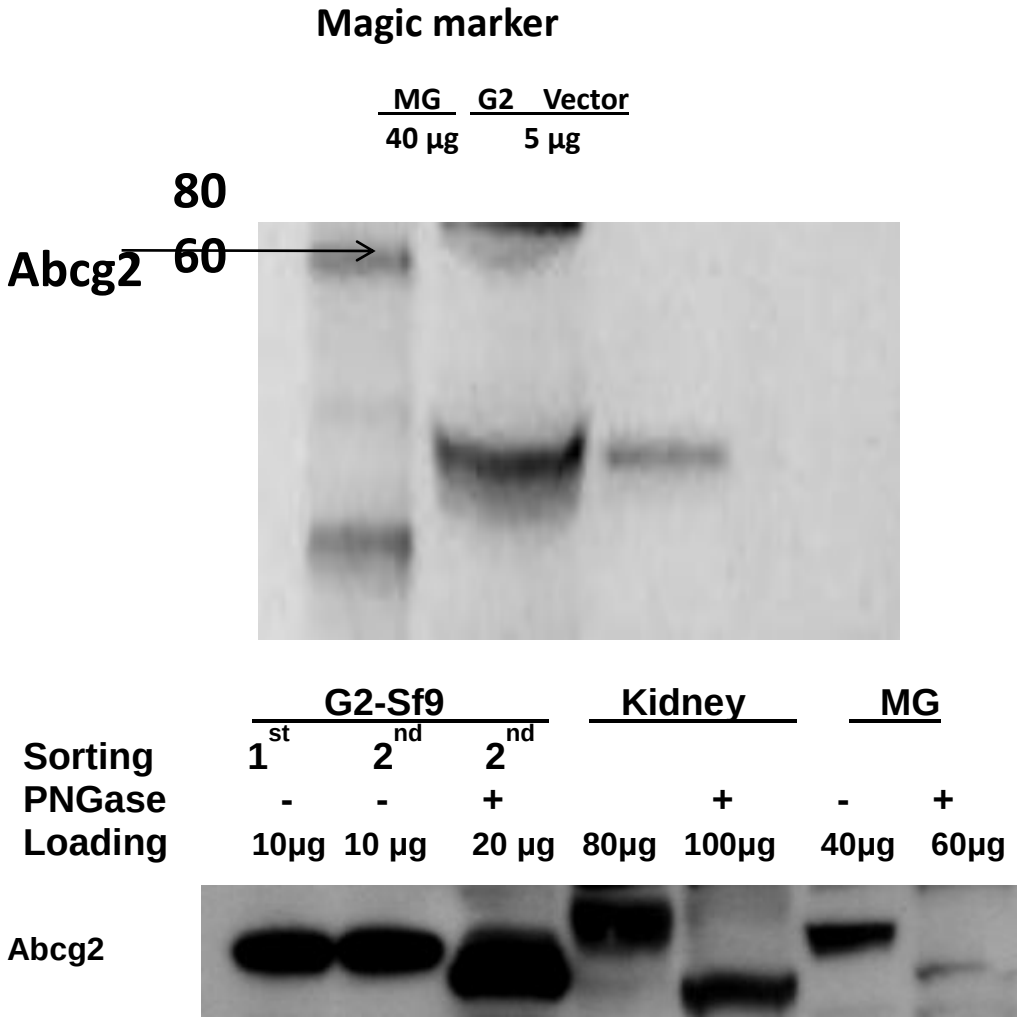

Figure 0-10 The Western result of rAbcg2 expression in Sf9 cells.

Function of rAbcg2 in Sf9

The plasma vesicles were prepared by the method in Leier's paper (Leier et al., 1994). ATP dependent methotrexate (1000μM) accumulation in vesicles at 20 minutes was performed according to the methods in Gerk's paper (Gerk et al., 2007). Forty μg vesicle proteins were used for each reaction of experiment. The results are shown in **Figure A-11**and time dependent experiment is shown in **Figure A-12**.

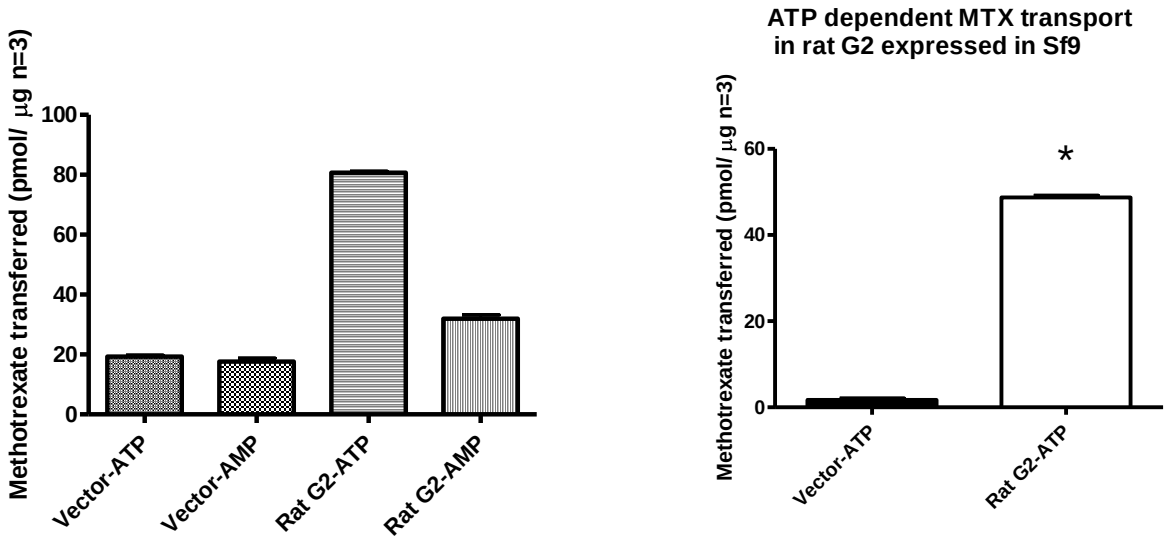

Figure 0-11 Methotrexate accumulated in presence of ATP or AMP in vesicle of vector or rAbcg2 in Sf9 cells (left panel). ATP dependent methotrexate transport by membrane vesicle from vector or rAbcg2 in Sf9 cells (right panel). Data are presented as mean±S.D (n=3).

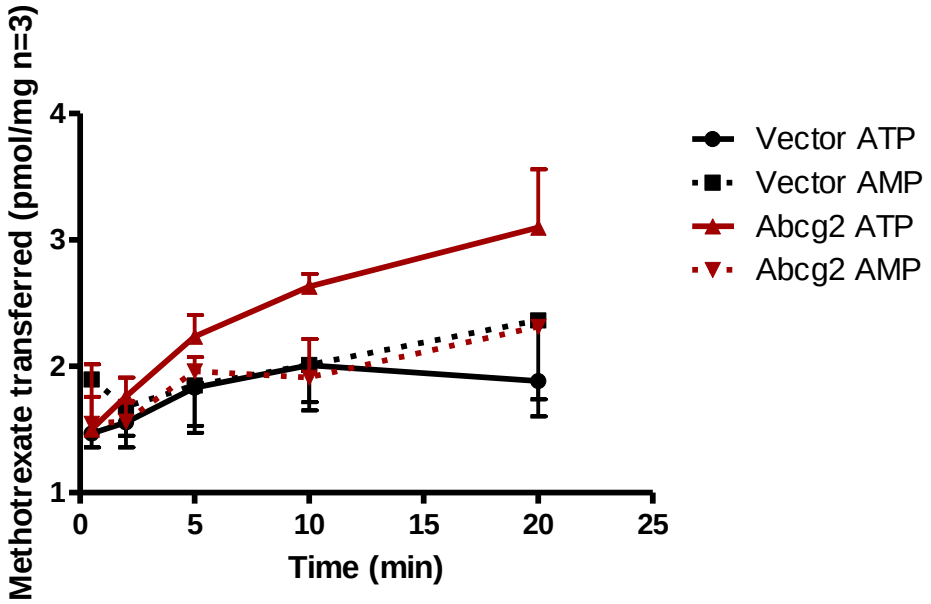

Figure 0-12 Time dependent of methotrexate accumulation in presence of ATP or AMP in vesicle of vector or rAbcg2 in Sf9 cells.

The problem of ABCG2/Abcg2-Sf9 vesicle experiment

In vesicle experiment the time dependent and concentration dependent experiments were performed for the estimation of K_m and V_{max} of Abcg2/ABCG2. The linear range of “uptake” of Abcg2/ABCG2 has been observed in time dependent experiment. Thus, the best incubation time could be determined. However, the saturation could not be clearly observed in concentration dependent experiment. The variability is big and could not see a smooth plateau. One of the possible reason is the Abcg2-Sf9 is a population not monoclonal cell line. Some of cells might have low Abcg2 expression and increased passive diffusion so that the active efflux mediated by Abcg2 can be masked.

Appendix I: The mass transport of pantoprazole isomers in human ABCG2 expressing in MDCKII cell lines at 3-200μM concentrations. (Note: this is the same data as shown in chapter 5. In this part, the data is shown as mass transfer rate from both directions vs donor concentration.**Figure A-13 and A-14**)

Note: Mass transport of a drug mediated by an active transporter vs donor concentration is a common method to describe the transport profile. From it, the kinetic parameters can be estimated, such as K_m and T_{max}. However, Transport data by Transwell model is different from that in vesicle transport studies. In order to get a direct picture and see how different between Transwell data and vesicle data, the mass transport of pantoprazole isomers in human ABCG2 expressing in MDCKII cell lines at 3-200 μM concentrations are shown as bellow.

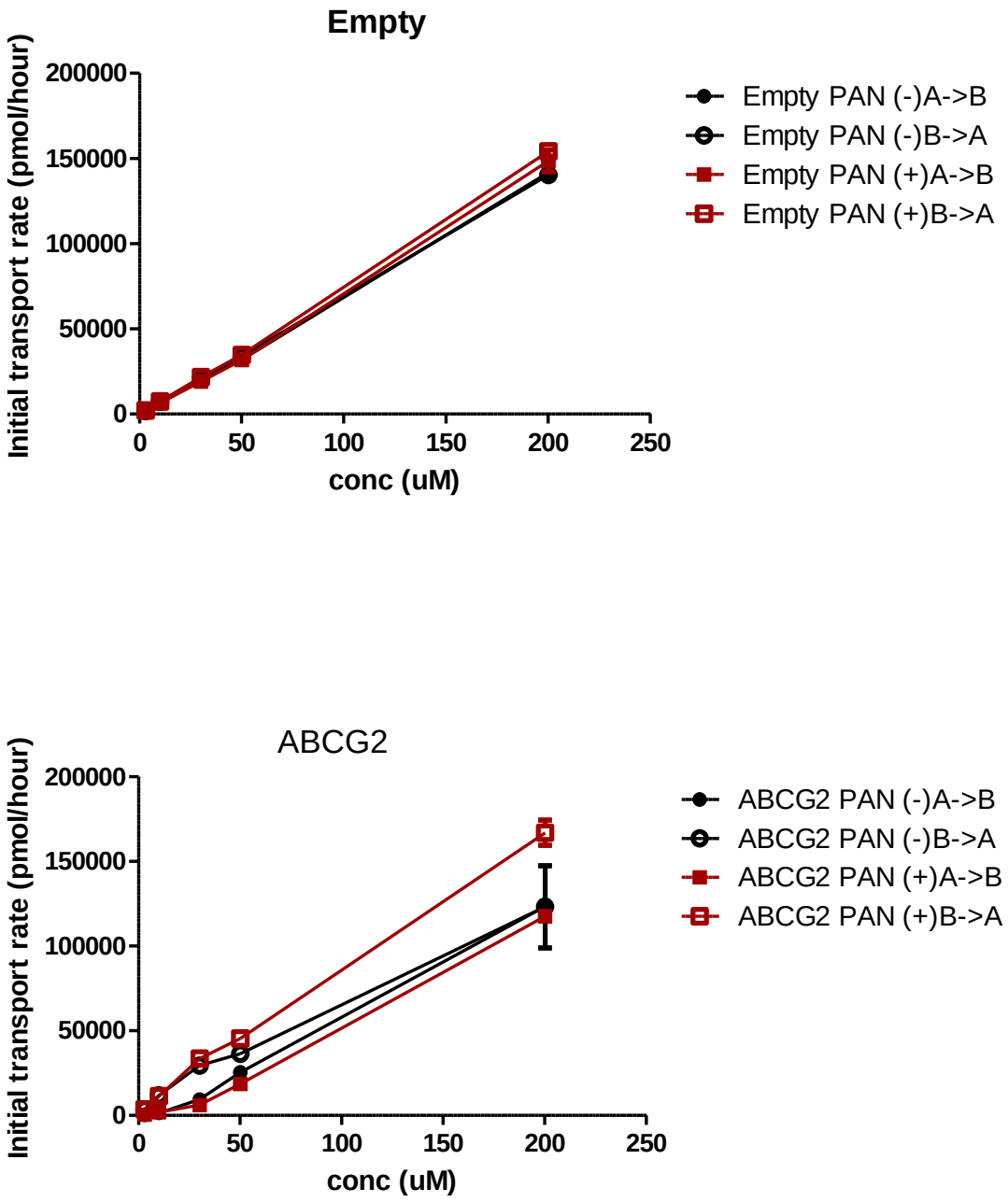

Figure 0-13 PAN isomers are transported in empty (upper) and ABCG2(lower) in MDCKII cells from 3-200μM concentrations.

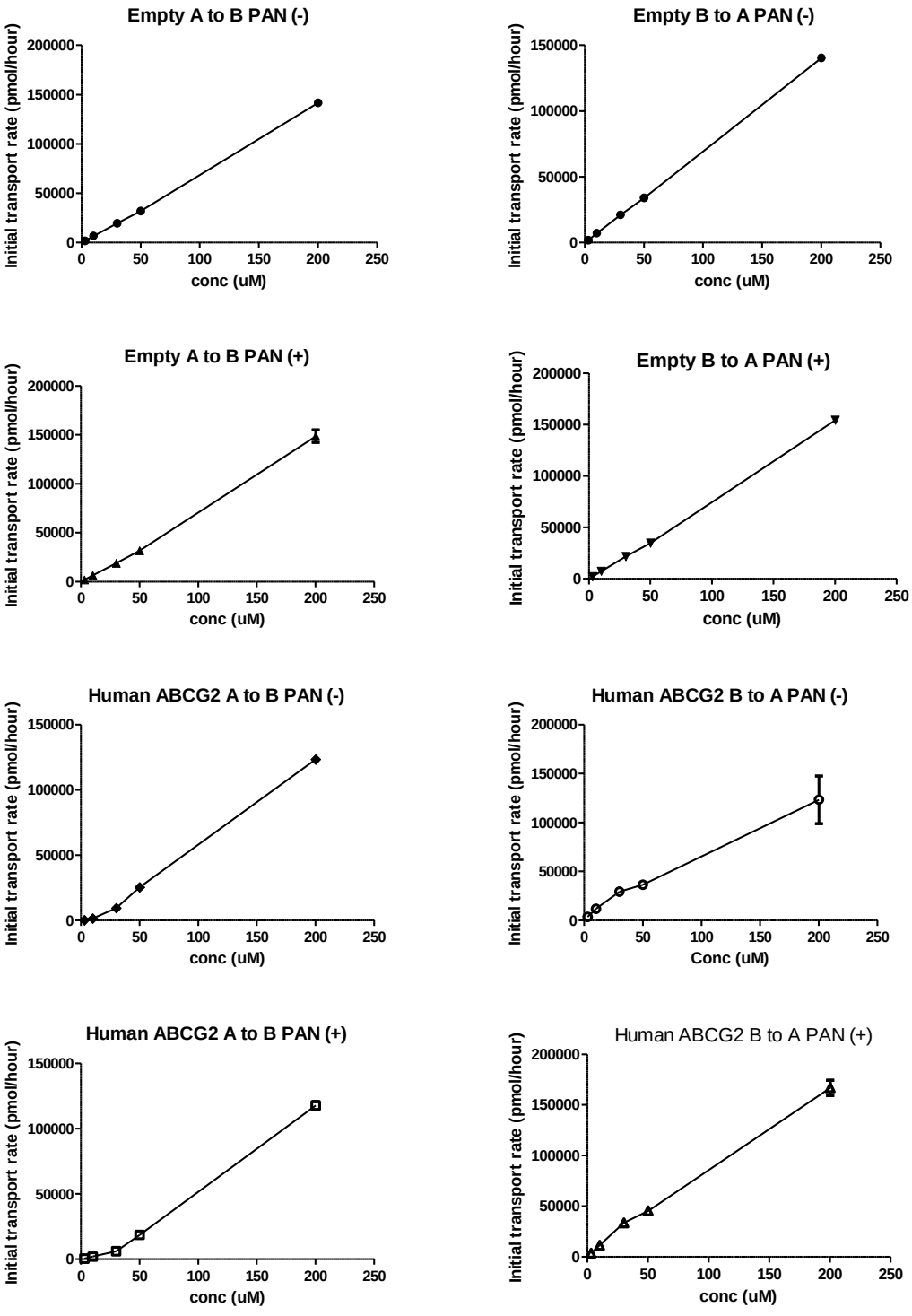

Figure 0-14 PAN isomers are transported from A to B or B to A direction in empty and ABCG2 in MDCKII cells at each concentration.

References:

Acharya P, O'Connor MP, Polli JW, Ayrton A, Ellens H and Bentz J (2008) Kinetic identification of membrane transporters that assist P-glycoprotein-mediated transport of digoxin and loperamide through a confluent monolayer of MDCKII-hMDR1 cells. *Drug Metab Dispos* **36:**452-460.

Adachi Y, Suzuki H and Sugiyama Y (2001) Comparative studies on in vitro methods for evaluating in vivo function of MDR1 P-glycoprotein. *Pharm Res* **18:**1660-1668.

Adkison KK, Vaidya SS, Lee DY, Koo SH, Li L, Mehta AA, Gross AS, Polli JW, Humphreys JE, Lou Y and Lee EJ (2009) Oral sulfasalazine as a clinical BCRP probe substrate: pharmacokinetic effects of genetic variation (C421A) and pantoprazole coadministration. *J Pharm Sci* **99:**1046-1062.

Afshar M and Thormann W (2006) Capillary electrophoretic investigation of the enantioselective metabolism of propafenone by human cytochrome P-450 SUPERSOMES: Evidence for atypical kinetics by CYP2D6 and CYP3A4. *Electrophoresis* **27:**1526-1536.

Agarwal S, Sane R, Gallardo JL, Ohlfest JR and Elmquist WF (2010) Distribution of gefitinib to the brain is limited by P-glycoprotein (ABCB1) and breast cancer resistance protein (ABCG2)-mediated active efflux. *J Pharmacol Exp Ther* **334:**147-155.

Ahmed-Belkacem A, Pozza A, Munoz-Martinez F, Bates SE, Castanys S, Gamarro F, Di Pietro A and Perez-Victoria JM (2005) Flavonoid structure-activity studies identify 6-prenylchrysin and tectochrysin as potent and specific inhibitors of breast cancer resistance protein ABCG2. *Cancer Res* **65:**4852-4860.

Alcorn J, Lu X, Moscow JA and McNamara PJ (2002) Transporter gene expression in lactating and nonlactating human mammary epithelial cells using real-time reverse transcription-polymerase chain reaction. *J Pharmacol Exp Ther* **303:**487-496.

Alcorn J and McNamara PJ (2002) Acyclovir, ganciclovir, and zidovudine transfer into rat milk. *Antimicrob Agents Chemother* **46:**1831-1836.

Anderson CM, Ganapathy V and Thwaites DT (2008) Human solute carrier SLC6A14 is the beta-alanine carrier. *J Physiol* **586:**4061-4067.

Andersson T (1996) Pharmacokinetics, metabolism and interactions of acid pump inhibitors. Focus on omeprazole, lansoprazole and pantoprazole. *Clin Pharmacokinet* **31:**9-28.

Andersson T and Weidolf L (2008) Stereoselective disposition of proton pump inhibitors. *Clin Drug Investig* **28:**263-279.

Arendt J (1997) Safety of melatonin in long-term use (?). *J Biol Rhythms* **12:**673-681.

Armstrong J and Reilly JJ (2002) Breastfeeding and lowering the risk of childhood obesity. *Lancet* **359:**2003-2004.

Aszalos A (2004) P-glycoprotein-based drug-drug interactions: preclinical methods and relevance to clinical observations. *Arch Pharm Res* **27:**127-135.

Badwan AAN, Lina N. ; Omari, M.M. Al; Daraghmeh, Nidal H; Ashour, Mahmoud K.; Abdoh, Ahmad M. and Jaber, A.M.Y. (2002) *Analytical profiles of drug substances and excipients*

Balakrishnan A, Hussainzada N, Gonzalez P, Bermejo M, Swaan PW and Polli JE (2007) Bias in estimation of transporter kinetic parameters from overexpression systems: Interplay of transporter expression level and substrate affinity. *J Pharmacol Exp Ther* **320:**133-144.

Balimane PV and Chong S (2005) A combined cell based approach to identify P-glycoprotein substrates and inhibitors in a single assay. *Int J Pharm* **301:**80-88.
Balimane PV, Patel K, Marino A and Chong S (2004) Utility of 96 well Caco-2 cell system for increased throughput of P-gp screening in drug discovery. *Eur J Pharm Biopharm* **58:**99-105.
Bartholome K, Rius M, Letschert K, Keller D, Timmer J and Keppler D (2007) Data-based mathematical modeling of vectorial transport across double-transfected polarized cells. *Drug Metab Dispos* **35:**1476-1481.
Bener A, Denic S and Galadari S (2001) Longer breast-feeding and protection against childhood leukaemia and lymphomas. *Eur J Cancer* **37:**234-238.
Bennet P (1988) *Drugs and human lactation*. Amsterdam: Elsevier.
Bentz J, Tran TT, Polli JW, Ayrton A and Ellens H (2005) The steady-state Michaelis-Menten analysis of P-glycoprotein mediated transport through a confluent cell monolayer cannot predict the correct Michaelis constant Km. *Pharm Res* **22:**1667-1677.
Bergman AM, Eijk PP, Ruiz van Haperen VW, Smid K, Veerman G, Hubeek I, van den Ijssel P, Ylstra B and Peters GJ (2005) In vivo induction of resistance to gemcitabine results in increased expression of ribonucleotide reductase subunit M1 as the major determinant. *Cancer Res* **65:**9510-9516.
Berlin CM, Jr., Paul IM and Vesell ES (2009) Safety issues of maternal drug therapy during breastfeeding. *Clin Pharmacol Ther* **85:**20-22.
Bharathi DV, Hotha KK, Jagadeesh B, Chatki PK, Thriveni K, Mullangi R and Naidu A (2009) Simultaneous estimation of four proton pump inhibitors--lansoprazole, omeprazole, pantoprazole and rabeprazole: development of a novel generic HPLC-UV method and its application to clinical pharmacokinetic study. *Biomed Chromatogr* **23:**732-739.
Bhatia P, Kolinski M, Moaddel R, Jozwiak K and Wainer IW (2008) Determination and modelling of stereoselective interactions of ligands with drug transporters: a key dimension in the understanding of drug disposition. *Xenobiotica* **38:**656-675.
Boumendjel A, Macalou S, Ahmed-Belkacem A, Blanc M and Di Pietro A (2007) Acridone derivatives: design, synthesis, and inhibition of breast cancer resistance protein ABCG2. *Bioorg Med Chem* **15:**2892-2897.
Breedveld P, Pluim D, Cipriani G, Wielinga P, van Tellingen O, Schinkel AH and Schellens JH (2005) The effect of Bcrp1 (Abcg2) on the in vivo pharmacokinetics and brain penetration of imatinib mesylate (Gleevec): implications for the use of breast cancer resistance protein and P-glycoprotein inhibitors to enable the brain penetration of imatinib in patients. *Cancer Res* **65:**2577-2582.
Breedveld P, Zelcer N, Pluim D, Sonmezer O, Tibben MM, Beijnen JH, Schinkel AH, van Tellingen O, Borst P and Schellens JH (2004) Mechanism of the pharmacokinetic interaction between methotrexate and benzimidazoles: potential role for breast cancer resistance protein in clinical drug-drug interactions. *Cancer Res* **64:**5804-5811.
Brimer C, Dalton JT, Zhu Z, Schuetz J, Yasuda K, Vanin E, Relling MV, Lu Y and Schuetz EG (2000) Creation of polarized cells coexpressing CYP3A4, NADPH cytochrome P450 reductase and MDR1/P-glycoprotein. *Pharm Res* **17:**803-810.
Brisken C, Heineman A, Chavarria T, Elenbaas B, Tan J, Dey SK, McMahon JA, McMahon AP and Weinberg RA (2000) Essential function of Wnt-4 in mammary gland development downstream of progesterone signaling. *Genes Dev* **14:**650-654.
Burdall SE, Hanby AM, Lansdown MR and Speirs V (2003) Breast cancer cell lines: friend or foe? *Breast Cancer Res* **5:**89-95.

Burger H, van Tol H, Brok M, Wiemer EA, de Bruijn EA, Guetens G, de Boeck G, Sparreboom A, Verweij J and Nooter K (2005) Chronic imatinib mesylate exposure leads to reduced intracellular drug accumulation by induction of the ABCG2 (BCRP) and ABCB1 (MDR1) drug transport pumps. *Cancer Biol Ther* **4:**747-752.

Cai X, Bikadi Z, Ni Z, Lee EW, Wang H, Rosenberg MF and Mao Q (2010) Role of basic residues within or near the predicted transmembrane helix 2 of the human breast cancer resistance protein in drug transport. *J Pharmacol Exp Ther* **333:**670-681.

Campo VL, Bernardes LS and Carvalho I (2009) Stereoselectivity in drug metabolism: molecular mechanisms and analytical methods. *Curr Drug Metab* **10:**188-205.

Cheng X and Klaassen CD (2009) Tissue distribution, ontogeny, and hormonal regulation of xenobiotic transporters in mouse kidneys. *Drug Metab Dispos* **37:**2178-2185.

Choong E, Dobrinas M, Carrupt PA and Eap CB (2010) The permeability P-glycoprotein: a focus on enantioselectivity and brain distribution. *Expert Opin Drug Metab Toxicol*.

Chu XY, Bleasby K, Yabut J, Cai X, Chan GH, Hafey MJ, Xu S, Bergman AJ, Braun MP, Dean DC and Evers R (2007) Transport of the dipeptidyl peptidase-4 inhibitor sitagliptin by human organic anion transporter 3, organic anion transporting polypeptide 4C1, and multidrug resistance P-glycoprotein. *J Pharmacol Exp Ther* **321:**673-683.

Chu XY, Strauss JR, Mariano MA, Li J, Newton DJ, Cai X, Wang RW, Yabut J, Hartley DP, Evans DC and Evers R (2006) Characterization of mice lacking the multidrug resistance protein MRP2 (ABCC2). *J Pharmacol Exp Ther* **317:**579-589.

Chulada PC, Arbes SJ, Jr., Dunson D and Zeldin DC (2003) Breast-feeding and the prevalence of asthma and wheeze in children: analyses from the Third National Health and Nutrition Examination Survey, 1988-1994. *J Allergy Clin Immunol* **111:**328-336.

Cisternino S, Mercier C, Bourasset F, Roux F and Scherrmann JM (2004) Expression, up-regulation, and transport activity of the multidrug-resistance protein Abcg2 at the mouse blood-brain barrier. *Cancer Res* **64:**3296-3301.

David T. Rossi MWS (2002) *Mass spectrometry in drug discovery* CRC Press, New York

Davis MK (1998) Review of the evidence for an association between infant feeding and childhood cancer. *Int J Cancer Suppl* **11:**29-33.

DE D (1993) The early history of stereochemistry: From the discovery of molecular asymmetry and the first resolution of a racemate to the asymmetrical chiral carbon of van't Hoff and Le Bel. , in: *Drug stereochemistry:* (Dekker M ed, pp 1-24, IW Wainer. , New York.

de Waart DR, Hausler S, Vlaming ML, Kunne C, Hanggi E, Gruss HJ, Oude Elferink RP and Stieger B (2010) Hepatic transport mechanisms of cholyl-L-lysyl-fluorescein. *J Pharmacol Exp Ther* **334:**78-86.

de Wolf C, Jansen R, Yamaguchi H, de Haas M, van de Wetering K, Wijnholds J, Beijnen J and Borst P (2008) Contribution of the drug transporter ABCG2 (breast cancer resistance protein) to resistance against anticancer nucleosides. *Mol Cancer Ther* **7:**3092-3102.

Delic D, Warskulat U, Borsch E, Al-Qahtani S, Al-Quraishi S, Haussinger D and Wunderlich F (2010) Loss of ability to self-heal malaria upon taurine transporter deletion. *Infect Immun* **78:**1642-1649.

Doyle LA and Ross DD (2003) Multidrug resistance mediated by the breast cancer resistance protein BCRP (ABCG2). *Oncogene* **22:**7340-7358.

Doyle LA, Yang W, Abruzzo LV, Krogmann T, Gao Y, Rishi AK and Ross DD (1998) A multidrug resistance transporter from human MCF-7 breast cancer cells. *Proc Natl Acad Sci U S A* **95:**15665-15670.

Edwards JE, Alcorn J, Savolainen J, Anderson BD and McNamara PJ (2005) Role of P-glycoprotein in distribution of nelfinavir across the blood-mammary tissue barrier and blood-brain barrier. *Antimicrob Agents Chemother* **49:**1626-1628.

Edwards JE, Rudy AC, Wermeling DP, Desai N and McNamara PJ (2003) Hydromorphone transfer into breast milk after intranasal administration. *Pharmacotherapy* **23:**153-158.

Feng B, Mills JB, Davidson RE, Mireles RJ, Janiszewski JS, Troutman MD and de Morais SM (2008) In vitro P-glycoprotein assays to predict the in vivo interactions of P-glycoprotein with drugs in the central nervous system. *Drug Metab Dispos* **36:**268-275.

Fleishaker JC (2003) Models and methods for predicting drug transfer into human milk. *Adv Drug Deliv Rev* **55:**643-652.

Fleishaker JC, Desai N and McNamara PJ (1987) Factors affecting the milk-to-plasma drug concentration ratio in lactating women: physical interactions with protein and fat. *J Pharm Sci* **76:**189-193.

Fleishaker JC and McNamara PJ (1988a) Effect of altered serum protein binding on propranolol distribution into milk in the lactating rabbit. *J Pharmacol Exp Ther* **244:**925-928.

Fleishaker JC and McNamara PJ (1988b) In vivo evaluation in the lactating rabbit of a model for xenobiotic distribution into breast milk. *J Pharmacol Exp Ther* **244:**919-924.

Friguls B, Joya X, Garcia-Algar O, Pallas CR, Vall O and Pichini S (2010) A comprehensive review of assay methods to determine drugs in breast milk and the safety of breastfeeding when taking drugs. *Anal Bioanal Chem*.

Gannon MK, 2nd, Holt JJ, Bennett SM, Wetzel BR, Loo TW, Bartlett MC, Clarke DM, Sawada GA, Higgins JW, Tombline G, Raub TJ and Detty MR (2009) Rhodamine inhibitors of P-glycoprotein: an amide/thioamide "switch" for ATPase activity. *J Med Chem* **52:**3328-3341.

Gdalevich M, Mimouni D and Mimouni M (2001) Breast-feeding and the risk of bronchial asthma in childhood: a systematic review with meta-analysis of prospective studies. *J Pediatr* **139:**261-266.

Gentile S (2005) The safety of newer antidepressants in pregnancy and breastfeeding. *Drug Saf* **28:**137-152.

Gerk PM, Hanson L, Neville MC and McNamara PJ (2002) Sodium dependence of nitrofurantoin active transport across mammary epithelia and effects of dipyridamole, nucleosides, and nucleobases. *Pharm Res* **19:**299-305.

Gerk PM, Kuhn RJ, Desai NS and McNamara PJ (2001a) Active transport of nitrofurantoin into human milk. *Pharmacotherapy* **21:**669-675.

Gerk PM, Li W, Megaraj V and Vore M (2007) Human multidrug resistance protein 2 transports the therapeutic bile salt tauroursodeoxycholate. *J Pharmacol Exp Ther* **320:**893-899.

Gerk PM, Oo CY, Paxton EW, Moscow JA and McNamara PJ (2001b) Interactions between cimetidine, nitrofurantoin, and probenecid active transport into rat milk. *J Pharmacol Exp Ther* **296:**175-180.

Giacomini KM, Huang SM, Tweedie DJ, Benet LZ, Brouwer KL, Chu X, Dahlin A, Evers R, Fischer V, Hillgren KM, Hoffmaster KA, Ishikawa T, Keppler D, Kim RB, Lee CA, Niemi M, Polli JW, Sugiyama Y, Swaan PW, Ware JA, Wright SH, Yee SW,

Zamek-Gliszczynski MJ and Zhang L (2010) Membrane transporters in drug development. *Nat Rev Drug Discov* **9:**215-236.
Gillman MW, Rifas-Shiman SL, Camargo CA, Jr., Berkey CS, Frazier AL, Rockett HR, Field AE and Colditz GA (2001) Risk of overweight among adolescents who were breastfed as infants. *Jama* **285:**2461-2467.
Giri N, Agarwal S, Pan G, Chen Y, Shaik N and Elmquist WF (2008) Substrate dependent Abcg2/Bcrp1-mediated interactions: consideration of multiple binding sites in in vitro assay design. *Drug Metab Dispos*.
Goldman AS, Chheda S, Garofalo R and Schmalstieg FC (1996) Cytokines in human milk: properties and potential effects upon the mammary gland and the neonate. *J Mammary Gland Biol Neoplasia* **1:**251-258.
Grummer-Strawn LM and Shealy KR (2009) Progress in protecting, promoting, and supporting breastfeeding: 1984-2009. *Breastfeed Med* **4 Suppl 1:**S31-39.
Gunaratna C and Kissinger PT (1998) Investigation of stereoselective metabolism of amphetamine in rat liver microsomes by microdialysis and liquid chromatography with precolumn chiral derivatization. *J Chromatogr A* **828:**95-103.
Gunderson EP (2008) Breast-feeding and diabetes: long-term impact on mothers and their infants. *Curr Diab Rep* **8:**279-286.
Gupta A, Zhang Y, Unadkat JD and Mao Q (2004) HIV protease inhibitors are inhibitors but not substrates of the human breast cancer resistance protein (BCRP/ABCG2). *J Pharmacol Exp Ther* **310:**334-341.
Ha HR and Follath F (2004) Metabolism of antiarrhythmics. *Curr Drug Metab* **5:**543-571.
He Y, Liu Y and Zeng S (2009) Stereoselective and multiple carrier-mediated transport of cetirizine across Caco-2 cell monolayers with potential drug interaction. *Chirality* **22:**684-692.
Hennighausen L and Robinson GW (2001) Signaling pathways in mammary gland development. *Dev Cell* **1:**467-475.
Hernadez MT, Paricio JM, Peman J, Sanchez M, Beseler B and Benlloch MJ (2009) [Breastfeeding and antiinfectious agents.]. *Rev Esp Quimioter* **22:**180-189.
Huang SM and Woodcock J (2010) Transporters in drug development: advancing on the Critical Path. *Nat Rev Drug Discov* **9:**175-176.
Huber R, Hartmann M, Bliesath H, Luhmann R, Steinijans VW and Zech K (1996a) Pharmacokinetics of pantoprazole in man. *Int J Clin Pharmacol Ther* **34:**S7-16.
Huber R, Hartmann M, Bliesath H, Luhmann R, Steinijans VW and Zech K (1996b) Pharmacokinetics of pantoprazole in man. *Int J Clin Pharmacol Ther* **34:**185-194.
Huber R, Kohl B, Sachs G, Senn-Bilfinger J, Simon WA and Sturm E (1995) Review article: the continuing development of proton pump inhibitors with particular reference to pantoprazole. *Aliment Pharmacol Ther* **9:**363-378.
Huls M, Brown CD, Windass AS, Sayer R, van den Heuvel JJ, Heemskerk S, Russel FG and Masereeuw R (2008) The breast cancer resistance protein transporter ABCG2 is expressed in the human kidney proximal tubule apical membrane. *Kidney Int* **73:**220-225.
Hunziker W and Kraehenbuhl JP (1998) Epithelial transcytosis of immunoglobulins. *J Mammary Gland Biol Neoplasia* **3:**287-302.
Ip S, Chung M, Raman G, Trikalinos TA and Lau J (2009) A summary of the Agency for Healthcare Research and Quality's evidence report on breastfeeding in developed countries. *Breastfeed Med* **4 Suppl 1:**S17-30.
Isaacs EB, Fischl BR, Quinn BT, Chong WK, Gadian DG and Lucas A (2009) Impact of breast milk on IQ, brain size and white matter development. *Pediatr Res*.

Ishikawa T, Tamura A, Saito H, Wakabayashi K and Nakagawa H (2005) Pharmacogenomics of the human ABC transporter ABCG2: from functional evaluation to drug molecular design. *Naturwissenschaften* **92:**451-463.
James DC and Lessen R (2009) Position of the American Dietetic Association: promoting and supporting breastfeeding. *J Am Diet Assoc* **109:**1926-1942.
Janneh O, Anwar T, Jungbauer C, Kopp S, Khoo SH, Back DJ and Chiba P (2009) P-glycoprotein, multidrug resistance-associated proteins and human organic anion transporting polypeptide influence the intracellular accumulation of atazanavir. *Antivir Ther* **14:**965-974.
Johnson BM, Zhang P, Schuetz JD and Brouwer KL (2006) Characterization of transport protein expression in multidrug resistance-associated protein (Mrp) 2-deficient rats. *Drug Metab Dispos* **34:**556-562.
Jonker JW, Merino G, Musters S, van Herwaarden AE, Bolscher E, Wagenaar E, Mesman E, Dale TC and Schinkel AH (2005) The breast cancer resistance protein BCRP (ABCG2) concentrates drugs and carcinogenic xenotoxins into milk. *Nat Med* **11:**127-129.
Kage K, Fujita T and Sugimoto Y (2005) Role of Cys-603 in dimer/oligomer formation of the breast cancer resistance protein BCRP/ABCG2. *Cancer Sci* **96:**866-872.
Kage K, Tsukahara S, Sugiyama T, Asada S, Ishikawa E, Tsuruo T and Sugimoto Y (2002) Dominant-negative inhibition of breast cancer resistance protein as drug efflux pump through the inhibition of S-S dependent homodimerization. *Int J Cancer* **97:**626-630.
Kalliokoski A and Niemi M (2009) Impact of OATP transporters on pharmacokinetics. *Br J Pharmacol* **158:**693-705.
Kalvass JC and Pollack GM (2007) Kinetic considerations for the quantitative assessment of efflux activity and inhibition: implications for understanding and predicting the effects of efflux inhibition. *Pharm Res* **24:**265-276.
Karunakaran S, Umapathy NS, Thangaraju M, Hatanaka T, Itagaki S, Munn DH, Prasad PD and Ganapathy V (2008) Interaction of tryptophan derivatives with SLC6A14 (ATB0,+) reveals the potential of the transporter as a drug target for cancer chemotherapy. *Biochem J* **414:**343-355.
Katsuki H, Hamada A, Nakamura C, Arimori K and Nakano M (2001) Role of CYP3A4 and CYP2C19 in the stereoselective metabolism of lansoprazole by human liver microsomes. *Eur J Clin Pharmacol* **57:**709-715.
Kempf J, Snook LA, Vonesch JL, Dahms TE, Pattus F and Massotte D (2002) Expression of the human mu opioid receptor in a stable Sf9 cell line. *J Biotechnol* **95:**181-187.
Keogh JP and Kunta JR (2006a) Development, validation and utility of an in vitro technique for assessment of potential clinical drug-drug interactions involving P-glycoprotein. *Eur J Pharm Sci* **27:**543-554.
Keogh JP and Kunta JR (2006b) Development, validation and utility of an in vitro technique for assessment of potential clinical drug-drug interactions involving P-glycoprotein. *Eur J Pharm Sci*.
Khaksari M, Shafiee M, Ghasemi A and Asl SZ (2009) Effect of orally administered propylthiouracil in pregnant and lactating rats on isolated aorta contractility of their adult male offspring. *Med Sci Monit* **15:**BR123-127.
Kim RB, Fromm MF, Wandel C, Leake B, Wood AJ, Roden DM and Wilkinson GR (1998) The drug transporter P-glycoprotein limits oral absorption and brain entry of HIV-1 protease inhibitors. *J Clin Invest* **101:**289-294.
Kim RB, Wandel C, Leake B, Cvetkovic M, Fromm MF, Dempsey PJ, Roden MM, Belas F, Chaudhary AK, Roden DM, Wood AJ and Wilkinson GR (1999)

Interrelationship between substrates and inhibitors of human CYP3A and P-glycoprotein. *Pharm Res* **16:**408-414.
Kitamura S, Maeda K, Wang Y and Sugiyama Y (2008) Involvement of multiple transporters in the hepatobiliary transport of rosuvastatin. *Drug Metab Dispos* **36:**2014-2023.
Klaassen CD and Aleksunes LM (2010) Xenobiotic, bile acid, and cholesterol transporters: function and regulation. *Pharmacol Rev* **62:**1-96.
Kodaira H, Kusuhara H, Ushiki J, Fuse E and Sugiyama Y (2010) Kinetic analysis of the cooperation of P-glycoprotein (P-gp/Abcb1) and breast cancer resistance protein (Bcrp/Abcg2) in limiting the brain and testis penetration of erlotinib, flavopiridol, and mitoxantrone. *J Pharmacol Exp Ther* **333:**788-796.
Kohl B, Sturm E, Senn-Bilfinger J, Simon WA, Kruger U, Schaefer H, Rainer G, Figala V and Klemm K (1992) (H+,K+)-ATPase inhibiting 2-[(2-pyridylmethyl)sulfinyl]benzimidazoles. 4. A novel series of dimethoxypyridyl-substituted inhibitors with enhanced selectivity. The selection of pantoprazole as a clinical candidate. *J Med Chem* **35:**1049-1057.
Kohler D, Kruse M, Stocker W and Sterchi EE (2000) Heterologously overexpressed, affinity-purified human meprin alpha is functionally active and cleaves components of the basement membrane in vitro. *FEBS Lett* **465:**2-7.
Koldovsky O (1995) Hormones in milk. *Vitam Horm* **50:**77-149.
Kooij G, Backer R, Koning JJ, Reijerkerk A, van Horssen J, van der Pol SM, Drexhage J, Schinkel A, Dijkstra CD, den Haan JM, Geijtenbeek TB and de Vries HE (2009) P-glycoprotein acts as an immunomodulator during neuroinflammation. *PLoS One* **4:**e8212.
Korjamo T, Kemilainen H, Heikkinen AT and Monkkonen J (2007) Decrease in intracellular concentration causes the shift in Km value of efflux pump substrates. *Drug Metab Dispos* **35:**1574-1579.
Kos V and Ford RC (2009) The ATP-binding cassette family: a structural perspective. *Cell Mol Life Sci* **66:**3111-3126.
Kostraba JN, Cruickshanks KJ, Lawler-Heavner J, Jobim LF, Rewers MJ, Gay EC, Chase HP, Klingensmith G and Hamman RF (1993) Early exposure to cow's milk and solid foods in infancy, genetic predisposition, and risk of IDDM. *Diabetes* **42:**288-295.
Kramer MS, Aboud F, Mironova E, Vanilovich I, Platt RW, Matush L, Igumnov S, Fombonne E, Bogdanovich N, Ducruet T, Collet JP, Chalmers B, Hodnett E, Davidovsky S, Skugarevsky O, Trofimovich O, Kozlova L and Shapiro S (2008) Breastfeeding and child cognitive development: new evidence from a large randomized trial. *Arch Gen Psychiatry* **65:**578-584.
Kruijtzer CM, Beijnen JH, Rosing H, ten Bokkel Huinink WW, Schot M, Jewell RC, Paul EM and Schellens JH (2002) Increased oral bioavailability of topotecan in combination with the breast cancer resistance protein and P-glycoprotein inhibitor GF120918. *J Clin Oncol* **20:**2943-2950.
Kuppens IE, Witteveen EO, Jewell RC, Radema SA, Paul EM, Mangum SG, Beijnen JH, Voest EE and Schellens JH (2007) A phase I, randomized, open-label, parallel-cohort, dose-finding study of elacridar (GF120918) and oral topotecan in cancer patients. *Clin Cancer Res* **13:**3276-3285.
Lagas JS, Fan L, Wagenaar E, Vlaming ML, van Tellingen O, Beijnen JH and Schinkel AH (2009a) P-glycoprotein (P-gp/Abcb1), Abcc2, and Abcc3 determine the pharmacokinetics of etoposide. *Clin Cancer Res* **16:**130-140.
Lagas JS, van der Kruijssen CM, van de Wetering K, Beijnen JH and Schinkel AH (2009b) Transport of diclofenac by breast cancer resistance protein (ABCG2)

and stimulation of multidrug resistance protein 2 (ABCC2)-mediated drug transport by diclofenac and benzbromarone. *Drug Metab Dispos* **37:**129-136.
Larson BL (1979) Biosynthesis and secretion of milk proteins: a review. *J Dairy Res* **46:**161-174.
Lechner C, Reichel V, Moenning U, Reichel A and Fricker G (2010) Development of a fluorescence-based assay for drug interactions with human Multidrug Resistance Related Protein (MRP2; ABCC2) in MDCKII-MRP2 membrane vesicles. *Eur J Pharm Biopharm* **75:**284-290.
Lee CG, Gottesman MM, Cardarelli CO, Ramachandra M, Jeang KT, Ambudkar SV, Pastan I and Dey S (1998) HIV-1 protease inhibitors are substrates for the MDR1 multidrug transporter. *Biochemistry* **37:**3594-3601.
Leggas M, Panetta JC, Zhuang Y, Schuetz JD, Johnston B, Bai F, Sorrentino B, Zhou S, Houghton PJ and Stewart CF (2006) Gefitinib modulates the function of multiple ATP-binding cassette transporters in vivo. *Cancer Res* **66:**4802-4807.
Leier I, Jedlitschky G, Buchholz U, Cole SP, Deeley RG and Keppler D (1994) The MRP gene encodes an ATP-dependent export pump for leukotriene C4 and structurally related conjugates. *J Biol Chem* **269:**27807-27810.
Lentz KA, Polli JW, Wring SA, Humphreys JE and Polli JE (2000) Influence of passive permeability on apparent P-glycoprotein kinetics. *Pharm Res* **17:**1456-1460.
Litman T, Jensen U, Hansen A, Covitz KM, Zhan Z, Fetsch P, Abati A, Hansen PR, Horn T, Skovsgaard T and Bates SE (2002) Use of peptide antibodies to probe for the mitoxantrone resistance-associated protein MXR/BCRP/ABCP/ABCG2. *Biochim Biophys Acta* **1565:**6-16.
Liu T, Chang LJ, Uss A, Chu I, Morrison RA, Wang L, Prelusky D, Cheng KC and Li C (2009) The impact of protein on Caco-2 permeability of low mass balance compounds for absorption projection and efflux substrate identification. *J Pharm Biomed Anal* **51:**1069-1077.
Luker GD, Rao VV, Crankshaw CL, Dahlheimer J and Piwnica-Worms D (1997) Characterization of phosphine complexes of technetium(III) as transport substrates of the multidrug resistance P-glycoprotein and functional markers of P-glycoprotein at the blood-brain barrier. *Biochemistry* **36:**14218-14227.
Lumen AA, Acharya P, Polli JW, Ayrton A, Ellens H and Bentz J (2010) If the KI is defined by the free energy of binding to P-glycoprotein, which kinetic parameters define the IC50 for the Madin-Darby canine kidney II cell line overexpressing human multidrug resistance 1 confluent cell monolayer? *Drug Metab Dispos* **38:**260-269.
Madadi P, Ross CJ, Hayden MR, Carleton BC, Gaedigk A, Leeder JS and Koren G (2009) Pharmacogenetics of neonatal opioid toxicity following maternal use of codeine during breastfeeding: a case-control study. *Clin Pharmacol Ther* **85:**31-35.
Mao Q and Unadkat JD (2005) Role of the breast cancer resistance protein (ABCG2) in drug transport. *Aaps J* **7:**E118-133.
Marchetti S, Oostendorp RL, Pluim D, van Eijndhoven M, van Tellingen O, Schinkel AH, Versace R, Beijnen JH, Mazzanti R and Schellens JH (2007) In vitro transport of gimatecan (7-t-butoxyiminomethylcamptothecin) by breast cancer resistance protein, P-glycoprotein, and multidrug resistance protein 2. *Mol Cancer Ther* **6:**3307-3313.
Mason T, Rabinovich CE, Fredrickson DD, Amoroso K, Reed AM, Stein LD and Kredich DW (1995) Breast feeding and the development of juvenile rheumatoid arthritis. *J Rheumatol* **22:**1166-1170.

Masubuchi N, Yamazaki H and Tanaka M (1998) Stereoselective chiral inversion of pantoprazole enantiomers after separate doses to rats. *Chirality* **10:**747-753.
Mather IH and Keenan TW (1998) Origin and secretion of milk lipids. *J Mammary Gland Biol Neoplasia* **3:**259-273.
Matsson P, Pedersen JM, Norinder U, Bergstrom CA and Artursson P (2009) Identification of novel specific and general inhibitors of the three major human ATP-binding cassette transporters P-gp, BCRP and MRP2 among registered drugs. *Pharm Res* **26:**1816-1831.
Matsushima S, Maeda K, Kondo C, Hirano M, Sasaki M, Suzuki H and Sugiyama Y (2005) Identification of the hepatic efflux transporters of organic anions using double-transfected Madin-Darby canine kidney II cells expressing human organic anion-transporting polypeptide 1B1 (OATP1B1)/multidrug resistance-associated protein 2, OATP1B1/multidrug resistance 1, and OATP1B1/breast cancer resistance protein. *J Pharmacol Exp Ther* **314:**1059-1067.
McManaman JL and Neville MC (2003) Mammary physiology and milk secretion. *Adv Drug Deliv Rev* **55:**629-641.
McNamara PJ, Burgio D and Yoo SD (1991) Pharmacokinetics of acetaminophen, antipyrine, and salicylic acid in the lactating and nursing rabbit, with model predictions of milk to serum concentration ratios and neonatal dose. *Toxicol Appl Pharmacol* **109:**149-160.
McNamara PJ, Burgio D and Yoo SD (1992a) Pharmacokinetics of caffeine and its demethylated metabolites in lactating adult rabbits and neonatal offspring. Predictions of breast milk to serum concentration ratios. *Drug Metab Dispos* **20:**302-308.
McNamara PJ, Burgio D and Yoo SD (1992b) Pharmacokinetics of cimetidine during lactation: species differences in cimetidine transport into rat and rabbit milk. *J Pharmacol Exp Ther* **261:**918-923.
McNamara PJ, Meece JA and Paxton E (1996) Active transport of cimetidine and ranitidine into the milk of Sprague Dawley rats. *J Pharmacol Exp Ther* **277:**1615-1621.
Merino G, Alvarez AI, Pulido MM, Molina AJ, Schinkel AH and Prieto JG (2006a) Breast cancer resistance protein (BCRP/ABCG2) transports fluoroquinolone antibiotics and affects their oral availability, pharmacokinetics and milk secretion. *Drug Metab Dispos*.
Merino G, Alvarez AI, Pulido MM, Molina AJ, Schinkel AH and Prieto JG (2006b) Breast cancer resistance protein (BCRP/ABCG2) transports fluoroquinolone antibiotics and affects their oral availability, pharmacokinetics, and milk secretion. *Drug Metab Dispos* **34:**690-695.
Merino G, Jonker JW, Wagenaar E, Pulido MM, Molina AJ, Alvarez AI and Schinkel AH (2005a) Transport of anthelmintic benzimidazole drugs by breast cancer resistance protein (BCRP/ABCG2). *Drug Metab Dispos* **33:**614-618.
Merino G, Jonker JW, Wagenaar E, van Herwaarden AE and Schinkel AH (2005b) The breast cancer resistance protein (BCRP/ABCG2) affects pharmacokinetics, hepatobiliary excretion, and milk secretion of the antibiotic nitrofurantoin. *Mol Pharmacol* **67:**1758-1764.
Meunier V, Bourrie M, Berger Y and Fabre G (1995) The human intestinal epithelial cell line Caco-2; pharmacological and pharmacokinetic applications. *Cell Biol Toxicol* **11:**187-194.
Meyer UA (1996) Metabolic interactions of the proton-pump inhibitors lansoprazole, omeprazole and pantoprazole with other drugs. *Eur J Gastroenterol Hepatol* **8 Suppl 1:**S21-25.

Mitomo H, Kato R, Ito A, Kasamatsu S, Ikegami Y, Kii I, Kudo A, Kobatake E, Sumino Y and Ishikawa T (2003) A functional study on polymorphism of the ATP-binding cassette transporter ABCG2: critical role of arginine-482 in methotrexate transport. *Biochem J* **373:**767-774.
Miura M and Uno T (2009) Clinical pharmacokinetics of fexofenadine enantiomers. *Expert Opin Drug Metab Toxicol* **6:**69-74.
Naruhashi K, Tamai I, Li Q, Sai Y and Tsuji A (2003) Experimental demonstration of the unstirred water layer effect on drug transport in Caco-2 cells. *J Pharm Sci* **92:**1502-1508.
Neville MC and Watters CD (1983) Secretion of calcium into milk: review. *J Dairy Sci* **66:**371-380.
Nguyen DA and Neville MC (1998) Tight junction regulation in the mammary gland. *J Mammary Gland Biol Neoplasia* **3:**233-246.
Nichols EL and Nichols VN (1981) Human milk: nutritional resource. *Prog Clin Biol Res* **61:**109-146.
Nobili V, Bedogni G, Alisi A, Pietrobattista A, Alterio A, Tiribelli C and Agostoni C (2009) A protective effect of breastfeeding on the progression of non-alcoholic fatty liver disease. *Arch Dis Child* **94:**801-805.
Noubarani M, Keyhanfar F, Motevalian M and Mahmoudian M (2010) Improved HPLC method for determination of four PPIs, omeprazole, pantoprazole, lansoprazole and rabeprazole in human plasma. *J Pharm Pharm Sci* **13:**1-10.
Nunez MC, Garcia-Rubino ME, Conejo-Garcia A, Cruz-Lopez O, Kimatrai M, Gallo MA, Espinosa A and Campos JM (2009) Homochiral drugs: a demanding tendency of the pharmaceutical industry. *Curr Med Chem* **16:**2064-2074.
O'Byrne SM, Kako Y, Deckelbaum RJ, Hansen IH, Palczewski K, Goldberg IJ and Blaner WS (2009) Multiple pathways ensure retinoid delivery to milk: studies in genetically modified mice. *Am J Physiol Endocrinol Metab* **298:**E862-870.
Ohashi A, Fukumuro M, Sawabe K, Mamada K, Sugawara Y, Matsuoka H and Hasegawa H (2009) Transcellular relocation of tetrahydrobiopterin across Caco-2 cells: a model study of tetrahydrobiopterin absorption through epithelial cells of intestinal mucosa. *J Inherit Metab Dis* **32:**73-78.
Ohtsu N, Anzai N, Fukutomi T, Kimura T, Sakurai H and Endou H (2010) [Human renal urate transpoter URAT1 mediates the transport of salicylate]. *Nippon Jinzo Gakkai Shi* **52:**499-504.
Ollivier-Bousquet M (1998) Transferrin and prolactin transcytosis in the lactating mammary epithelial cell. *J Mammary Gland Biol Neoplasia* **3:**303-313.
Oo CY, Kuhn RJ, Desai N and McNamara PJ (1995) Active transport of cimetidine into human milk. *Clin Pharmacol Ther* **58:**548-555.
Oo CY, Paxton EW and McNamara PJ (2001) Active transport of nitrofurantoin into rat milk. *Adv Exp Med Biol* **501:**547-552.
Oostendorp RL, Buckle T, Beijnen JH, van Tellingen O and Schellens JH (2009) The effect of P-gp (Mdr1a/1b), BCRP (Bcrp1) and P-gp/BCRP inhibitors on the in vivo absorption, distribution, metabolism and excretion of imatinib. *Invest New Drugs* **27:**31-40.
Ormandy CJ, Camus A, Barra J, Damotte D, Lucas B, Buteau H, Edery M, Brousse N, Babinet C, Binart N and Kelly PA (1997) Null mutation of the prolactin receptor gene produces multiple reproductive defects in the mouse. *Genes Dev* **11:**167-178.
Pan G, Giri N and Elmquist WF (2007) Abcg2/Bcrp1 mediates the polarized transport of antiretroviral nucleosides abacavir and zidovudine. *Drug Metab Dispos* **35:**1165-1173.

Pan G, Winter TN, Roberts JC, Fairbanks CA and Elmquist WF (2009) Organic cation uptake is enhanced in bcrp1-transfected MDCKII cells. *Mol Pharm* **7:**138-145.
Pan G, Winter TN, Roberts JC, Fairbanks CA and Elmquist WF (2010) Organic cation uptake is enhanced in bcrp1-transfected MDCKII cells. *Mol Pharm* **7:**138-145.
Pavek P, Merino G, Wagenaar E, Bolscher E, Novotna M, Jonker JW and Schinkel AH (2005) Human breast cancer resistance protein: interactions with steroid drugs, hormones, the dietary carcinogen 2-amino-1-methyl-6-phenylimidazo(4,5-b)pyridine, and transport of cimetidine. *J Pharmacol Exp Ther* **312:**144-152.
Pedersen JM, Matsson P, Bergstrom CA, Norinder U, Hoogstraate J and Artursson P (2008) Prediction and identification of drug interactions with the human ATP-binding cassette transporter multidrug-resistance associated protein 2 (MRP2; ABCC2). *J Med Chem* **51:**3275-3287.
Penttila IA (2010) Milk-derived transforming growth factor-beta and the infant immune response. *J Pediatr* **156:**S21-25.
Perez M, Blazquez AG, Real R, Mendoza G, Prieto JG, Merino G and Alvarez AI (2009) In vitro and in vivo interaction of moxidectin with BCRP/ABCG2. *Chem Biol Interact* **180:**106-112.
Petri N, Tannergren C, Rungstad D and Lennernas H (2004) Transport characteristics of fexofenadine in the Caco-2 cell model. *Pharm Res* **21:**1398-1404.
Pettitt DJ, Forman MR, Hanson RL, Knowler WC and Bennett PH (1997) Breastfeeding and incidence of non-insulin-dependent diabetes mellitus in Pima Indians. *Lancet* **350:**166-168.
Plagemann A and Harder T (2005) Breast feeding and the risk of obesity and related metabolic diseases in the child. *Metab Syndr Relat Disord* **3:**222-232.
Plante L, Ferron GM, Unruh M and Mayer PR (2004) Excretion of pantoprazole in human breast. *J Reprod Med* **49:**825-827.
Planting AS, Sonneveld P, van der Gaast A, Sparreboom A, van der Burg ME, Luyten GP, de Leeuw K, de Boer-Dennert M, Wissel PS, Jewell RC, Paul EM, Purvis NB, Jr. and Verweij J (2005) A phase I and pharmacologic study of the MDR converter GF120918 in combination with doxorubicin in patients with advanced solid tumors. *Cancer Chemother Pharmacol* **55:**91-99.
Pollex EK, Anger G, Hutson J, Koren G and Piquette-Miller M (2010) Breast cancer resistance protein (BCRP)-mediated glyburide transport: effect of the C421A/Q141K BCRP single-nucleotide polymorphism. *Drug Metab Dispos* **38:**740-744.
Powers HJ (2003) Riboflavin (vitamin B-2) and health. *Am J Clin Nutr* **77:**1352-1360.
Press B and Di Grandi D (2008) Permeability for intestinal absorption: Caco-2 assay and related issues. *Curr Drug Metab* **9:**893-900.
Prost F and Thormann W (2003) Capillary electrophoresis to assess drug metabolism induced in vitro using single CYP450 enzymes (Supersomes): application to the chiral metabolism of mephenytoin and methadone. *Electrophoresis* **24:**2577-2587.
Radhofer-Welte S (1999) Pharmacokinetics and metabolism of the proton pump inhibitor pantoprazole in man. *Drugs Today (Barc)* **35:**765-772.
Roberts SA (2001) High-throughput screening approaches for investigating drug metabolism and pharmacokinetics. *Xenobiotica* **31:**557-589.
Robey RW, Obrzut T, Shukla S, Polgar O, Macalou S, Bahr JC, Di Pietro A, Ambudkar SV and Bates SE (2009) Becatecarin (rebeccamycin analog, NSC 655649) is a transport substrate and induces expression of the ATP-binding cassette transporter, ABCG2, in lung carcinoma cells. *Cancer Chemother Pharmacol* **64:**575-583.

Rocchi E, Khodjakov A, Volk EL, Yang CH, Litman T, Bates SE and Schneider E (2000) The product of the ABC half-transporter gene ABCG2 (BCRP/MXR/ABCP) is expressed in the plasma membrane. *Biochem Biophys Res Commun* **271:**42-46.
Rodriguez-Palmero M, Koletzko B, Kunz C and Jensen R (1999) Nutritional and biochemical properties of human milk: II. Lipids, micronutrients, and bioactive factors. *Clin Perinatol* **26:**335-359.
Roerig DL, Audi SH and Ahlf SB (2004) Kinetic characterization of P-glycoprotein-mediated efflux of rhodamine 6G in the intact rabbit lung. *Drug Metab Dispos* **32:**953-958.
Rohde JE (1981) Mother milk and the Indonesian economy: a major national resource. *Indian J Pediatr* **48:**125-132.
Sachs G (1997) Proton pump inhibitors and acid-related diseases. *Pharmacotherapy* **17:**22-37.
Schmitz A, Thormann W, Moessner L, Theurillat R, Helmja K and Mevissen M (2010) Enantioselective CE analysis of hepatic ketamine metabolism in different species in vitro. *Electrophoresis* **31:**1506-1516.
Schoenfeld P, Kimmey MB, Scheiman J, Bjorkman D and Laine L (1999) Review article: nonsteroidal anti-inflammatory drug-associated gastrointestinal complications--guidelines for prevention and treatment. *Aliment Pharmacol Ther* **13:**1273-1285.
Schwab D, Fischer H, Tabatabaei A, Poli S and Huwyler J (2003) Comparison of in vitro P-glycoprotein screening assays: recommendations for their use in drug discovery. *J Med Chem* **46:**1716-1725.
Scott LJ, Dunn CJ, Mallarkey G and Sharpe M (2002) Esomeprazole: a review of its use in the management of acid-related disorders in the US. *Drugs* **62:**1091-1118.
Shen H, Smith DE, Yang T, Huang YG, Schnermann JB and Brosius FC, 3rd (1999) Localization of PEPT1 and PEPT2 proton-coupled oligopeptide transporter mRNA and protein in rat kidney. *Am J Physiol* **276:**F658-665.
Shen S, He Y and Zeng S (2007) Stereoselective regulation of MDR1 expression in Caco-2 cells by cetirizine enantiomers. *Chirality* **19:**485-490.
Shigeta J, Katayama K, Mitsuhashi J, Noguchi K and Sugimoto Y (2010) BCRP/ABCG2 confers anticancer drug resistance without covalent dimerization. *Cancer Sci*.
Shirasaka Y, Konishi R, Funami N, Kadowaki Y, Nagai Y, Sakaeda T and Yamashita S (2009) Expression levels of human P-glycoprotein in in vitro cell lines: correlation between mRNA and protein levels for P-glycoprotein expressed in cells. *Biopharm Drug Dispos* **30:**149-152.
Smith SW (2009) Chiral toxicology: it's the same thing...only different. *Toxicol Sci* **110:**4-30.
Stanley LA, Horsburgh BC, Ross J, Scheer N and Wolf CR (2009) Drug transporters: gatekeepers controlling access of xenobiotics to the cellular interior. *Drug Metab Rev* **41:**27-65.
Su Y, Lee SH and Sinko PJ (2004) Practical aspects of transporter model systems: a case study involving SQV. *Drug Metab Rev* **36:**377-389.
Sugano K, Kansy M, Artursson P, Avdeef A, Bendels S, Di L, Ecker GF, Faller B, Fischer H, Gerebtzoff G, Lennernaes H and Senner F (2010) Coexistence of passive and carrier-mediated processes in drug transport. *Nat Rev Drug Discov* **9:**597-614.
Sun H, Chow EC, Liu S, Du Y and Pang KS (2008) The Caco-2 cell monolayer: usefulness and limitations. *Expert Opin Drug Metab Toxicol* **4:**395-411.
Sun H and Pang KS (2008) Permeability, transport, and metabolism of solutes in Caco-2 cell monolayers: a theoretical study. *Drug Metab Dispos* **36:**102-123.

Sun H and Scott DO (2009) Structure-based drug metabolism predictions for drug design. *Chem Biol Drug Des* **75:**3-17.
Suzuki K, Doki K, Homma M, Tamaki H, Hori S, Ohtani H, Sawada Y and Kohda Y (2009) Co-administration of proton pump inhibitors delays elimination of plasma methotrexate in high-dose methotrexate therapy. *Br J Clin Pharmacol* **67:**44-49.
Tachibana T, Kitamura S, Kato M, Mitsui T, Shirasaka Y, Yamashita S and Sugiyama Y (2010) Model analysis of the concentration-dependent permeability of P-gp substrates. *Pharm Res* **27:**442-446.
Takahashi H (2008) [Warfarin resistance and related pharmacogenetic information]. *Brain Nerve* **60:**1365-1371.
Tam D, Sun H and Pang KS (2003) Influence of P-glycoprotein, transfer clearances, and drug binding on intestinal metabolism in Caco-2 cell monolayers or membrane preparations: a theoretical analysis. *Drug Metab Dispos* **31:**1214-1226.
Tan B, Piwnica-Worms D and Ratner L (2000) Multidrug resistance transporters and modulation. *Curr Opin Oncol* **12:**450-458.
Tanaka M, Ohkubo T, Otani K, Suzuki A, Kaneko S, Sugawara K, Ryokawa Y and Ishizaki T (2001) Stereoselective pharmacokinetics of pantoprazole, a proton pump inhibitor, in extensive and poor metabolizers of S-mephenytoin. *Clin Pharmacol Ther* **69:**108-113.
Tanaka M, Yamazaki H, Hakusui H, Nakamichi N and Sekino H (1997) Differential stereoselective pharmacokinetics of pantoprazole, a proton pump inhibitor in extensive and poor metabolizers of pantoprazole--a preliminary study. *Chirality* **9:**17-21.
Tateishi T, Miura M, Suzuki T and Uno T (2008) The different effects of itraconazole on the pharmacokinetics of fexofenadine enantiomers. *Br J Clin Pharmacol* **65:**693-700.
Tenberken O, Thiermann H, Worek F and Reiter G (2010) Chromatographic preparation and kinetic analysis of interactions between tabun enantiomers and acetylcholinesterase. *Toxicol Lett* **195:**142-146.
Thorn CF, Klein TE and Altman RB (2009) Codeine and morphine pathway. *Pharmacogenet Genomics* **19:**556-558.
Titus-Ernstoff L, Rees JR, Terry KL and Cramer DW (2009) Breast-feeding the last born child and risk of ovarian cancer. *Cancer Causes Control* **21:**201-207.
Toddywalla VS, Kari FW and Neville MC (1997) Active transport of nitrofurantoin across a mouse mammary epithelial monolayer. *J Pharmacol Exp Ther* **280:**669-676.
Tournier N, Chevillard L, Megarbane B, Pirnay S, Scherrmann JM and Decleves X (2009) Interaction of drugs of abuse and maintenance treatments with human P-glycoprotein (ABCB1) and breast cancer resistance protein (ABCG2). *Int J Neuropsychopharmacol***:**1-11.
Uhl K, Peat R, Toigo T, Kennedy DL and Kweder SL (2003) Review of drug labeling for information regarding lactation. *Clin Pharmacol Ther* **73:**P39.
Vaidya SS, Walsh SW and Gerk PM (2009) Formation and efflux of ATP-binding cassette transporter substrate 2,4-dinitrophenyl-S-glutathione from cultured human term placental villous tissue fragments. *Mol Pharm* **6:**1689-1702.
van Herwaarden AE, Jonker JW, Wagenaar E, Brinkhuis RF, Schellens JH, Beijnen JH and Schinkel AH (2003) The breast cancer resistance protein (Bcrp1/Abcg2) restricts exposure to the dietary carcinogen 2-amino-1-methyl-6-phenylimidazo[4,5-b]pyridine. *Cancer Res* **63:**6447-6452.
van Herwaarden AE and Schinkel AH (2006) The function of breast cancer resistance protein in epithelial barriers, stem cells and milk secretion of drugs and xenotoxins. *Trends Pharmacol Sci* **27:**10-16.

van Herwaarden AE, Wagenaar E, Karnekamp B, Merino G, Jonker JW and Schinkel AH (2006) Breast cancer resistance protein (Bcrp1/Abcg2) reduces systemic exposure of the dietary carcinogens aflatoxin B1, IQ and Trp-P-1 but also mediates their secretion into breast milk. *Carcinogenesis* **27:**123-130.

van Herwaarden AE, Wagenaar E, Merino G, Jonker JW, Rosing H, Beijnen JH and Schinkel AH (2007) Multidrug transporter ABCG2/breast cancer resistance protein secretes riboflavin (vitamin B2) into milk. *Mol Cell Biol* **27:**1247-1253.

Villegas R, Gao YT, Yang G, Li HL, Elasy T, Zheng W and Shu XO (2008) Duration of breast-feeding and the incidence of type 2 diabetes mellitus in the Shanghai Women's Health Study. *Diabetologia* **51:**258-266.

Vlaming ML, Lagas JS and Schinkel AH (2009) Physiological and pharmacological roles of ABCG2 (BCRP): recent findings in Abcg2 knockout mice. *Adv Drug Deliv Rev* **61:**14-25.

Walker A (2010) Breast milk as the gold standard for protective nutrients. *J Pediatr* **156:**S3-7.

Wang B, Dukarevich M, Sun EI, Yen MR and Saier MH, Jr. (2009a) Membrane porters of ATP-binding cassette transport systems are polyphyletic. *J Membr Biol* **231:**1-10.

Wang L, Leggas M, Goswami M, Empey PE and McNamara PJ (2008) N-(4-[2-(1,2,3,4-tetrahydro-6,7-dimethoxy-2-isoquinolinyl)ethyl]-phenyl)-9 ,10-dihydro-5-methoxy-9-oxo-4-acridine carboxamide (GF120918) as a chemical ATP-binding cassette transporter family G member 2 (Abcg2) knockout model to study nitrofurantoin transfer into milk. *Drug Metab Dispos* **36:**2591-2596.

Wang L and McNamara PJ (2010) Stereoselective transport of pantoprazole by rAbcg2/ABCG2. *In preparation*.

Wang X and Morris ME (2007) Effects of the flavonoid chrysin on nitrofurantoin pharmacokinetics in rats: potential involvement of ABCG2. *Drug Metab Dispos* **35:**268-274.

Wang XD, Meng MX, Gao LB, Liu T, Xu Q and Zeng S (2009b) Permeation of astilbin and taxifolin in Caco-2 cell and their effects on the P-gp. *Int J Pharm* **378:**1-8.

Warmann S, Gohring G, Teichmann B, Geerlings H and Fuchs J (2002) MDR1 modulators improve the chemotherapy response of human hepatoblastoma to doxorubicin in vitro. *J Pediatr Surg* **37:**1579-1584.

Washington CB, Duran GE, Man MC, Sikic BI and Blaschke TF (1998) Interaction of anti-HIV protease inhibitors with the multidrug transporter P-glycoprotein (P-gp) in human cultured cells. *J Acquir Immune Defic Syndr Hum Retrovirol* **19:**203-209.

Weinglass AB, Kohler MG, Nketiah EO, Liu J, Schmalhofer W, Thomas A, Williams B, Beers L, Smith L, Hafey M, Bleasby K, Leone J, Tang YS, Braun M, Ujjainwalla F, McCann ME, Kaczorowski GJ and Garcia ML (2008) Madin-Darby canine kidney II cells: a pharmacologically validated system for NPC1L1-mediated cholesterol uptake. *Mol Pharmacol* **73:**1072-1084.

White RE (2000) High-throughput screening in drug metabolism and pharmacokinetic support of drug discovery. *Annu Rev Pharmacol Toxicol* **40:**133-157.

Xiao Y, Davidson R, Smith A, Pereira D, Zhao S, Soglia J, Gebhard D, de Morais S and Duignan DB (2006) A 96-well efflux assay to identify ABCG2 substrates using a stably transfected MDCK II cell line. *Mol Pharm* **3:**45-54.

Xie Z, Zhang Y, Xu H and Zhong D (2005) Pharmacokinetic differences between pantoprazole enantiomers in rats. *Pharm Res* **22:**1678-1684.

Xu J, Liao L, Ning G, Yoshida-Komiya H, Deng C and O'Malley BW (2000) The steroid receptor coactivator SRC-3 (p/CIP/RAC3/AIB1/ACTR/TRAM-1) is required for

normal growth, puberty, female reproductive function, and mammary gland development. *Proc Natl Acad Sci U S A* **97:**6379-6384.

Xu J, Liu Y, Yang Y, Bates S and Zhang JT (2004) Characterization of oligomeric human half-ABC transporter ATP-binding cassette G2. *J Biol Chem* **279:**19781-19789.

Yamashita S, Hattori E, Shimada A, Endoh Y, Yamazaki Y, Kataoka M, Sakane T and Sezaki H (2002) New methods to evaluate intestinal drug absorption mediated by oligopeptide transporter from in vitro study using Caco-2 cells. *Drug Metab Pharmacokinet* **17:**408-415.

Yamazaki M, Neway WE, Ohe T, Chen I, Rowe JF, Hochman JH, Chiba M and Lin JH (2001) In vitro substrate identification studies for p-glycoprotein-mediated transport: species difference and predictability of in vivo results. *J Pharmacol Exp Ther* **296:**723-735.

Yokooji T, Murakami T, Yumoto R, Nagai J and Takano M (2007) Role of intestinal efflux transporters in the intestinal absorption of methotrexate in rats. *J Pharm Pharmacol* **59:**1263-1270.

Zhang C, Kwan P, Zuo Z and Baum L (2010) In vitro concentration dependent transport of phenytoin and phenobarbital, but not ethosuximide, by human P-glycoprotein. *Life Sci* **86:**899-905.

Zhang L, Zhang YD, Strong JM, Reynolds KS and Huang SM (2008) A regulatory viewpoint on transporter-based drug interactions. *Xenobiotica* **38:**709-724.

Zhang L, Zhang YD, Zhao P and Huang SM (2009) Predicting drug-drug interactions: an FDA perspective. *Aaps J* **11:**300-306.

Zhang Y, Wang H, Unadkat JD and Mao Q (2007) Breast cancer resistance protein 1 limits fetal distribution of nitrofurantoin in the pregnant mouse. *Drug Metab Dispos* **35:**2154-2158.

Zhao R, Raub TJ, Sawada GA, Kasper SC, Bacon JA, Bridges AS and Pollack GM (2009) Breast cancer resistance protein interacts with various compounds in vitro, but plays a minor role in substrate efflux at the blood-brain barrier. *Drug Metab Dispos* **37:**1251-1258.

Zheng LS, Wang F, Li YH, Zhang X, Chen LM, Liang YJ, Dai CL, Yan YY, Tao LY, Mi YJ, Yang AK, To KK and Fu LW (2009) Vandetanib (Zactima, ZD6474) antagonizes ABCC1- and ABCG2-mediated multidrug resistance by inhibition of their transport function. *PLoS One* **4:**e5172.

Zhou L, Naraharisetti SB, Wang H, Unadkat JD, Hebert MF and Mao Q (2008) The breast cancer resistance protein (Bcrp1/Abcg2) limits fetal distribution of glyburide in the pregnant mouse: an Obstetric-Fetal Pharmacology Research Unit Network and University of Washington Specialized Center of Research Study. *Mol Pharmacol* **73:**949-959.

Zhou W, Madrid P, Fluitt A, Stahl A and Xie XS (2010) Development and validation of a high-throughput screening assay for human long-chain fatty acid transport proteins 4 and 5. *J Biomol Screen* **15:**488-497.

VITA

Lipeng Wang was born on March 22, 1971 in Nenjiang, Heilongjiang Province in China. She majored in Veterinary Medicine and received her bachelor degree in the College of Veterinary Medicine at Heilongjiang Argricultural University (Heilongjiang, China) in 1993 and master degree in the College of Veterinary Medicine at China Argricultural University (Beijing, China) in 2000. In 2001, Lipeng joined Dr. James Y Kang's lab as a research associate in the Department of Pharmacology and Toxicology at University of Louisvile. Her research focused on molecular mechanisms of alcoholic fatty liver, zinc homeostasis and alcoholic liver disease. She also successfully established alcohol-induced myocardial fibrosis model in metallothionein -null mice. She is the author or co-author in 12 papers of the work in this period.

Lipeng entered the Doctor of Philosophy program in the Department of Pharmaceutical Science at the University of Kentucky in 2005 and persued her studies under the direction of Dr. Patrick J. McNamara. Lipeng received the First Place Poster Award for 2010 Rho Chi Research day. She received Graduate School Travel Award for 2009 AAPS annual meeting at University of Kentucky. She was also Drug transporter meeting Travelship Award Winner in Drug Transporters meeting: 2007 AAPS Workshop on Transporters in ADME. Lipeng is a member of American Association of Pharmaceutical Scientists (AAPS) and American Association for the Advancement of Science (AAAS).

Publications:

1. **Wang L,** Leggas M, Goswami M, Empey PE, McNamara PJ. N-(4-[2-(1,2,3,4-tetrahydro-6,7-dimethoxy-2-isoquinolinyl)ethyl]-phenyl)-9,10-dihydro-5-methoxy-9-oxo-4-acridine carboxamide (GF120918) as a chemical ATP-binding cassette transporter family G member 2 (Abcg2) knockout model to study nitrofurantoin transfer into milk. *Drug Metab Dispos.* 2008 Dec; 36(12):2591-6. Epub 2008 Sep 17.
2. ***Wang L***, Zhou Z, Kang YJ. Alcohol-induced myocardial fibrosis in metallothionein-null mice. *Am J Pathol.* 2005 Aug;167(2):337-44.

   Comment in: A murine model of alcoholic cardiomyopathy: a role for zinc and metallothionein in fibrosis. *Am J Pathol.* 2005 Aug;167(2):301-4.
3. Li Y, **Wang L,** Schuschke DA., Zhou Z, Saari JT, and Kang YJ. Marginal Dietary Copper Restriction Induces Cardiomyopathy in Rats. *J Nutr.* 2005 Sep; 135(9):2130-6
4. Cai L, Wang J, Li Y, Sun X, **Wang L,** Zhou Z, and Kang YJ. Inhibition of superoxide generation and associated nitrosative damage is involved in

metallothionein prevention of diabetic cardiomyopathy. *Diabetes.* 2005 June (54): 1829-1837

5. Zhou Z, **Wang L,** Saari JT, McClain CJ, Kang YJ. Zinc supplementation prevents alcohol-induced liver injury through attenution of oxidative stress. *Am J Pathol.* 2005 June; 166 (6): 1681-1690
6. Song Z, Zhou Z, Uriarte S, **Wang L,** Kang YJ, Chen T, Barve S, McClain CJ. S-adenosylhomocysteine sensitizes to TNF-alpha hepatotoxicity in mice and liver cells: a possible etiological factor in alcoholic liver disease. *Hepatology.* 2004 Oct;40(4):989-97.
7. Kannan M, **Wang L,** Kang YJ. Myocardial oxidative stress and toxicity induced by acute ethanol exposure in mice. *Exp Biol Med (Maywood).* 2004 Jun;229(6):553-9.
8. Lambert JC, Zhou Z, **Wang L,** Song Z, McClain CJ, and Kang YJ. Preservation of intestinal structural integrity by zinc is independent of metallothionein in alcohol-intoxicated mice. *Am J Pathol.* 2004 Jun;164(6):1959-66.
9. Zhou Z, **Wang L,** Song Z, Saari JT, McClain CJ, Kang YJ. Abrogation of NF-κB activation is involved in zinc inhibition of Lipopolysacchride-induced tumor necrosis factor-α production and liver injury. *Am J Pathol.* 2004 May;164(5):1547-56..
10. Elsherif L, **Wang L,** Saari JT, Kang YJ. Regression of dietary copper restriction-induced cardiomyopathy by copper repletion in mice. *J Nutr.* 2004 Apr;134(4):855-60.
11. Zhou Z, **Wang L,** Song Z, Lambert JC, McClain CJ, and Kang YJ.A critical involvement of oxidative stress in acute alcohol-induced hepatic TNF-α production. *Am J Pathol.* 2003;163:1137-1146
12. Lambert JC, Zhou Z, **Wang L,** Song Z, McClain CJ, and Kang YJ. Prevention of alterations in intestinal permeability is involved in zinc inhibition of acute ethanol-induced liver damage in mice. *J Pharmacol Exp Ther* 2003;305:880-886
13. Li Y, Sun X, **Wang L,** Zhou Z, and Kang YJ. Myocardial toxicity of arsenic trioxide in a mouse model. *Cardiovascular Toxicology,* 2002, (2): 63-73